UC San Diego

UC San Diego Electronic Theses and Dissertations

Title

Genetic analysis of proteoglycan-mediated clearance of triglycerides

Permalink

https://escholarship.org/uc/item/1q16k6hq

Author

Stanford, Kristin Irene

Publication Date

2009

Peer reviewed|Thesis/dissertation

eScholarship.org Powered by the California Digital Library
University of California

UNIVERSITY OF CALIFORNIA, SAN DIEGO

GENETIC ANALYSIS OF PROTEOGLYCAN-MEDIATED CLEARANCE OF TRIGLYCERIDES

A dissertation submitted in partial satisfaction of the requirements

of the degree Doctor of Philosophy

in

Biomedical Sciences

by

Kristin Irene Stanford

Committee in Charge:

Professor Jeffrey D. Esko, Chair
Professor Linda K. Curtiss
Professor Richard L. Gallo
Professor Randolph Y. Hampton
Professor Michael C. Hogan
Professor Joseph L. Witztum

2009

Copyright

Kristin Irene Stanford, 2009

All rights reserved.

The dissertation of Kristin Irene Stanford is approved, and it is acceptable in quality and form for publication on microfilm and electronically:

_____

_____

_____

_____

_____

_____
Chair

University of California, San Diego

2009

To my Giagia, who was my biggest fan and supporter.

Not to worry, Gia – proceeds from this work won't be used for cigs or beer.

“A goal, a love, and a dream give you total control over your life”

John Wayne Schlatter

TABLE OF CONTENTS

Signature Page……...iii

Dedication……..iv

Epigraph……..v

Table of Contents……...vi

List of Symbols…….xii

List of Figures and Tables……...xiii

Acknowledgements……...xv

Vita……..xvii

Abstract of the Dissertation……...xix

CHAPTER 1 INTRODUCTION: HEPARAN SULFATE PROTEOGLYCANS AND LIPOPROTEIN REMNANT METABOLISM……..……..1

1.1 Summary…….1

1.2 Hypertriglyceridemia……..1

1.3 Lipoprotein metabolism……..2

1.4 Receptors involved in lipoprotein remnant clearance…….5

1.5 Hepatic HSPGs facilitate clearance of TRLs……..……6

1.6 Relative contribution of receptors involved in TRL clearance……..…8

1.7 Heparan sulfate proteoglycans: structure and function……13

1.8 How does HS structure affect lipoprotein metabolism?.....16

1.9 Which proteoglycans are relevant to TRL clearance……17

1.10 Conclusions and Future Directions……...19

1.11 References…….20

CHAPTER 2 HEPARAN SULFATE 2-*O*-SULFOTRANSFERASE IN HEPATOCYTES IS REQUIRED FOR TRIGLYCERIDE-RICH LIPOPROTEIN CLEARANCE……..…….39

2.1 Summary……...39

2.2 Introduction……...40

2.3 Results……...42

2.3.1 Conditional targeting of Hs2st……..42

2.3.2 Hepatocyte-specific Hs2st gene disruption alters heparan sulfate in the liver……43

2.3.3 *Hs2st$^{f/f}$AlbCre^{+}* mice accumulate triglyceride-rich lipoproteins……46

2.3.4 Hs2st-deficient mice exhibit slower plasma clearance of triglycerides and VLDL……48

2.3.5 Binding and uptake of ^{125}I-VLDL particles is delayed in Hs2st-deficient hepatocytes……..51

2.3.6 Binding of VLDL shows specificity…….52

2.4 Discussion…….54

2.5 Experimental Procedures……..58

2.5.1 Mice derivation and Animal husbandry……58

2.5.2 HS purification and analysis…….59

2.5.3 Lipoprotein analysis……..60

2.5.4 VLDL plasma clearance……60

2.5.5 Vitamin A fat tolerance testing……61

2.5.6 Lipoprotein uptake by hepatocytes……...61

2.5.7 Statistics……62

2.6 Acknowledgements……..63

2.7 References……64

2.8 Supplementary Experimental Procedures……68

2.8.1 Heparan sulfate 2-*O*-sulfotransferase assay……..68

2.9 Supplementary results……...68

2.9.1 Generation of conditional Hs2st mice……...69

2.9.2 Conditional inactivation of Hs2st……70

2.9.3 zpHs2st$^{-/-}$ mice exhibit reduced 2-*O*-sulfotransferase activity……..71

2.9.4 Hs2st$^{-/-}$ mice exhibit nearly complete absence of 2-*O*-sulfation……71

2.10 Supplementary figure legends……...72

CHAPTER 3 SYNDECAN-1 IS THE PRIMARY HEPARAN SULFATE PROTEOGLYCAN MEDIATING HEPATIC CLEARANCE OF TRIGLYCERIDE-RICH LIPOPROTEINS *IN VIVO*……..75

3.1 Summary……...75

3.2 Introduction……...76

3.3 Results……...78

3.3.1 *Sdc1*$^{-/-}$ mice accumulate plasma triglycerides……...78

3.3.2 *Sdc1*$^{-/-}$ mice exhibit delayed plasma clearance of both VLDL and dietary triglycerides……82

3.3.3 Syndecan-1 is the primary heparan sulfate proteoglycan mediating clearance……...86

3.3.4 Syndecan-1 is localized on microvilli of hepatocytes in the space of Disse……88

3.3.5 Syndecan-1 can mediate binding, uptake, and degradation of VLDL……89

3.4 Discussion……93

3.5 Experimental Procedures……..98

3.5.1 Mice and animal husbandry……..98

3.5.2 Adenovirus……99

3.5.3 Quantitative RT-PCR of membrane HSPGs…….99

3.5.4 Lipoprotein Analysis……...100

3.5.5 Analysis of apolipoprotein composition…….100

3.5.6 VLDL plasma clearance……..101

3.5.7 Vitamin A excursion studies……...101

3.5.8 Immunofluorescence microscopy……...102

3.5.9 Immunogold electron microscopy……..103

3.5.10 Lipoprotein binding and uptake by hepatocytes…….104

3.5.11 Statistics……..105

3.6 Acknowledgements……106

3.7 References……...107

3.8 Supplemental Figure Legends…….114

CHAPTER 4 THE RELATIVE CONTRIBUTION OF HEPARAN SULFATE PROTEOGLYCANS, LDL-RECEPTOR, AND LDL-RECEPTOR-RELATED PROTEIN IS ESSENTIAL FORCLEARANCE OF TRIGLYCERIDE- AND CHOLESTEROL-RICH PARTICLES……116

4.1 Summary…….116

4.2 Introduction……117

4.3 Results…….119

4.3.1 Generalized hyperlipidemia is observed in mutant mice……119

4.3.2 *Ldlr*$^{-/-}$*Ndst1*$^{f/f}$*Lrp1*$^{f/f}$*AlbCre*$^{+}$ mice exhibit greater delay in plasma clearance of dietary triglycerides compared to other mutant mice.....123

4.3.3 LDLR and HS mediate binding, uptake, and degradation of VLDL……..125

4.3.4 The three receptors, LDLR, HS, and LRP1 do not compensate for each other……...128

4.4 Discussion……...130

4.5 Experimental Procedures……134

4.5.1 Mice and animal husbandry……134

4.5.2 Lipoprotein analysis……135

4.5.3 Vitamin A excursion studies……...135

4.5.4 Analysis of apolipoprotein composition…….136

4.5.5 Triglyceride secretion rate……...136

4.5.6 Immunofluorescence microscopy……...137

4.5.7 Quantitative RT-PCR of membrane HSPGs……...138

4.5.8 Lipoprotein binding and uptake by hepatocytes…….138

4.5.9 Statistics……..139

4.6 Acknowledgements…….140

4.7 References……...141

CHAPTER 5 CONCLUSIONS AND FUTURE DIRECTIONS……..146

5.1 Summary…….146

5.2 *N*- and 2-*O*-sulfation are required for the binding and uptake of triglyceride-rich lipoproteins……...146

5.2.1 Determine the ligand required for VLDL binding to heparan sulfate……148

5.3 Why do large particles accumulate in the *Ldlr*$^{-/-}$*HS*$^{-/-}$*Lrp1*$^{-/-}$ mice?.....152

5.4 Syndecan 1 is the primary hepatocyte HSPG involved in lipoprotein remnant metabolism…….153

5.4.1 Regulation of Sdc1 uptake by dietary triglyceride……..155

5.5 Conclusions…….156

5.6 References……...158

APPENDIX A DELETION OF BASEMENT MEMBRANE HEPARAN SULFATE PROTEOGLYCAN TYPE XVIII COLLAGEN CAUSES HYPERTRIGLYCERIDEMIA……...166

LIST OF SYMBOLS

For the purposes of this dissertation gene names will be written in lower case italics (i.e., *Ndst1*), whereas protein names will be written in capitals (i.e., NDST1), regardless of species.

NDST/*Ndst*	N-deacetylase N-sulfotransferase
OST/*Ost*	O-sulfotranferase
AlbCre	Cre transgene driven by rat albumin promoter
GlcNAc	N-acetyl-D-glucosamine
GlcA	D-glucuronic acid
IdoA	L-iduronic acid
apoE/*Apoe*	apolipoprotein E
apoB	apolipoprotein B
apoA	apolipoprotien A
apoC	apolipoprotein C
LDLR/*Ldlr*	LDL receptor
LRP/*Lrp*	LDL receptor-related protein
Lpl	lipoprotein lipase
HL	hepatic lipase
VLDL	very low density lipoprotein
LDL	low density lipoprotein
HDL	high density lipoprotein

LIST OF FIGURES AND TABLES

Table 1-1. Hyperlipidemias in humans……2

Table 1-2. Lipoprotein particle characterization……..3

Figure 1-1. Hyperlipidemia in heparan sulfate deficient mice……..8

Figure 1-2. Model of possible roles for hepatic HSPGs……..12

Figure 1-3. Scheme of HS chain biosynthesis…….15

Figure 2-1. *Hs2st* conditional knockout……...45

Figure 2-2. Disaccharide analysis of liver HS…….46

Table 2-1. Distribution of sulfate groups in wild-type and mutant hepatocytes…46

Figure 2-3. Hypertriglyceridemia in *Hs2st*$^{f/f}$*AlbCre*$^{+}$ mice……..48

Figure 2-4. *Hs2st*$^{f/f}$*AlbCre*$^{+}$ mice exhibit delayed plasma clearance of VLDL and dietary triglycerides……50

Figure 2-5. Hs2st mediates binding, uptake, and degradation of VLDL…….52

Figure 2-6. Incubation with various desulfated heparins effects binding of ^{125}I-VLDL…….54

Table 2-2. Apolipoproteins known to bind Heparin/Heparan Sulfate……56

Table 2-3. Various organisms deficient in Hs2st……...57

Figure 2-S1. Genotyping Hs2st mice…….73

Figure 2-S2. Heparan sulfate 2-O-sulfotransferase enzyme activity and disaccharide analyses…….74

Figure 3-1. RT-PCR analysis of membrane HSPGs and hypertriglyceridemia in *Sdc1*$^{-/-}$ mice……80

Figure 3-2. Hypertriglyceridemia and delayed plasma clearance of VLDL in *Sdc*$^{-/-}$ mice……..82

Figure 3-3. *Sdc1*$^{-/-}$ mice exhibit delayed plasma clearance of dietary triglycerides……...85

Figure 3-4. Hypertriglyceridemia in *Sdc1*$^{-/-}$ and *Ndst1*$^{f/f}$*AlbCre*$^{+}$ mice is not Additive……87

Figure 3-5. Syndecan-1 is localized on microvilli of hepatocytes in the space of Disse……..89

Figure 3-6. Syndecan-1 mediates the binding of VLDL…….92

Figure 3-7. Binding, uptake, and degradation of VLDL at 37^{o}……...93

Figure 3-S1. Supplemental figure 1…….115

Figure 4-1. Hyperlipidemia in *Ldlr*$^{-/-}$*Ndst1*$^{f/f}$*Lrp1*$^{f/f}$*AlbCre*$^{+}$ mice…….120

Table 4-1. Hyperlipidemia in mutant mice……...121

Figure 4-2. Hyperlipidemia in *Ldlr*$^{-/-}$*Ndst1*$^{f/f}$*Lrp1*$^{f/f}$*AlbCre*$^{+}$ mice is similar to *ApoE*$^{-/-}$ mice……122

Figure 4-3. *Ldlr*$^{-/-}$*Ndst1*$^{f/f}$*Lrp1*$^{f/f}$*AlbCre*$^{+}$ mice exhibit delayed plasma clearance of dietary triglycerides……124

Figure 4-4. HS, LDLR mediates binding of VLDL……...127

Figure 4-5. Binding, uptake, and degradation of VLDL at 37^{o}C……...128

Figure 4-6. RT-PCR analysis of hepatocyte lipoprotein receptors……130

ACKNOWLEDGEMENTS

Many people helped me accomplish the research presented in this thesis. First of all, I'd like to thank my thesis advisor, Jeff Esko, for his continual support and guidance throughout my graduate career, and for creating an environment in which I could be successful. I also thank my thesis committee members, Linda Curtiss, Richard Gallo, Randy Hampton, Michael Hogan, and Joseph Witztum for their helpful feedback and advice throughout this process. I am very grateful to past and present members of the Esko lab, especially Rusty Bishop, Erin Foley, Roger Lawrence, and Danyin Song, for their collaborative help in the work presented in this thesis. Many others at UCSD assisted in my research: David Ditto in the Hematology Core collected blood samples from my mice. From the Witztum laboratory, Joe Juliano analyzed plasma cholesterol and triglyceride samples for me, Jennifer Pattison showed me how to isolate lipoproteins by FPLC and preparative ultracentrifugation, Fely Alamazen showed me how to ^{125}I-label VLDL, and Elizabeth Miller taught me her ELISA technique and allowed me to use her equipment and reagents repeatedly. Ingrid Niesman also offered technical support and advice with immunofluorescence microscopy.

Work presented in chapter 2 will be submitted for publication to the *Journal of Biological Chemistry* with coauthors Joseph R., Bishop, Danyin Song, Roger Lawrence, Lianchun Wang, and Jeffrey D. Esko. I was the primary author of the work contained in the paper. I'd like to thank David Ditto and Joseph Juliano for excellent technical assistance. Work was conducted within the department of Cellular and

Molecular Medicine, the Department of Medicine, and the Glycobiology Research and Training Center, University of California, San Diego, La Jolla, California.

Work presented in chapter 3 has been submitted in for publication to the *Journal of Clinical Investigation* with coauthors Joseph R. Bishop, Ingrid R. Niesman, Joseph L. Witztum, and Jeffrey D. Esko. I was the primary author of the work contained in this chapter. I'd like to thank Joseph Juliano, Fely Alamazen and Jennifer Pattison at UCSD, David Ditto of the Hematology/Coagulation/Chemistry Core supported by NIH grant HL57345, and National Institutes of Health Grants GM33063 and HL57345 (J.D.E.), NIH HL088093 and the Leducq Foundation (J.L.W.), and a Scientist Development Grant from the American Heart Association (J.R.B).

Work presented in chapter 4 will be submitted for publication to the *Journal of Biological Chemistry* with coauthors Erin M. Foley, Ingrid R. Niesman, Joseph L. Witztum, and Jeffrey D. Esko. I was the primary author of this work, and I'd like to thank Joseph Juliano, Fely Alamazen and Jennifer Pattison at UCSD, and David Ditto of the Hematology/Coagulation/Chemistry Core.

Last, but not least, I would like to thank my parents and my sister for their unwavering support, and my future pool manager, Nicole Lacayo, for her continual support and encouragement, even though she hates those 'patocytes.

CURRICULUM VITA

2002	Bachelor of Science, Kinesiology - Exercise Science Indiana University, Bloomington, Indiana
2004	Master of Science, Kinesiology – Exercise Physiology Indiana University, Bloomington, Indiana
2009	Doctor of Philosophy, Biomedical Sciences University of California, San Diego

Stanford KI, Bishop JR, Niesman I, Witztum JL, Esko JD. Syndecan-1 is the Primary Heparan Sulfate Proteoglycan Mediating Hepatic Clearance of Triglyceride-Rich Lipoproteins *In Vivo*. *In Review* 2009.

Bishop JR, Passos-Bueno MR, **Stanford KI**, Gonzales, JC, Yeh E, Bensadoun, Moulton KS, Esko JD. Deletion of the basement membrane heparan sulfate proteoglycan Type XVIII Collagen causes hypertriglyceridemia in humans and mice. *Submitted* 2009.

Stanford KI, Bishop JR, Song D, Castagnola J, Lawrence R, Wang L, Esko JD. Heparan Sulfate 2-*O*-sulfotransferase in hepatocytes is required for Triglyceride-Rich Lipoprotein clearance. *In preparation* 2009.

Stanford KI, Foley EM, Witztum JL, and Esko JD. The relative contribution of heparan sulfate proteoglycans, LDL-receptor, and LDL-receptor-related protein is essential for clearance of triglyceride- and cholesterol-rich particles. *In preparation* 2009.

Bishop JR, **Stanford KI**, Esko JD. Heparan sulfate proteoglycans and triglyceride-rich lipoprotein metabolism. *Current Opinions in Lipidology* 2008; 19(3): 307-13.

MacArthur JM, Bishop JR, **Stanford KI**, Wang L, Bensadoun A, Witztum JL, Esko JD. Liver heparan sulfate proteoglycans mediate clearance of triglyceride-rich lipoproteins independently of LDL receptor family members. *Journal of Clinical Investigation* 2007; 117(1): 153-64.

Stanford KI, Mickleborough TD, Ray S, Lindley MR, Koceja DM, Stager JM. Influence of menstrual cycle phase on pulmonary function in asthmatic athletes *European Journal of Applied Physiology* 2006; 96(6): 703-10.

Wade CE, **Stanford KI**, Stein TP, Greenleaf JE. Intensive exercise training suppresses testosterone during bed rest. *Journal of Applied Physiology* 2005; 99(1): 59-63.

ABSTRACT OF THE DISSERTATION

GENETIC ANALYSIS OF PROTEOGLYCAN-MEDIATED CLEARANCE OF TRIGLYCERIDES

by

Kristin Irene Stanford

Doctor of Philosophy in Biomedical Sciences

University of California, San Diego, 2009

Professor Jeffrey D. Esko, Chair

Heparan sulfate proteoglycans regulate various aspects of lipoprotein metabolism through their interaction with apolipoproteins and lipases. In the liver, one or more proteoglycans facilitates the clearance of remnant triglyceride-rich lipoproteins. This dissertation describes the role of various sulfate groups on heparan sulfate necessary for lipoprotein binding and uptake, the identity of the heparan sulfate proteoglycan receptor in the hepatocytes, and the relative contribution of heparan sulfate proteoglycans and members of the low density lipoprotein family of receptors to clearance. Chapter 1 reviews literature regarding lipoprotein metabolism, hypertriglyceridemia, and relevant work implicating heparan sulfate proteoglycans in lipoprotein clearance. Chapter 2 describes the requirement of 2-O-sulfation of uronic

acids in heparan sulfate for binding and uptake of lipoprotein remnants using a mouse model in which the relevant biosynthetic enzyme (Hs2st) was selectively inactivated in hepatocytes. Chapter 3 provides genetic evidence for syndecan-1 as the relevant proteoglycan involved in lipoprotein binding and uptake in the liver. Chapter 4 presents insight into the relative contribution of three receptors, syndecan-1, low-density lipoprotein receptors (LDLR), and low-density lipoprotein-related protein-1 (LRP-1) to hepatic clearance. A new mouse model in which all three hepatocyte lipoprotein receptors have been inactivated is described. These mice accumulated triglycerides and cholesterol, demonstrating that heparan sulfate proteoglycans participate in the clearance of cholesterol-rich lipoproteins as well as triglyceride-rich remnants. Chapter 5 proposes future studies into the application of these findings with regards to human disease.

CHAPTER 1

INTRODUCTION:
HEPARAN SULFATE PROTEOGLYCANS AND LIPOPROTEIN REMNANT METABOLISM

1.1 Summary

Lipoproteins transport insoluble triglyceride, cholesterol, and cholesterol esters in the blood. In the liver, lipoproteins bind to and are internalized by various endocytic receptors, including LDL receptors (LDLR), LDL receptor-related proteins (LRPs), and heparan sulfate proteoglycans (HSPG). It is the goal of this thesis to determine if a specific heparan sulfate proteoglycan acts as a clearance receptor in the liver, the heparan sulfate sulfotransferases involved in forming the binding sites for lipoproteins, and the relative contributions of the various receptors to lipoprotein clearance. This chapter describes how these lipoprotein particles travel through the circulation and are acted on by various receptors, and the role that heparan sulfate proteoglycans are thought to play in this process.

1.2 Hypertriglyceridemia

Hypertriglyceridemia is prevalent in the United States, affecting as many as 10-20% of the population (162-164), and is characterized by the accumulation of triglyceride-rich lipoproteins (TRLs) in the circulation. Some hypertriglyceridemias are caused by monogenic defects from deficiencies in receptors, apolipoproteins, and lipases, while the majority are acquired through diet, drug treatment, or hormone

deficiencies. Acquired hypertriglyceridemia has a complex etiology and may arise from conditions such as uncontrolled diabetes mellitus, metabolic syndrome, chronic alcohol consumption, hypothyroidism, steroids (estrogen), and certain drug treatments (2). Patients with hypertriglcyeridemia have an increased risk of atherosclerosis, coronary artery disease, and pancreatitis, and thus much interest exists in understanding its etiology. Hypertriglyceridemias were first categorized by the Fredrickson classification system; types I, IIb, III, IV, and V are characterized by variable levels of triglycerides (Table 1-1). In type I, IIb, III, and V, serum cholesterol levels are also elevated (1).

Table 1-1. Hyperlipidemias in humans

	Lipids	**Lipoproteins**	**Primary Disorder**	**Mouse Model**
Type I	Very high triglycerides	Chylomicrons	Defect in lipoprotein lipase, apolipoprotein CII deficiency	*Lpl*$^{-/-}$ mice
Type IIa	High Cholesterol	LDL	Defect in LDL receptor	*Ldlr*$^{-/-}$ mice
Type IIb	High cholesterol + triglycerides	LDL + VLDL	Defect in LDL receptor + ?	?
Type III	High cholesterol + triglycerides	IDL + remnants	Defect in apoE	Like *ApoE*$^{-/-}$ mice
Type IV	High triglycerides	VLDL	Defect in ABCA1, or ?	?
Type V	Very high triglycerides	Chylomicrons + VLDL	Defect in lipoprotein lipase, apolipoprotein CII deficiency	*Lpl*$^{-/-}$ mice
?	Vesicular and discoidal lipoproteins	HDL	LCAT deficiency	*LCAT*$^{-/-}$ mice

1.3 Lipoprotein metabolism

Triglyceride-rich lipoproteins arise from exogenous and endogenous pathways. The exogenous source of triglycerides is dietary fat, which is absorbed by the intestine and packaged into large, buoyant, triglyceride-rich chylomicrons, and secreted into the lymphatic system (Table 1-2). These chylomicrons possess apoB48 (a truncated form of apoB), as well as apoCII and apoE. ApoCII is a cofactor for lipoprotein lipase (Lpl), the enzyme in capillaries that hydrolyzes chylomicron triglycerides into free fatty acids. Animals deficient in Lpl die perinatally, with triglyceride levels of ~30,000 mg/dL; animals deficient in apoCII display a mild hypertriglyceridemia (~100 mg/dL) (70), due to an inability of Lpl to hydrolyze the particle. During hydrolysis, the free fatty acids and monoacylglycerls are released from the particle and the chylomicron decreases in size and loses apoCII. These processed particles are now called chylomicron remnants (CRs) and are now small enough to pass through the fenestrated endothelium of the liver sinusoids and into the space of Disse (3-6).

Table 1-2. Lipoprotein particle characterization.

Lipoprotein	Density (mg/dL)	Electrophoretic Mobility	Diameter (nm)	Molecular Weight (kDa)	Apoproteins
Chylomicrons	< 0.93	Origin	75 - 1200	50 - 1000 x 10^6	B48, E, CII
VLDL	<0.93 – 1.006	Pre-β	30 - 80	10 – 80 x 10^6	B100, E, AV, CI, II, III
IDL	1.006 – 1.019	Slow pre-β	25 - 35	5 – 10 x 10^6	B100, E
LDL	1.019 – 1.063	β	18 - 25	2 – 3 x 10^6	B100
HDL	1.063 – 1.21	α	5 - 12	1.8 – 3.6 x 10^5	AI, II, IV

The liver packages lipids derived from endogenous fats and secretes them as very low density lipoproteins (VLDL). In humans, the VLDL particles contain the full length apoB, apoB100. Once in circulation, these VLDL particles gain apoCII and apoE. ApoE is an essential structural component and appears to be required for

binding and uptake of VLDL, as mice deficient in apoE have hypercholesteremia with an accumulation of cholesterol in the VLDL particles. ApoAV also appears to drive plasma hydrolysis of triglycerides from TRLs by facilitating interactions with Lpl. ApoAV deficient mice have four times more plasma triglyceride than littermate controls (60, 61). Like chylomicrons, VLDL is a substrate for Lpl in the capillaries, and its hydrolysis releases fatty acids to nearby tissues for storage and energy. The VLDL particle that has lost its triglycerides becomes a VLDL remnant, or intermediate density lipoprotein (IDL), which, like CRs, may now enter the space of Disse and by cleared by receptors in the liver (3-6).

The IDL that remains in circulation undergoes further processing by cholesterol ester transfer protein (CETP) (in humans) and hepatic lipase (HL). HL hydrolyzes the triglycerides and phospholipids of the lipoprotein particle in the liver; humans deficient in HL have an accumulation of large, buoyant, triglyceride- and phospholipid-enriched lipoproteins (1, 94). After processing of IDL, this smaller, cholesterol-enriched particle becomes low density lipoprotein (LDL). LDL is cleared primarily through the LDL receptor (LDLR) through the binding of its primary apolipoprotein, apoB100. Animals deficient in LDLR have an accumulation of LDL cholesterol accompanied by a slight accumulation of triglycerides (28-30). High density lipoprotein (HDL) is secreted by the liver with apoAI as its primary apolipoprotein. ApoAI acts as a structural component of HDL to gather surplus cholesterol from the periphery and transport it back into the liver, a process called reverse cholesterol transport (3-6). Mouse models with decreased apoAI result in

decreased HDL; overexpression of apoAI result in an increase in HDL cholesterol (122).

1.4 Receptors involved in lipoprotein remnant clearance

Clearance of triglyceride-rich lipoproteins (TRLs), chylomicrons and VLDL remnants occurs in the liver when the particles enter the space of Disse and undergo endocytosis and degradation by hepatocytes (141). Microvilli protrude from the hepatocyte basal membrane facing the blood sinusoids and contain several types of endocytic receptors that facilitate clearance of lipoproteins, as well as plasma glycoproteins and glycans (17-19).

Three receptors have been shown to play a role in lipoprotein remnant clearance. The most well known is the LDL receptor (LDLR), which was initially described by Brown and Goldstein (20, 21). The LDLR has a primary role in the endocytosis of LDLs; in the absence of the LDLR, accumulation of these small, cholesterol-enriched particles is observed in mice, rabbits, and humans (28-30).

It had been demonstrated that LDL are internalized and degraded primarily in the liver (28-30). Remnant lipoproteins also bind the LDLR, via apoE as opposed to apoB100. While animals deficient in LDLR demonstrate an accumulation of cholesterol, only a mild accumulation of triglyceride-rich remnants was observed. Interestingly in a patient population deficient in LDLR there is no accumulation of remnant particles. This suggests that an LDLR-independent mechanism involved in the clearance of TRLs exists. A receptor was then identified based on homology to LDLR, which revealed a family of LDL receptor-related proteins (LRP) (22). LRP

was shown to recognize only apoE, and not apoB100, implying that it had the ability to take up apoE-enriched remnants. In cultured cells, LRP was shown to bind and internalize TRLs, however the absence of Lrp1 or Lrp5 *in vivo* does not result in any accumulation of remnant particles (37). This led to the hypothesis that a third class of receptors was involved in lipoprotein remnant clearance. While several receptors were suggested, the laboratories of K.J. Williams (23) and R.W Mahley (24) showed that heparan sulfate proteoglycans (HSPGs) were the third class of receptors facilitating the clearance of TRLs. Interestingly, several apolipoproteins (such as apoE, apoB) and lipases (Lpl, HL) involved in lipoprotein uptake and clearance bind heparin and heparan sulfate. This interaction could suggest a potential role for apolipoproteins and lipases as a mechanism of binding and potential uptake by HSPGs.

1.5 Hepatic HSPGs facilitate clearance of TRLs

Cell surface HSPGs have been hypothesized to work either independently or in concert with other receptors in the clearance of TRLs. In cell culture models, pharmacologic (using chlorate and xylosides), enzymatic (heparinases), or genetic alteration of heparan sulfate changes the uptake of model lipoproteins (23, 24). In most cases, the studies employed lipoproteins enriched with apoE or Lpl in order to increase their affinity for HS. In vivo evidence supporting a role for HS was derived from experiments in which heparinase was perfused through the liver resulting in a decreased clearance of ^{125}I-VLDL and chylomicron remnants and decreased binding of VLDL (142).

HSPGs have been shown to bind HL, Lpl, and apoE. Interestingly, there are several rare apoE alleles that exhibit reduced binding to HS and cause severe hyperlipoproteinemia (40-42). Mice bearing Lpl defective in HS binding fail to traffic lipids to tissues properly (166).

All of this evidence points to fact that alterations in HS, or in HS binding proteins, can affect clearance of TRLs; but is this data physiologically relevant? Recently, MacArthur *et al.* (25) showed that alteration of hepatocyte heparan sulfate *in vivo* results in an accumulation of triglyceride-rich VLDL-like particles, thus establishing that hepatocyte HS plays a critical role in clearance *in vivo*. Overall sulfation of the hepatocyte heparan sulfate was achieved by inactivating a specfic sulfotransferase, *Ndst1*. *Ndst1* encodes one of four related isozymes expressed in mice (143). Systemic inactivation of *Ndst1* causes perinatal lethality, but inactivating the gene in the liver using Cre recombinase under the control of the rat albumin promoter (*AlbCre*) did not affect the overall health or reproductive capacity of mice (144).

Analysis of plasma samples from adult mutant mice fasted overnight showed a 2.5-fold elevation of total plasma triglyceride levels, whereas total plasma cholesterol remained unchanged (Fig. 1-1). Triglycerides accumulated in VLDL-like particles (density > 1.019 g/ml) bearing apoB48, apoB100, apoE, and apoCs. Through a series of experiments, MacArthur et al. showed that the VLDL-like particles accumulated due to delayed clearance from the circulation as opposed to excess triglyceride secretion. Post-prandial studies showed a sharp delay in clearance of dietary lipid as well. Thus, hepatic HSPGs facilitate the clearance of a portion of plasma triglycerides derived either from the diet or the liver.

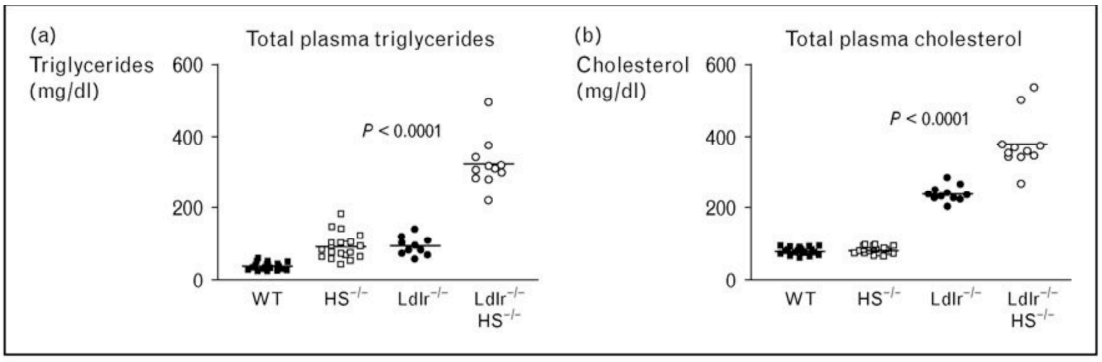


Figure 1-1. Hyperlipidemia in heparan sulfate deficient mice. Total triglycerides **(A)** and cholesterol **(B)** were measured in plasma samples from individual mice bearing the indicated mutation. Figure adapted from (25) with permission. WT, *Ldlr*$^{+/+}$*Ndst1*$^{f/f}$*AlbCre*$^{-}$; HS$^{-/-}$, *Ldlr*$^{+/+}$*Ndst1*$^{f/f}$*AlbCre*$^{+}$; Ldlr$^{-/-}$, *Ldlr*$^{-/-}$*Ndst1*$^{f/f}$*AlbCre*$^{-}$; Ldlr$^{-/-}$HS$^{-/-}$, *Ldlr*$^{-/-}$*Ndst1*$^{f/f}$*AlbCre*$^{+}$.

1.6 Relative contribution of receptors involved in TRL clearance

More profound effects on TRL clearance were observed in HS-deficient mice lacking LDLR (25). Strikingly, compound mutants exhibited a 7-fold increase in plasma triglycerides compared to wild-type animals (> 3-fold compared to LDLR-deficiency alone). Furthermore, these mice showed low binding and uptake of VLDL in vivo as well as markedly delayed clearance of post-prandial TRLs. These findings indicate that HSPGs and LDLR work in parallel to clear both hepatic and dietary TRLs from the circulation. The synergistic effect of inactivating both molecules suggests that LDLR and HSPGs in the liver can compensate for each other. Interestingly, compound mutants also exhibited a 2-fold increase in plasma cholesterol mainly found in VLDL remnants (IDL) and LDL. Thus, HSPGs could facilitate the clearance of IDL/LDL in the absence of LDLR, but this may be the result of excess remnants residing in the circulation long enough to be converted to LDLs by peripheral lipases and exchange factors.

Ndst1-deficient mice differ in phenotype from strains altered in classical lipoprotein receptors (LDLR, LRP), revealing the unique function of proteoglycans in liver-mediated clearance. LDLR deficiency leads to a large increase in levels of apoB100 bearing cholesterol-rich LDL and an increase in the level of triglyceride-rich particles (31) whereas inactivation of LRP1 in the liver (37) or systemic inactivation of LRP5 has no effect on lipoprotein clearance under normal physiological conditions (167). Compounding deficiencies in LRP1 and LDLR results in a slight increase in plasma cholesterol and triglyceride levels (37), suggesting that LRP1 can aid in the metabolism of lipoproteins, but its activity is masked by LDLR under normal conditions. In contrast, inactivation of *Ndst1* in the liver resulted in accumulation of a distinct set of lipoproteins, containing apoB100, apoB48, and apoE, and rich in triglycerides but low in cholesterol. Compound mutants lacking both *Ndst1* and *Ldlr* accumulated high levels of TRLs, as well as cholesterol-rich lipoproteins IDL and LDL. Thus, hepatocyte HS plays a central in the metabolism of all subclasses of lipoproteins, with the exception of HDL (168).

The relationship between HSPGs and LRP has remained somewhat elusive; the two receptors have been shown to interact (54), however the nature of the interaction has not been characterized. It has been hypothesized that the HSPG-LRP pathway can mediate uptake either by transfer of the remnants from the HSPG to the LRP for internalization or by binding of the remnant lipoproteins to HSPG forming a tertiary complex with the LRP that is then internalized. In this model, HSPGs are critical for the internalization via the HSPG-LRP pathway (51, 169, 170).

While this information suggests that HSPGs and LRP work together, and HSPGs and LRP both interact with HL, apoE, and apoB, there has been no genetic data to suggest that the interaction of HS with remnant lipoproteins is dependent on LRP. Additionally, while MacArthur et al (25) showed that in the absence of LDLR and HS a synergistic accumulation of triglyceride and cholesterol is observed, the relative contribution of each receptor remains unknown. The relative abundance of the LDLR, LRP, and HSPGs on the hepatocyte plasma membrane differs significantly. The number of each receptor can be estimated from binding studies, yielding values of 10^3-10^4 for LDLR in mouse hepatocytes (158, 159), ~$3.8x10^5$ for LRP in rat hepatocytes (171), and 10^5-10^6 for HSPGs (K.I.S. and J.D.E., unpublished results). The rates of internalization differ as well, with approximate $t_{1/2}$ values of ~5-10 min for LDLR (21), ~60 min for LRP (171) and 60-120 min for HSPGs (148, 153). These differences in receptor number and rates of internalization would appear to balance one another, yielding comparable capacity to take up particles. The mechanism of uptake may also differ (clathrin-coated pits for LDLR and LRP vs. a caveolin-dependent mechanism for HSPGs (23, 160)), which could affect the rate of degradation of the lipoproteins after internalization. Since degradation of particles was not measured by MacArthur et al. (25), more work is needed to determine the fate of the lipoproteins, the mechanism of endocytosis in hepatocytes, and if the HSPG dependent route is regulated in ways similar to or different from the LDLR. These questions, as well as how these receptors interact with one another, will be addressed in Chapter 4, when a mouse model genetically deficient in hepatocyte HS and LRP1,

as well as a mouse deficient in hepatocyte HS, LRP1, and systemic absence of LDLR, are presented. A potential model of this system can be seen in Figure 1-2.

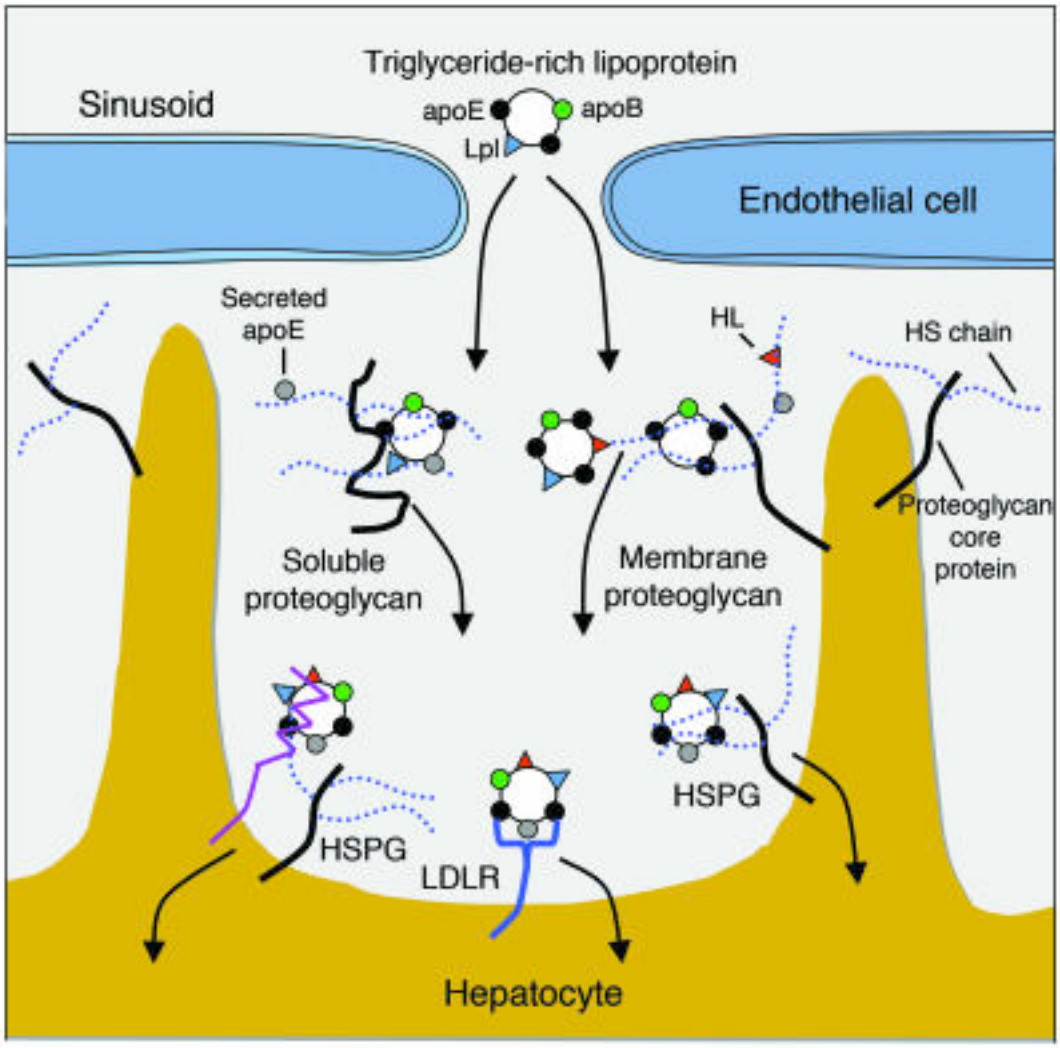


Figure 1-2. Model of possible roles for hepatic HSPGs in TRL clearance. Hepatocytes and endothelial cells produce membrane-bound HSPGs and secrete proteoglycans into the space of Disse. After lipolytic processing of lipoproteins in the circulation by Lpl (blue triangles), apoE-enriched (black circles) remnant lipoproteins enter the space of Disse through fenestrations in the endothelium. Remnant lipoproteins are thought to be sequestered near the hepatocyte cell surface via apoE-HS binding or lipase-HS bridging on secreted HSPGs. Lipoproteins are further processed in the space of Disse by transfer of soluble apoE (gray circles) and by HL (red triangles) bound via HS. apoE, HL, and Lpl can potentially serve as ligands of TRLs. Endocytosis of lipoprotein particles occurs via LDLR (blue) or LRP (purple) in association with HSPGs or independently by proteoglycans. Figure adapted from (25) with permission.

1.7 Heparan sulfate proteoglycans: structure and function

HSPGs consist of a core protein with one or more heparan sulfate glycosaminoglycan chains linked to a serine residue in the core protein. The heparan sulfate chains assemble while attached to the core protein and generally do not occur as free chains. The core proteins contain amino acid determinates that specify the number and type of glycosaminoglycan (GAG) chains, and determine whether the proteoglycan is secreted, tethered to the plasma membrane, or located in intracellular granules. They can also determine cellular function, as endocytic receptors, co-receptors for signaling, or cell adhesion components. Membrane-associated HSPGs include syndecans 1-4, glypicans 1-6 (glycosylphosphatidylinositol anchored), CD44v3, and betaglycan. The extracellular matrix proteoglycans consist of agrin, collagen XVIII, and perlecan. Haematopoietic cells also contain a secretory vesicle proteoglycan, serglycin. The HSPGs on the cell surface (membrane-bound) can be shed by proteolytic cleavage of the core protein, and processed by endoglycosidic cleavage of the HS chains by extracellular heparanase. HSPGs contain one or more GAG chains; some HSPGs may also contain chondroitin sulfate/dermatan sulfate (CS/DS), a GAG chain that differs from heparan sulfate (HS) in its sugar components – the former containing *N*- acetylgalactosamine (GalNAc) and glucuronic (GlcA)/ Iduronic (IdoA) residues; the latter containing *N*-acetylglucosamine (GlcNAc) and GlcA/IdoA residues. This thesis will concentrate primarily on HSPGs (8).

Synthesis of the side chain begins with the assembly of a tetrasaccharide linker glucuronic acid, β1,3-galactose, β1,3-galactose, and β1,4-xylose region attached to a specific serine residue in the core protein of the proteoglycan, (Figure 1-3). The

assembly and subsequent processing of the HS chain depends on an array of enzymes. The glycosyltransferases exostosin 1 and 2 (Ext1 and Ext2) assemble HS as a polymer of alternating *N*-acetyl-D-glucosamine (GlcNAc) and D-glucuronic acid (GlcA) units. A family of four GlcNAc *N*-deacetylase/*N*-sulfotransferases (Ndst) replace glucosamine *N*-acetyl groups with *N*-sulfates. A C5-epimerase then changes adjacent GlcA to L-iduronic acids (IdoA), which can be sulfated at C2 by a 2-*O*-sulfotransferase (Hs2st). Near the end of the modification process are 6-*O*-sulfotransferases (Hs6st) and 3-*O*-sulfotransferases (Hs3st) which add sulfate groups to the C6 or C3 of glucosamine units, respectively. Processing may also occur by plasma-membrane bound endosulfatases (Sulf1 and Sulf2) which remove specific 6-*O*-sulfate groups from the chains (10, 11). Heparan sulfate biosynthesis has been extensively reviewed (7, 12) and is depicted in Figure 1-3.

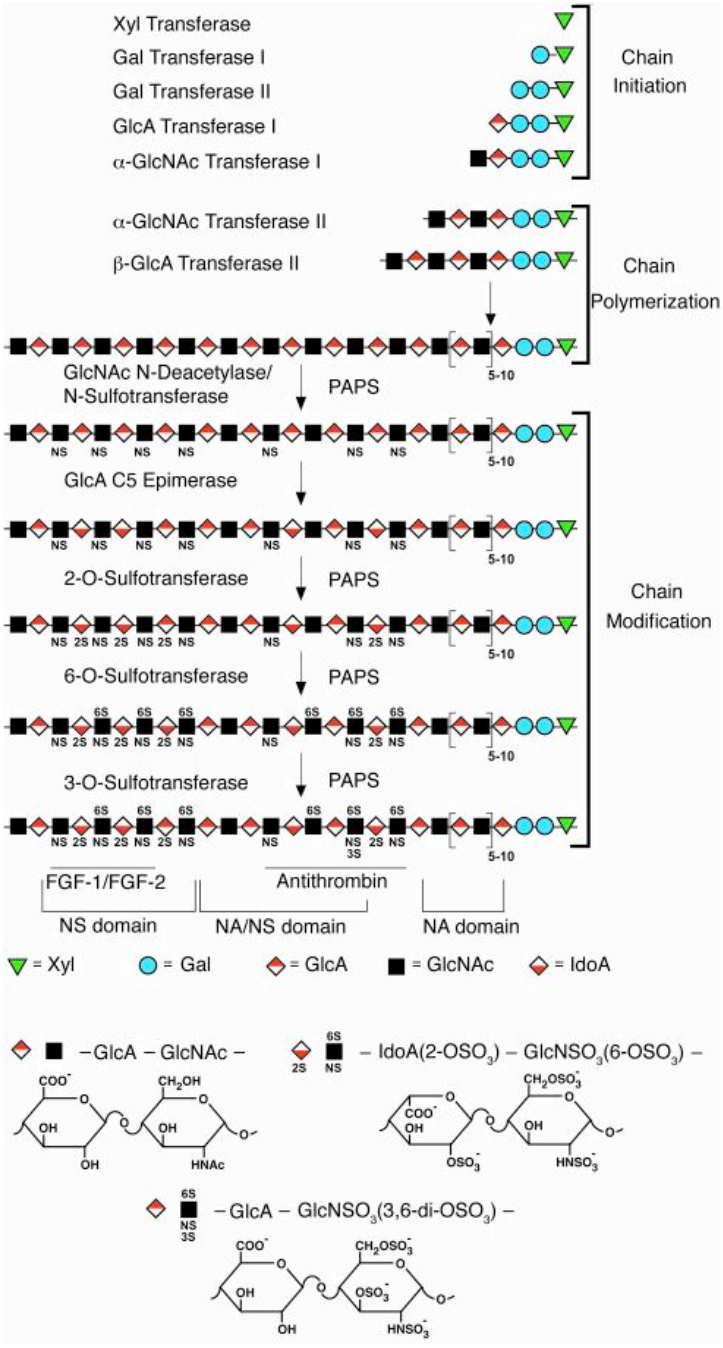


Figure 1-3. Scheme of HS chain biosynthesis. The symbols used are defined by the structures shown below the scheme. Structural domains (NA, NA/NS, NS) are defined with regard to the distribution of GlcN N-substituents as indicated. Also shown are regions that have been implicated in binding of specific ligands, such as FGF-1/FGF-2 and antithrombin. Reprinted with permission (12).

The types of HSPGs, as well as the extent and degree of sulfation of the heparan sulfate chains, vary among tissues, suggesting cell type specific control of proteoglycan biosynthesis. Different cell types have the ability to regulate expression of these biosynthetic enzymes, thus producing heparan sulfate chains of variable length and fine structure. Thus, the heparan sulfate on a hepatocyte is not the same molecule as the heparan sulfate found on an endothelial cells, even though the chains may be attached to the same core protein. Hepatocyte heparan sulfate is more highly sulfated than HS found in other cell types, and is about 14-25 kDa which translates into an average chain composed of 50-100 monosaccharides (45). This may explain the ability of hepatocyte heparan sulfate to bind lipoproteins and facilitate clearance with greater affinity than HS produced in other cells (6).

1.8 How does HS structure affect lipoprotein metabolism?

Previous work by MacArthur et al., as well as from the labs of Mahley and Williams, examined how overall reduction of sulfation of the heparan sulfate chain, or partial removal of HS (23-25) affected clearance. Since these methods do not result in complete loss of HS, the contribution of HS to TRL clearance may be underestimated. More profound alteration of HS structure, e.g., by mutation of the copolymerase (Ext1 and Ext2), C5 epimerase, or other sulfotransferases (Hs2st, Hs6st, or Hs3st), might lead to greater effects. Furthermore, this approach could help sort out the various roles of apoE, Lpl, and HL in clearance if differences in binding to HS with respect to *N*-, 2-*O*, 6-*O*-sulfation and epimerization exist. In Chapter 2, the structural significance of 2-*O*-sulfation with respect to lipoprotein clearance will be addressed.

2-*O*-sulfated iduronic acid is required for the binding of HS to many members of the fibroblast growth factor (FGF) family and is essential for the initiation of FGF-mediated signal transduction pathways. Additionally, the preferred binding site for apoE to HS; contains IdoA2S, establishing that 2-*O*-sulfation is required for the binding of apoE to HS. Chapter 2 presents data showing that in the absence of hepatocyte 2-*O*-sulfation causes accumulation of triglycerides is observed, implying that a specific structural alteration in hepatocyte heparan sulfate may be enough to cause a defect in clearance of TRLs.

1.9 Which proteoglycans are relevant to TRL clearance?

MacArthur et al. clearly established that a decrease in overall sulfation of hepatocyte HS caused a reduction in binding and uptake of VLDL particles. However, the identity of the PG mediating clearance has not been established. Transmembrane HSPGs, like syndecan, contain a short cytoplasmic domain that interacts with adapter proteins involved in cytoskeletal organization , endocytosis, and signaling (57). These proteoglycans are internalized and delivered to lysosomes by an endosomal route, and ligands bound to the chains can be delivered to the interior of the cell in this way, but the precise route followed by the ligand and the proteoglycan has not been worked out. Evidence suggests that membrane HSPGs turn over constitutively (153), but can be induced to internalize by binding of ligands (148). Some evidence suggests that they can be recycled as well (154-156).

There are several HSPGs expressed in hepatocytes; syndecans-1, -2, and -4, glypican-4, agrin, and collagen XVIII (25). Syndecan-1 emerged as a primary

candidate for TRL clearance as several reports suggest that, as a cell surface HSPG, syndecan-1 can facilitate the uptake of lipoproteins in cultured cells (55, 148). In a recent paper by Wilsie, fibroblasts lacking LDLR with fully functional LRP were unable to bind and internalize ^{125}I-VLDL particles, but transfection with syndecan-1 cDNA conferred uptake (149). Syndecan-1 can also mediate binding and uptake of chylomciron remnants by HepG2 liver cells *in vitro* based on antisense and antibody inhibition experiments (55). The evidence pointing to specific hepatic proteoglycans mediating TRL clearance *in vivo* is more indirect. Yu et al. found that chylomicron remnants labeled with a fluorescent dye cocluster with syndecan-1 on hepatocytes in the space of Disse (150), consistent with cell culture data indicating that clustering of syndecan may facilitate its internalization by endocytosis (148, 151). However, overexpression of hepatic syndecan-1 by infection with an adenoviral construct actually induced hyperlipidemia (152). In Chapter 3, we examined available mutants in membrane HSPGs and found that mice deficient in syndecan-1 (*Sdc1*$^{-/-}$) had elevated plasma triglycerides under fasting conditions and exhibited delayed hepatic clearance of dietary triglycerides and injected VLDL. Reconstitution of syndecan-1 expression in hepatocytes *in vivo* restored normal triglyceride metabolism. The absence of syndecan-1 in hepatocytes also caused a decrease in the binding, uptake, and degradation of VLDL particles in isolated primary hepatocytes. These findings show that syndecan-1 is the hepatic HSPG receptor involved in TRL clearance.

Upon examination of the various proteoglycans, it was also determined that mice deficient in the basement membrane proteoglycan Collagen XVIII accumulate triglycerides. This phenotype, however, appeared to be result of an inability to present

Lpl on the endothelial cell surface and thus results in hyperchylomicronemia. This finding is independent of the hepatocyte defect found in mice deficient in hepatocyte-deficient HS, and will be discussed in appendix A.

1.10 Conclusions and Future Directions

Studies over the last year, coupled with a large body of evidence derived from earlier in vitro studies demonstrate that HSPGs function at multiple levels in the metabolism of TRLs. In the periphery, HSPGs work with Lpl and apoA-V to facilitate hydrolysis of TRLs as they circulate. In the liver, highly sulfated HS produced by hepatocytes facilitates clearance of TRLs from the circulation, working in concert with but independently of LDLR. Furthermore, HSPGs aid in the clearance of cholesterol-rich particles that accumulate in the absence of LDL receptors. To fully understand the role of hepatocyte HSPGs in the clearance of lipoproteins from circulation much work remains to be done. More information is needed on the structure of the binding site in HS, the identity of the relevant protein ligands on TRLs, and the identity of the relevant HSPGs. It is the goal of this thesis to address these questions and clearly establish the role for HSPGs in lipoprotein remnant clearance.

1.11 References

1. **Citkowitz E, Gambert SR, Talavera F, Shenker Y, Cooper M, and Griffing GT. 2005. Hypertriglyceridemia (www.emedicine.com/med/topic2921.htm).**

2. **Witztum JL. 1996. Drugs used in the treatment of hyperlipoproteinemias. In Goodman and Gilman's The Pharmacological Basis of Therapeutics, JG Hardman, LE Limbird, PB Molinoff, RW Ruddon, and AG Gilman, eds. (New York: McGraw-Hill), pp. 875-897**

3. **Davis RA, and Vance JE. 1996. Structure, assembly, and secretion of liporptoeins. In Biochemistry of Lipids, Lipoproteins, and Membranes, DE Vance, and JE Vance, eds. (New York: Elsevier), pp. 473-493.**

4. **Havel RJ, and Kane JP. (2001). Structure and metabolism of plasma lipoproteins. In The Metabolic and Molecular Bases of Inherited Disease, CR Scriver, VS Sly, B Childs, AL Beaudet, D Valle, KW Kinzler, and B Vogelstein, eds. (New York: McGraw-Hill), pp. 2705-2716.**

5. **Schneider WJ (1996). Removal of lipoproteins from plasma. In Biochemistry of Lipids, Lipoproteins, and Membranes, DE Vance, and JE Vance, eds. (New York: Elsevier), pp 517-541.**

6. **Bernfield M, Gotte M, Park PW, Reizes O, Fitzgerald ML, Lincecum J, and Zako M. 1999. Functions of cell surface heparan sulfate proteoglycans. *Annu Rev Biochem* 68, 729-777.**

7. **Conrad HE. 1998. Heparin-Binding Proteins (San Diego: Academic Press).**

8. **Bishop JR, Schuksz M, and Esko JD. 2007. Heparan sulfate proteoglycans fine-tune mammalian physiology. *Nature* 446: 1030-36.**

9. **Fielding PE, and Fielding CJ. 1996. Intracellular transport of low density lipoprotein derived free cholesterol begins at clathrin-coated pits and terminates at cell surface caveolae. *Biochemistry* 35(47): 14932-8.**

10. **Dhoot GK, Gustafsson MK, Ai X, Sun W, Standiford DM, and Emerson CP Jr. 2001. Regulation of Wnt signalin and embryo patterning by an extracellular sulfatase. *Science* 293(5535): 1663-6.**

11. Morimoto-Tomita M, Uchimura K, Werb Z, Hemmerich S, and Rosen SD. 2002. Cloning and characterization of two extracellular heparin-degrading endosulfatases in mice and humans. *J Biol Chem* 277(51): 49175-85.

12. Esko JD, and Lindahl U. 2001. Molecular diversity of heparan sulfate. *J Clin Invest* 108: 169-173.

13. Alexopoulou AN, Multhaupt HA, and Couchman JR. 2001. Syndecans in wound healing, inflammation, and vascular biology. *Int J Biochem Cell Biol* 39: 505-528.

14. Couchman JR, Chen LG, and Woods A. 2001. Syndecans and cell adhesion. *Int Rev Cytol* 207: 113-150.

15. Kirkpatrick CA, Knox SM, Staatz WD, Fox B, Lercher DM, and Selleck SB. 2006. The function of a *Drosophila* glypican does not depend entirely on heparan sulfate modification. *Dev Biol* 300: 570-582.

16. Cooper AD. 1997. Hepatic uptake of chylomicron remnants. *J Lipid Res* 38: 2173-2192.

17. Weiss P, and Ashwell G. 1989. Ligand-induced modulation of the hepatic receptor of asialoglycoproteins. Evidence for the role of cell surface hyposialytion. *J Biol Chem* 264(20): 11572-4.

18. Woodworth A, and Baenziger JU. 2001. The man/GalNAc-4-SO4-receptor has multiple specificities and functions. *Results Probl Cell Differ* 33:123-38.

19. Weigel PH, and Yik JH. 2002. Glycans as endocytosis signals: the cases of the asialoglycoprotein and hyaluronan/chondroitin sulfate receptors. *Biochim Biophys Acta* 1572(2-3): 341-63.

20. Brown MS, Kovanen PT, and Goldstein JL. 1981. Regulation of plasma cholesterol by lipoprotein receptors. *Science* 212(4495): 628-35.

21. Brown MS, and Goldstein JL. 1986. A receptor-mediated pathway for cholesterol homeostasis. *Science* 232(4746): 34-47.

22. Herz J, Hamann U, Rogne S, Myklebost O, Gausepohl H, and Stanley KK. 1988. Surface location and high affinity for calcium of a 500-kd

liver membrane protein closely related to the LDL-receptor suggest a physiological role as lipoprotein receptor. ***EMBO J*** **7(13): 4119-27.**

23. Williams KJ, and Fuki IV. 1997. Cell-surface heparan sulfate proteoglycans: dynamic molecules mediating ligand catabolism. ***Curr Opin Lipidol*** **8(5): 253-62.**

24. Mahley RW, Ji ZS. 1999. Remnant lipoprotein metabolism: key pathways involving cell-surface heparan sulfate proteoglycans and apolipoprotein E. ***J Lipid Res*** **40(1): 1-16.**

25. MacArthur, J.M., Bishop, J.R., Wang, L., Stanford, K.I., Bensadoun, A., Witztum, J.L., and Esko, J.D. 2007. Liver heparan sulfate proteoglycans mediate clearance of triglyceride-rich lipoproteins independently of LDL receptor family members. ***J Clin Invest*** **117:153-164.**

26. Plump AS, Smith JD, Hayek T, Aalto-Setala K, Walsh A, Verstuyft JG, Rubin EM, and Breslow JL. 1992. Severe hypercholesterolemia and atherosclerosis in apolipoprotein E-deficient mice created by homologous recombination in ES cells. ***Cell*** **71(2): 343-53.**

27. Zhang SH, Reddick RL, Piedrahita JA, and Maeda N. 1992. Spontaneous hypercholesterolemia and arterial lesions in mice lacking apolipoprotein E. ***Science*** **258(5081): 468-71.**

28. Ishibashi S, Goldstein JL, Brown MS, Herz J, and Burns DK. 1994. Massive xanthomatosis and atherosclerosis in cholesterol-fed low density receptor-negative mice. ***J Clin Invest*** **93(5): 1885-93.**

29. Herz J, Qiu SQ, Oesterle A, DeSilva HV, Shafi S, and Havel RJ. 1995. Initial hepatic removal of chylomicron remnants is unaffected but endocytosis is delayed in mice lacking the low density lipoprotein receptor. ***Proc Natl Acad Sci*** **92(10): 4611-15.**

30. Mortimer BC, Beveridge DJ, Martins IJ, and Redgrave TG. 1995. Intracellular localization and metabolism of chylomicron remnants in the livers of low density lipoprotein receptor-deficient mice and apoE-deficient mice. Evidence for slow metabolism via an alternative apoE-dependent pathway. ***J Biol Chem*** **270(48): 28767-76.**

31. Ishibashi S, Herz J, Maeda N, Goldstein JL, and Brown MS. 1994. The two-receptor model of lipoprotein clearance: tests of the hypothesis in "knockout" mice lacking the low density lipoprotein receptor, apolipoprotein E, or both proteins. ***Proc Natl Acad Sci*** **91(10): 4431-5.**

32. Ishibashi S, Perrey S, Chen Z, Osuga J, Shimada M, Ohashi K, Harada K, Yazaki Y, and Yamada N. 1996. Role of the low density lipoprotein (LDL) receptor pathway in the metabolism of chylomicron remnants. A quantitative study in knockout mice lacking the LDL receptor, apolipoprotein E, or both. ***J Biol Chem*** **271(37): 22322-7.**

33. Hussain MM, Maxfield FR, Mas-Oliva J, Tabas I, Ji ZS, Innerartiy TL, and Mahley RW. 1991. Clearance of chylomicron remnants by the low density lipoprotein receptor-related protein/alpha 2-macroglobulin receptor. ***J Biol Chem*** **266(21): 13936-40.**

34. Mokuno H, Brady S, Kotite L, Herz J, and Havel RJ. 1994. Effect of the 39-kDa receptor-associated protein on the hepatic uptake and endocytosis of chylomicron remnants and low density lipoproteins in the rat. ***J Biol Chem*** **269(18): 13238-43.**

35. Willnow TE, Sheng Z, Ishibashi S, and Herz J. 1994. Inhibition of hepatic chylomicron remnant uptake by gene transfer of a receptor antagonist. ***Science*** **263(5164): 1471-4.**

36. Willnow TE, Armstrong SA, Hammer RE, and Herz J. 1995. Functional expression of low density lipoprotein receptor-related protein is controlled by receptor-associated protein ***in vivo*****.** ***Proc Natl Acad Sci*** **92(10): 4537-41.**

37. Rohlmann A, Gotthardt M, Hammer RE, and Herz J. 1998. Inducible inactivation of hepatic LRP gene by cre-mediated recombination confirms role of LRP in clearance of chylomicron remnants. ***J Clin Invest*** **101(3): 689-95.**

38. Veniant MM, Ziot CH, Walzem RL, Pierotti V, Driscoll R, Dichek D, Herz J, and Young SG. 1998. Lipoprotein clearance mechanisms in LDL receptor-deficient "Apo-B48-only" and "Apo-B100-only" mice. ***J Clin Invest*** **102(8): 1559-68.**

39. Mahley RW, and Rall SC Jr. 2001. Type III hyperlipoproteinemia (dysbetalipoproteinemia): to role of apolipoprotein E in normal and abnormal lipoprotein metabolism. In The Metabolic and Molecular Bases of Inherited Disease, CR Scriver, WS Sly, B Childs, AL Beaudet, D Valle, KW Kinzler, and B Vogelstein, eds. (New York: McGraw-Hill) pp. 2835-2862.

40. Ji ZS, Fazio S, and Mahley RW. 1994. Variable heparan sulfate proteoglycan binding of apolipoprotein E variants may modulate the expression of type III hyperlipoproteinemia. *J Biol Chem* 269: 13421-28.

41. Mann WA, Lohses P, Gregg RE, Ronan R, Hoeg JM, Zech LA, and Brewer HB Jr. 1995. Dominant expression of type III hyperlipoproteinemia. Pathophysiological insights derived from the structural and kinetic characteristics of ApoE-1 (Lys146->Glu). *J Clin Invest* 96: 1100-1107.

42. Mann WA, Meyer N, Wever W, Meyer S, Greten H, and Beisiegel U. 1995. Apolipoprotein E isoforms and rare mutations: parallel reduction in binding to cells and to heparin reflects severity of associated type III hyperlipoproteinemia. *J Lipid Res* 36: 517-525.

43. Libeu CP, Lund-Katz S, Phillips MC, Wehrli S, Hernaiz MJ, Capila I, Linhardt RJ, Raffai RL, Newhouse YM, Zhou F, and Weisgraber KH. 2001. New insights into the heparan sulfate proteoglycan-binding activity of apolipoprotein E. *J Biol Chem* 276: 39138-44.

44. Dong J, Peters-Libeu CA, Weisgraber KH, Segelke BW, Rupp B, Capila I, Hernaiz MJ, LeBrun LA, and Linhardt RJ. 2001. Interaction of the N-terminal domain of apolipoprotein E4 with heparin. *Biochemistry* 40: 2826-34.

45. Lyon M, Deakin JA, and Gallagher JT. 1994. Liver heparan sulfate structure. A novel molecular design. *J Biol Chem* 269: 11208-15.

46. Willnow TE. 1997. Mechanisms of hepatic chylomicron remnant clearance. *Diabet Med* 14 Suppl 3:S75-80.

47. Yu KC, Jiang Y, Chen W, and Cooper AD. 1999. Evaluation of the components of the chylomicron remnant removal mechanism by use of the isolated perfused mouse liver. *J Lipid Res* 40: 1899-1910.

48. **Ji ZS, Sanan DA, and Mahley RW. 1995. Intravenous heparinase inhibits remnant lipoprotein clearance from the plasma and uptake by the liver: in vivo role of heparan sulfate proteoglycans. *J Lipid Res* 36: 583-92**

49. **Windler E, Greeve J, Robenek H, Rinninger F, Greten H, and Jackle S. 1996. Differences in the mechanisms of uptake and endocytosis of small and large chylomicron remnants by rat liver. *Hepatology* 24: 344-51**

50. **Al-Haideri M, Goldberg IJ, Galeano NF, Gleeson A, Vogel T, Gorecki M, Sturley SL, and Deckelbaum RJ. 1997. Heparan sulfate proteoglycan-mediated uptake of apolipoprotein E-triglyceride-rich lipoprotein particles: a major pathway at physiological particle. *Biochemistry* 36: 12766-72.**

51. **Ji ZS, Brecht WJ, Miranda RD, Hussain MM, Innerarity TL, and Mahley RW. 1993. Role of heparan sulfate proteoglycans in the binding and uptake of apolipoprotein E-enriched remnant lipoproteins by cultured cells. *J Biol Chem* 268: 10160-67.**

52. **Ji ZA, Fazio S, Lee YL, and Mahley RW. 1994. Secretion-capture role for apolipoprotein E in remnant lipoprotein metabolism involving cell surface heparan sulfate proteoglycans. *J Biol Chem* 269: 2764-72.**

53. **Ji ZS, Pitas RE, and Mahley RW. 1998. Differential cellular accumulation/retention of apolipoprotein E mediated by cell surface heparan sulfate proteoglycans. Apolipoproteins E3 and E2 greater than E4. *J Biol Chem* 273: 13452-60.**

54. **Wilsie LC, and Orlando RA. 2003. The low density lipoprotein receptor-related protein complexes with cell surface heparan sulfate proteoglycans to regulate proteoglycan-mediated lipoprotein catabolism. *J Biol Chem* 278: 15758-64.**

55. **Zeng BJ, Mortimer BC, Martins IJ, Seydel U, and Redgrave TG. 1998. Chylomicron remnant uptake is regulated by the expression and function of heparan sulfate proteoglycan in hepatocytes. *J Lipid Res* 39: 845-60.**

56. Goldberg IJ, Wagner WD, Pang L, Paka L, Curtiss LK, DeLozier JA, Shelness GS, young CS, and Pillarisetti S. 1998. The NH2-terminal region of apolipoprotein B is sufficient for lipoprotein association with glycosaminoglycans. *J Biol Chem* 273: 35355-61.

57. Boren J, Lee I, Zhu W, Arnold K, Taylor S, and Innerarity TL. 1998. Identification of the low density lipoprotein receptor-binding site in apolipoprotein B100 and the modulation of its binding activity by the carboxyl terminus in familial defective apo-B100. *J Clin Invest* 101(5): 1084-93.

58. Flood C, Gustafsson M, Richardson PE, Harvey SC, Segrest JP, and Boren J. 2002. Identification of the proteoglycan binding site in apolipoprotein B48. *J Biol Chem* 277: 32228-33.

59. Olsson U, Ostergren-Lunden G, and Moses J. 2001. Glycosaminoglycan-lipoprotein interaction. *Glycoconj J* 18: 789-97.

60. O'Brien PJ, Alborn WE, Sloan JH, Ulmer M, Boodhoo A, Knierman MD, Schultze AE, and Konrad RJ. 2005. The novel apolipoprotein A5 is present in human serum, is associated with VLDL, HDL, and chylomicrons, and circulates at very low concentrations compared with other apolipoproteins. *Clin Chem* 51(2): 351-9.

61. Grosskopf I, Baroukh N, Lee SJ, Kamari Y, Harats D, Rubin EM, Pennacchio LA, and Cooper AD. 2005. Apolipoprotein A-V deficiency results in marked hypertriglyceridemia attributable to decreased lipolysis of triglyceride-rich lipoproteins and removal of their remnants. *Arterioscler Thromb Vasc Biol* 25(12): 2573-9.

62. Nilsson SK, Lookene A, Beckstead JA, Gliemann J, Ryan RO, and Olivercrona G. 2007. Apolipoprotein A-V interaction with members of the low density lipoprotein receptor gene family. *Biochemistry* 46(12): 3896-904.

63. Lookene A, Beckstead JA, Nilsson S, Olivercrona G, and Ryan RO. 2005. Apolipoprotein A-V-heparin interactions: implications for plasma lipoprotein metabolism. *J Biol Chem* 280(27): 25383-7.

64. Merkel M, Loeffler B, Kluger M, Fabig N, Geppert G, Pennacchio LA, Laatsch A, and Heeren J. 2005. Apolipoprotein AV accelerates

plasma hydrolysis of triglyceride-rich lipoproteins by interaction with proteoglycan-bound lipoprotein lipase. *J Biol Chem* 280(22): 21553-60.

65. Fruchart-Najib J, Bauge E, Niculescu LS, Pham T, Thomas B, Rommens C, Majd , Brewer B, Pennacchio LA, and Fruchart JC. 2004. Mechanism of triglyceride lowering in mice expressing human apolipoprotein A5. *Biochem Biophys Res Commun* 319(2): 397-404.

66. Schaap FG, Rensen PC, Voshol PH, Vrins C, van der Vliet HN, Chamuleau RA, Havekes LM, Groen AK, van Dijk KW. 2004. ApoAV reduces plasma triglycerides by inhibiting very low density lipoprotein-triglyceride (VLDL-TG) production and stimulating lipoprotein lipase-mediated VLDL-TG hydrolysis. *J Biol Chem* 279(27): 27941-7.

67. Sun G, Bi N, Li G, Zhu X, Zeng W, Wu G, Xue H, and Chen B. 2006. Identification of lipid binding and lipoprotein lipase activation domains of human apoAV. *Chem Phys Lipids* 143(1-2): 22-8.

68. Windler E, Chao Y, and Havel RJ. 1980. Regulation of the hepatic uptake of triglyceride-rich lipoproteins in the rat. Opposing effects of homologous apolipoprotein E and individual C apoproteins. *J Bio Chem*. 255(17): 8303-7.

69. Aalto-Setala K, Fisher EA, Chen X, Chajek-Shaul T, Hayek T, Zechner R, Walsh A, Ramakrishnan R, Ginsberg HN, and Breslow JL. 1992. Mechanism of hypertriglyceridemia in human apolipoprotein (apo) CIII transgenic mice Diminished very low density lipoprotein fractional catabolic rate associated with increased apo CIII and reduced apo E on the particles. *J Clin Invest* 90(5): 1889-900.

70. Shachter NS, Hayek T, Leff T, Smith JD, Rosenberg DW, Walsh A, Ramakrishnan R, Goldberg IJ, Ginsberg HN, and Breslow JL. 1994. Overexpression of apolipoprotein CII causes hypertriglyceridemia in transgenic mice. *J Clin Invest* 93(4): 1683-90.

71. Shachter NS, Ebara T, Ramakrishnan R, Steiner G, Breslow JL, Ginsberg HN, and Smith JD. 1996. Combined hyperlipidemia in transgenic mice overexpressing human apolipoprotein CI. *J Clin Invest* 98(3): 846-55.

72. Parthasarathy S, Morales AJ, and Murphy AA. 1994. Antioxidant: a new role for RU-486 and related compounds. *J Clin Invest* 94(5): 1990-5.

73. Spillmann D, Lookene A, and Olivercrona G. 2006. Isolation and characterization of low sulfated heparan sulfate sequences with affinity for lipoprotein lipase. *J Biol Chem* 281(33): 23405-13.

74. Anfinsen CB, Boyle E, and Brown RK. 1952. The role of Heparin in Lipoprotein Metabolism. *Science* 115(2996): 583-586.

75. Beigneux AP, Davies BS, Gin P, Weinstein MM, Farber E, Qiao X, Peale F, Bunting S, Walzem RL, Wong JS, Blaner WS, Ding ZM, Melford K, Wongsiriroj N, Shu X, de Sauvage F, Ryan RO, Fong LG, Bensadoun A, and Young SG. 2007. Glycosylphosphatidylinositol-anchored high-density lipoprotein 1 plays a critical role in the lipolytic processing of chylomicrons. *Cell Metab* 5(4): 279-91.

76. Young SG, Davies BS, Fong LG, Gin P, Weinstein MM, Bensadoun A, and Beigneux AP. 2007. GPIHBP1: an endolthelial cell molecule important for the lipolytic processing of chylomicrons. *Curr Opin Lipidol* 18(4): 389-96.

77. Wallinder L, Peterson J, Olivercrona T, and Bengtsson-Olivercrona G. 1984. Hepatic and extrahepatic uptake of intravenously injected lipoprotein lipase. *Biochim Biophys Acta* 795(3): 513-24.

78. Olivercrona T. 1962. Plasma and liver lipids of ethionine-treated rats. *Acta Physiol Scand* 55:291-302.

79. Brunzell JD and Deeb SS. 2001. Familial lipoprotein lipase deficiency, apoC-II deficiency, and hepatic lipase deficiency. In The Metabolic and Molecular Bases of Inherited Disease, CR Scriver, WS Sly, B Childs, AL Beaudet, D Valle KW Kinzler, and B Vogelstein, eds. (New York: McGraw-Hill) pp. 2789-2816.

80. Beisiegel U, and Heeren J. 1997. Lipoprotein lipase (EC 3.1.1.34) targeting of lipoproteins to receptors. *Proc Nutr Soc* 56(2): 731-7.

81. Beisiegel U, Weber W, and Bengtsson-Olivercrona G. 1991. Lipoprotein lipase enhances the binding of chylomicrons to low density lipoprotein receptor-related protein. *Proc Natl Acad Sci* 88(19): 8342-6.

82. Eisenberg S, Sehayek E, Olivercrona T, and Vlodavsky I. 1992. Lipoprotein lipase enhances binding of lipoproteins to heparan sulfate on cell surfaces and extracellular matrix. *J Clin Invest* 90(5): 2013-21.

83. Mulder M, Lombardi P, Jansen H, van Berkel TJ, Frants RR, and Havekes LM. 1993. Low density lipoprotein receptor internalizes low density and very low density lipoproteins that are bound to heparan sulfate proteoglycans via lipoprotein lipase. *J Biol Chem* 268(13): 9369-75.

84. Mannn WA, Meyer N, Weber W, Rinninger F, Greten H, and Beisiegel U. 1995. Apolipoprotein E and lipoprotein lipase co-ordinately enhance binding and uptake of chylomicrons by human hepatocytes. *Eur J Clin Invest* 25: 880-2.

85. Mann WA, Meyer N, Berg D, Greten H, and Beisiegel U. 1999. Lipoprotein lipase compensates for the defective function of apoE variants in vitro by interacting with proteoglycans and lipoprotein receptors. *Atherosclerosis* 145: 61-69.

86. Huff MW, Miller DB, Wolfe BM, Connelly PW, and Sawyez CG. 1997. Uptake of hypertriglyceridemic very low density lipoproteins and their remnants by HepG2 cells: the role of lipoprotein lipase, hepatic triglyceride lipase, and cell surface proteoglycans. *J Lipid Res* 38(7): 1318-33.

87. Krapp A, Zhang H, Ginzinger D, Liu MS, Lindberg A, Olivercrona G, Hayden MR, and Beisiegel U. 1995. Structural features in lipoprotein lipase necessary for the mediation of lipoprotein uptake into cells. *J Lipid Res* 36(11): 2362-73.

88. Williams KJ, Fless GM, Petrie KA, Snyder ML, Brocia RW, and Swenson TL. 1992. Mechanisms by which lipoprotein lipase alters cellular metabolism of lipoprotein(a), low density lipoprotein, and nascent lipoproteins. Roles for low density lipoprotein receptors and heparan sulfate proteoglycans. *J Biol Chem* 267(19): 13284-92.

89. Chang S, Maeda N, and Borensztajn J. 1996. The role of lipoprotein lipase and apoprotein E in the recognition of chylomicrons and chylomicron remnants by cultured isolated mouse hepatocytes. *Biochem J* 318(Pt 1): 29-34.

90. Merkel M, Kako Y, Radner H, Cho IS, ramasamy R, Brunzell JD, Goldberg IJ, and Breslow JL. 1998. Catalytically inactive lipoprotein lipase expression in muscle of transgenic mice increases very low density lipoprotein uptake: direct evidence that lipoprotein lipase bridging occurs in vivo. *Proc Natl Acad Sci* 95(23): 13841-6.

91. Merkel M, Eckel RH, and Goldberg IJ. 2002. Lipoprotein lipase: genetics, lipid uptake, and regulation. *J Lipid Res* 43(12): 1997-2006.

92. Fernandez-Borja M, Bellido D, Vilella E, Olivercrona G, and Vilaro S. 1996. Lipoprotein lipase-mediated uptake of lipoprotein in human fibroblasts: evidence for an LDL receptor-independent internalization pathway. *J Lipid Res* 37(3): 464-81.

93. Skottova N, Savonen R, Lookene A, Hultin M, and Olivercrona G. 1995. Lipoprotein lipase enhances removal of chylomicrons and chylomicron remnants by the perfused rat liver. *J Lipid Res* 36(6): 1334-44.

94. Deeb SS, Zambon A, Carr MC, Ayyobi AF, and Brunzell JD. 2003. Hepatic lipase and dyslipidemia: Interactions among genetic variants, obesity, gender, and diet. *J Lipid Res* 44(7): 1279-86.

95. Heeren J, Niemeier A, Merkel M, and Beisiegel U. 2002. Endothelial-derived lipoprotein lipase is bound to postprandial triglyceride-rich lipoproteins and mediates their hepatic clearance in vivo. *J Mol Med* 80(9): 576-84.

96. De Faria E, Fong LG, Komaromy M, Cooper AD. 1996. Relative roles of the LDL receptor, LDL receptor-like protein, and hepatic lipase in chylomicron remnant removal by the liver. *J Lipid Res* 37(1): 197-209.

97. Diard P, Malewiak MI, Lagrange D, and Griglio S. 1994. Hepatic lipase may act as a ligand in the uptake of artificial chylomicron remnant-like particles by isolated rat hepatocytes. *Biochem J* 299(Pt 3): 889-94.

98. Dichek HL, Brecht W, Fan J, Ji ZS, McCormick SP, Akeefe H, Conzo L, Sanan DA, Weisgraber KH, Young SG, Taylor JM, and Mahley RW. 1998. Overexpression of hepatic lipase in transgenic mice decreases apolipoprotein B-containing and high density lipoproteins. Evidence that hepatic lipase acts as a ligand for lipoprotein uptake. *J Biol Chem* 273(4): 1896-903.

99. Dichek HL, Johnson SM, Akeefe H, Lo GT, Sage E, Yap CE, and Mahley RW. 2001. Hepatic lipase overexpression lowers remnant and LDL levels by a noncatalytic mechanism in LDL receptor-deficient mice. *J Lipid Res* 42: 201-210.

100. Ji ZS, Lauer SJ, Fazio S, Bensadoun A, Taylor JM, and Mahley RW. 1994. Enhanced binding and uptake of remnant lipoproteins by

hepatic lipase-secreting hepatoma cells in culture. *J Biol Chem* 269: 13429-36.

101. Krapp A, Ahle S, Kersting S, Hua Y, Kneser K, Nielsen M, Gliemann J, and Beisiegel U. 1996. Hepatic lipase mediates the uptake of chylomicrons and beta-VLDL into cells via the LDL receptor-related protein (LRP). *J Lipid Res* 37(5): 926-36.

102. Lee SJ, Kadambi S, Yu KC, David C, Azhar S, Cooper AD, and Choi SY. 2005. Removal of chylomicron remnants in transgenic mice overexpressing normal and membrane-anchored hepatic lipase. *J Lipid Res* 46(1): 27-35.

103. Daggy BP, and Bensadoun A. 1986. Enrichment of apolipoprotein B-48 in the LDL density class following in vivo inhibition of hepatic lipase. *Biochim Biophys Acta* 877: 252-61.

104. Sultan F, Lagrange D, Jansen H, and Griglio S. 1990. Inhibition of hepatic lipase activity impairs chylomicron remnant-removal in rats. *Biochim Biophys Acta* 1042: 150-2.

105. Shafi S, Brady SE, Bensadoun A, and Havel RJ. 1994. Role of hepatic lipase in the uptake and processing of chylomicron remnants in rat liver. *J Lipid Res* 35(4): 709-20.

106. Homanics GE, de Silva HV, Osada J, Zhang SH, Wong H, Borensztajn J, and Maeda N. 1995. Mild dyslipidemia in mice following targeted inactivation of the hepatic lipase gene. *J Biol Chem* 270(7): 2974-80.

107. Fan J, Wang J, Bensadoun A, Lauer SJ, Dang Q, Mahley RW, and Taylor JM. 1994. Overexpression of hepatic lipase in transgenic rabbits leads to a marked reduction of plasma high density lipoproteins and intermediate density lipoproteins. *Proc Natl Acad Sci* 91(18): 8724-8.

108. Dichek HL, Qian K, and Agrawal N. 2004. The bridging function of hepatic lipase clears plasma cholesterol in LDL receptor-deficient "apoB-48-only" and apoB-100-only" mice. *J Lipid Res* 45: 551-60.

109. Ji ZS, Dichek HL, Miranda RD, and Mahley RW. 1997. Heparan sulfate proteoglycans participate in hepatic lipase and apolipoprotein E-mediated binding and uptake of plasmalipoproteins, including high density lipoproteins. *J Biol Chem* 272: 31285-92.

110. Brown RJ, Gauthier A, Parks RJ, McPherson R, Sparks DL, Schultz JR, and Yao Z. 2004. Severe hypoalphalipoproteinemia in mice expressing human hepatic lipase deficient in binding to heparan sulfate proteoglycans. *J Biol Chem* 279: 42403-409.

111. Kounnas MZ, Chappell DA, Wong H, Argraves WS, and Strickland DK. 1995. The cellular internalization and degradation of hepatic lipase is mediated by low density lipoprotein receptor-related protein and requires cell surface proteoglycans. *J Biol Chem* 270(16): 9307-12.

112. Sehayek E, and Eisenberg S. 1996. Cellular metabolism of triglyceride-rich lipoproteins: role of heparan sulfate, lipoprotein lipase and lipoprotein receptors. *Z Gastroenterol* 34 Suppl 3: 110-2.

113. Verges M, Bensadoun A, Herz J, Belcher JD, and Havel RJ. 2004. Endocytosis of hepatic lipase and lipoprotein lipase into rat liver hepatocytes in vivo is mediated by the low density lipoprotein receptor-related protein. *J Biol Chem* 279: 9030-36.

114. Fuki IV, Blanchard N, Jin W, Marchadier DH, Millar JS, Glick JM, and Rader DJ. (2003). Endogenously produced endothelial lipase enhances binding and cellular processing of plasma lipoproteins via HSPG-mediated pathway. *J Biol Chem* 278(36): 34331-8.

115. Broedl UC, Maugeais C, Marchadier D, Glick JM, and Rader DJ. 2003. Effects of nonlipolytic ligand function of endothelial lipase on high density lipoprotein metabolism in vivo. *J Biol Chem* 278: 40688-93.

116. Oram JF, Johnson CJ, and Brown TA. 1987. Interaction of high density lipoprotein with its receptor on cultured fibroblasts and macrophages. Evidence for reversible binding at the cell surface without internalization. *J Biol Chem* 262(5): 2405-10.

117. Graham DL, and Oram JF. 1987. Identification and characterization of a high density lipoprotein-binding protein in cell membranes by ligand blotting. *J Biol Chem* 262(16): 7439-42

118. Oram JF, Mendez AJ, Slotte JP, and Johnson TF. 1991. High density lipoprotein apolipoproteins mediate removal of sterol from intracellular pools but not from plasma membranes of cholesterol-loaded fibroblasts. *Arterioscler Thromb* 11(2): 403-14.

119. Barbaras R, Puchois P, Fruchart JC, Pradines-Figueres A, and Ailhaud G. 1990. Purification of apolipoprotein A binding protein from mouse adipose cells. *Biochem J* 269(3): 767-73.

120. Huang Y, von Eckardstein A, and Assmann G. 1993. Cell-derived unesterified cholesterol cycles between different HDLs and LDL for its effective esterification in plasma. *Arterioscler Thromb* 13(3): 445-58.

121. Fielding CJ, Fielding PE. 1995. Molecular physiology of reverse cholesterol transport. *J Lipid Res* 36(2): 211-28.

122. Hennessy LK, Kunitake ST, and Kane JP. 1993. Apolipoprotein A-I-containing lipoproteins, with or without apolipoprotein A-II as progenitors of pre-beta high-density lipoprotein particles. *Biochemistry* 32(22): 5759-65.

123. Agellon LB, Zhang P, Jiang ZC, Mendelsohn L, and Tall AR. 1992. The CCAAT/enhancer-binding proteins trans-activates the human cholesteryl ester transfer protein gene promoter. *J Biol Chem* 267(31): 22336-9.

124. Son YS, and Zilversmit DB. 1986. Increased lipid transfer activities in hyperlipidemic rabbit plasma. *Arteriosclerosis* 6(3): 345-51.

125. Quinet EM, Agellon LB, Kroon PA, Marcel YL, Lee YC, Whitlock ME, and Tall AR. 1990. Atherogenic diet increases cholesteryl ester transfer protein messenger RNA levels in rabbit liver. *J Clin Invest* 85(2): 357-63.

126. Jiang XC, Masucci-Magoulas L, Mar J, Lin M, Walsh A, Breslow JL, and Tall A. 1993. Down-regulation of mRNA for the low density lipoprotein receptor in transgenic mice containing the gene for human cholesteryl ester transfer protein. Mechanism to explain accumulation of lipoprotein B particles. *J Biol Chem* 268(36): 27406-12.

127. Castelli WP. 1984. Epidemioloy of coronary heart disease: the Framingham study. *Am J Med* 76(2A): 4-12.

128. Gordon DJ, Probstfield JL, Garrison RJ, Neaton JD, Castelli WP, Knoke JD, Jacobs DR Jr., Bangdiwala S, and Tyroler HA. 1989. High-density lipoprotein cholesterol and cardiovascular disease. Four prospective American studies. *Circulation* 79(1): 8-15.

129. Veniant MM, Sullivan MA, Kim SK, Ambroziak P, Chu A, Wilson MD, Hellerstein MK, Rudel LL, Walzem RL, and Young SG. 2000.

Defining the atherogenicity of large and small lipoproteins containing apolipoprotein B100. *J Clin Invest* 106(12): 1501-10.

130. Nordestgaard BJ, and Zilversmit DB. 1988. Large lipoprotein are excluded from the arterial wall in diabetic cholesterol-fed rabbits. *J Lipid Res* 29(11): 1491-500.

131. Tsao BP, Curtiss LK, and Edgington TS. 1982. Immunochemical heterogeneity of human plasma apolipoprotein B. II. Expression of apolipoprotein B epitopes on native lipoproteins. *J Biol Chem* 257(24): 15222-8.

132. Gustafsson M, and Boren J. 2004. Mechanism of lipoprotein retention by the extracellular matrix. *Curr Opin Lipidol* 15: 505-14.

133. Stary HC, Blankenhorn DH, Chandler AB, Glagov S, Insull W Jr., Richardson M, Rosenfeld ME, Schaffer SA, Schwartz CJ, Wagner WD, et al. 1992. A definition of the intima of human arteries and of its atherosclerosis-prone regions. A report from the Committee on Vascular Lesions of the Council on Arteriosclerosis, American Heart Association. *Circulation* 85(1): 391-405.

134. Cherchi GM, Coinu R, Demuro P, Formato M, Sanna G, Tidore M, Tirra ME, and De Luca G. 1990. Structural and functional modifications of human aorta proteoglycans in atherosclerosis. *Matrix* 10: 362-72.

135. Pillarisetti S. 2000. Lipoprotein modulation of subendothelial heparan sulfate proteoglycans (perlecan) and atherogenicity. *Trends Cardiovasc Med* 10(2): 60-5.

136. Meyers CD, Tannock LR, Wight TN, and Chait A. 2003. Statin-exposed vascular smooth muscle cells secrete proteoglycans with decreased biding affinity for LDL. *J Lipid Res* 44: 2152-60.

137. Tannock LR, Little PJ, Wight TN, and Chait A. 2002. Arterial smoot muscle cell proteoglycans synthesized in the presence of glucosamine demonstrate reduced binding to LDL. *J Lipid Res* 43: 149-57.

138. Little PJ, Tannock L, Olin KL, Chait A, and Wight TN. 2002. Proteoglycans synthesized by arterial smooth muscle cells in the presence of transforming growth factor-beta 1 exhibit increased binding to LDLs. *Arterioscler Thromb Vasc Biol* 22: 55-60.

139. Chang MY, Potter-Perigo S, Tsoi C, Chait A, and Wight TN. 2000. Oxidized low density lipoproteins regulate synthesis of monkey aortic smooth muscle cell proteoglycans that have enhanced native low density lipoprotein binding properties. *J Biol Chem* 275: 4766-73.

140. Edwards IJ, Wagner JD, Vogi-Willis CA, Litwak KN, and Cefalu WT. 2004. Arterial heparan sulfate is negatively associated with hyperglycemia and atherosclerosis in diabetic monkeys. *Cardiovasc Diabetol* 3: 6.

141. Havel RJ, and Hamilton RL. 2004. Hepatic catabolism of remnant lipoproteins: where the action is. *Arterioscler Thromb Vasc Biol* 24: 213-215.

142. Ji ZS, Sanan DA, and Mahley RW. 1995. Intravenous heparinase inhibits remnant lipoprotein clearance from the plasma and uptake by the liver: *in vivo* role of heparan sulfate proteoglycans. *J Lipid Res* 36: 583-92.

143. Aikawa J, Grobe K, Tsujimoto M, and Esko JD. 2001. Multiple isozymes of heparan sulfate/heparin GlcNAc N-deacetylase/N-sulfotransferase: structure and activity of the fouth member, NDST4. *J Biol Chem* 276: 5876-82.

144. Postic C, and Magnuson MA. (2000). DNA excision in liver by an albumin-Cre transgene occurs progressively with age. *Genesis* 26: 149-50.

145. Beauvais DM, and Rapraeger AC. 2003. Syndecan-1-mediated cell spreading requires signaling by alphavbeta3 integrins in human breast carcinoma cells. *Exp Cell Res* 286: 219-32.

146. Wong K, and Ryan RO. 2007. Characterization of apolipoprotein A-V structure and mode of plasma triacylglycerol regulation. *Curr Opin Lipidol* 18: 319-24.

147. Condac E, Silasi-Mansat R, Kosanke S *et al*. 2007. Polycystic disease caused by deficiency in xylosyltransferase 2, an initiating enzyme of glycosaminoglycan biosynthesis. *Proc Natl Acad Sci USA* 104: 9416-21

148. Fuki IV, Kuhn KM, Lomazov IR *et al*. 1997. The syndecan family of proteoglycans. Novel receptors mediating internalization of atherogenic lipoproteins *in vitro*. *J Clin Invest* 100: 1611-22.

149. Wilsie LC, Gonzales AM, and Orlando RA. 2006. Syndecan-1 mediates internalization of apoE-VLDL through a low density lipoprotein receptor-related (LRP)-independent, non-clathrin-mediated pathway. *Lipids Health Dis* 5: 23.

150. Yu K.C., Chen W., and Cooper A.D. 2001. LDL receptor-related protein mediates cell surface clustering and hepatic sequestration of chylomicron remnants in LDLR-deficient mice. *J Clin Invest* 107:1387-1394.

151. Fuki I.V., Meyer M.E., and Williams K.J. 2000. Transmembrane and cytoplasmic domains of syndecan mediate a multi-step endocytic pathway involving detergent insolublemembrane rafts. *Biochem J* 351:607-612.

152. Cortes V., Amigo L., Donoso K., Valencia I., Quinones V., Zanlungo S., Brandan E., and Rigotti A. 2007. Adenovirus-mediated hepatic syndecan-1 overexpression induces hepatocyte proliferation and hyperlipidaemia in mice. *Liver Int* 27:569-581.

153. Yanagisihita M, and Hascall V. 1992. Cell surface heparan sulfate proteoglycans. *J Biol Chem* 267: 9451-54.

154. Takeuchi Y, Yanagishita M, and Hascall VC. 1992. Recycling of transferin receptors and heparan sulfate proteoglycans in a rat parathyroid cell line. *J Biol Chem* 267: 14685-90.

155. Fransson LA, Belting M, Cheng F *et al.* 2004. Novel aspects of glypican glycobiology. *Cell Mol Life Sci* 61: 1016-24.

156. Zimmermann P, Zhang Z, Degeest G *et al.* 2005. Syndecan recycling [corrected] is controlled by syntenin-PIP2 interaction and Arf6. *Dev Cell* 9:377-88.

157. Bullock SL, Fletcher JM, Beddington RSP, and Wilson VA. 1998. Renal agenesis in mice homozygous for a gene trap mutation in the gene encoding heparan sulfate 2-sulfotransferase. *Genes and Dev* 12: 1894-1906.

158. Truong TQ, Auger A, Denizeau F, and Brissette L. 2000. Analysis of low-density lipoprotein catabolism by primary cultures of hepatic

cells from normal and low-density lipoprotein receptor knockout mice. *Biochim Biophys Acta* 1484: 307-15.

159. Auger A, Truong TQ, Rhainds D *et al.* 2001. Low and high density lipoprotein metabolism in primary cultures of hepatic cells from normal and apolipoprotein E knockout mice. *Eur J Biochem* 268: 2322-30.

160. Payne CK, Jones SA, Chen C, and Zhuang X. 2007. Internalization and trafficking of cell surface proteoglycans and proteoglycan-binding ligands. *Traffic* 8: 389-401.

161. Shimano H, Namba Y, Ohsuga J *et al.* 1994. Secretion-recapture process of apolipoprotein E in hepatic uptake of chylomicron remnants in transgenic mice, *J Clin Invest* 93: 2215-23.

162. Nordestegaard BG, Benn M, Schnohr P, and Tybjaerg-Hansen A. 2007. Nonfasting triglycerides and risk of myocardial infarction, ischemic heard disease, and death in men and women. *JAMA* 298: 299-308.

163. Bansal S, Buring JE, Rifai N, *et al.* 2007. Fasting compared with nonfasting triglycerides and risk of cardiovascular events in women. *JAMA* 24: 213-15.

164. Yuan G, Al-Shlai KZ, and Hegele RA. 2007. Hypertriglyceridemia: its etiology, effects, and treatment. *CMAJ* 176: 1113-20.

165. Rodriguez-Lee M, Bondjers G, and Camejo G. 2007. Fatty acid-induced atherogenic changes in extracellular matrix proteoglycans. *Curr Opin Lipidol* 18: 546-53.

166. Lutz, E.P., et al. 2001. Heparin-binding defective lipoprotein lipase is unstable and causes abnormalities in lipid delivery to tissues. *J. Clin. Invest.* 107: 1183-1192.

167. Magoori, K., et al. 2003. Severe hypercholesterolemia, impaired fat tolerance, and advanced atherosclerosis in mice lacking both low density lipoprotein receptor-related protein and apolipoprotein E. *J. Biol. Chem.* 278: 11331-11336.

168. Fui, I.V., Iozzo, R.V., and Williams, K.J. 2000. Perlecan heparan sulfate proteoglycan. A novel receptor that mediates a distinct pathway for ligand catabolism. *J. Biol. Chem.* 275: 25742-25750.

169. Mahley, R.W. 1996. Heparan sulfate proteoglycan/low density lipoprotein receptor-related protein pathway involved in type III hyperlipoproteinemia and Alzheimer's disease. *Isr. J. Med. Sci.* 32: 414-429.

170. Mahley, R.W., Ji, Z.S., Brecht, W.J., Miranda, R.D., and He, D. 1994. Role of heparan sulfate proteoglycans and the LDL receptor-related protein in remnant lipoprotein metabolism. *Ann. NY Acad. Sci.* 737: 39-52.

171. Iadonato, S.P., Bu, G., Maksymovitch, E.A., and Schwartz, A.L. 1993. Interaction of a 39 kDa protein with the low-density-lipoprotein-receptor-related protein (LRP) on rat hepatoma cells. *Biochem. J.* 296: 867-875.

CHAPTER 2

HEPARAN SULFATE 2-*O*-SULFOTRANSFERASE IN HEPATOCYTES IS REQUIRED FOR TRIGLYCERIDE-RICH LIPOPROTEIN CLEARANCE

2.1 Summary

Triglyceride-rich lipoprotein uptake in the liver depends on low-density lipoprotein receptors and one or more heparan sulfate proteoglycans made by hepatocytes. We previously showed that diminished sulfation of the heparan sulfate chains by hepatocytes induced by a conditional inactivation of N-acetylglucosamine (GlcNAc) N-deacetylase/N-sulfotransferase 1 (Ndst1) causes accumulation of plasma triglyceride-rich lipoproteins (7). Inactivation of Ndst1 led to decreased overall sulfation of the chains due to coupling of the various modifications (epimerization and O-sulfation) to N-sulfation of GlcNAc residues. To determine if the hypertriglyceridemia was caused by decreased overall charge, we created a conditional loxP-flanked allele of uronyl 2-O-sulfotransferase (Hs2st) and inactivated the gene in hepatocytes by crossing the mutant to mice bearing the rat AlbCre transgene. Analysis of $Hs2st^{f/f}AlbCre^{+}$ mice showed accumulation of plasma triglycerides to the same extent as observed in $Ndst1^{f/f}AlbCre^{+}$ mice. Hs2st-deficient mice synthesized VLDL normally, but exhibited delayed clearance of injected human VLDL and intestinally derived chylomicrons. Altering the expression of Hs2st in this way diminished uronyl 2-O-sulfation, but led to increased glucosamine N-sulfation and 6-O-sulfation as

observed in other systems. Binding, uptake and degradation of ^{125}I-VLDL was diminshed in hepatocytes isolated from the mutant. Incubation of isolated hepatocytes from wildtype mice with various chemically desulfated heparins showed that heparin and 6-O-desulfated heparin blocked ^{125}I-VLDL binding, but 2-O-desulfated or N-desulfated/re-N-acetylated heparin did not. Taken together, these findings show that VLDL binding and uptake by way of heparan sulfate proteoglycans on hepatocytes depends on both N-sulfaton and 2-O-sulfation of the chains, but not 6-O-sulfation.

2.2 Introduction

Heparan sulfate proteoglycans (HSPGs) act as co-receptors for various growth factors, chemokines, enzymes, and cell adhesion proteins (1-3). They also act as endocytic receptors, facilitating the uptake of various ligands and metabolites (4, 5). Although the mechanism of uptake has not been analyzed in detail in most cell types, available data suggests that ligands bound to the heparan sulfate chains most likely "piggy-back" into the cell during macropinocytosis of the proteoglycan. Binding and uptake via this mechanism has physiological relevance based on the discovery that triglycride-rich lipoprotein uptake by hepatocytes via heparan sulfate proteoglycans represents a major clearance pathway for remnant lipoproteins derived from VLDL and chylomicrons (7-11).

In previous studies we showed that lipoprotein uptake in the liver was sensitive to the degree of sulfation of the chains based on hypertriglyceridemia induced in mice by a selectively altering the expression of N-acetylglucosamine N-deacetylase/N-sulfotransferase-1 (Ndst1) in hepatocytes. Ndst1 belongs to a family of four enzymes

and initiates the modification of heparan sulfate chains. An epimerase (HsEpi) converts adjacent D-glucuronic acid units to L-iduronic acid, and then a group of *O*-sulfotransferases add sulfate to C2 of uronic acids (Hs2st) and to C6 (Hs6st1-3) and C3 (Hs3st1-6) of glucosamine units. These modifications occur in contiguous blocks of sugars along the chain in an incomplete manner, resulting in domains of variable size and sulfation (1, 3). Sets of modified sugars act as binding sites for different proteins, often with great specificity and affinity. Because Ndsts act prior to these other enzymes, altering the level of N-sulfation leads to altered levels of sulfation at other positions along the chain. The changes that occur depend on the specific cell type under study, but in hepatocytes inactivation of Ndst1 led to significantly decreased 2-O-sulfation of uronic acids with a lesser effect on 6-O-sulfation (7). Thus, altered lipoprotein uptake in Ndst1-deficient mice could result from altered sulfation at any of these positions. Although the ligand responsible for lipoprotein binding to heparan sulfate has not been defined, understanding the requirement for specific groups of sulfate residues can help determine if binding of known ligands is relevant.

One way to analyze this problem further is to inactivate the other enzymes involved in O-sulfation. Since uronyl 2-O-sulfation is most dramatically reduced in Ndst1 deficient hepatocytes, we decided to examine the imporatnce of Hs2st in lipoprotein clearance. This has not been possible since systemic inactivation of the gene causes renal agenesis, over-mineralized skeletons, retardation of eye development, and neonatal death (12). To circumvent this problem, we generated a conditional loxP-flanked allele of Hs2st and inactivated it selectively in hepatocytes. The mutation led to hypertriglyceridemia identical to that observed in Ndst1-deficient

animals, and altered binding and uptake of VLDL particles in isolated hepatocytes. Competition studies using variously disulfated heparins showed that both N-suflation and 2-O-sulfation, but not 6-O-sulfation are crucial features of the chains required for lipoprotein clearance.

2.3 Results

2.3.1 Conditional targeting of Hs2st

Systemic inactivation of *Hs2st* in mice causes neonatal lethality, primarily due to renal agenesis (12). To study the role of *Hs2st* in liver physiology, we produced a loxP-flanked allele of Hs2st (Experimental Procedures). At the time that this study was initiated the intron-exon boundaries of the gene was not fully established in 129Sv/J mice. Thus, one of the loxP recombination sites was inadvertently inserted in the short 5'-UTR, flanking exon 2 and encoding the start codon and 40 amino acids upstream from the start site of translation. qPCR of Hs2st transcripts in $Hs2st^{f/f}$ mice showed that the presence of the loxP site had no effect on transcript levels. Furthermore, enzyme assays of extracts prepared from $Hs2st^{f/f}$ embryos had normal activity and the composition of heparan sulfate was identical to that observed in wild-type animals. This allele could be conditionally deleted by crossbreeding $Hs2st^{f/+}$ and Zp3Cre mice, which led to heterozygosity at the locus in growing oocytes (see Supplementary Information). Subsequently, inbreeding of heterozygotes showed that the homozygous null animals ($Hs2st^{-/-}$) suffered from kidney agenesis and died as neonates, exactly as described previously for conventionally targeted mice. Analysis

of Hs2st enzyme activity and disaccharide analyses showed that homozygous null embryos were grossly defective in 2-O-sulfation compared to the wild-type.

2.3.2 Hepatocyte-specific Hs2st gene disruption alters heparan sulfate in the liver. To inactivate Hs2st in hepatocytes, *Hs2st*$^{f/f}$ were crossbred to transgenic mice expressing Cre recombinase under control of the rat albumin promoter (*AlbCre*) to drive selective inactivation of the gene in hepatocytes (20). Expression of the *AlbCre* transgene occurs after postnatal day 10. From these breedings, we established a colony of hepatocyte-specific *Hs2st* knockout mice (*Hs2st*$^{f/f}$*AlbCre*$^{+}$) with littermate controls of genotype *Hs2st*$^{f/f}$*AlbCre*$^{-}$. All genotypes were backcrossed more than 10 generations with C57BL/6J mice.

Hepatocytes were isolated from adult mice to measure the extent of *Hs2st* inactivation by Southern blotting. Cre-mediated recombination deleted exon 2, removing an *EcoRI* restriction site and yielding a fragment of 2.2 kb, whereas the wild-type allele generated a 3.0 kb fragment. DNA from hepatocytes of 8-week old homozygous mutant mice (*Hs2st*$^{f/f}$*AlbCre*$^{+}$) showed that ~90% of the *Hs2st*$^{f/f}$ alleles had undergone recombination (Fig. 2-1A).

Inactivation of *Hs2st* induced significant changes in liver heparan sulfate composition. Heparan sulfate was isolated from whole livers of adult mice (n = 3 per genotype) and depolymerized into its constituent disaccharides by bacterial heparinases (Figure 2-1B). The disaccharides were quantitated using an aniline tagging method and liquid chromatography/mass spectrometry (15) (Figure 2-2A). The level of sulfation at the various positions (N-, 2- and 6-) were then determined by

summing the number of disaccharides bearing each type of modification (Table 2-1). The level of 2-O-sulfation of uronic acids (sum of D2S0 and D2S6) decreased ~5-fold, from 21 2-O-sulfate groups/100 disaccharides in wild-type to 4 in the mutant. The residual sulfation arose presumably from incomplete inactivation of the gene and the presence of endothelial cells and other cell types in whole liver. Interestingly, the number of N-sulfate groups increased in *Hs2st*$^{f/f}$*AlbCre*$^{+}$ mice to 69/100 disaccharides from 48/100 disaccharides in the wild-type and the extent of glucosamine 6-*O*-sulfation (DOA6, D0S6, D2S6) increased as well, from 19 sulfates/100 disaccharides in the wild-type to 48/100 disaccharides in the mutant. These results are similar to those observed previously in mice carrying a systemic null allele of Hs2st and Chinese hamster ovary cells lacking the uronyl 2-O-sulfotransferase. For comparison, we reexamined the composition of *Ndst1*$^{f/f}$*AlbCre*$^{+}$ mice as well using mass spectrometry (Fig 2-2). Livers from *Ndst1*$^{f/f}$*AlbCre*$^{+}$ mice exhibited reduced levels of N-sulfation (18 sulfates/100 disaccharides, 2-O-sulfation (6/100 disaccharides) and 6-O-sulfation (9/100 disaccharides).

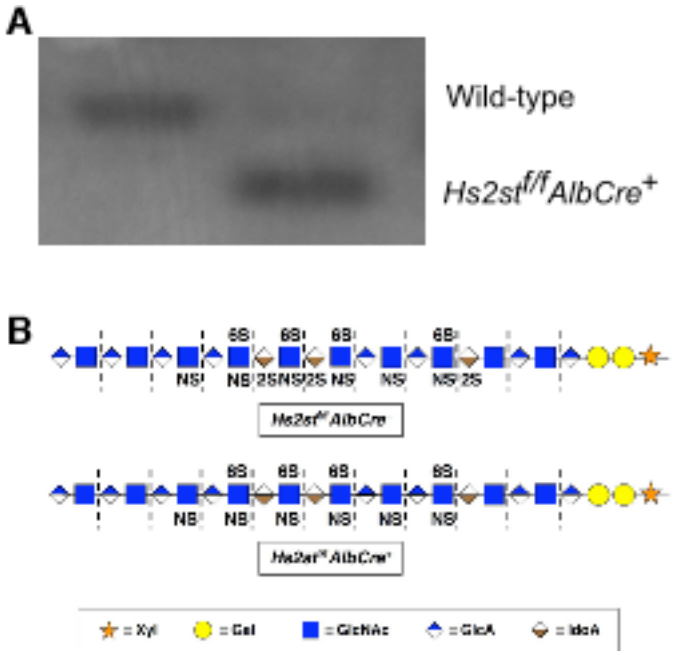


Figure 2-1. *Hs2st* conditional knockout. (A) Southern blot to determine Cre-mediated recombination of *Hs2st* floxed alleles. Hepatocyte genomic DNA was digested with *EcoRI* and probed for *Hs2st* alleles. The deleted allele gave a fragment of 2.2 kb, and the wild-type allele gave a fragment of 3 kb. Quantification of the bands indicated 90-95% recombination in *AlbCre*$^{+}$ hepatocytes. (B) Heparan sulfate chains from wildtype and Hs2stf/fALbCre+ mice are depicted using the indicated symbol nomenclature for the individual sugar residues (http://grtc.ucsd.edu). The dashed lines indicate the sites where heparinases cleave the chains into individual disaccharides.

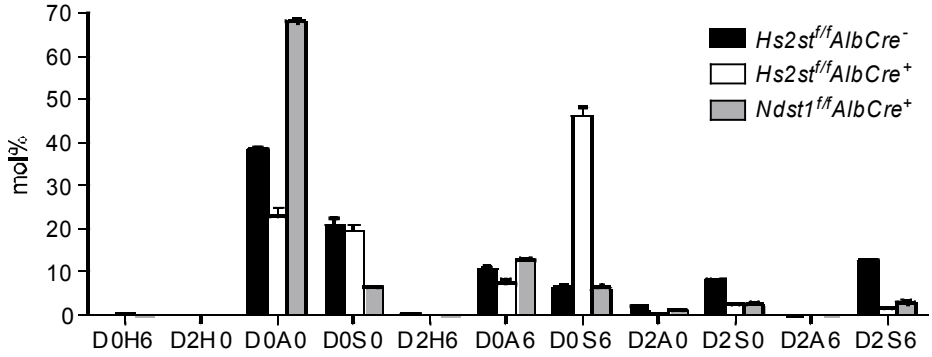


Figure 2-2. Disaccharide analysis of liver HS. (A) HS chains from *Hs2st*$^{f/f}$*AlbCre*$^{-}$ (black bars), *Hs2st*$^{f/f}$*AlbCre*$^{+}$ (white bars), and *Ndst1*$^{f/f}$*AlbCre*$^{+}$ (grey bars) livers were digested with heparin lyases I, II, and III, and the disaccharides were resolved by aniline tagging (n = 2 per genotype). (B) Average sums of total *N*-, 2-*O*-, and 6-*O*-sulfation are displayed. *N*-sulfation was decreased in *Ndst1*$^{f/f}$*AlbCre*$^{+}$ livers, 2-*O*-sulfation was decreased in *Ndst1*$^{f/f}$*AlbCre*$^{+}$ and *Hs2st*$^{f/f}$*AlbCre*$^{+}$ mice, and 6-*O*-sulfation was increased in *Hs2st*$^{f/f}$*AlbCre*$^{+}$ livers.

Table 2-1. Distribution of sulfate groups in wild-type and mutant hepatocytes.

	Hs2st$^{f/f}$*AlbCre*$^{-}$	*Hs2st*$^{f/f}$*AlbCre*$^{+}$	*Ndst1*$^{f/f}$*AlbCre*$^{+}$
	Sulfates per 100 disaccharides		
N-sulfates	49 $\pm$ 0.8	69 $\pm$ 0.7	18 $\pm$ 0.7
2-O-sulfates	21 $\pm$ 0.2	4 $\pm$ 0.1	6 $\pm$ 0.2
6-O-sulfates	19 $\pm$ 0.7	48 $\pm$ 2.6	9 $\pm$ 0.4

2.3.3 *Hs2st*$^{f/f}$*AlbCre*$^{+}$ mice accumulate triglyceride-rich lipoproteins.

Analysis of plasma samples from overnight-fasted 8-week-old mice showed that total plasma triglyceride levels were approximately 2.0 fold higher in Hs2st-deficient mice (58 ± 7 mg/dl in control mice vs. 100 ± 10 mg/dl; n = 10; $P < 0.003$) (Figure 2-3A). Total plasma cholesterol was not affected (96 ± 3 mg/dl versus 98 ± 4;

$n = 10$; $P = 0.62$) (Figure 2-3B). Buoyant density ultracentrifugation of fasting plasma lipoproteins from *Hs2st*$^{f/f}$*AlbCre*$^{+}$ and *Hs2st*$^{f/f}$*AlbCre*$^{-}$ mice showed that triglyceride-rich lipoproteins of $\delta < 1.006$ g/ml and 1.006-1.019 g/ml accumulated in mutant mice (Fig. 2-3C). There was no significant difference in cholesterol in these fractions and only a minor reduction in HDL cholesterol (Fig 2-3D). Analysis of lipoproteins of density $\delta < 1.006$ g/ml by SDS-PAGE showed the presence of apoB-48, apoB-100, apoE and apoCs characteristic of VLDL particles and chylomicron remnants (data not shown).

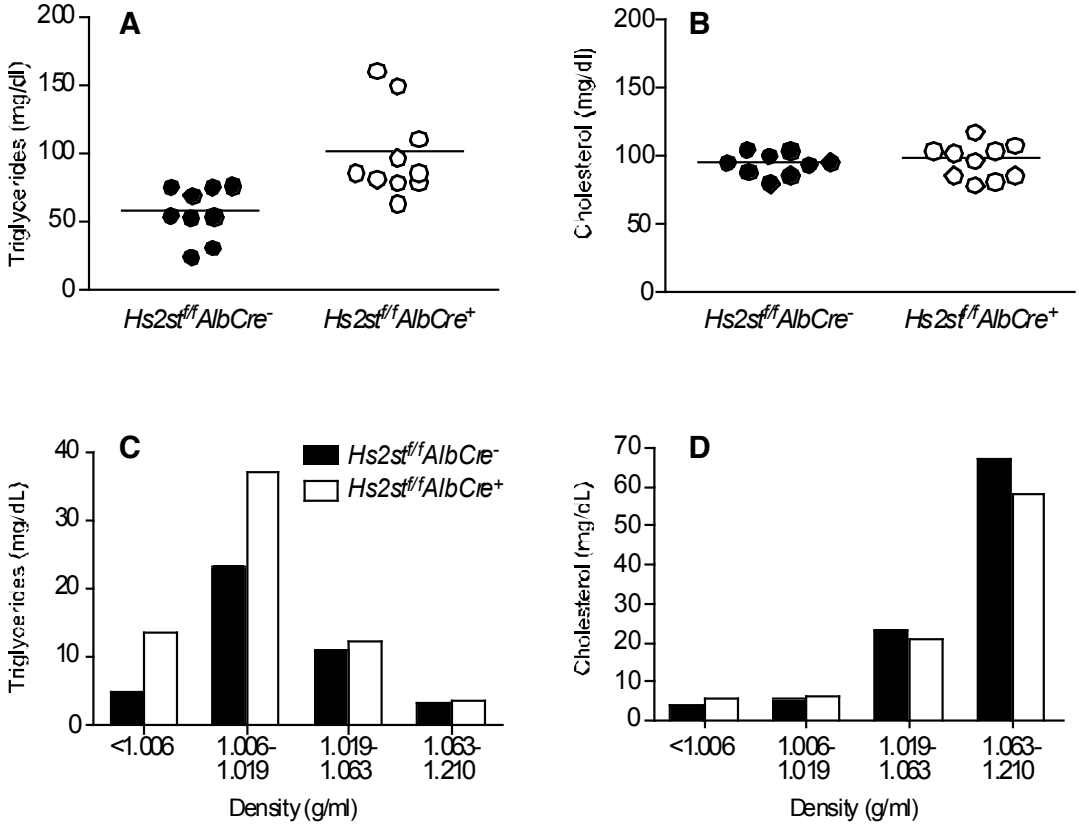


Figure 2-3. Hypertriglyceridemia in *Hs2st*$^{f/f}$*AlbCre*$^{+}$ mice. Total triglycerides (A) and total cholesterol (B) were measured in plasma samples (*n*=9 *Hs2st*$^{f/f}$*AlbCre*$^{-}$, *n*=10 *Hs2st*$^{f/f}$*AlbCre*$^{+}$, mixed males and females, horizontal bars indicate mean values). Triglyceride (C) and cholesterol (D) content of lipoproteins fractionated by preparative ultracentrifugation was determined. Each value is from 1 set of pooled plasma derived from 10 mice.

2.3.4 *Hs2st*-deficient mice exhibit slower plasma clearance of triglycerides and VLDL

Clearance rates of intestinally derived triglyceride-rich lipoproteins were measured in mice lacking hepatocyte *Hs2st* by a vitamin A fat tolerance test. Overnight-fasted mice were given a bolus mixture of [^{3}H]retinol and corn oil by gavage, and blood was sampled at various time points from the retro-orbital sinus.

The retinol is converted to retinyl esters and packaged with dietary lipids in chylomicron particles. The disappearance of [^{3}H]retinyl esters from the circulation is measure of hepatic clearance. The retinyl ester excursion curves showed that *Hs2st*$^{f/f}$*AlbCre*$^{+}$ mice cleared intestinally derived lipoproteins at a significantly slower rate than *Hs2st*$^{f/f}$*AlbCre*$^{-}$ mice (area under the curve (AUC) – 4123 vs. 9554; $P = 0.0033$), but most of the particles were cleared by 12 hr (Figure 2-4A). Plasma triglyceride clearance matched the retinyl ester excursion curves (data not shown).

Clearance of VLDL was also affected based on experiments in which a bolus of human VLDL was injected intravenously and the circulating level of human VLDL was determined by ELISA using mAb MB47, which is specific for human apoB-100 (17) (Figure 2-4B). The rate of turnover was reduced in mutant mice, yielding apparent half-lives (calculated by extrapolation from the curves) of 125 $\pm$ 10 minutes in control mice and 360 $\pm$ 117 minutes in mutant mice ($n = 6$ per genotype; $P < 0.0001$). Thus, hepatocyte Hs2st plays a crucial role in the clearance of both intestinally and liver derived lipoprotein particles.

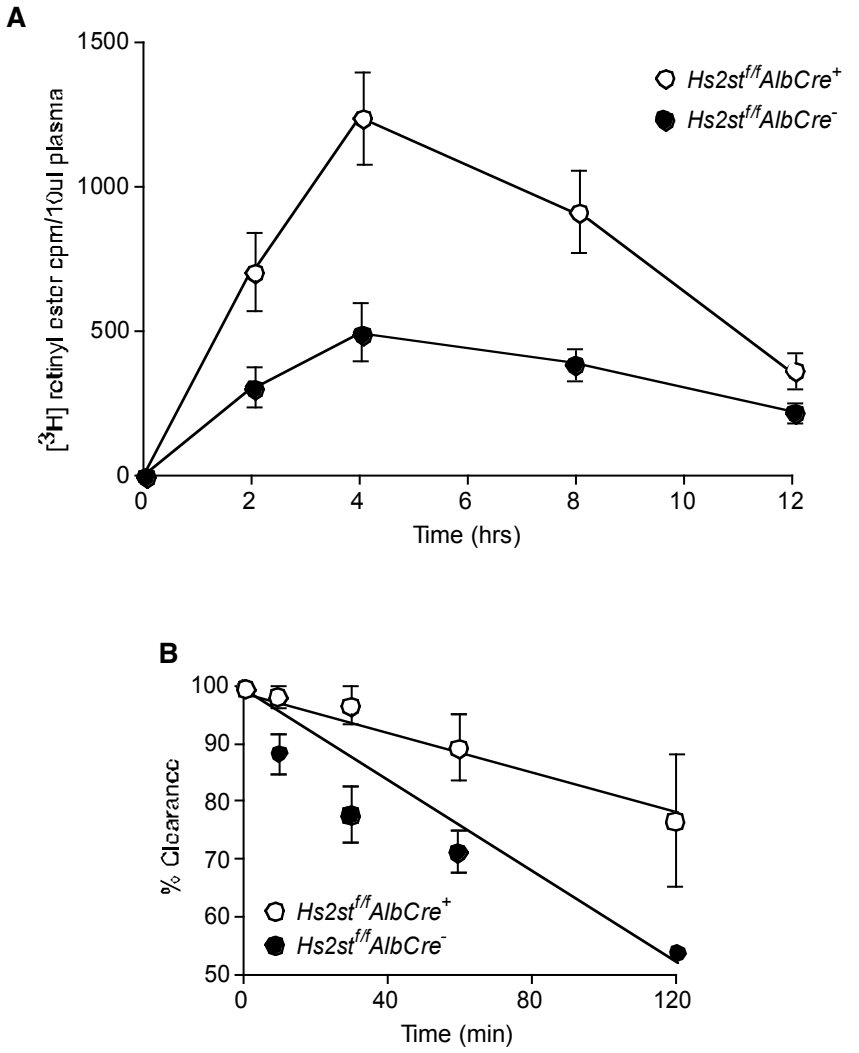


Figure 2-4. *Hs2st$^{f/f}$AlbCre^{+}* mice exhibit delayed plasma clearance of VLDL and dietary triglycerides. (A) Retinyl ester excursions were measured at the times indicated in *Hs2st$^{f/f}$AlbCre^{+}* mice (open circles, $n = 3$) compared with *Hs2st$^{f/f}$AlbCre^{-}* (closed circles, $n = 3$). Overnight-fasted animals of the indicated genotypes were given 200μl of corn oil containing 5.4μCi [^{3}H] retinol by gavage. Blood samples were taken at the indicated times, and radioactivity remaining in 10 μl of serum was determined scintillation counting in triplicate. Clearance was significantly delayed in the *Hs2st$^{f/f}$AlbCre^{+}* mice ($P < 0.0001$). Plasma clearance of human VLDL apoB-100 (B) was measured by ELISA using human apoB-100-specific monoclonal antibody MB47 (see methods). *Hs2st$^{f/f}$AlbCre^{-}* mice (filled circles; $t_{1/2} = 125$ min; $n = 6$ mice) and *Hs2st$^{f/f}$AlbCre^{+}* mice (open circles; $t_{1/2} = 259$ min; $n = 6$ mice). The difference in $t_{1/2}$ between the genotypes was significant ($P = 0.0007$).

2.3.5 Binding and uptake of ^{125}I-VLDL particles is delayed in *Hs2st*-deficient

hepatocytes

To determine how altering Hs2st would affect binding and uptake of VLDL in isolated hepatocytes, cells were isolated from *Hs2st*$^{f/f}$*AlbCre*$^{-}$ and *Hs2st*$^{f/f}$*AlbCre*$^{+}$ mice and incubated with 20μg ^{125}I-VLDL. *Hs2st*$^{f/f}$*AlbCre*$^{+}$ hepatocytes showed decreased binding at 4^{o}C compared to *Hs2st*$^{f/f}$*AlbCre*$^{-}$ mice (1.8 $\pm$ .8 μg VLDL/mg cell protein vs. 0.5 $\pm$ .1 in the mutant), and reduced binding/uptake of ^{125}I-VLDL at 37^{o} (5 $\pm$ 0.3 μg VLDL/mg cell protein vs. 0.9 $\pm$ 0.1 μg VLDL/mg cell protein) (Figure 5A). Significant degradation of VLDL occurred during the one hour incubation based on recovery of non-chloroform extractable acid-soluble counts (iodo-tyrosine) in the growth medium. *Hs2st*$^{f/f}$*AlbCre*$^{+}$ hepatocytes showed a dramatic decrease in degradation as well (Fig. 2-5A). Similar reduction in binding, uptake and degradation were obtained when *Ndst1*$^{f/f}$*AlbCre*$^{+}$ were assayed (Fig. 5A) and the differences between the mutants was not significant (P = 0.1345, P = 0.768, P = 0.928). Binding and uptake of ^{125}I-VLDL particles was also measured in wild-type hepatocytes after treatment with heparin lyases to remove cell surface heparan sulfate. A three-fold decrease in uptake compared to untreated hepatocytes was observed (4 $\pm$ 2 μg VLDL/mg cell protein vs. 1.3 $\pm$ 0.2 μg VLDL/mg cell protein), consistent with the studies of the mutants (Figure 2-5B).

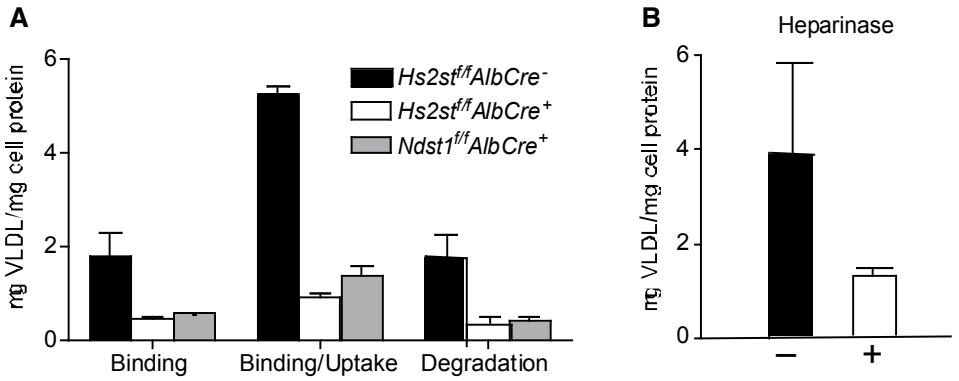


Figure 2-5. Hs2st mediates binding, uptake, and degradation of VLDL. (A) Incubation with ^{125}I-VLDL at 4^{o} revealed increased binding of *Hs2st$^{f/f}$AlbCre^{-}* (filled bars) hepatocytes compared to *Hs2st$^{f/f}$AlbCre^{+}* (open bars) hepatocytes approximately (3.7-fold). There was no difference between *Hs2st$^{f/f}$AlbCre^{+}* hepatocytes and *Ndst1$^{f/f}$AlbCre^{+}* hepatocytes (grey bars). Binding and uptake (measured at 37^{o}) was increased approximately 5.5-fold in *Hs2st$^{f/f}$AlbCre^{-}* vs. *Hs2st$^{f/f}$AlbCre^{+}* hepatocytes ($P < 0.01$). There was no difference in uptake and degradation between *Hs2st$^{f/f}$AlbCre^{+}* hepatocytes and *Ndst1$^{f/f}$AlbCre^{+}* hepatocytes (grey bars; $P = 0.1345$). (B) *Hs2st$^{f/f}$AlbCre^{-}*hepatocytes were incubated with heparin lyases I, II, and III. Incubation with heparin lyases at 37^{o} resulted in a 3-fold decrease in binding compared to *Hs2st$^{f/f}$AlbCre^{-}* hepatocytes ($P < 0.01$).

2.3.6 Binding of VLDL shows specificity

The altered binding of VLDL to heparan sulfate deficient cells predicted that the addition of heparin, which is more highly sulfated than hepatoctye heparan sulfate, should also block binding and uptake. Incubation with increasing concentrations of heparin resulted in a decrease in binding of ^{125}I-VLDL (Fig. 2-6), with an extracted IC_{50} value of 0.1 μg/ml.

The inhibition of VLDL binding by heparin suggested another way to examine the role of different sulfate groups in the interaction, specifically by assaying the inhibitory activity of selectively desulfated preparations. Both *N*-desulfated and 2,3-*O*-desulfated heparin had only mild effect on VLDL binding, which supports the genetic studies showing that these groups were crucial for clearance in vivo and binding,

uptake and degradation in isolated cells. In contrast, 6-O-desulfated heparin had nearly the same potency as native heparin, with a calculated IC_{50} value of 0.1 μg/ml.

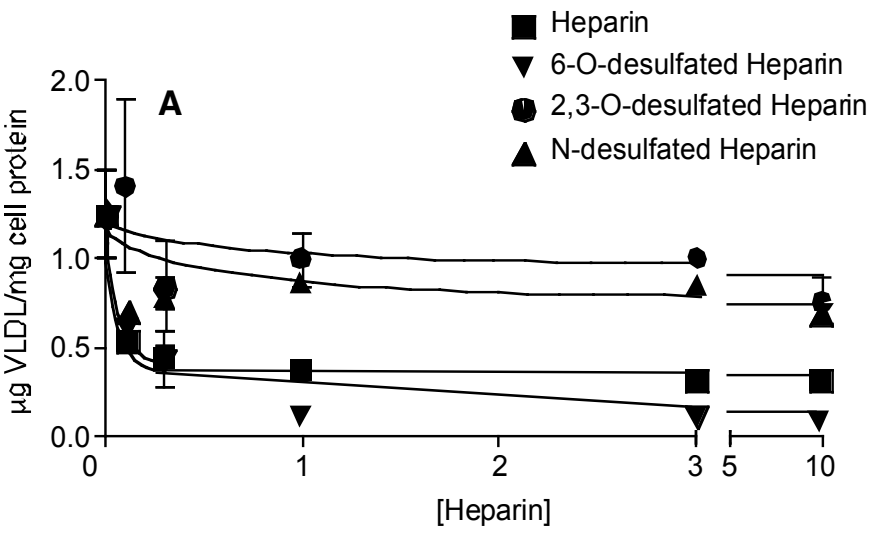


Figure 2-6. Incubation with various desulfated heparins effects binding of ^{125}I-VLDL. Incubation of ^{125}I-VLDL with various desulfated heparins at 4^{O}. Wild-type heparin (filled squares) and 6-O-desulfated heparin (filled inverted triangles) showed complete inhibition. 2,3-O-desulfated heparin (filled circles) and N-desulfated heparin (filled triangles) showed almost no inhibition. There was no difference between 2-O-desulfated heparin and N-desulfated heparin ($P = 0.2$) or heparin and 6-O-desulfated heparin ($P = 0.66$). There was a significant difference between 2-O-desulfated heparin and heparin ($P = 0.016$).

2.4 Discussion

Prior studies have suggested that uptake of triglyceride-rich lipoproteins remnants can occur through a heparan sulfate-mediated pathway in cells. Recently, we provided direct genetic evidence that hepatocyte heparan sulfate fulfills this function in vivo, by altering the biosynthesis of the chains through a tissue-specific inactivation of Ndst1. In this report, we have advanced these studies by demonstrating that clearance depends on both N-sulfated glucosamine residues and 2-O-sulfated uronic acids in the chain, but independently of 6-O-sulfation of glucosamine units. Because of coupling between several of the biosynthetic enzymes, sulfation occurs in domains of variable size (so-called NS domains). These segments make up the binding

sites for most ligands, in this case the sites where apolipoproteins or lipases carried by triglyceride-rich lipoproteins associate. In other studies, we have demonstrated that syndecan-1 constitutes the primary proteoglycan receptor present in hepatocytes that facilitates clearance of remnant particles. Thus, this implies that the heparan sulfate chains on syndecan represent the relevant subpopulation of heparan sulfate that interact with remnant lipoprotein particles. Additional studies are needed to determine if lipoprotein binding is unique to the chains present on syndecan-1 in the liver, or if other hepatic proteoglycans or syndecan-1 derived from other tissues could bind as well.

Several mechanisms have been suggested to explain how heparan sulfate interactions with apolipoproteins and/or enzymes affect lipoprotein processing in the liver. Mahley et al have suggested that remnant lipoprotein particles entering the space of Disse bind to HSPGs via apoE, resulting in their sequestration prior to further processing and receptor-mediated endocytosis (24). Lipoprotein lipase and hepatic lipase also can act in this way, since both enzymes can bind to heparan sulfate and to the lipoprotein particles, thus acting a bridging molecule (4, 24). Apparently, one or more of these ligands contains a binding site that requires N-sulfation and 2-*O*-sulfation. Potential ligands of VLDL that bind to heparin include apoE, apoB, lipoprotein lipase, and hepatic lipase (Table 2). Many of these ligands can interact with heparan sulfate oligosaccharides of variable sulfation, and most avidly to segments enriched in the tri-sulfated disaccharide, GlcNS6S-IdoA2S. Thus, the available structural data does not allow us to determine which if any of these proteins serve as the relevant ligand for heparan sulfate dependent clearance.

Table 2-2. Apolipoproteins known to bind Heparin/Heparan Sulfate

Ligand	Binding specificity	References
ApoE	Sequences rich in GlcNS6S-IdoA2S	26, 27
ApoB	Heparin, highly sulfated regions of HS	28-30
HL	Heparin, highly sulfated regions of HS	31, 32
Lpl	Heparin, highly sulfated regions of HS; tighter interaction with *O*-sulfated disaccharides, sequences rich in GlcNS6S-IdoA2S	33-38

One of the interesting effects of altering 2-O-sulfation of heparan sulfate in hepatocytes is the nearly stoichiometric increase in N-sulfation and 6-O-sulfation, which maintains the overall charge of the chain. In spite of this "compensation", triglycerides accumulate in the mutant and VLDL uptake is reduced in isolated hepatocytes, suggesting that the ligand on the lipoprotein particles exhibits specificity for the arrangement of sulfate residues. Similar "compensation" occurs in Chinese hamster ovary cells containing a mutation in Hs2st and model organisms lacking the Hs2st orthologs. The mechanism responsible for these coordinated changes in sulfation remain unknown. GlcNAc N-deacetylation and N-sulfation precedes all of the other modification reactions and creates the preferred substrate for HsC5epi, which epimerizes glucuronic acids located to the reducing side of the N-sulfoglucosamine units to L-iduronic (IdoA). The resulting IdoA is then preferentially sulfated at C-2 by Hs2st, although the enzyme can also work less efficiently on glucuronic acids. Although we have not measured GlcNAc N-deacetylase/N-sulfotransferase activity in mutant hepatocytes, *N*-sulfotransferase activity in Hs2st-deficient CHO cells was

unchanged, suggesting that the presence of 2-*O*-sulfated residues somehow decreases the rate or extent of the *N*-deacetylase/*N*-sulfotransferase reaction. This explanation suggests that the length of the N-sulfated blocks might be greater in the absence of Hs2st, which is borne out by analysis of the sulfated segments (NS-domains) in mouse gene trap mutant alleled in Hs2st (40).

Table 2-3. Various organisms deficient in Hs2st.

Organism/Tissue	Compensation	Phenotype of Mutant	References
CHO cells	Increase in *N*-, 6-*O*-sulfation	Decreased binding of FGF	39
Drosophila	Increase in *N*-, 6-*O*-sulfation	Cell adhesion and guidance defect	42, 43, 44
C. elegans	Increase in *N*-, 6-*O*-sulfation	Cell migration defect	41
Mice	Increase in *N*-, 6-*O*-sulfation	Renal agenesis, defects in eye and skeletal development, neonatal lethality	12, 40

The selective elevation of plasma triglycerides without accumulation of plasma cholesterol in Hs2st-deficient mice is similar to that observed in patients with hypertriglyceridemia associated with elevated levels of VLDL particles (25). These patients persistently exhibit elevated plasma triglyceride levels, but plasma cholesterol and phospholipid levels usually remain close to normal levels. Mutations that affect triglyceride levels in humans include genes encoding Lpl, apoAV, apoCII, apoCIII, and GPIHBP1. We can now add Hs2st to the growing list of genes involved in heparan sulfate proteoglycan formation that could affect triglyceride clearance. Patients predisposed to mild but clinically relevant hyperlipidemias should be screened for changes in 2-*O*-sulfation and polymorphisms in the relevant genes involved in 2-*O*-sulfation.

2.5 Experimental Procedures

2.5.1 Mice derivation and Animal Husbandry

All animals were housed under barrier conditions in AAALAC approved vivaria in the School of Medicine, University of California San Diego, following standards and procedures approved by the local Institutional Animal Care and Use Committee. Mice were weaned at 3 weeks, maintained on a 12 h light-dark cycle, and fed water and standard rodent chow *ad libitum*. To measure fasting plasma lipids chow was removed from the cages at approximately 8 am in the morning and 4 hrs later samples of blood were drawn from the retroorbital plexus.

Mice bearing a conditional loxP-flanked allele of *Hs2st* were prepared in the thymidine kinase-neomycin phosphotransferase based targeting vector described previously. *loxP* recombination sites were inserted upstream from the ATG start codon in exon 2 , which includes most of the 5'-untranslated region and encodes 40 of 356 amino acids of the open reading frame of Hs2st. The final targeting vector was linearized using *SalI* before transfection of E9.5 R1 129Sv/J embryonic stem (ES) cells by electroporation. The transfected ES cells were selected with G418, and homologous recombinants were identified by Southern blotting and PCR analysis. One clone with normal karyotypes was transfected with a Cre-expression vector, followed by gancyclovir selection. Finally, one recombinant ES cell lines bearing

loxP sites flanking the *HS2st* exon 2 was selected based on Southern blotting and PCR analysis and injected in C57BL/6J blastocysts. One mouse line derived from the ES cell clone was obtained and backcrossed into a C57BL/6 background for >10 generations. Mice were genotyped by PCR using the following primers: Primer 1 (5`-gtgcggccgtggggtcc-3`), Primer 2 (5`-atggggctcctcaggattatgatgc-3`), and Primer 3 (5`-tgccctaggctcaggcatg-3`). The primer pair P1/P3 generated PCR bands at 1178, 876 and 360 bp, corresponding to $HS2st^{f}$, $HS2st^{+}$ and $HS2st^{-}$ respectively.

Southern blots were performed on DNA isolated from isolated hepatocytes using a DNeasy Tissue Kit (QIAGEN). Genomic DNA (25μg) was digested overnight with the *EcoRI* and separated on 1% agarose before transfer overnight to nitrocellulose. The membrane was UV-crosslinked and hybridized to an *Hs2st*-specific probe double-labeled with [α^{32}P]dCTP and [α^{32}P]dATP (EasyTides; PerkinElmer). The membrane was washed and exposed to x-ray film. Films were scanned and bands were quantitated using Adobe Photoshop.

2.5.2 HS purification and analysis

HS was isolated from whole liver as previously described (7, 14). Livers were homogenized in PBS and treated overnight with Pronase to degrade proteins followed by purification of glycopeptides by anion exchange chromatography using DEAE sepharose. The columns were washed, and the glycans eluted with high salt. Disaccharide analysis was carried out as described (15). Briefly, HS chains were digested with heparin lyases I, II and III and labeled with C12 aniline. Labeled HS was combined with known quantities of HS disaccharide standards labeled with C13

aniline and were subjected to liquid chromatography followed by mass spectroscopy to separate and identify individually labeled disaccharides. Ratiometric analysis of the ^{12}C and ^{13}C-labeled disaccharides provided a quantitative way to determine the level of *N*-, 2-*O*-, and 6-*O*-sulfation.

2.5.3 Lipoprotein Analysis

Total lipids were measured in blood samples drawn from overnight-fasted animals by retro-orbital sinus bleeds. Total cholesterol and triglyceride levels were determined enzymatically using an automated reader (Cobas Mira; Roche Diagnostics) and kits: Cholesterol High-Performance Reagent (Roche Diagnostics) and Triglyceride-SL (Diagnostic Chemicals Ltd.).

Lipoproteins were prepared from blood drawn by cardiac puncture using sequential preparative ultracentrifugation according to established methods (16). TRLs (δ = 1.006 g/ml) were prepared from pooled plasma samples (n = 10 mice, vol = 5 ml) by centrifugation for 12 hours at 45,000 x rpm in a Beckman 50.3Ti rotor. VLDL remnants and IDL were then collected as the δ = 1.006 - 1.019 g/ml fraction and subsequently LDL and HDL as the δ = 1.019-1.063, and δ = 1.063-1.21g/ml fractions, respectively. The isolated lipoproteins were dialyzed against phosphate-buffered saline (PBS) (16) and analyzed for lipid content.

2.5.4 VLDL plasma clearance

Human VLDL (d < 1.006g/ml) was isolated from healthy, fasting volunteers. Mice were fasted for 6 hours and injected with 20μg human VLDL proteins via the

tail vein. Serial samples were taken by retro-orbital sinus bleeds at 2, 10, 30, 60, and 120 minutes after injection. The amount of human VLDL remaining in the plasma was determined by sandwich ELISA, utilizing mAb MB47 specific for human apoB-100 (17). MB47 does not bind to murine apoB-100. U-bottom 96-well plates were coated overnight with MB47 at 5μg/ml in Tris-buffered saline, followed by addition of nonsaturating amounts of plasma (typically, 1:100 dilution of mouse plasma) to capture human VLDL. Bound VLDL was detected using biotinylated goat anti-human apoB-100 (BIODESIGN International), followed by alkaline phosphatase-labeled neutrAvidin (Pierce Biotechnology). Plates were developed with Lumi-Phos 530 (Lumigen) and read in a DYNEX Technologies MLX Microtiter Plate Luminometer. Half-times were calculated using linear regression to extrapolate the clearance rates.

2.5.5 Vitamin A fat tolerance testing

Vitamin A fat tolerance testing was done essentially as described previously (10). Briefly, 27.0μCi [11,12-^{3}H] retinol (44.4Ci/mmol; PerkinElmer) in ethanol was mixed with 1ml of corn oil (Sigma-Aldrich). Each mouse received 200μl by oral gavage. Blood was sampled at the times indicated by retro-orbital sinus bleed, and radioactivity was measured in triplicate (10μl serum) by scintillation counting.

2.5.6 Lipoprotein uptake by hepatocytes

Human VLDL ($\delta < 1.006$ g/ml, 21 mg protein) was iodinated using 3 mCi and $Na^{125}I$ (1.9×10^{2} cpm/ng, NEN/Perkin Elmer) using Iodogen (18). Under these conditions, 13% of the label was lipid soluble. Isolated hepatocytes were treated with

the indicated concentration of ^{125}I-VLDL in DMEM media with 2.5 mg/ml lipoprotein-free serum (Biomedical Technologies, Inc., Boston, MA). Cells were incubated at 4^{o}C or 37^{o}C for 1 hr, rinsed three times with PBS and then solubilized with 0.1M NaOH. Protein concentration was determined by Bradford (BioRad) and radioactivity was measured by gamma counting. Degradation of ^{125}I-VLDL was measured by precipitation of 0.25 mL of conditioned media with an equal volume of 50% trichloroacetic acid (19). After 30 min at 4 ^{o}C, the samples were centrifuged for 30 min. The supernatant was placed in a fresh glass tube, and 5 µL of 40% potassium iodide was added as a carrier. Hydrogen peroxide (30%) was added, and lipid soluble material was extracted by the addition of 2 ml of chloroform. An aliquot of the upper aqueous phase containing iodotyrosine was counted as measure of degradation (19).

In competition experiments, wild-type hepatocytes were treated simultaneously with varying concentrations of heparin or de-sulfated heparins and ^{125}I-VLDL at 4^{o}C for 1 hr. Porcine intestinal heparin (M_r = 12,000-15,000) was a kind gift from Dr. Patrick Shaklee (Scientific Protein Laboratories Inc., Milwaukee, Wisconsin, USA). Desulfated heparins (O-desulfated and 6-O-desulfated) were from Neoparin (Alameda, California, USA). Insome experiments, wildtype cells were incubated at 37 ^{o}C for 1.5 hr with 15 mU heparin lyases I, II, and III (a gift from Jian Liu, University of North Caroline). The media was then replaced with fresh media containing ^{125}I-VLDL and heparin lyase I, II, and III. Binding and uptake were analyzed as described above.

2.5.7 Statistics

Statistical analyses were performed using PRISM (GraphPad Software). All data is expressed as mean values $\pm$ SD unless otherwise indicated. Significance was determined using an unpaired Student's (two-tailed) t test. Significance was taken as $P < 0.05$.

2.6 Acknowledgements

This work in full will be submitted for publication to the *Journal of Biological Chemistry* with coauthors Joseph R., Bishop, Danyin Song, Roger Lawrence, Lianchun Wang, and Jeffrey D. Esko. The dissertation author was the primary author of the work contained in the paper. Together with her coauthors she thanks David Ditto and Joseph Juliano for excellent technical assistance. Work was conducted within the department of Cellular and Molecular Medicine, the Department of Medicine, and the Glycobiology Research and Training Center, University of California, San Diego, La Jolla, California.

2.7 References

1. **Conrad H.E. (1998). Heparin-binding proteins. Academic Press. San Diego, California, USA. 527 pp.**

2. **Bernfield, M., Gotte M., Park, P.W., Reizes, O., Fitzgerald, M.L., Lincecum, J., and Zako, M. (1999). *Annu. Rev. Biochem.* 68, 729 – 777.**

3. **Esko, J.D., and Selleck, S.B. (2002). *Annu. Rev. Biochem.* 71, 435 – 471.**

4. **Williams, K.J., and Fuki, I.V. (1997). *Curr. Opin. Lipidol.* 8, 253- 262.**

5. **Belting, M. (2003). *Trends Biochem. Sci.* 28: 145-151.**

6. **Williams, K.J., Fless G.M., Petrie, K.A., Snyder, M.L., Brocia, R.W., and Swenson, T.L. (1992). *J. Biol. Chem.* 267, 13284-13292.**

7. **MacArthur, J.M., Bishop, J.R., Stanford, K.I., Wang, L., Bensadoun, A., Witztum, J.L., and Esko, J.D. (2007). *J Clin Invest.* 117, 153-164.**

8. **Rubinsztein, D.C., Cohen, J.C., Berger, G.M., van der Westhuyzen, D.R., Coetzee, G.A., and Gevers, W. (1990). *J. Clin. Invest.* 86, 1306-1312.**

9. **Kita, T., Brown, M.S., Bilheimer, D.W., and Goldstein, J.L. (1982). *Proc. Natl. Acad. Sci.* 79, 3623-3627.**

10. **Ishibashi, S., Perrey, S., Chen, Z., OSuga, J., Shimada, M., Ohashi, K., Harada, K., Yazaki, Y., and Yamada, N. (1996). *J. Biol. Chem.* 271, 22422-22427.**

11. **Cooper, A.D. (1997). *J. Lipid. Res.* 38, 2173-2192.**

12. **Bullock, S.L., Fletcher, J.M., Beddington, R.S.P., and Wilson, V.A. (1998). *Genes and Dev.* 12, 1894-1906.**

13. **Horton, J.D., Shimaon, H., Hamilton, R.L., Brown, M.S., and Goldstein, J.L. (1999). *J. Clin. Invest.* 103, 1067-1076.**

14. **Grobe, K., Inatani, M., Palleria, S.R., Castagnola, J., Yamaguchi, Y., and Esko, J.D. (2005). *Development* 132, 3777-3786.**

15. **Lawrence, R., Lu, H., Rosenburg, R.D., Esko, J.D., and Zhang, L. (2008).** ***Nat Methods*** **5, 291-2.**

16. **Kelley, J.L., Kruski, A.W. (1986).** ***Methods Enzymol.*** **128, 170-181.**

17. **Young S.G., Smith, R.S., Hogel, D.M., Curtiss, L.K., and Witztum, J.L. (1986).** ***Clin. Chem.*** **32, 1484-1490.**

18. **Salcinski, P.R., McLean, C., Sykes, J.E., Clement-Jones, V.V., and Lowry, P.J. (1981).** ***Anal. Biochem.*** **117, 136-146.**

19. **Williams, K.J. (2001).** ***Methods Mol. Biol.*** **171, 457-477.**

20. **Postic, C., and Magnuson, M.A. (2000).** ***Genesis*** **26, 149-150.**

21. **Rohlmann, A., Gotthardt, M., Hammer, R.E., and Herz, J. (1998).** ***J. Clin. Invest.*** **101, 689-695.**

22. **Ishibashi, S., Brown, M.S., Goldstein, J.L., Gerard, R.D., Hammer, R.E., and Herz J. (1993).** ***J. Clin. Invest.*** **92, 883-893.**

23. **Magoori, K., Kang, M.J., Ito, M.R., Kakuuchi, H., Ioka, R.X, Kamataki, A., Kim, D.H., Asaba, H., Iwasaki, S., Takei, Y.A., Sasaki, M., Usui, S., Okazaki, M., Takahashi, S., Ono, M., Nose, M., Sakai, J., Fujino, T., and Yamamoto, T.T. (2003).** ***J. Biol. Chem.*** **278, 11331-11336.**

24. **Mahley, J., and Ji, Z.S. (1999).** ***J. Lipid Res.*** **40, 1-16.**

25. **Havel, R.J., and Kane, J.P. (2001). Structure and metabolism of plasma lipoproteins. In The metabolic and molecular bases of inherited disease. C.R. Scriver et al., editors. McGraw-Hill. New York, New York, USA. 2705-2716.**

26. **Libeu, C.P., Lunk-Katz, S., Phillips, M.C., et al. 2001. New insights into the heparan sulfate proteoglycan-binding activity of apolipoprotein E.** ***E. J. Biol. Chem.*** **276: 39138-39144.**

27. **Dong, J., Peters-Libeu, C.A., Weisgraber, K.H., et al. 2001. Interaction of the N-terminal domain of apolipoprotein E4 with heparin.** ***Biochemistry*** **40: 2826-2834.**

28. **Goldberg, I.J., Wagner, W.D., Pang, L., Curtiss, L.K., DeLozier, J.A., Shelness, G.S., Young, C.S., and Pillarisetti, S. 1998. The NH2-**

terminal region of apolipoprotein B is sufficient for lipoprotein assocation with glycosaminoglycans. *J. Biol. Chem.* 273: 35355-35361.

29. Boren J., Olin, K., Lee, I., Chait, A., Wight, T.N., and Innerarity, T.L. 1998. Identification of the principal proteoglycan-binding site in LDL. A single-point mutation in apoB100 severely affects proteoglycan interaction without affecting LDL receptor binding. *J. Clin. Invest.* 101: 2658-2664.

30. Flood, C., Gustafsson, M., Richardson, P.E., Harvey, S.C., Segrest, J.P., and Boren, J. 2002. Identification of the proteoglyacn binding site in apolipoprotein B48. *J. Biol. Chem.* 277: 32228-32233.

31. Dichek, H.L., Brecht, W., Fan, J., Ji, Z.S., McCormick, S.P., Akeefe, H., Conzo, L., Sanan, D.A., Weisgraver, K.., Young, S.G., et al. 1998. Overexpression of hepatic lipase in transgenic mice decreases apolipoprotein B-containing and high density lipoproteins. Evidence that hepatic lipase acts as a ligand for lipoprotein uptake. *J. Biol. Chem.* 273: 1896-1903.

32. Dichek, H.L., Johnson, S.M., Akeefe, H., Lo, G.T., Sage, E., Yap, C.E., and Mahley, R.W. 2001. Hepatic lipase overexpression lowers remnant and LDL levels by a noncatalytic mechanism in LDL receptor-deficient mice. *J. Lipid Res.* 42: 201-210.

33. Shimada, K., Gill, P.J., Silbert, J.E., Douglas, W.H., and Fanburg, B.L. 1981. Involvement of cell surface heparan sulfate in the binding of lipoprotein lipase to cultured bovine endothelial cells. *J. Clin. Invest.* 68: 995-1002.

34. Parthasarathy, N., Goldberg, I.J., Sivaram, P., Mulloy, B., Flory, D.M., and Wagner, W.D. 1994. Oligosaccharide sequences of endothelial cell surface heparan sulfate proteoglycan with affinity for lipoprotein lipase. *J. Biol. Chem.* 269: 22391-22396.

35. Spillmann, D., Lookene, A., and Olivercrona, G. 2006. Isolation and characterization of low sulfated heparan sulfate sequences with affinity for lipoprotein lipase. *J. Biol. Chem.* 281: 23405-23413.

36. Kinnunen, T., Raulo, E., Nolo, R., Maccarana, M., Lindahl, U., and Rauvala, H. 1996. Neurite outgrowth in brain neurons induced by heparin-binding growth-associated molecule (HB-GAM) depends on the specific interaction of HB-GAM with heparan sulfate at the cell surface. *J. Biol. Chem.* 27: 2243-2248.

37. Ledin, J., Staatz, W., Li, J.P., Gotte, M., Selleck, S., Kjellen, L., and Spillmann, D. 2004. Heparan sulfate structure in mice with genetically modified heparan sulfate production. *J. Biol. Chem.* 279: 42732-42741.

38. Safaiyan, F., Lindahl, U., and Salmivirta, M. 2000. Stuctural diversity of N-sulfated heparan sulfate domains: distinct modes of glucuronyl C5 epimerization, iduronic acid, 2-O-sulfation, and glucosaamine 6-O-sulfation. *Biochemistry* 39: 10823-10830.

39. Bai, X., and Esko, J.D. 1996. An animal cell mutant defective in heparan sulfate hexuronic acid 2-O-sulfation. *J. Biol. Chem.* 271: 17711-117717.

40. Merry, C.L., Bullock, S.L., Swan, D.C., Backen, A.C., Lyon, M., Beddington, R.S., Wilson, V.A., and Gallagher, J.T. 2001. The molecular phonetype of heparan sulfate in the Hs2st$^{-/-}$ mutant mouse. *J. Biol. Chem.* 276: 35429-35434.

41. Hudson, M.L., Kinnunen, T., Cinar, H.N., and Chisholm, A.D. 2006. C. elegans Kallmann syndrome protein KAL-1 interacts with syndecan and glypican to regulate neuronal cell migrations. *Dev. Biol.* 294: 352-365.

42. Bulow, H.E., Berry, K.L., Topper, L.H., Peles, E., and Hobert, O. 2002. Heparan sulfate proteoglycan-dependent induction of axon branching and axon misrouting by the Kallmann syndrome gene kal-1. *Proc. Natl. Acad. Sci., U.S.A.* 99: 6346-6351.

43. Bulow, H.E., and Hobert, O. 2004. Differential sulfations and epimerization define heparan sulfate specificity in nervous system development. *Neuron* 41: 723-736.

44. Kamimura, K., Koyama, T., Habuchi, H., Ueda, R., Masu, M., Kimata, K., and Nakato, H. 2006. Specific and flexible role of heparan sulfate modifications in Drosophila FGF signaling. *J. Cell. Biol.* 174: 773-778.

2.8 Supplementary Experimental Procedures

2.8.1 Heparan sulfate 2-O-Sulfotransferase Assay

Two embryos from each mouse genotype (zp*HS2st*$^{+/+}$, zp*HS2st*$^{+/-}$ *and zpHS2st*$^{-/-}$) were homogenized using Polytron organ homogenizer in 50mM MES (pH 6) containing protease inhibitors (Sigma). Each sample was centrifuged and the supernatant was used as the cell lysate and kept frozen at -80 ^{o}C. The HS2st enzymatic activity was measured as reported previously. Briefly, the 2-O-sulfotrasnferase assay (25 ml) contained: 50 mM MES (pH 6.5), 1% TX-100, 10 mM $MgCl_2$, 10 mM $MnCl_2$, 5 mM $CaCl_2$, 87.5 mM NaF, ~2.7 x 10^5 cpm/nmol [^{35}S]PAPS, 1 mg 2-O-desulfated heparin as an acceptor substrate and 150 mg cell lysate protein as the enzyme source. The reaction was incubated for 1 h at 37^{o}C and stopped by quenching with 0.1N EDTA. Standard chondroitin sulfate was added (2 mg) as a carrier and the volume was increased to 500 ml with water. The sample was applied to 0.25-ml column of DEAE-Sephacel in disposable polypropylene tips as described[2]. The column was washed with 10 ml of 0.25 M NaCl, 20 mM sodium acetate (pH 6.0) and eluted with 2.5 ml of a 1 M NaCl, 20 mM sodium acetate (pH 6.0). An aliquot (1 ml) was counted by liquid scintillation (Ultima Gold X-R, Packard BioScience). *P. Chrysogenum* APS Kinase was a kind gift from Dr. Irwin Segel, University of California, and was used to prepare [^{35}S]PAPS as described [3].

2.9 Supplementary Results

2.9.1 Generation of Conditional Hs2st mice.

Vertebrates contain one *HS2st* which is ubiquitously expressed in all tissue examined. Mice with a gene-trap mutation of the *HS2st* (*gtHS2st*$^{-/-}$) die in the neonatal period, exhibiting bilateral renal agenesis and defects of the eye and the skeleton. The onset of abnormalities in the *gtHS2st*$^{-/-}$ mice occurs only after midgestation. 2-O-sulfated uronic acid residues were not detected in the HS preparations from various organs of the *gtHS2st*$^{-/-}$ mice, demonstrating a complete loss of function of *HS2st* and also confirming that only one *HS2s*t isozyme exists in mouse genome. To study the role of *HS2st* at later developmental stage and in survival animal, a conditional allele of murine *HS2st was* generated by placing *loxP* recombination sites flanking exon 2 which encodes part of the 5'-UTR, the start codon, and 40 amino acids of the enzyme (*HS2st1*^{f}) (Fig. S1A). PCR analyses was developed to distinguish the conditional or mutant *HS2st* (*Hs2st*$^{-}$) from wild-type (*Hs2st*$^{+}$) by using Primers 1, 2 and -3. The DNA sequences of the Primers are: Primer 1 (5`-gtgcggccgtggggtcc-3`), Primer 2 (5`-atggggctcctcaggattatgatgc-3`), and Primer 3 (5`-tgccctaggctcaggcatg-3`). The primer pair P1/P3 generated PCR bands at 1178, 876 and 360 bp, corresponding to *HS2st*^{f}, *HS2st*$^{+}$ and *HS2st*$^{-}$ respectively (Fig. S1B). One line of *HS2st*$^{f/+}$ was established from the ES cell line. Interbreeding of *HS2st1*$^{f/+}$ mice yielded pups in the expected Mendelian ratio (23% +/+, 54% f/+, and 23% f/f, n = 70), indicating that the presence of the *loxP* recombination sites has no deleterious effect on survival of the *HS2st1*$^{f/f}$ mice.

2.9.2 Conditional inactivation of Hs2st

Conditional inactivation of the targeted *HS2st* was examined by interbreeding *HS2st1*$^{f/f}$ mice with transgenic *Zp3-Cre* mice, in which the expression of Cre recombinase is under control of the regulatory sequences of the mouse zona pellucida 3 (ZP3) gene[6]. The *Zp3-Cre* is exclusively expressed in the growing oocyte prior to the completion of the first meiotic division. The Cre-medicated recombination inactivated the single copy of *HS2st*^{f}, generating *HS2st*$^{-}$ mutant allel, and heterogyzous (*zpHS2st*$^{+/-}$*)* mice. The *zpHS2st*$^{+/-}$ mice thrived, reproduced normally, and were indistinguishable in health and behavior from wild-type littermates (*HS2st1*$^{f/+}$*Zp3-Cre*$^{-}$). The interbreeding of *zpHS2st1*$^{+/-}$ mice yielded pups in the expected Mendelian ratio (24% +/+, 53% f/+, and 23% f/f, n= 53) at birth, but the *zpHS2st*$^{-/-}$ neonates died within a day after birth, indicating the deficiency of *HS2st* is not compatible with life. Gross anatomy observed that the organs of *zpHS2st*$^{-/-}$ mice developed closely normal, except kidney agenesis (n = 10). The developmental defect and neonatal death phenotype of the *zpHS2st*$^{-/-}$ mice are similar to that of the reported *gtHS2st*$^{-/-}$ mice, indicating that the *HS2st*$^{f/f}$ can be efficiently excised by Cre-recombinase *in vivo*.

To establish the efficiency of Zp3-Cre-mediated inactivation of *HS2st*, genomic DNA was isolated from *zpHS2st*$^{+/+}$, *zpHS2st*$^{+/-}$ and *zpHS2st*$^{-/-}$ neonates, and examined by PCR analysis using primer pair P1/P2. As shown in **Fig. S1C**, both the wildtype band (876 bp) and deletion band (360 bp) are amplified from the *zpHS2st*$^{+/-}$ genomic DNA, but only the deletion band was generated from the *zpHS2st*$^{-/-}$ genomic DNA, demonstrating that that Zp3-Cre-mediated inaction of HS2st reached 100%

(**Fig. S1C**). This observation also confirmed the high efficiency of the Zp3-Cre-mediated inactivation *in vivo* as reported[6].

2.9.3 zpHs2st$^{-/-}$ mice exhibit reduced 2-O-sulfotransferase activity

Previous study characterized the *gtHS2st*$^{-/-}$ mice, uronate 2-O-sulfates were not detected in the mutant HS, indicating a complete loss of the HS2st function in the *gtHS2st*$^{-/-}$ mice and there is only one *HS2st*$^{-/-}$ isoenzyme in mouse genome. To establish the consequence of *HS2st* inactivation on HS 2-O-sulfotranse enzymatic activity in *zpHS2st*$^{-/-}$ mice, the whole neonate mouse bodies were homogenized and centrifuged, the supernatants were applied for measurement of 2-O-sulfotrasnferase activity using [^{35}S]PAPS as sulfate donor and 2-O-desulfated heparin as acceptor substrate. The assay was proportional to time up to 60 min and to the amount of tissue protein up to 300 μg[7, 8]. Radiation activity of the transferred [35]sulfate was measured. zp*HS2st*$^{+/+}$ showed the enzymatic activity at 3700 ± 650 cpm (mean ± SD), however the *zpHS2st*$^{-/-}$ had enzymatic activity at 700 ± 300 cpm, which was close, but above the background level, indicating there were residual 2-O-sulfotransferase activity in the *zpHS2st*$^{-/-}$ mice (Fig. S2A).

2.9.4 Hs2st$^{-/-}$ mice exhibit nearly complete absence of 2-O-sulfation

The observation of residual HS2st enzymatic activity in the *zpHS2st*$^{-/-}$ mice led to further examine HS composition. Total HS was extracted from neonates and digested into disaccharide residues for compositional analysis. Disaccharides from *zpHS2st*$^{+/+}$ and *zpHS2st*$^{-/-}$ embryos were compared to HS disaccharide standards for quantitation using an anion exchange/post column derivatizing method previously

described. The results demonstrated that of the four 2-*O*-sulfated disaccharides expressed in *zpHS2st*$^{+/+}$ HS, only small amounts of a disaccharide with a retention time consistent with DUA2S-GlcNS6S was detected in HS isolated from the *zpHS2st*$^{-/-}$ mice (Fig. S2B). Quantitation of the individual disaccharides showed that 2-O-sulfated species were reduced from 21% in the wild-type (*zpHS2st*$^{+/+}$) to 1.8% in the *zpHS2st*$^{-/-}$ mutant, showing > 90% reduction of 2-O-sulfate in *zpHS2st*$^{-/-}$ HS (Fig. S2B). To determine the identity of the species in the *zpHS2st*$^{-/-}$ sample which was co-eluted with the DUA2S-GlcNS6S standard in the anion exchange column, HS residues from both wild type and *zpHS2st*$^{-/-}$ embryos were analyzed using LC/MS. In the wild type sample, the mass spectra for DUA2S-GlcNS6S (Fig. 3A) shows six ions related to this species: (1) $[M-2H]^{-2}$, (2) $[M-3H+DBA]^{-2}$, (3) $[M-HSO_3]^-$, (4) $[M-H]^-$, (5) $[M-2H+DBA]^-$, and (6) $[M-3H+2DBA]^-$, with the *m/z* for the free molecular ion equal to 576. In the *zpHS2st*$^{-/-}$ HS, the same 6 species were detected thus confirming the presence of this disaccharide residue (Fig. 3B). Taken together, these results demonstrated that the *zpHS2st*$^{-/-}$ mice, while expressing no detectable DUA2S-GlcNS, still express a small amount (less than 20% of normal) of DUA2S-GlcNS6S disaccharide, and further suggested residual HS2st activity in the *zpHS2st*$^{-/-}$ mice. In mouse genome, only one *HS2st* exists. The residual HS2st activity is most likely from maternal source during the embryonic development.

2.10 Supplementary Figure Legends

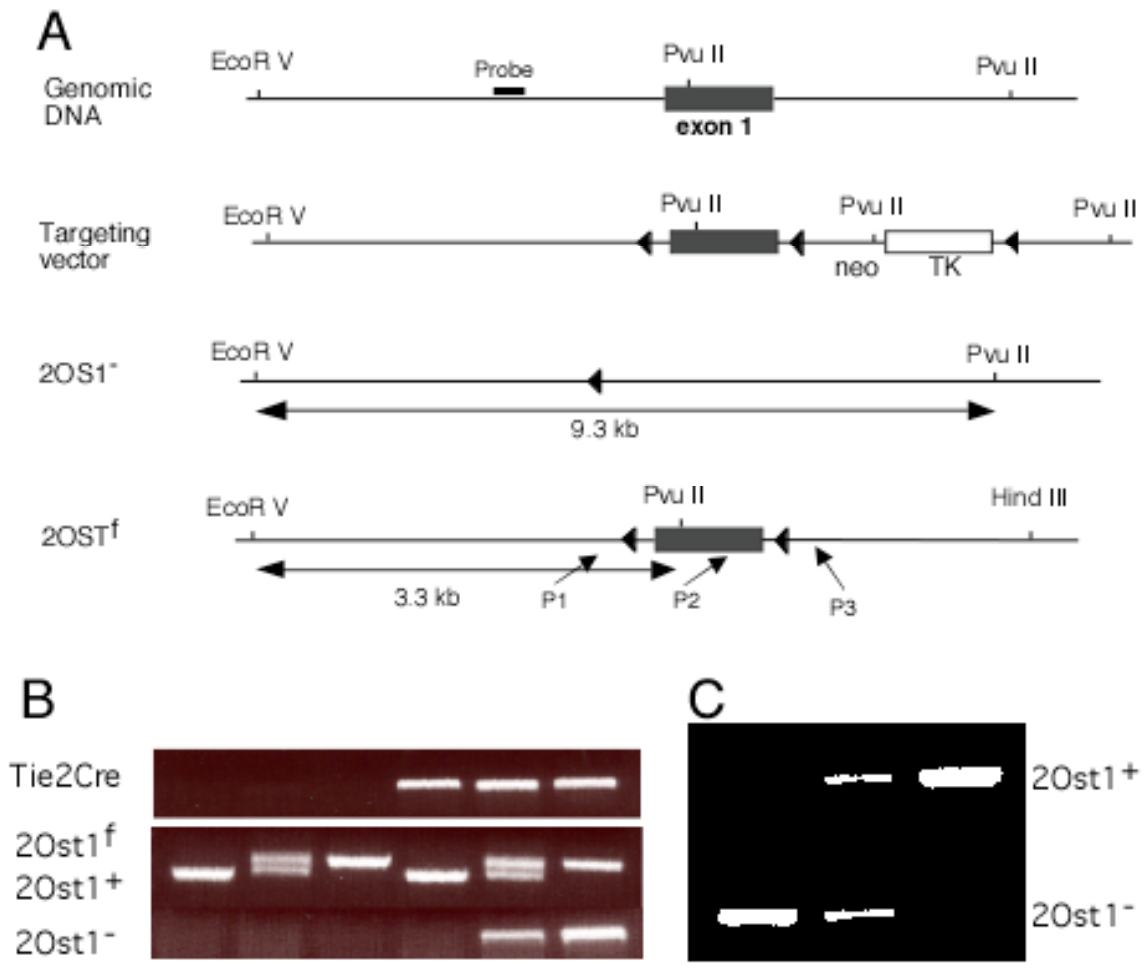
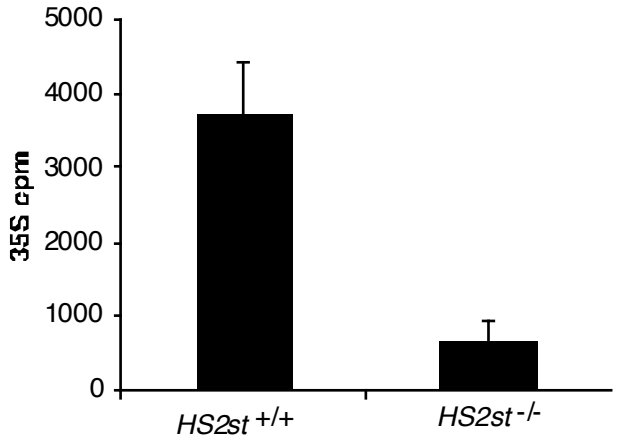


Figure 2-S1. Genotyping Hs2st mice. (A) Gene-targeting scheme. The genomic arrangement of exon 2, the targeting vector, the heterozygous allele, and homozygous null allele is depicted. (B) PCR analysis of DNA samples showing genotypes of *Hs2st*$^{f/+}$, *Hs2st*$^{+/+}$, and *Hs2st*$^{-/-}$ cells after Tie2Cre-mediated inactivation using primer pair P2/P3. (C) PCR analyses showing genotypes of *Hs2st*$^{+/-}$ and *Hs2st*$^{-/-}$ after ZP3Cre-mediated inactivation using primer pair P1/P3.



B

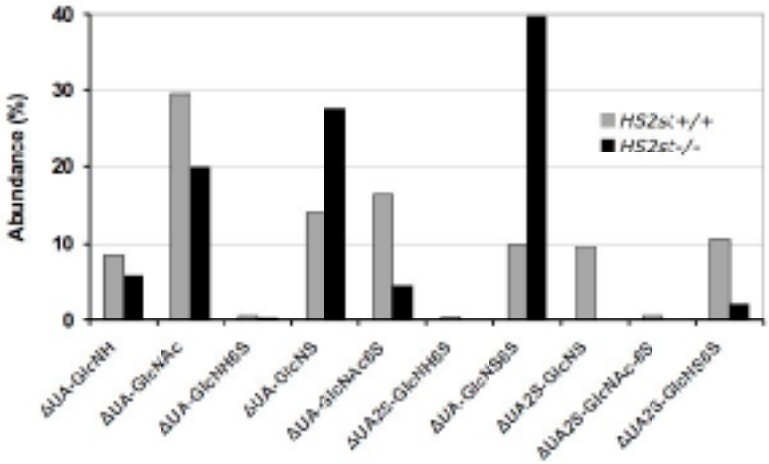


Figure 2-S2. Heparan sulfate 2-O-sulfotransferase enzyme activity and disaccharide analyses. Inactivation of Hs2st results in dramatically reduced heparan sulfate 2-O-sulfotransferase enzymatic activity and 2-O-sulfate groups in isolated heparan sulfate.

CHAPTER 3

SYNDECAN-1 IS THE PRIMARY HEPARAN SULFATE PROTEOGLYCAN MEDIATING HEPATIC CLEARANCE OF TRIGLYCERIDE-RICH LIPOPROTEINS *IN VIVO*

3.1 Summary

Diminished sulfation of heparan sulfate in hepatocytes results in accumulation of plasma triglyceride-rich lipoproteins. In this study, we sought to identify genetically the relevant heparan sulfate proteoglycan(s) in the liver that mediate lipoprotein clearance. RT-PCR analysis demonstrated the expression of the membrane proteoglycans syndecans-1, -2, and -4, and glypicans-1 and -4. Analysis of available proteoglycan-deficient mice showed that only syndecan-1 mutants (*Sdc1*$^{-/-}$) accumulated plasma triglycerides. *Sdc1*$^{-/-}$ mice also exhibited prolonged circulation of injected human VLDL and intestinally derived chylomicrons, and adenovirus containing syndecan-1 corrected the clearance defect *in vivo*. Crossbreeding mutants defective in syndecan-1 and heparan sulfate did not accentuate triglyceride accumulation, identifying syndecan-1 as the primary proteoglycan mediating clearance. Immunoelectron microscopy showed expression of syndecan-1 on the microvilli of hepatocyte basal membranes facing the space of Disse where lipoprotein uptake occurs. Syndecan-1 receptors are abundant on hepatocytes, exhibit saturable binding of VLDL and inhibition by heparin, and facilitate degradation of VLDL.

Adenovirus containing syndecan-1 corrected the clearance defect *in vivo* and restored binding, uptake, and degradation of VLDL in isolated hepatocytes. These findings provide the first in vivo genetic evidence showing that syndecan-1 is the primary hepatocyte proteoglycan receptor mediating the clearance of both hepatic and intestinally derived triglyceride-rich lipoproteins.

3.2 Introduction

Because elevated plasma triglycerides constitute an independent risk factor for premature atherosclerosis, much interest exists in determining the factors that affect their synthesis and turnover (1, 2). Circulating triglyceride-rich lipoproteins (TRLs) arise from dietary fats in the intestine (chylomicrons) and *de novo* synthesized lipids in the liver (VLDL). In the circulation, chylomicron and VLDL triglycerides undergo hydrolysis by lipoprotein lipase (LPL), which is immobilized on receptors on endothelial cells (3, 4). The surrounding tissues then take up the liberated free fatty acids for energy generation, membrane lipid synthesis, or storage as lipid droplets. Remnant lipoproteins arising from LPL-mediated lipolysis are cleared in the liver by multiple endocytic receptors, including the LDL receptor (LDLR) and heparan sulfate proteoglycans (HSPGs) (5-8). Recent genetic studies in mice demonstrated the importance of these two classes of receptors in TRL clearance *in vivo* (9, 10).

The identity of the physiologically relevant HSPG in hepatocytes that mediates remnant particle clearance in vivo has not been determined. Animal cells express multiple HSPGs, including four transmembrane syndecans, six glycosylphosphatidylinositol-linked-anchored glypicans, an alternatively spliced form

of CD44 (v3), TGF-β Type III receptors (betaglycan), and four secreted proteoglycans, perlecan, agrin, collagen XVIII, and serglycin (11). Syndecans (5-9, 12, 15, 20) have been shown to mediate the internalization of model remnant lipoproteins or TRL preparations enriched in LPL or apoE. Syndecan-1 can also mediate binding and uptake of chylomicron remnants by HepG2 liver cells *in vitro* based on antisense and antibody inhibition experiments (21). The evidence pointing to specific hepatic proteoglycans mediating TRL clearance *in vivo* is more indirect. Yu et al. (22) found that chylomicron remnants labeled with a fluorescent dye co-cluster with syndecan-1 on hepatocytes in the space of Disse, consistent with cell culture data indicating that clustering of syndecan may facilitate its internalization by endocytosis (15, 17). However, the authors opposed a functional role for syndecan-1 as a remnant receptor, suggesting that syndecan-1 acted merely as a chaperone to other receptors. As an added complication, overexpression of hepatic syndecan-1 in mice by infection with an adenoviral construct actually induced hyperlipidemia (23), but this may have reflected liver damage indicated by marked hepatocyte proliferation, cell-isolated apoptosis and increased plasma alanine aminotransferase (ALT) levels.

Determining the relevant HSPG in the liver and its functional role in remnant clearance is important since it would set the stage for further mechanistic studies of TRL uptake and processing and provide a candidate gene for allelic analysis in individuals with hypertriglyceridemia. In the current study, we examined available mutants in membrane HSPGs and found that mice deficient in syndecan-1 ($Sdc1^{-/-}$) had elevated plasma triglycerides under fasting conditions and exhibited delayed hepatic clearance of dietary triglycerides and injected VLDL. Reconstitution of

syndecan-1 expression in hepatocytes *in vivo* restored normal triglyceride metabolism. The absence of syndecan-1 in hepatocytes also caused a decrease in the binding, uptake, and degradation of VLDL particles in isolated primary hepatocytes. Our findings show that syndecan-1 is the hepatic HSPG receptor involved in TRL clearance.

3.3 Results

3.3.1 *Sdc1*$^{-/-}$ mice accumulate plasma triglycerides

To identify the relevant HSPGs in hepatic clearance, we first determined the array of proteoglycan core proteins expressed by murine hepatocytes. Quantitative reverse transcription polymerase chain reaction (qRT-PCR) using intron spanning primers to all of the known membrane proteoglycans (see Supplemental Table S1) showed that freshly purified hepatocytes expressed transcripts for syndecans -1, -2, and -4 and glypicans -1 and -4 (n = 3) (Fig. 3-1A). Since the probe sets were validated with preparations of RNA from other tissues, the absence of detectable mRNA for other proteoglycans (e.g. syndecan-3, other glypicans, betaglycan and CD44v3) was judged significant.

Of the five membrane proteoglycan transcripts detected in hepatocytes, mutants containing systemic null alleles for syndecans-1 and -4 were available for further study. Analysis of fasted animals showed that only *Sdc1*$^{-/-}$ mice had elevated

plasma triglycerides, which were approximately two-fold higher compared to wild-type mice (95 + 11mg/dl in *Sdc1*$^{-/-}$ mice (n = 13) vs. 44 + 19 mg/dl in wild-type mice (n = 14); $P < 0.0001$). As an added control we examined *Sdc3*$^{-/-}$ mice and found that they had normal plasma triglyceride levels (n = 8) (Fig. 3-1B). Plasma cholesterol levels were unaffected in *Sdc1*$^{-/-}$ mice (70 + 1mg/dl in *Sdc1*$^{-/-}$ (n = 13) vs. 74 + 5mg/dl in the wild type (n = 14); $P = 0.3782$).

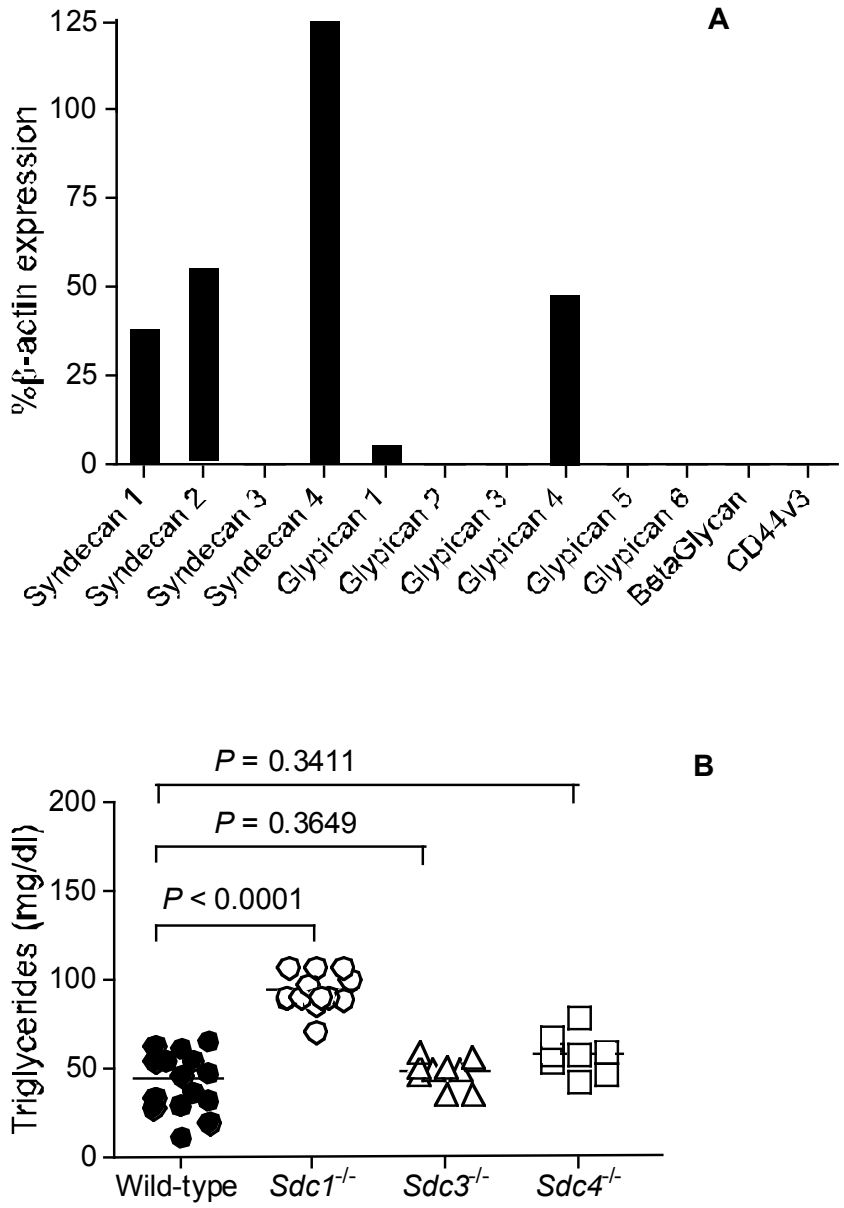


Figure 3-1. RT-PCR analysis of membrane HSPGs and hypertriglyceridemia in *Sdc1-/-* mice. (A) Transcript levels of the membrane proteoglycan core proteins were measured in isolated hepatocytes. The numbers represent the level of expression compared to the housekeeping gene β-actin, using C_T values from triplicate assays according to Stratagene manual. Error bars are not shown because they are factored into the final calculation. Comparable results were obtained in two independent assays. (B) Triglycerides were measured in plasma samples from fasted male and female mice of indicated genotypes. Wild-type (n = 14), *Sdc1*$^{-/-}$ (n =13), *Sdc3*$^{-/-}$ (n = 10), *Sdc4*$^{-/-}$ (n = 8) (horizontal bars indicate mean values).

Buoyant density ultracentrifugation of fasting plasma lipoproteins from *Sdc1*$^{-/-}$ and wild-type mice showed that triglyceride accumulation occurred in particles of $\delta <$ 1.006 g/ml and δ = 1.006 - 1.019 g/ml in *Sdc1*$^{-/-}$ mice, whereas LDL and HDL triglycerides were unaffected (Fig. 3-2A). Only minor differences in the amounts of cholesterol in the separated lipoprotein classes was noted (Fig. 3-2B). Analysis of the lipoproteins by gel filtration fast-phase liquid chromatography (FPLC) showed that the triglyceride-rich particles eluted like chylomicron remnants and VLDL with no obvious change in cholesterol content (Fig. 3-2C and D). A small increase in cholesterol was noted in small high density particles, but this material has not been characterized further. Analysis of lipoproteins of $\delta <$ 1.019 g/ml by SDS-PAGE showed they had apoB-48, apoB-100, apoE and apoCs, characteristic of VLDL particles and chylomicron remnants (data not shown). The apolipoprotein composition of these lipoproteins is the same as that observed in Ndst1$^{f/f}$AlbCre^{+} mice which produce undersulfated chains in liver hepatocytes (9).

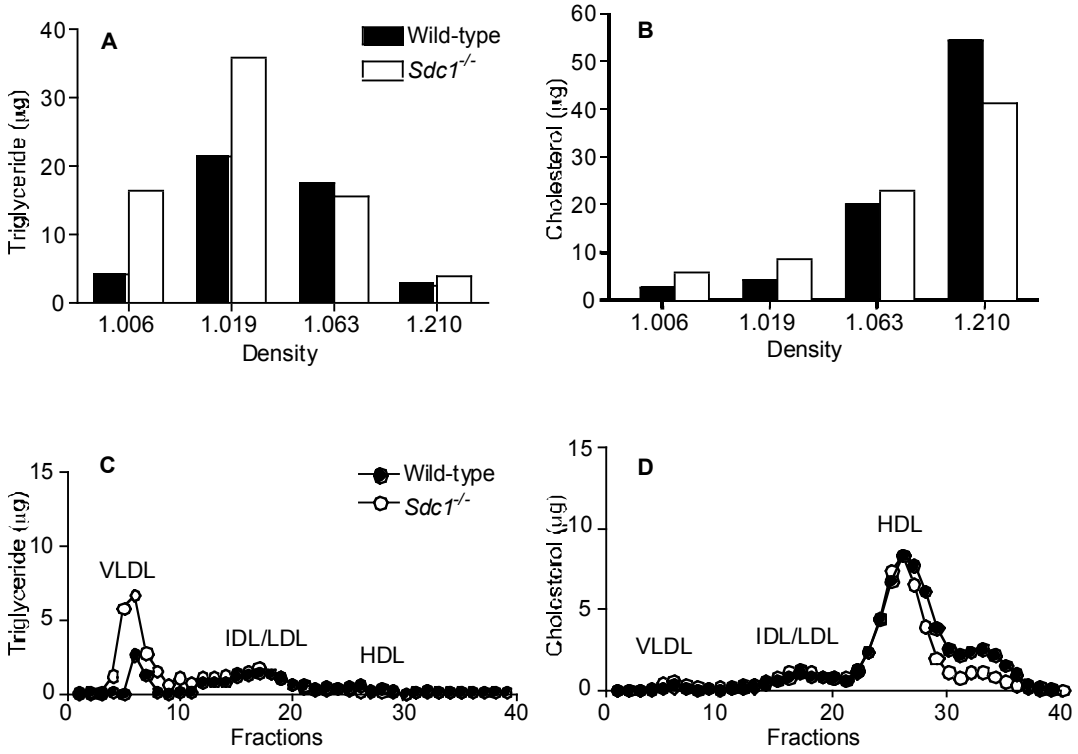


Figure 3-2. Hypertriglyceridemia and delayed plasma clearance of VLDL in *Sdc1*$^{-/-}$ mice. Triglyceride (A) and cholesterol (B) were measured in lipoprotein subclasses separated by preparative density ultracentrifugation. Each value is from pooled plasma derived from 10 mice. Plasma Triglycerides (C) and cholesterol (D) were also analyzed by FPLC. Wild-type, filled circles; *Sdc1*$^{-/-}$, open circles.

3.3.2 *Sdc1*$^{-/-}$ mice exhibit delayed plasma clearance of both VLDL and dietary triglycerides

Prior studies showed that mice bearing a defect in sulfation of hepatic heparan sulfate displayed altered hepatic clearance of triglycerides, suggesting that *Sdc1*$^{-/-}$ mice might exhibit a similar phenotype (9). VLDL clearance was therefore measured by intravenous injection of a bolus of human VLDL and periodic blood sampling to measure the circulating level of human VLDL by ELISA using mAb MB47, which is specific for human apoB-100. As shown in Fig. 3-3A, the initial rate of clearance of

VLDL was reduced about 2-fold in *Sdc1*$^{-/-}$ mice compared to the wild-type ($t_{1/2}$ = 92 ± 18 min in *Sdc1*$^{-/-}$ mice vs. 46 ± 7 min in wild-type mice, determined by extrapolation, P = 0.0009, n = 6). Although the absolute clearance rates differed from previous data obtained from studies of Ndst1-deficient mice, the fold difference between mutant and wildtype mice was comparable (9).

The clearance rate of intestinally-derived TRLs was also measured by vitamin A-excursion studies. Fasted mice were given a bolus mixture of [^{3}H]retinol and corn oil by oral gavage, and blood was sampled at various time points to determine the plasma level of ^{3}H-counts. In the intestine, [^{3}H]retinol is converted to fatty acid esters and incorporated into newly made chylomicrons and its only route of removal is through clearance in the liver. As shown in Fig. 3-3B, the area under the curve for *Sdc1*$^{-/-}$ mice (open circles) was 2-fold greater than the wild-type (filled circles) (area under the curve (AUC) = 8400 vs. 4100), indicating that the mutant cleared intestinally derived lipoproteins at a slower rate (P = 0.0034). After 12 hours, most of the tracer had been cleared in both mutant and wild-type animals, consistent with previous data showing that LDL receptors also can clear plasma TRLs (9, 34, 37). The data presented in Figs. 3-3A and 3-3B indicate that syndecan-1 plays a key role in the clearance of both hepatic (VLDL) and intestinally-derived TRLs.

Since *Sdc1*$^{-/-}$ mice were created by conventional gene targeting methods, syndecan-1 expression was diminished in all tissues. Thus, to directly test the role of hepatic syndecan-1 in hepatic clearance, *Sdc1*$^{-/-}$ mice were intravenously injected with adenovirus containing either *Sdc1* or *GFP* cDNAs. Under these conditions, more than 95% of the adenovirus is cleared by the liver (38), leading to hepatic-specific

expression of Sdc1. Three weeks after infection, a bolus of [^{3}H]retinol and corn oil was administered by gavage and the rate of clearance was measured. Infection with AdSdc1 partially restored expression of Sdc1 (Supplemental Fig. 3-S1A), but nevertheless normalized clearance compared to *Sdc1*$^{-/-}$ mice infected with AdGFP (P = 0.0037) and the excursion curve was similar to wild-type mice (Fig. 3-3C). These findings show that hepatic syndecan-1 is both necessary and sufficient to clear plasma triglycerides. These findings contrast a previous study showing that syndecan-1 overexpression leads to hypertriglyceridemia , which may reflect differences in viral load or timing of the lipid analyses relative to viral infection.

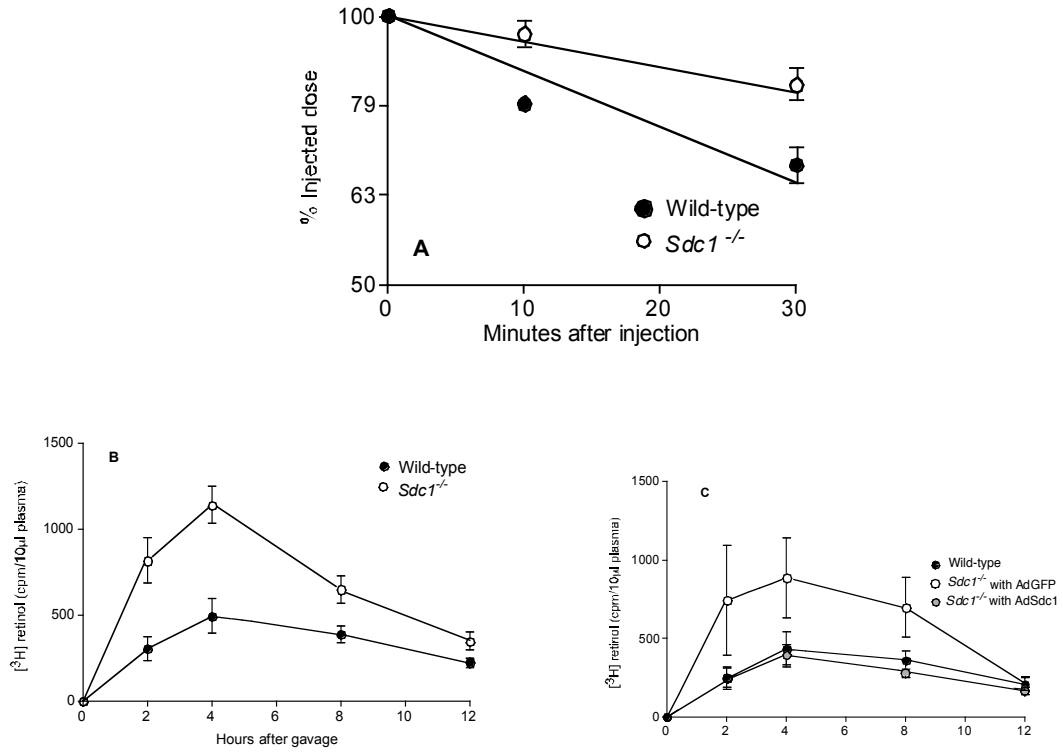


Figure 3-3. *Sdc1*$^{-/-}$ mice exhibit delayed plasma clearance of dietary triglycerides. (A) Plasma clearance of human VLDL apoB-100 was measured by ELISA using human apoB-100-specific monoclonal antibody MB47 (see Methods). Representative data from three different experiments is shown. Wild-type mice (filled circles; $t_{1/2}$ = 46 min; *n* = 6 mice); *Sdc1*$^{-/-}$ mice (open circles; $t_{1/2}$ = 92 min; *n* = 6 mice). The difference in $t_{1/2}$ between the genotypes was significant (P = 0.0009). (B) Retinol ester clearance was measured at the times indicated in wild-type (filled circles, n= 3), and *Sdc1*$^{-/-}$ (open circles, *n* = 3) mice. Animals were fasted for 4 hours in the morning and given 200 µl of corn oil containing 5.4 µCi [^{3}H] retinol by gavage. Blood samples were taken at the indicated times, and radioactivity remaining in 10 µl of serum was determined by scintillation counting. The values are expressed as mean + SD. Clearance was significantly delayed in the *Sdc1*$^{-/-}$ mice compared to wild-type (*P* = 0.0034). (C) *Sdc1*$^{-/-}$ mice were injected with AdSdc1 (filled circles; 4 x 10^{11} particles per mouse; *n* = 6 mice) or AdGFP (open circles; 4 x 10^{11} particles per mouse, *n* = 6 mice). Plasma retinol ester levels were measured at the times indicated. Animals treated with AdSdc1 demonstrated clearance similar to that of wild-type animals (grey circles, *P* = 0.1272) and significantly faster than that of *Sdc1*$^{-/-}$mice treated with AdGFP (*P* = 0.0037).

3.3.3 Syndecan-1 is the primary heparan sulfate proteoglycan mediating clearance

The selective hyperlipidemia in *Sdc1*$^{-/-}$ mice resembles the phenotype of *Ndst1*$^{f/f}$*AlbCre*$^{+}$ mice, which produce undersulfated heparan sulfate chains in hepatocytes due to a deficiency of a specific sulfotransferase, *N-deacetylase/N-sulfotransferase-1* (*Ndst1*). To test if other hepatocyte HSPGs can affect plasma triglyceride levels, *Sdc1*$^{-/-}$ mice were interbred with *Ndst1*$^{f/f}$*AlbCre*$^{+}$ mice, which results in undersulfation of heparan sulfate chains on syndecan as well as other hepatocyte derived proteoglycans. Analysis of fasting plasma triglycerides showed that compounding the mutations did not result in accumulation of triglycerides to a greater extent than in either single mutant (Fig. 3-4A, compare open circles and open squares; $P = 0.1373$). The double mutant also displayed delayed [^{3}H]retinol clearance of to the same extent as in *Sdc1*$^{-/-}$ and *Ndst1AlbCre*$^{+}$ mutants (Fig. 3-4B). The slightly diminished effect in the double mutant was not significant ($P = 0.6670$). These data indicate that the heparan sulfate chains on syndecan-1 are responsible for plasma triglyceride clearance mediated by hepatic proteoglycans.

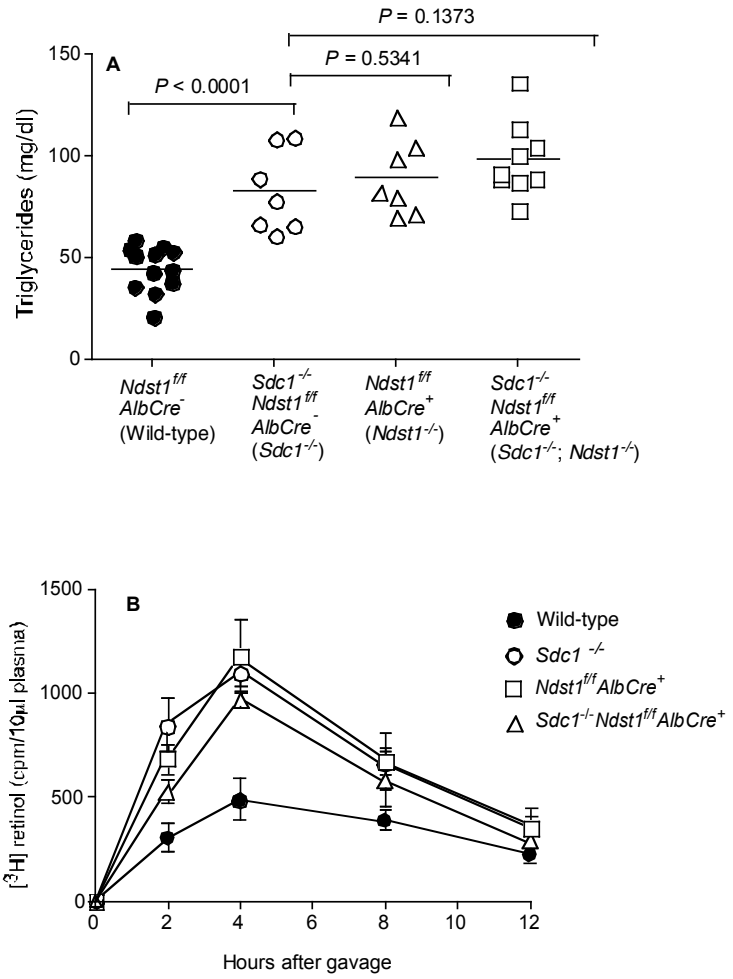


Figure 3-4. Hypertriglyceridemia in *Sdc1*$^{-/-}$ and *Ndst1*$^{f/f}$*AlbCre*$^{+}$ mice is not additive. (A) Plasma triglycerides were measured in plasma samples from fasted mice. There was no difference in plasma triglycerides in *Sdc1*$^{-/-}$*Ndst1*$^{f/f}$*AlbCre*$^{+}$ (n = 9), *Sdc1*$^{-/-}$ *Ndst1*$^{f/f}$*AlbCre*$^{-}$ (n = 7), and *Ndst1*$^{f/f}$*AlbCre*$^{+}$ (n = 7) mice, although all three genotypes were significantly elevated above the wild-type, *Ndst1*$^{f/f}$*AlbCre*$^{-}$ (n = 13). (B) Retinol ester excursions were measured at the times indicated in wild-type (filled circles, n= 3), and *Sdc1*$^{-/-}$ (open circles, n = 3), *Ndst1*$^{f/f}$*AlbCre*$^{-}$ (filled circles, n = 3), and *Sdc1*$^{-/-}$ *Ndst1*$^{f/f}$*AlbCre*$^{+}$(open circles, n = 3) mice. Animals were fasted for 4 hr in the morning and given 200 µl of corn oil containing 5.4 µCi [^{3}H] retinol by gavage. Blood samples were taken at the indicated times, and radioactivity remaining in 10 µl of serum was determined by scintillation counting. The values are expressed as mean + SD. Clearance was significantly delayed in the *Sdc1*$^{-/-}$ mice compared to wild-type (P = 0.0034), while the difference observed between *Sdc1*$^{-/-}$ and *Sdc1*$^{-/-}$*Ndst1*$^{f/f}$*AlbCre*$^{+}$ animals was not significant (P = 0.1373).

3.3.4 Syndecan-1 is localized on microvilli of hepatocytes in the space of Disse

Based on these results, we predicted that syndecan-1 should be located on basal membrane of the hepatocytes facing the space of Disse. Immunofluorescence micrographs of cryosections prepared from *Sdc1*$^{-/-}$ livers revealed no staining, confirming the specificity of the antibody (Fig. 3-5B). Sections prepared from wild-type mouse livers showed syndecan-1 localization around the sinusoids (Fig. 3-5A), as reported previously (39, 40). Additionally, sections prepared from *Ndst1*$^{f/f}$*AlbCre*$^{+}$mice indicated that syndecan-1 was localized around the sinusoids as in wild-type liver sections, indicating that altering the sulfation of the heparan sulfate chains has not effect on distribution of Sdc1 (data not shown). In contrast to these findings, syndecan-2 was present mainly on sinusoidal endothelial cells, whereas syndecan-4 was ubiquitously expressed over the entire hepatocyte surface (data not shown). Electron microscopy of immunogold-labeled sections showed enrichment of syndecan-1 on the microvilli extending from the basal surface of the hepatocytes (Fig. 3-5C). Thus, syndecan-1 is positioned appropriately to encounter remnant TRLs entering the space of Disse.

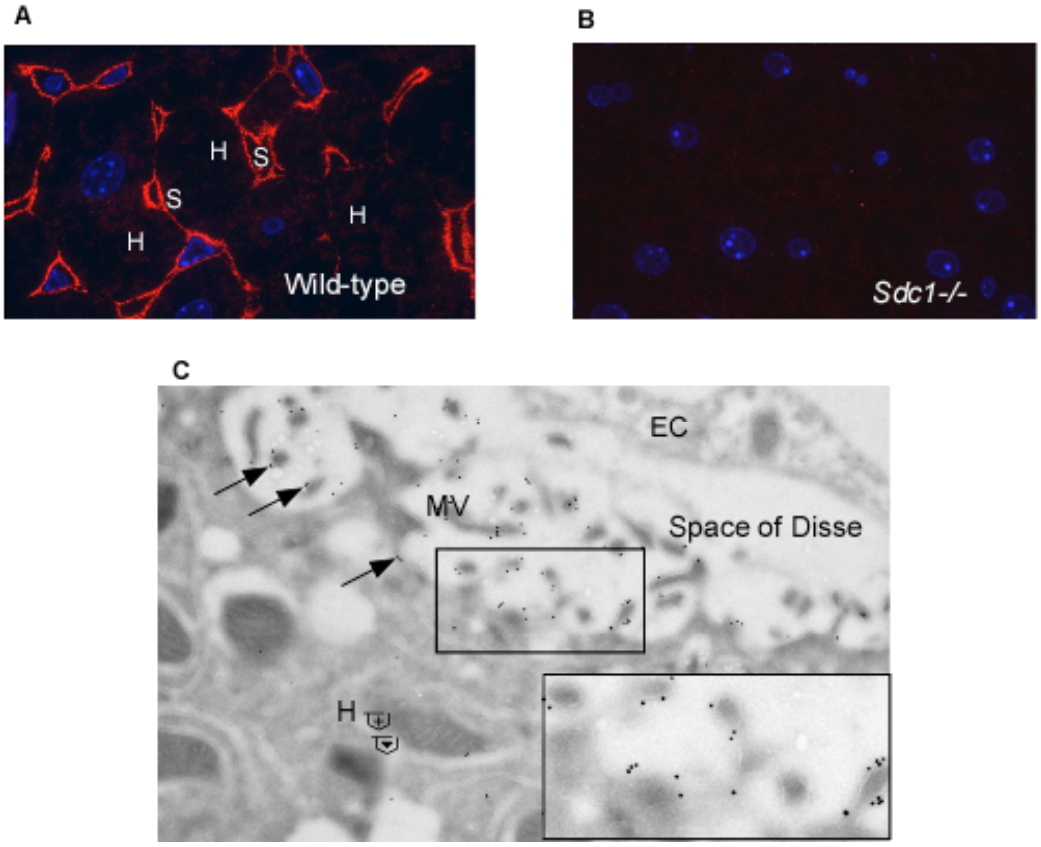


Figure 3-5. Syndecan-1 is localized on microvilli of hepatocytes in the space of Disse. (A) Immunofluorescence micrographs of wild-type mouse livers stained with rabbit polyclonal antibody to syndecan-1 and goat anti-rabbit secondary antibody conjugated to Alexa fluor-594 (red). Nuclei were stained with DAPI (blue). Syndecan-1 was localized around the sinusoids (H, hepatocytes, S, sinusoid). (B) *Sdc1*$^{-/-}$ livers were used as a control to show specificity of the syndecan-1 antibody. (C) Electron microscopy of immunogold-labeled sections revealed syndecan-1 on the microvilli extending from the basal surface of the hepatocytes.

3.3.5 Syndecan-1 can mediate binding, uptake and degradation of VLDL

To determine if syndecan-1 could directly mediate binding of unmodified VLDL, hepatocytes were isolated from wild-type mice and incubated with ^{125}I-VLDL at 4^{o}C. Normal hepatocytes bound VLDL in a saturable manner, and the signal was reduced by the addition of heparin (Fig. 3-6A). Specific binding was then determined

by subtracting the counts obtained in the presence of heparin from the counts obtained in its absence (Fig. 6A, broken line). Fitting the data to a conventional single-site binding equation yielded a B_{max} value of 8.2 ± 1.1 μg VLDL protein/mg cell protein (~1.4 x 10^6 sites per cell) and a K_D of 43 ± 10 μg/ml (~2.2 nM) (R^2 = .9760), assuming that the average size particle had a diameter of 40 nm, a mass of 2 x 10^7 Da, and that protein represents 1.8% of the mass. Binding was also sensitive to dilution with non-radioactive VLDL, yielding specific binding data that was comparable to that obtained by heparin inhibition (Fig.3-6B, circles) (B_{max} value of 9.1 ± 1 μg VLDL protein/mg cell protein and a K_D of 51 ± 9 μg/ml, R^2 = .9871). To determine if binding depended on syndecan-1, hepatocytes were isolated from *Sdc1*$^{-/-}$ mice and challenged with ^{125}I-VLDL. As shown in Fig. 3-6B (squares), the absence of syndecan-1 significantly reduced binding compared to wild-type hepatocytes. Specific binding was reduced on average by 6 ± 1-fold (Fig. 3-6C). These findings are consistent with previous studies of other cell types and modified lipoproteins (15, 20, 21).

Prior studies also have shown that Sdc1 can mediate lipoprotein uptake and degradation (15, 17). Therefore, we examined uptake and degradation of VLDL by incubating wild-type and mutant hepatocytes with 20 μg/ml of ^{125}I-VLDL at 37^{o}C. After one hour, wild-type cells bound and internalized 4.1 ± 0.4 μg VLDL/mg cell protein (Fig. 3-7A), which was ~30% higher than the amount bound at 4^{o}C (3.2 μg/mg cell protein at 20 μg/ml VLDL, Fig. 3-6B). Uptake via syndecan-1 led to degradation of 2.4 μg/mg of cell protein in one hour, as measured by the appearance of acid-soluble, non-chloroform extractable ^{125}I-counts in the growth medium. *Sdc1*$^{-/-}$ hepatocytes showed a dramatic decrease in both uptake (1.5 ± 0.4 μg VLDL/mg cell

protein; $P < .005$) and degradation (0.4 ± 0.1 μg VLDL/mg cell protein; $P < 0.02$) under these conditions.

To confirm that altered uptake and degradation in *Sdc1*$^{-/-}$ hepatocytes resulted from loss of syndecan-1, we analyzed hepatocytes isolated from *Sdc1*$^{-/-}$ mice infected with AdSdc1 or AdGFP. AdSdc1-treated hepatocytes showed increased binding, uptake, and degradation of ^{125}I-VLDL compared to hepatocytes derived from mice treated with AdGFP (Fig. 3-7B; $P < 0.02$). Finally, we examined uptake and degradation in hepatocytes derived from mice deficient in LDL receptors and in combination with a deficienct of Ndst1. As shown in Fig. 3-7C, the LDL receptor contributes to binding and uptake, but to a lesser extent that Together, these data indicate that syndecan-1 accounts for the majority of ^{125}I-VLDL bound, taken up, and degraded by wild-type cells.

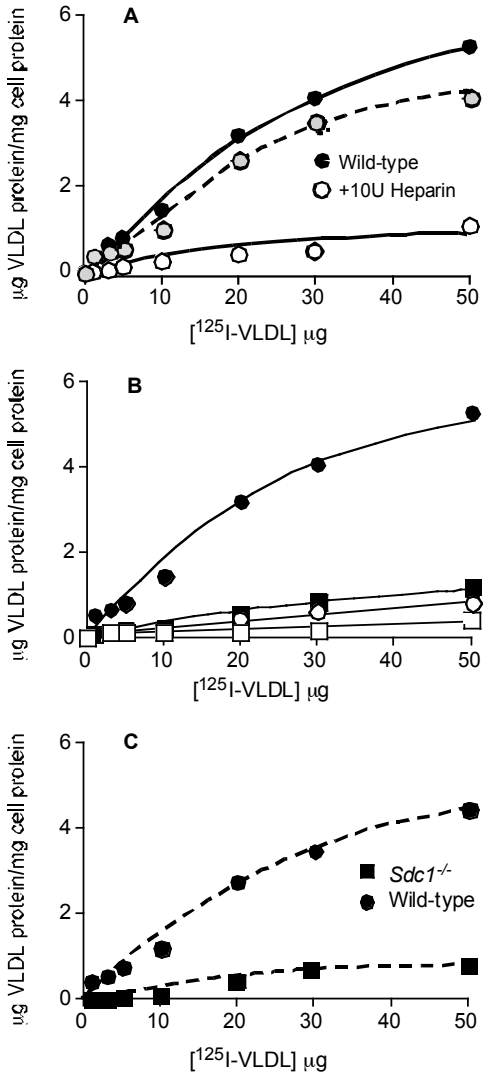


Figure 3-6. Syndecan-1 mediates binding of VLDL. (A) Wild-type cells were incubated with the indicated concentrations of ^{125}I-VLDL the absence (filled circles) or presence (open circles) of 10 U heparin for 1 hour at 4°C. The amount of binding observed in the presence of heparin was subtracted from the total to obtain specific binding (dashed curve). (B) Wild-type (filled circles) and *Sdc1*$^{-/-}$ (filled squares) hepatocytes were incubated with the indicated concentrations of ^{125}I-VLDL for 1 hour at 4°C. A parallel set of cells was incubated under identical conditions with 250 μg/ml of non-radioactive VLDL. Addition of non-radioactive VLDL decreased binding in wild-type hepatocytes (open circles) to nearly the level measured in *Sdc1*$^{-/-}$ cells (open squares). (C) The counts bound in the presence of excess non-radioactive VLDL in panel B were subtracted from the data and the net counts were converted to μg VLDL protein bound/mg of cell protein based on radiospecific activity of the particles (140 cpm/ng). Deletion of syndecan-1 reduced maximal binding.

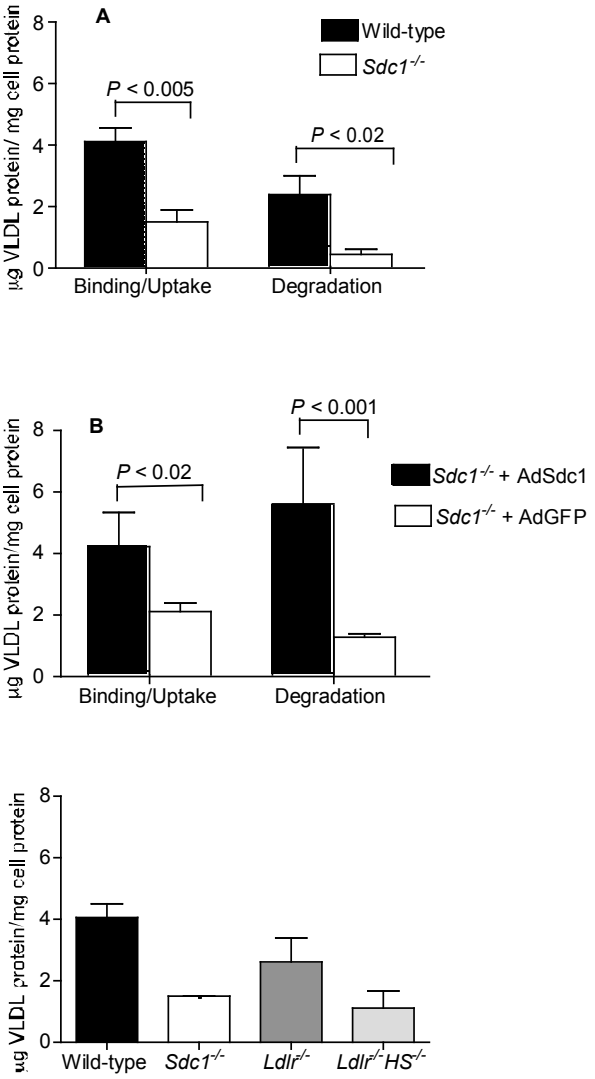


Figure 3-7. Binding, uptake and degradation of VLDL at 37°C. (A) Uptake and degradation of VLDL was measured in wild-type (filled bars) and mutant (open bars) hepatocytes after 1 hr incubation with 20 µg/ml of ^{125}I-VLDL. The bars represent the sum of binding and internalization under these conditions, or the amount of degradation as determined by acid soluble, non-chloroform extractable counts in the medium. Binding plus uptake was reduced 2.7 fold in *Sdc1*$^{-/-}$ cells. Degradation was reduced by nearly 6-fold. (B) Hepatocytes isolated from *Sdc1*$^{-/-}$ mice treated with AdSdc1 (filled bars) showed enhanced binding and uptake and increased degradation of ^{125}I-VLDL compared to hepatocytes isolated from *Sdc1*$^{-/-}$ mice treated with AdGFP (open bars) ($P < 0.02$).

3.4 Discussion

The major finding presented in this report is that syndecan-1 mediates hepatic clearance of TRLs *in vivo*. This conclusion is based on the observation that TRLs resembling VLDL and VLDL remnants accumulate in fasted *Sdc1*$^{-/-}$ mice (Figs. 3-1 and 3-2) and that the mutant exhibits delayed clearance of TRLs derived from dietary fat (Fig. 3-3). Importantly, syndecan-1 appears to be the principal hepatic HSPG involved in TRL clearance since compounding the syndecan-1 deficiency with a mutation that affects sulfation of all heparan sulfate chains on hepatocyte HSPGs did not increase the extent of triglyceride accumulation (Fig. 3-4). Syndecan-1, poised on the microvilli of hepatocytes (Fig. 3-5), can encounter circulating TRLs that enter the space of Disse. Binding to syndecan-1 showed saturability and inhibition by heparin (Fig. 3-6), and increasing the expression of syndecan-1 by viral transduction corrected the deficiency in postprandial clearance in the mutant (Fig. 3-3C) and enhanced the uptake and degradation of VLDL in isolated hepatocytes (Fig. 3-7). Taken together, these data provide direct genetic evidence that syndecan-1 is the primary hepatic proteoglycan receptor mediating TRL clearance.

Our genetic studies of hepatic heparan sulfate proteoglycans extend previous observations showing that syndecans can mediate lipoprotein uptake in cultured cells. Fuki et al introduced several syndecan core proteins into Chinese hamster ovary cells, which increased cell association and degradation of lipoproteins enriched in lipoprotein lipase, a protein that may mediate binding to the heparan sulfate chains on syndecan-1 (15). Subsequently, Zeng et al. showed by antisense and antibody inhibition that the

uptake of chylomicron remnants by HepG2 liver cells was mediated in part by syndecan-1 (21). Uptake by cultured cells depends on the heparan sulfate chains based on analysis of mutants altered in heparan sulfate biosynthesis, treatment of cells with heparinases that degrade the heparan sulfate chains, or pharmacological manipulation of glycosaminoglycan biosynthesis. Conversely, overexpression of human syndecan-1 increased binding and uptake of VLDL by human fibroblasts (20). The data presented here demonstrates that TRL binding and uptake in the liver occurs by way of syndecan-1 and establishes the physiologically relevance of these earlier findings *in vivo*.

Syndecan-1, first described by Merton Bernfield and colleagues on mammary epithelial cells, is a trans-membrane proteoglycan of diverse function, mediating cell adhesion and motility, growth factor activation, tumor growth, and microbial infection (41-47). Like other proteoglycans, syndecan also undergoes endocytosis and degradation in lysosomes (48). Thus, ligands bound to the heparan sulfate chains can "piggy-back" into the cell (5), which operationally defines syndecan-1 as an endocytic receptor of broad specificity. Syndecan-1 also undergoes proteolytic processing, resulting in shedding of ectodomains containing the attached glycosaminoglycan chains (49). Although to our knowledge the shedding process has not been studied in liver, cultured hepatocytes accumulate ectodomains in the conditioned medium (J.R.B. and J.D.E., unpublished results). This finding raises the possibility that shed syndecan-1 ectodomains might bind plasma lipoproteins in the space and Disse and either prevent

their escape back into the plasma or facilitate their further processing prior to uptake. The fact that compounding syndecan-1 deficiency with a mutation that affects all heparan sulfate chains produced by hepatocytes has no greater effect on lipoprotein clearance than either mutation alone (Fig. 3-4) would suggest that syndecan-1 could also be responsible for sequestration of lipoproteins in the space of Disse as suggested previously (6-8, 50, 51).

Syndecan-1 has three attachment sites for heparan sulfate clustered near its N-terminus and up to two chondroitin chains located in the membrane proximal region, although the glycosaminoglycan composition of liver syndecan-1 has not been determined. The binding of TRLs to the heparan sulfate chains presumably occurs through electrostatic interactions between negatively charged sulfate and carboxyl groups with complementary positively charged domains in the apolipoproteins (apoB and apoE) or lipases (lipoprotein lipase or hepatic lipase) associated with the particles. In general, only 8-12 monosaccharide residues are needed to bind to many proteins, including LPL and apoE (52-55), but the pattern of sulfate groups and uronic acids that mediate TRL binding is unknown. Liver heparan sulfate is unusual in that it contains more highly sulfated chains than heparan sulfate in other tissues (56). Thus, the high degree of sulfation of the heparan sulfate chains in hepatocyte syndecan-1 might ensure selective binding of remnant lipoprotein particles to liver syndecan-1. Binding and/or internalization might depend on the multiple interactions between one or more chains on syndecan-1 or syndecan multimers with multiple protein ligands

associated with the particles. Clustering of syndecan may in fact trigger internalization by endocytosis (15, 17).

The abundance of VLDL binding sites on isolated hepatocytes is also interesting. We estimate from saturation binding curves that wild-type cells express over a million VLDL binding sites, and that syndecan-1 apparently accounts for the majority of them (Fig. 3-6). In most cells, endocytosis of syndecans occurs in a clathrin-independent manner with relatively slow kinetics ($t_{1/2}$ = 20-60 min) (17, 20, 58) compared to clathrin-mediated uptake of ligands, e.g. uptake of LDL by LDL receptors ($t_{1/2}$ = 5-10 min) (59). Since LDL receptors are much less abundant (~10^4 - 5 x 10^4 receptors/cell) than syndecan-1 receptors (~10^6 receptors/cell), their faster rate of internalization offsets the higher level of expression of syndecan, resulting in equal contribution to uptake and clearance. Additional studies of binding, uptake and degradation in isolated hepatocytes are underway to obtain more quantitative data, but our studies of heparan sulfate-deficient and LDL receptor-deficient mice confirm that these two receptors appear to work with comparable efficiency (9).

A third class of receptors, LDL receptor related proteins (LRPs), have also been implicated in TRL clearance (60). LRP apparently can form a complex with HSPGs (61) and modulate their capacity to bind VLDL. However, inactivation of LRP1 or LRP5 in hepatocytes has no effect on fasting plasma triglyceride levels (60, 62), whereas inactivation of syndecan-1 increases fasting triglycerides, suggesting that syndecan-1 most likely acts independently of LRP receptors under these conditions. LRPs may aid in the metabolism of lipoproteins after dietary challenge or under conditions where other receptors are occupied or rendered non-operational (60, 62).

Sorting out the relative contribution of these receptors will require studies of various double mutants lacking syndecan-1, LDLR and LRPs (K.I.S. and J.D.E, unpublished results). Whether these three receptors undergo coordinate regulation dependent on plasma triglyceride levels remains unknown. Preliminary experiments show that the relative expression of mRNAs for LDLR and LRP1 in hepatocytes of *Sdc1*$^{-/-}$ mice are not elevated compared to transcripts in wild-type hepatocytes (K.I.S. and J.D.E., unpublished results). However, this issue needs to be examined in double mutants fed normal and high fat diets.

In conclusion, we have determined that syndecan-1 acts as a primary receptor for remnant TRL clearance in the liver. While further work needs to be done to determine the relative contribution of syndecan-1 and other receptors to TRL clearance, the data presented here suggests that mutations affecting the expression of syndecan-1 or the assembly of the heparan sulfate chains could explain some forms of human dyslipidemias. Studies of patients with unexplained hypertriglyceridemia are underway to explore this possibility.

3.5 Experimental Procedures

3.5.1 Mice and Animal Husbandry

Mice deficient in syndecan-1 (*Sdc1*$^{-/-}$), syndecan-3 (*Sdc3*$^{-/-}$), and syndecan–4 (*Sdc4*$^{-/-}$) were described previously (24-26). *Ndst1*$^{f/f}$*AlbCre*$^{+}$ mice were described by MacArthur et al. (9). All mice were backcrossed >10 generations on a C57BL/6

background. All animals were housed and bred in vivaria approved by the Association for Assessment and Accreditation of Laboratory Animal Care located in the School of Medicine, University of California, San Diego, following standards and procedures approved by the local Institutional Animal Care and Use Committee. Mice were weaned at 3 weeks, maintained on a 12 hr light-dark cycle, and fed *ad libitum* with water and standard rodent chow (Harlan-TekLad). Genotyping was performed as described in the cited publications.

3.5.2 Adenovirus

Adenovirus containing syndecan-1 cDNA (AdSdc1) was a kind gift from Pyong Woo Park (Harvard Medical School) (27). AdSdc1 and AdGFP were amplified by the UCSD Vector Development Core Facility. Approximately 4×10^{11} particles in phosphate buffered saline (PBS) (28) were injected via the tail vein (29). Mice were used after 3 weeks the experimental procedures indicated in the text.

3.5.3 Quantitative RT-PCR of Membrane HSPGs

Total RNAs from mouse, liver, heart, and brain were purchased from Ambion. RNA was isolated from purified hepatocytes from C57BL/6 mice as described previously (30). Samples were reverse transcribed (Superscript III, Invitrogen) and amplified using intron spanning primers (see Supplemental Table S1). Quantitation was done by the $2^{-\Delta\Delta Ct}$ method using β-actin as control RNAs (31). C_T values from triplicate assays were used to calculate fold-expression as compared to β-actin

according to the Stratagene manual. Results were verified in three independent assays.

3.5.4 Lipoprotein Analysis

Plasma samples were prepared from blood drawn by retro-orbital bleeding from mice fasted for 6 hr in the morning. Total cholesterol and triglyceride levels were determined enzymatically using an automated reader (Cobas Mira; Roche Diagnostics) and kits (Cholesterol High-Performance Reagent, Roche Diagnostics and Triglyceride-SL, Diagnostic Chemicals Ltd).

Lipoproteins were prepared from blood drawn by cardiac puncture using sequential preparative ultracentrifugation according to established methods (32). TRLs (δ = 1.006 g/ml) were prepared from pooled plasma samples (*n* = 10 mice, vol = 5 ml) by centrifugation for 12 hours at 45,000 x rpm in a Beckman 50.3Ti rotor. VLDL remnants and IDL were then collected as the δ = 1.006 - 1.019 g/ml fraction and subsequently LDL and HDL were collected as the δ = 1.019-1.063, and δ = 1.063-1.21g/ml fractions, respectively. The isolated lipoproteins were dialyzed against PBS and analyzed for lipid content using kits. Plasma lipoproteins were also separated by gel filtration FPLC. Pooled plasma samples were loaded on a Superose 12 FPLC column (Amersham Biosciences) in 0.15 M sodium chloride containing 1 mM EDTA and 0.02% sodium azide, pH 7.4, and 0.25-ml fractions were collected (0.1 ml/min).

3.5.5 Analysis of apolipoprotein composition

Equal volumes of the δ < 1.006 g/ml float fraction were concentrated on the Microcon-30s (Millipore), and proteins were resolved by SDSPAGE on 4%-15% Ready Gels (Bio-Rad). Proteins were visualized by Coomassie blue andsilver stain.

3.5.6 VLDL plasma clearance

Human VLDL (δ < 1.006 g/ml) was isolated from healthy, fasting volunteers by ultracentrifugation. Mice were fasted for 6 hrs and injected with 10 μg human VLDL protein via the tail vein. Serial samples were taken by retro-orbital bleeds at the indicated times. The amount of human VLDL remaining in the plasma was determined by sandwich ELISA, utilizing mAb MB47 specific for human apoB-100 (33). MB47 does not bind to murine apoB-100 and therefore it can be used to trace the clearance of injected human VLDL. U-bottom 96-well plates were coated overnight with MB47 at 5 μg/ml in Tris-buffered saline, followed by addition of nonsaturating amounts of plasma (typically, 1:100 dilution of mouse plasma) to capture human VLDL. Bound VLDL was detected using biotinylated goat anti-human apoB-100 (BIODESIGN International), followed by alkaline phosphatase labeled neutrAvidin (Pierce Biotechnology). Plates were developed with Lumi-Phos 530 (Lumigen) and read in a DYNEX Technologies MLX Microtiter Plate Luminometer.

3.5.7 Vitamin A excursion studies

Clearance of chylomicrons derived from dietary triglyceridewas measured by

Vitamin A excursion essentially as described (34). Briefly, 27 μCi of [11,12-^{3}H]-retinol (Perkin-Elmer, 44.4Ci/mmol) in ethanol was mixed with 1 ml of corn oil (Sigma) and administered by oral gavage (200 μl/mouse). Retro-orbital sinus blood was sampled at the times indicated and radioactivity was measured in triplicate (10 μl of serum) by scintillation counting. Triglycerides were measured enzymatically using a plate reader and kits.

3.5.8 Immunofluorescence microscopy

Livers were perfused at 7 ml/min with 30 ml of PBS/EDTA followed by 30 ml of 4% paraformaldehyde. Livers were snap-frozen, and 20-μm sections were cut on a cryostat. Sections were plated on glass coverslips precoated with laminin (2 μg/cm2). They were then fixed with 2% paraformaldehyde in PBS for 10 min at room temperature, incubated for 10 min with 100 mM glycine, pH 7.4, to quench aldehyde groups, permeabilized in 0.1 % Triton X-100 for 10 min, blocked for 20 min with a solution of 1% bovine serum albumin (BSA) and 0.05% Tween in PBS, and then incubated for 2 hr at room temperature with primary antibodies (syndecan-1, 1: 250; syndecan-2, 1:250; syndecan-4, 1:100) in blocking solution. Rabbit polyclonal antibodies raised against the various syndecans were a kind gift of Alan Rapraeger, University of Wisconsin. Excess antibody was removed by incubation for 15 min with 0.1% Tween in PBS. Samples were then incubated for 1 hr with Alexa fluor-594-conjugated goat anti-rabbit secondary antibody (1:250, Invitrogen) and then washed 6

times at 5-min intervals with 0.1% Tween in PBS and incubated for 20 min with the nuclear stain DAPI (1:5000) diluted in PBS. Images were captured with a DeltaVision Restoration microscope system (AppliedPrecision) using a Photometrics Sony CoolSAP HQ charge-coupled device (CCD) camera system attached to an inverted, wide-field fluorescence microscope (Nikon TE200). Optical sections were acquired using a 63x Nikon (NA 1.3) oil immersion objective in 0.2-μm steps in the *z*-axis. Fluorescence was detected using a standard DAPI and Texas Red filter set. Images were saved, processed, and analyzed on SGI workstations (O2, Octane) using the DeltaVision software package softWoRx (version 2.50). Quantification of fluorescence was accomplished using only the linear range of the digital camera.

3.5.9 Immunogold electron microscopy

Samples were fixed in 4% paraformaldehyde in 10mM phosphate buffer, pH 7.4, cryoprotected, and frozen in liquid nitrogen. Ultrathin cryosections were cut at 4^{o}C using a Leica Ultracut UCT Microtome with an EMFCS cryoattachment (Leica), and placed on glow-discharged nickel grids. Samples were stored on 2% gelatin in PBS at 4^{o}C, and incubated with primary antibodies followed by goat anti-mouse IgG conjugated to 5 or 10 nm gold particles (Amersham Biosciences) in PBS supplemented with 10% fetal bovine serum. Grids were absorption-stained with 0.2% neutral uranyl acetate, 0.2% methylcellulose, and 3.2% polyvinyl alcohol. Images were obtained using a JEOL 1200EX II (JEOL, Peabody, MA) transmission electron microscope and

photographed using a Gatan digitalcamera (Gatan, Pleasanton, CA).

3.5.10 Lipoprotein binding and uptake by hepatocytes

Human VLDL ($\delta < 1.006$ g/ml, ~1.1 mg protein) was iodinated using 3 mCi and $Na^{125}I$ (1.4×10^2 cpm/ng, NEN/Perkin Elmer) using Iodogen (35). Under these conditions, 13% of the label was lipid soluble. Isolated hepatocytes were treated with the indicated concentration of ^{125}I-VLDL in DMEM media with 2.5 mg/ml lipoprotein-free serum (Biomedical Technologies, Inc., Boston, MA). Cells were incubated at 4°C or 37°C for 1 hr, rinsed three times with PBS and then solubilized with 0.1M NaOH. Protein concentration was determined by Bradford (BioRad) and radioactivity was measured by gamma counting. Degradation of ^{125}I-VLDL was measured by precipitation of 0.25 mL of conditioned media with an equal volume of 50% trichloroacetic acid (36). After 30 min at 4°C, the samples were centrifuged for 30 min. The supernatant was placed in a fresh glass tube, and 5 μL of 40% potassium iodide was added as a carrier. Hydrogen peroxide (30%) was added, and lipid soluble material was extracted by the addition of 2 ml of chloroform. An aliquot of the upper aqueous phase containing iodotyrosine was counted as measure of degradation.

Porcine intestinal heparin (M_r = 12,000-15,000, 180 U/mg) was a kind gift from Dr. Patrick Shaklee (Scientific Protein Laboratories Inc., Milwaukee, Wisconsin, USA). In competition experiments, wild-type hepatocytes were treated simultaneously with varying concentrations of heparin and ^{125}I-VLDL and incubated

at 4^{o}C for 1 hr. The signal obtained in the presence of heparin was subtracted from the total binding in order to calculate specific binding.

3.5.11 Statistics

Statistical analyses were performed using PRISM (GraphPad Software). All data is expressed as mean values $\pm$ SD unless otherwise indicated. Significance was determined using an unpaired Student's (two-tailed) t-test or ANOVA. Significance was taken as $P < 0.05$.

3.6 Acknowledgements

This work has been submitted in for publication to the *Journal of Clinical Investigation* with coauthors Joseph R. Bishop, Ingrid R. Niesman, Joseph L. Witztum, and Jeffrey D. Esko. The dissertation author was the primary author of the work contained in this chapter. Together with her coauthors, she thanks Joseph Juliano, Fely Alamazen and Jennifer Pattison at UCSD, David Ditto of the Hematology/Coagulation/Chemistry Core supported by NIH grant HL57345, and National Institutes of Health Grants GM33063 and HL57345 (J.D.E.), NIH HL088093 and the Leducq Foundation (J.L.W.), and a Scientist Development Grant from the American Heart Association (J.R.B). Work was conducted within the department of Cellular and Molecular Medicine, the Department of Medicine, and the Glycobiology Research and Training Center, University of California, San Diego, La Jolla, California.

3.7 References

1. **Nordestgaard, B.G., Benn, M., Schnohr, P., and Tybjaerg-Hansen, A. 2007. Nonfasting triglycerides and risk of myocardial infarction, ischemic heart disease, and death in men and women. *Jama* 298:299-308.**

2. **Bansal, S., Buring, J.E., Rifai, N., Mora, S., Sacks, F.M., and Ridker, P.M. 2007. Fasting compared with nonfasting triglycerides and risk of cardiovascular events in women. *Jama* 298:309-316.**

3. **Beigneux, A.P., Davies, B.S., Gin, P., Weinstein, M.M., Farber, E., Qiao, X., Peale, F., Bunting, S., Walzem, R.L., Wong, J.S., et al. 2007. Glycosylphosphatidylinositolanchored high-density lipoprotein-binding protein 1 plays a critical role in the lipolytic processing of chylomicrons. *Cell Metab* 5:279-291.**

4. **Young, S.G., Davies, B.S., Fong, L.G., Gin, P., Weinstein, M.M., Bensadoun, A., and Beigneux, A.P. 2007. GPIHBP1: an endothelial cell molecule important for the lipolytic processing of chylomicrons. *Curr Opin Lipidol* 18:389-396.**

5. **Williams, K.J., and Fuki, I.V. 1997. Cell-surface heparan sulfate proteoglycans: dynamic molecules mediating ligand catabolism. *Curr. Opin. Lipidol.* 8:253-262.**

6. **Mahley, R.W., and Ji, Z.S. 1999. Remnant lipoprotein metabolism: key pathwaysinvolving cell-surface heparan sulfate proteoglycans and apolipoprotein E. *J Lipid Res* 40:1-16.**

7. **Mahley, R.W., and Huang, Y. 2007. Atherogenic remnant lipoproteins: role for proteoglycans in trapping, transferring, and internalizing. *J Clin Invest* 117:94-98.**

8. **Williams, K.J. 2008. Molecular processes that handle -- and mishandle -- dietary lipids. *J Clin Invest* 118:3247-3259.**

9. **MacArthur, J.M., Bishop, J.R., Wang, L., Stanford, K.I., Bensadoun, A., Witztum, J.L., and Esko, J.D. 2007. Liver heparan sulfate proteoglycans mediate clearance of triglyceride-rich lipoproteins independently of LDL receptor family members. *J Clin Invest* 117:153-164.**

10. Bishop, J.R., Stanford, K.I., and Esko, J.D. 2008. Heparan sulfate proteoglycans and triglyceride-rich lipoprotein metabolism. *Curr Opin Lipidol* 19:307-313.

11. Bishop, J.R., Schuksz, M., and Esko, J.D. 2007. Heparan sulphate proteoglycans finetune mammalian physiology. *Nature* 446:1030-1037.

12. Williams, K.J., Fless, G.M., Petrie, K.A., Snyder, M.L., Brocia, R.W., and Swenson, T.L. 1992. Mechanisms by which lipoprotein lipase alters cellular metabolism of lipoprotein(a), low density lipoprotein, and nascent lipoproteins. Roles for low density lipoprotein receptors and heparan sulfate proteoglycans. *J.Biol.Chem.* 267:13284-13292.

13. Ji, Z.S., Fazio, S., and Mahley, R.W. 1994. Variable heparan sulfate proteoglycan binding of apolipoprotein E variants may modulate the expression of type III hyperlipoproteinemia. *J Biol Chem* 269:13421-13428.

14. Mann, W.A., Meyer, N., Weber, W., Meyer, S., Greten, H., and Beisiegel, U. 1995. Apolipoprotein E isoforms and rare mutations: parallel reduction in binding to cells and to heparin reflects severity of associated type III hyperlipoproteinemia. *J Lipid Res* 36:517-525.

15. Fuki, I.V., Kuhn, K.M., Lomazov, I.R., Rothman, V.L., Tuszynski, G.P., Iozzo, R.V., Swenson, T.L., Fisher, E.A., and Williams, K.J. 1997. The syndecan family of proteoglycans. Novel receptors mediating internalization of atherogenic lipoproteins invitro. *J Clin Invest* 100:1611-1622.

16. Ji, Z.S., Dichek, H.L., Miranda, R.D., and Mahley, R.W. 1997. Heparan sulfate proteoglycans participate in hepatic lipase- and apolipoprotein E-mediated binding and uptake of plasma lipoproteins, including high density lipoproteins. *J. Biol. Chem.* 272:31285-31292.

17. Fuki, I.V., Meyer, M.E., and Williams, K.J. 2000. Transmembrane and cytoplasmic domains of syndecan mediate a multi-step endocytic pathway involving detergent insolublemembrane rafts. *Biochem J* 351:607-612.

18. Fuki, I.V., Iozzo, R.V., and Williams, K.J. 2000. Perlecan heparan sulfate proteoglycan - A novel receptor that mediates a distinct pathway for ligand catabolism. *J. Biol. Chem.*275:25742-25750.

19. Ebara, T., Conde, K., Kako, Y., Liu, Y., Xu, Y., Ramakrishnan, R., Goldberg, I.J., and Shachter, N.S. 2000. Delayed catabolism of apoB-48 lipoproteins due to decreased heparan sulfate proteoglycan production in diabetic mice. *J Clin Invest* 105:1807-1818.

20. Wilsie, L.C., Gonzales, A.M., and Orlando, R.A. 2006. Syndecan-1 mediates internalization of apoE-VLDL through a low density lipoprotein receptor-related protein (LRP)-independent, non-clathrin-mediated pathway. *Lipids Health Dis* 5:23.

21. Zeng, B.J., Mortimer, B.C., Martins, I.J., Seydel, U., and Redgrave, T.G. 1998. Chylomicron remnant uptake is regulated by the expression and function of heparansulfate proteoglycan in hepatocytes. *J. Lipid Res.* 39:845-860.

22. Yu, K.C., Chen, W., and Cooper, A.D. 2001. LDL receptor-related protein mediates cell surface clustering and hepatic sequestration of chylomicron remnants in LDLR-deficient mice. *J Clin Invest* 107:1387- 1394.

23. Cortes, V., Amigo, L., Donoso, K., Valencia, I., Quinones, V., Zanlungo, S., Brandan, E., and Rigotti, A. 2007. Adenovirus-mediated hepatic syndecan-1 overexpression induces hepatocyte proliferation and hyperlipidaemia in mice. *Liver Int* 27:569-581.

24. Park, P.W., Pier, G.B., Hinkes, M.T., and Bernfield, M. 2001. Exploitation of syndecan-1 shedding by Pseudomonas aeruginosa enhances virulence. *Nature* 411:98-102.

25. Reizes, O., Lincecum, J., Wang, Z., Goldberger, O., Huang, L., Kaksonen, M., Ahima,R., Hinkes, M.T., Barsh, G.S., Rauvala, H., et al. 2001. Transgenic expression of syndecan-1 uncovers a physiological control of feeding behavior by syndecan-3. *Cell* 106:105-116.

26. Echtermeyer, F., Streit, M., Wilcox-Adelman, S., Saoncella, S., Denhez, F., Detmar, M., and Goetinck, P. 2001. Delayed wound repair and impaired angiogenesis in mice lacking syndecan-4. *J Clin Invest*

107:9-14.

27. Hayashida, K., Johnston, D.R., Goldberger, O., and Park, P.W. 2006. Syndecan-1 expression in epithelial cells is induced by transforming growth factor beta through a PKA-dependent pathway. *J Biol Chem* 281:24365-24374.

28. Dulbecco, R., and Vogt, M. 1954. Plaque formation and isolation of pure cell lines with poliomyelitis viruses. *J.Exp.Med.* 99:167-182.

29. Rohlmann, A., Gotthardt, M., Willnow, T.E., Hammer, R.E., and Herz, J. 1996. Sustained somatic gene inactivation by viral transfer of Cre recombinase. *Biotechnology* 14:1562-1565.

30. Bishop, J.R., and Esko, J.D. 2005. The elusive role of heparan sulfate in Toxoplasma gondii infection. *Mol Biochem Parasitol* 139:267-269.

31. Livak, K.J., and Schmittgen, T.D. 2001. Analysis of relative gene expression data using real-time quantitative PCR and the 2(-Delta Delta C(T)) Method. *Methods* 25:402-408.

32. Kelley, J.L., and Kruski, A.W. 1986. Density gradient ultracentrifugation of serum lipoproteins in a swinging bucket rotor. *Methods Enzymol* 128:170-181.

33. Young, S.G., Smith, R.S., Hogle, D.M., Curtiss, L.K., and Witztum, J.L. 1986. Two new monoclonal antibody-based enzyme-linked assays of apolipoprotein B. *Clin Chem* 32:1484-1490.

34. Ishibashi, S., Perrey, S., Chen, Z., Osuga, J., Shimada, M., Ohashi, K., Harada, K., Yazaki, Y., and Yamada, N. 1996. Role of the low density lipoprotein (LDL) receptor pathway in the metabolism of chylomicron remnants. A quantitative study in knockout mice lacking the LDL receptor, apolipoprotein E, or both. *J Biol Chem* 271:22422-22427.

35. Salacinski, P.R., McLean, C., Sykes, J.E., Clement-Jones, V.V., and Lowry, P.J. 1981. Iodination of proteins, glycoproteins, and peptides using a solid-phase oxidizing agent, 1,3,4,6-tetrachloro-3 alpha,6 alpha-diphenyl glycoluril (Iodogen). *Anal Biochem* 117:136-146.

36. Williams, K.J. 2001. Interactions of lipoproteins with proteoglycans.

Methods Mol Biol **171:457-477.**

37. Horton, J.D., Shimano, H., Hamilton, R.L., Brown, M.S., and Goldstein, J.L. 1999. Disruption of LDL receptor gene in transgenic SREBP-1a mice unmasks hyperlipidemia resulting from production of lipid-rich VLDL. ***J Clin Invest*** **103:1067-1076.**

38. Ishibashi, S., Brown, M.S., Goldstein, J.L., Gerard, R.D., Hammer, R.E., and Herz, J. 1993. Hypercholesterolemia in low density lipoprotein receptor knockout mice and its reversal by adenovirus-mediated gene delivery. ***J Clin Invest*** **92:883-893.**

39. Hayashi, K., Hayashi, M., Jalkanen, M., Firestone, J.H., Trelstad, R.L., and Bernfield, M. 1987. Immunocytochemistry of cell surface heparan sulfate proteoglycan in mouse tissues. A light and electron microscopic study. ***J.Histochem.Cytochem.*** **35:1079-1088.**

40. Roskams, T., Moshage, H., De Vos, R., Guido, D., Yap, P., and Desmet, V. 1995. Heparan sulfate proteoglycan expression in normal human liver. ***Hepatology*** **21:950-958.**

41. Bernfield, M., Kokenyesi, R., Kato, M., Hinkes, M.T., Spring, J., Gallo, R.L., and Lose, E.J. 1992. Biology of the syndecans: a family of transmembrane heparan sulfate proteoglycans. ***Annu.Rev.Cell Biol.*** **8:365-393.**

42. Bernfield, M., Gotte, M., Park, P.W., Reizes, O., Fitzgerald, M.L., Lincecum, J., and Zako, M. 1999. Functions of cell surface heparan sulfate proteoglycans. ***Annu Rev Biochem*** **68:729-777.**

43. Park, P.W., Reizes, O., and Bernfield, M. 2000. Cell surface heparan sulfate proteoglycans: Selective regulators of ligand-receptor encounters. ***J.Biol. Chem.*** **275:29923-29926.**

44. Bellin, R., Capila, I., Lincecum, J., Park, P.W., Reizes, O., and Bernfield, M.R. 2002. Unlocking the secrets of syndecans: Transgenic organisms as a potential key. ***Glycoconj J*** **19:295-304.**

45. Sanderson, R.D., and Yang, Y. 2008. Syndecan-1: a dynamic regulator of the myeloma microenvironment. ***Clin Exp Metastasis*** **25:149-159.**

46. Bartlett, A.H., Hayashida, K., and Park, P.W. 2007. Molecular and

cellular mechanisms of syndecans in tissue injury and inflammation. *Mol Cells* 24:153-166.

47. Tumova, S., Woods, A., and Couchman, J.R. 2000. Heparan sulfate proteoglycans on the cell surface: versatile coordinators of cellular functions. *Int.J.Biochem.Cell Biol.* 32:269-288.

48. Burbach, B.J., Friedl, A., Mundhenke, C., and Rapraeger, A.C. 2003. Syndecan-1 accumulates in lysosomes of poorly differentiated breast carcinoma cells. *Matrix Biol* 22:163-177.

49. Fitzgerald, M.L., Wang, Z.H., Park, P.W., Murphy, G., and Bernfield, M. 2000. Shedding of syndecan-1 and-4 ectodomains is regulated by multiple signaling pathways and mediated by a TIMP-3-sensitive metalloproteinase. *J.Cell Biol.* 148:811-824.

50. Mahley, R.W. 1996. Heparan sulfate proteoglycan/low density lipoprotein receptor related protein pathway involved in type III hyperlipoproteinemia and Alzheimer's disease. *Isr J Med Sci* 32:414-429.

51. Cooper, A.D. 1997. Hepatic uptake of chylomicron remnants. *J Lipid Res* 38:2173-2192.

52. Parthasarathy, N., Goldberg, I.J., Sivaram, P., Mulloy, B., Flory, D.M., and Wagner, W.D. 1994. Oligosaccharide sequences of endothelial cell surface heparan sulfate proteoglycan with affinity for lipoprotein lipase. *J. Biol. Chem.* 269:22391-22396.

53. Spillmann, D., Lookene, A., and Olivecrona, G. 2006. Isolation and characterization of low sulfated heparan sulfate sequences with affinity for lipoprotein lipase. *J Biol Chem* 281:23405-23413.

54. Libeu, C.P., Lund-Katz, S., Phillips, M.C., Wehrli, S., Hernaiz, M.J., Capila, I., Linhardt, R.J., Raffai, R.L., Newhouse, Y.M., Zhou, F., et al. 2001. New insights into the heparan sulfate proteoglycan-binding activity of apolipoprotein E. *J Biol Chem* 276:39138-39144.

55. Dong, J., Peters-Libeu, C.A., Weisgraber, K.H., Segelke, B.W., Rupp, B., Capila, I., Hernaiz, M.J., LeBrun, L.A., and Linhardt, R.J. 2001. Interaction of the N-terminal domain of apolipoprotein E4 with heparin. *Biochemistry* 40:2826-2834.

56. **Lyon, M., Deakin, J.A., and Gallagher, J.T. 1994. Liver heparan sulfate structure. A novel molecular design. *J. Biol. Chem.* 269:11208-11215.**

57. **Thankamony, S.P., and Knudson, W. 2006. Acylation of CD44 and its association with lipid rafts are required for receptor and hyaluronan endocytosis. *J Biol Chem* 281:34601-34609.**

58. **Tkachenko, E., Lutgens, E., Stan, R.V., and Simons, M. 2004. Fibroblast growth factor 2 endocytosis in endothelial cells proceed via syndecan-4-dependent activation of Rac1 and a Cdc42-dependent macropinocytic pathway. *J Cell Sci* 117:3189-3199.**

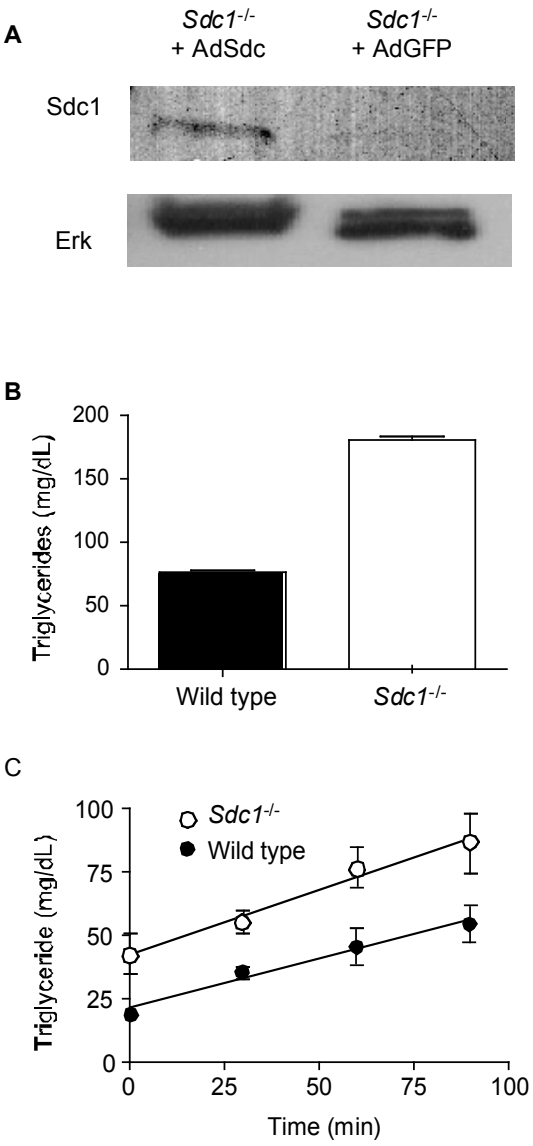
59. **Brown, M.S., Anderson, R.G., and Goldstein, J.L. 1983. Recycling receptors: the roundtrip itinerary of migrant membrane proteins. *Cell* 32:663-667.**

60. **Rohlmann, A., Gotthardt, M., Hammer, R.E., and Herz, J. 1998. Inducible inactivation of hepatic LRP gene by cre-mediated recombination confirms role of LRP in clearance of chylomicron remnants. *J Clin Invest* 101:689-695.**

61. **Wilsie, L.C., and Orlando, R.A. 2003. The low density lipoprotein receptor-related protein complexes with cell surface heparan sulfate proteoglycans to regulate proteoglycan-mediated lipoprotein catabolism. *J Biol Chem* 278:15758-15764.**

62. **Magoori, K., Kang, M.J., Ito, M.R., Kakuuchi, H., Ioka, R.X., Kamataki, A., Kim, D.H., Asaba, H., Iwasaki, S., Takei, Y.A., et al. 2003. Severe hypercholesterolemia, impaired fat tolerance, and advanced atherosclerosis in mice lacking both low density lipoprotein receptor-related protein 5 and apolipoprotein E. *J Biol Chem* 278:11331-11336.**

3.8 Supplemental Figure Legends



Supplemental Figure 1. (A) Syndecan 1 expression was measured in isolated hepatocytes from wild-type mice, *Sdc1*$^{-/-}$ mice treated with AdSdc1, and *Sdc1*$^{-/-}$ mice treated with AdGFP. Erk was measured as a loading control. **(B)** Overnight-fasted animals of the indicated genotypes, wild-type ($n = 3$) and *Sdc1*$^{-/-}$ ($n = 3$), were given 200μl of corn oil containing 5.4μCi [^{3}H] retinol by gavage. Blood samples were taken 4 hours after gavage, and plasma triglyceride levels were measured. **(C)** Triglyceride secretion rates, as determined by injection of Triton WR-1339, did not differ between *Sdc1*$^{-/-}$ (0.51 ± 0.11 mg/min; $n = 3$) and wild-type (0.38 ± 0.07; $n = 3$), $P = 0.63$.

CHAPTER 4

THE RELATIVE CONTRIBUTION OF HEPARAN SULFATE PROTEOGLYCANS, LDL-RECEPTOR, AND LDL-RECEPTOR-RELATED PROTEIN IS ESSENTIAL FOR CLEARANCE OF TRIGLYCERIDE- AND CHOLESTEROL-RICH PARTICLES

4.1 Summary

To study the relative contribution of HSPGs, LDL receptors (LDLR) and LDL receptor related protein-1 (LRP1) in clearance, double and triple mutants were generated and characterized. Combining *Ldlr*$^{-/-}$ with *Lrp1*$^{f/f}$*AlbCre*$^{+}$ or *Ndst1*$^{f/f}$*AlbCre*$^{+}$ with *Lrp1*$^{f/f}$*AlbCre*$^{+}$ did not result in additional accumulation of triglyceride-rich lipoproteins compared to *Ldlr*$^{-/-}$ or *Ndst1*$^{f/f}$*AlbCre*$^{+}$ mice, resepectively. In contrast, combining *Ndst1*$^{f/f}$*AlbCre*$^{+}$ and *Ldlr*$^{-/-}$ resulted in greatly enhanced accumulation of triglyceride- and cholesterol-rich particles (triglycerides 205 $\pm$ 26 mg/dl vs. 43 $\pm$ 3 mg/dl in wild-type; cholesterol 216 $\pm$ 15 mg/dl vs. 67 $\pm$ 3 mg/dl in wild-type). Mice deficient in all three receptors (*Ldlr*$^{-/-}$*Lrp1*$^{f/f}$*Ndst1*$^{f/f}$*AlbCre*$^{+-}$) further accentuated accumulation of triglyceride- and cholesterol-rich lipoprotein particles (triglyceride 629 $\pm$ 122; cholesterol 1088 $\pm$ 80). The particles that accumulated in these *Ldlr*$^{-/-}$ *Ndst1*$^{f/f}$*Lrp1*$^{f/f}$*AlbCre*$^{+}$ were triglyceride- and cholesterol-rich VLDL. These findings provide the first genetic evidence showing that HS, LDLR, and LRP1 all work independently of each other, and are involved in the clearance of different types of

particles, and that HSPGs can mediate clearance of both triglyceride and cholesterol rich particles independently of LDLR and LRP1.

4.2 Introduction

Remnant lipoproteins are triglyceride- and cholesterol-enriched particles derived from the lipolytic processing of intestinal chylomicrons and hepatic very low density lipoproteins (VLDL). VLDL are synthesized by hepatocytes; as these triglycercide-rich lipoproteins (TRLs) circulate through the body, the triglycerides are hydrolyzed by lipoprotein lipose (Lpl), resulting in the formation of chylomicron remnants (CRs) and intermediate-density lipoproteins (IDLs) from VLDLs (1). The TRL remnants also obtain apoE by transfer reactions from other lipoproteins in the circulation, or by enrichment in the liver. VLDL contain apoB-48, apoB-100, apoE, and Lpl.

The mechanism of hepatic clearance of TRLs remains controversial. The particles may first be sequestered in the liver perisinusoidal space (space of Dissse), where they undergo further processing by hepatic lipase (HL) and Lpl, both of which are detectable in the space of Disse and may remain associated with TRLs (2-4). After hydrolysis of the triglycerides, a group of hepatic lipoprotein receptors then endocytoses the lipoproteins, leading to their lysosomal catabolism. There are three receptors known to play a role in the hepatic clearance of TRLs; LDL receptor (LDLR) (5-7), LDLR-related protein (LRP) (8-10), and HSPGs (11).

The LDLR, initially described by Brown and Goldstein, has its primary role in the endocytosis of LDLs, based on the accumulation of cholesterol-rich particles in

mice, rabbits, and humans with inactivating mutations in LDLR (5-7). The LDLR deficiency causes a mild accumulation of TRLs, and a two-fold accumulation of cholesterol-rich particles. This caused speculation that there were other receptors involved, thus leading to the identification of the LRPs. Mice deficient in hepatic LRP1, however, show no accumulation of TRLs or cholesterol-rich particles (8-10). This suggested that a third receptor, heparan sulfate proteoglycans (HSPGs) (1, 12-21) was involved in the clearance of TRLs. The absence of hepatic heparan sulfate (HS) results in a 2.5-fold accumulation of triglycerides (density < 1.006) without a corresponding increase in cholesterol (11). Syndecan-1 has since been identified as the HSPG involved in TRL clearance, and the *Sdc1*$^{-/-}$ mice have the same two-fold accumulation of triglycerides with no increase in cholesterol (22). While the absence of these individual receptors cause a slight alteration in lipoprotein metabolism, the relative contribution of each individual receptor remains unknown.

Previous work has demonstrated that the various receptors may work in concert with each other (7, 9, 11). The absence of any two receptors results in a greater accumulation of both plasma triglycerides or plasma cholesterol compared to the additive effect of mice deficient in just one receptor. Compound mutants, mice deficient in LDLR and HS, showed a seven-fold increase in plasma triglycerides compared with wild-type animals (and three-fold over mice deficient solely in LDLR or HS) (11). In addition, while the absence of hepatic LRP1 does not result in remnant particle accumulation, combining LRP1 with LDLR mutations results in a modest increase in accumulation of TRLs, and a three-fold increase in LDL compared to mice deficient in LDLR alone (9).

The question remains, however, as to the interaction between LRP and HSPGs, and to the interaction between all three receptors. Previous work by Mahley et al. has suggested an HSPG-LRP pathway in which these two receptors work together as a sequestration-uptake hand-off mechanism (15, 21). Also, it is possible that in the absence of one or two of these receptors, the third receptor compensates; and that these three receptors work together to facilitate lipoprotein remnant clearance. In the current study, we sought to determine the relative contribution of each of three receptors, specifically by creating a mouse model deficient in the various receptors. While the compound mutant deficient in hepatocyte HS and LRP does not show an increased accumulation of triglycerides greater than the HS mutant mouse alone, the mouse deficient in all three receptors demonstrated an increase in plasma triglycerides eight-fold over wild-type mice, and an increase in plasma cholesterol twelve-fold over wild-type mice.

4.3 Results

4.3.1 Generalized hyperlipidemia is observed in mutant mice.

To study the relative contribution of HSPGs, LDL receptors (LDLR) and LDL receptor related protein-1 (LRP1), in clearance of triglycerides and cholesterol, double and triple mutants were generated and characterized. Combining *Ldlr*$^{-/-}$ with *Lrp1*$^{f/f}$*AlbCre*$^{+}$ or *Ndst1*$^{f/f}$*AlbCre*$^{+}$ with *Lrp1*$^{f/f}$*AlbCre*$^{+}$ did not result in additional accumulation of triglyceride-rich lipoproteins compared to *Ldlr*$^{-/-}$ or *Ndst1*$^{f/f}$*AlbCre*$^{+}$ mice, respectively. In contrast, combining *Ndst1*$^{f/f}$*AlbCre*$^{+}$ and *Ldlr*$^{-/-}$ resulted in

greatly enhanced accumulation of triglyceride- and cholesterol-rich particles (triglycerides 205 ± 26 mg/dl vs. 43 ± 3 mg/dl in wild-type; cholesterol 216 ± 15 mg/dl vs. 67 ± 3 mg/dl in wild-type). Mice deficient in all three receptors (*Ldlr*$^{-/-}$ *Lrp1*$^{f/f}$*Ndst1*$^{f/f}$*AlbCre*$^{+-}$) further accentuated accumulation of triglyceride- and cholesterol-rich lipoprotein particles (triglyceride 629 ± 122; cholesterol 1088 ± 80) (Fig. 4-1A-D). Numerical representation of the data, as well as from the *Ldlr*$^{-/-}$ *Lrp*$^{f/f}$*AdCre* mouse (9) is shown in Table 4-1.

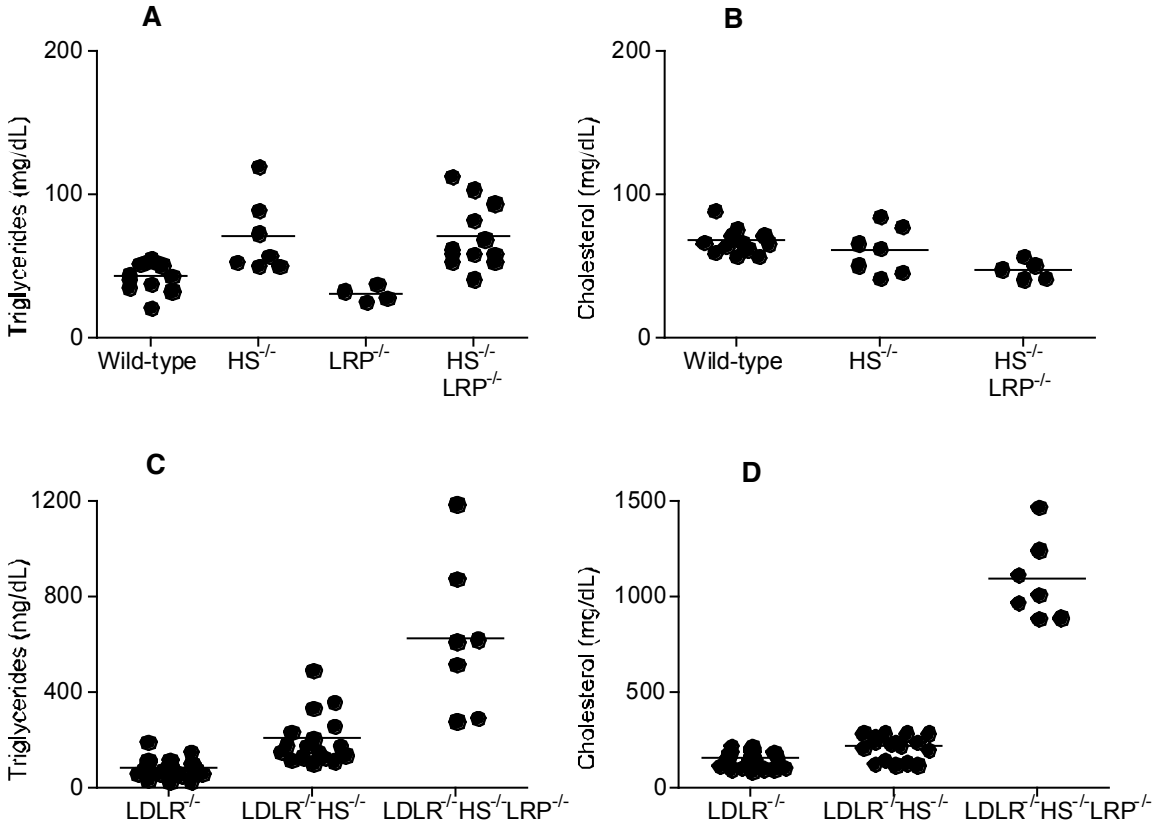


Figure 4-1. Hyperlipidemia in *Ldlr*$^{-/-}$*Ndst1*$^{f/f}$*Lrp1*$^{f/f}$*AlbCre*$^{+}$ mice. Total triglycerides **(A, C)** and cholesterol **(B, D)** were measured in Wild-type (n = 9), *HS*$^{-/-}$ (n = 7), *HS*$^{-/-}$*Lrp*$^{-/-}$ (n = 12), *Ldlr*$^{-/-}$ (n = 13), *Ldlr*$^{-/-}$*HS*$^{-/-}$ (n = 17), and *Ldlr*$^{-/-}$*HS*$^{-/-}$*Lrp1*$^{-/-}$ (n = 7) mice.

Table 4-1. Hyperlipidemia in mutant mice.

Genotype	Triglycerides (mg/dL)	Cholesterol (mg/dL)
Wild-type	43 ± 3	67 ± 3
HS$^{-/-}$	70 ± 10	62 ± 6
HS$^{-/-}$*Lrp1*$^{-/-}$	71 ± 6	48 ± 7
Ldlr$^{-/-}$	86 ± 7	154 ± 8
Ldlr$^{-/-}$*HS*$^{-/-}$	205 ± 26	216 ± 15
Ldlr$^{-/-}$*HS*$^{-/-}$*Lrp1*$^{-/-}$	629 ± 122	1088 ± 80
Ldlr$^{-/-}$*Lrp*$^{-/-*}$	187 ± 47	503 ± 110
ApoE$^{-/-}$	582 ± 54	62 ± 4

*This data was taken from Rohlmann et al (9) and injected with AdCre instead of AlbCre.

Buoyant density ultracentrifugation of fasting plasma lipoproteins from *Ldlr*$^{-/-}$, *Ldlr*$^{-/-}$*Ndst1*$^{f/f}$*AlbCre*$^{+}$, and *Ldlr*$^{-/-}$*Ndst1*$^{f/f}$*AlbCre*$^{+}$*Lrp1*$^{f/f}$*AlbCre*$^{+}$ mice showed that triglyceride accumulation occurred primarily in particles of $\delta < 1.006$ g/ml in *Ldlr*$^{-/-}$ *Ndst1*$^{f/f}$*AlbCre*$^{+}$*Lrp1*$^{f/f}$*AlbCre*$^{+}$ mice, while LDL and HDL triglycerides were only slightly affected (Fig 4-2A). Additionally, the *Ldlr*$^{-/-}$*Ndst1*$^{f/f}$*AlbCre*$^{+}$*Lrp1*$^{f/f}$*AlbCre*$^{+}$ mice also accumulated cholesterol in VLDL, or particles of $\delta < 1.006$ g/ml, as well as LDL (Fig 4-2B). Interestingly, this is similar to the phenotype observed in the *ApoE*$^{-/-}$ mouse. FPLC profiles of all genotypes confirm this data (2C); FPLC from *Ldlr*$^{-/-}$ *Lrp*$^{f/f}$*AdCre* mouse shown for comparison (Fig 4-2D).

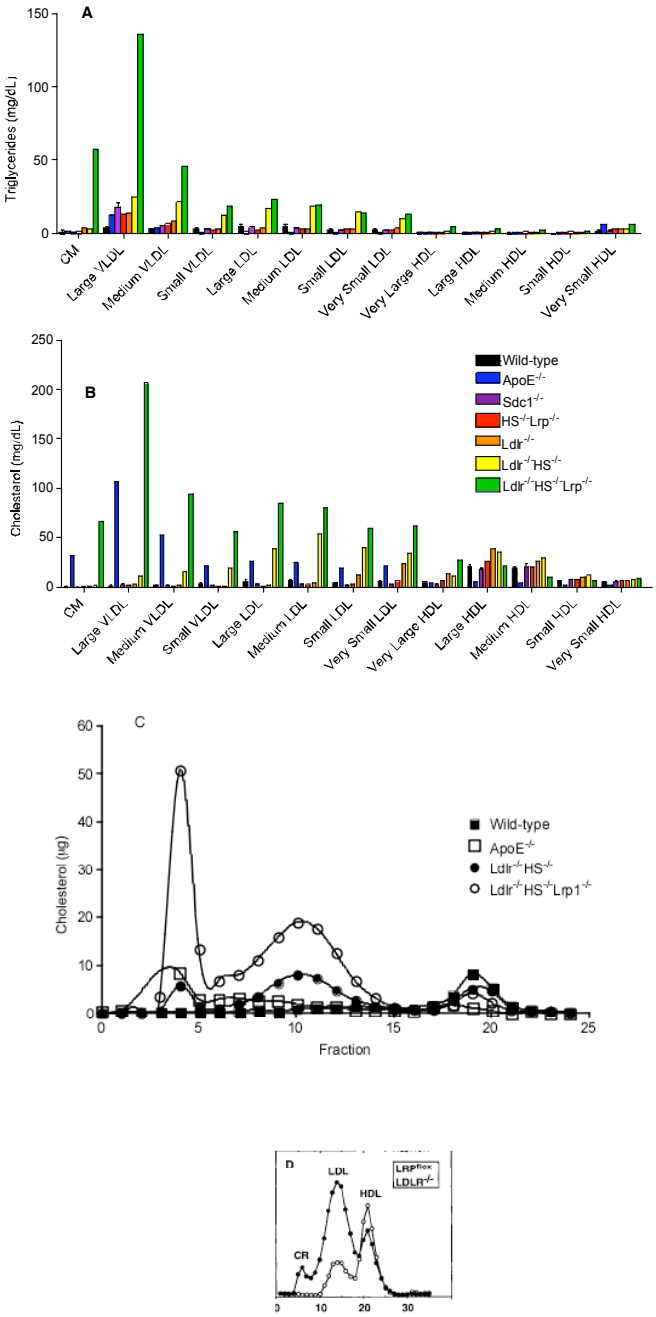


Figure 4-2. Hyperlipidemia in *Ldlr*$^{-/-}$*Ndst1*$^{f/f}$*Lrp1*$^{f/f}$*AlbCre*$^{+}$ mice is similar to *ApoE*$^{-/-}$ mice. Triglyceride (A) and cholesterol (B) distribution across plasma lipoprotein subclasses. Plasma was pooled from 4 mice of each genotype and triglyceride in lipoprotein size classes was determined by LipoSEARCH HPLC. Chylomicron (CM) > 80 nm particle diameter; VLDL, 30-80 nm; LDL, 16-30 nm; and HDL, 8-16nm. (C) FPLC fractions were pooled from mice of each genotype. Lipid peaks labeled to indicate VLDL, IDL/LDL, and HDL. (D) FPLC of *Ldlr*$^{-/-}$*Lrp*$^{f/f}$*AdCre* from Rohlmann et al is shown for comparison (9).

4.3.2 *Ldlr*$^{-/-}$*Ndst1*$^{f/f}$*Lrp1*$^{f/f}$*AlbCre*$^{+}$ mice exhibit greater delay in plasma clearance of dietary triglycerides compared to other mutant mice.

Prior studies showed that mice bearing a defect in sulfation of hepatic heparan sulfate (*Ndst1*$^{f/f}$*AlbCre*$^{+}$), syndecan-1, or compound mutants in *Ldlr*$^{-/-}$*Ndst1*$^{f/f}$*AlbCre*$^{+}$ displayed altered hepatic clearance of triglycerides and intestinally-derived TRLs. Clearance of intestinally-derived TRLs was measured by vitamin A-excursion studies. Fasted mice were given a bolus mixture of [^{3}H]retinol and corn oil by oral gavage, and blood was sampled at various time points to determine the plasma level of ^{3}H-counts. In the intestine, [^{3}H]retinol in converted to fatty acid esters and incorporated into newly made chylomicrons and its only route of removal is to be cleared through the liver. As shown in figure 3A, the area under the curve for the *Ndst1*$^{f/f}$*AlbCre*$^{+}$ and *Ndst1*$^{f/f}$*Lrp1*$^{f/f}$*AlbCre*$^{+}$ mice was 2.5-fold greater than wild-type mice (AUC = 4468 and 5319 vs. 1591), indicating that the mutant cleared intestinally derived lipoproteins at a slower rate ($P = 0.0067$). After 12 hours, most of the tracer had been cleared in both *Ndst1*$^{f/f}$*AlbCre*$^{+}$ and *Ndst1*$^{f/f}$*Lrp1*$^{f/f}$*AlbCre*$^{+}$ and wild-type animals. Interestingly, as shown in figure 3B, the area under the curve for the *Ldlr*$^{-/-}$*Ndst1*$^{f/f}$*AlbCre*$^{+}$ and *Ldlr*$^{-/-}$*Ndst1*$^{f/f}$*Lrp1*$^{f/f}$*AlbCre*$^{+}$ mice was elevated 4.5-fold and 18-fold, respectively, compared to the *Ldlr*$^{-/-}$ mice (AUC = 13166 and 50392 vs. 3331) ($P < 0.0001$). In the *Ldlr*$^{-/-}$*Ndst1*$^{f/f}$*Lrp1*$^{f/f}$*AlbCre*$^{+}$ mice, there was virtually no clearance detected 24 hours post-gavage, indicating that all three receptors play an important role in the clearance of dietary lipids.

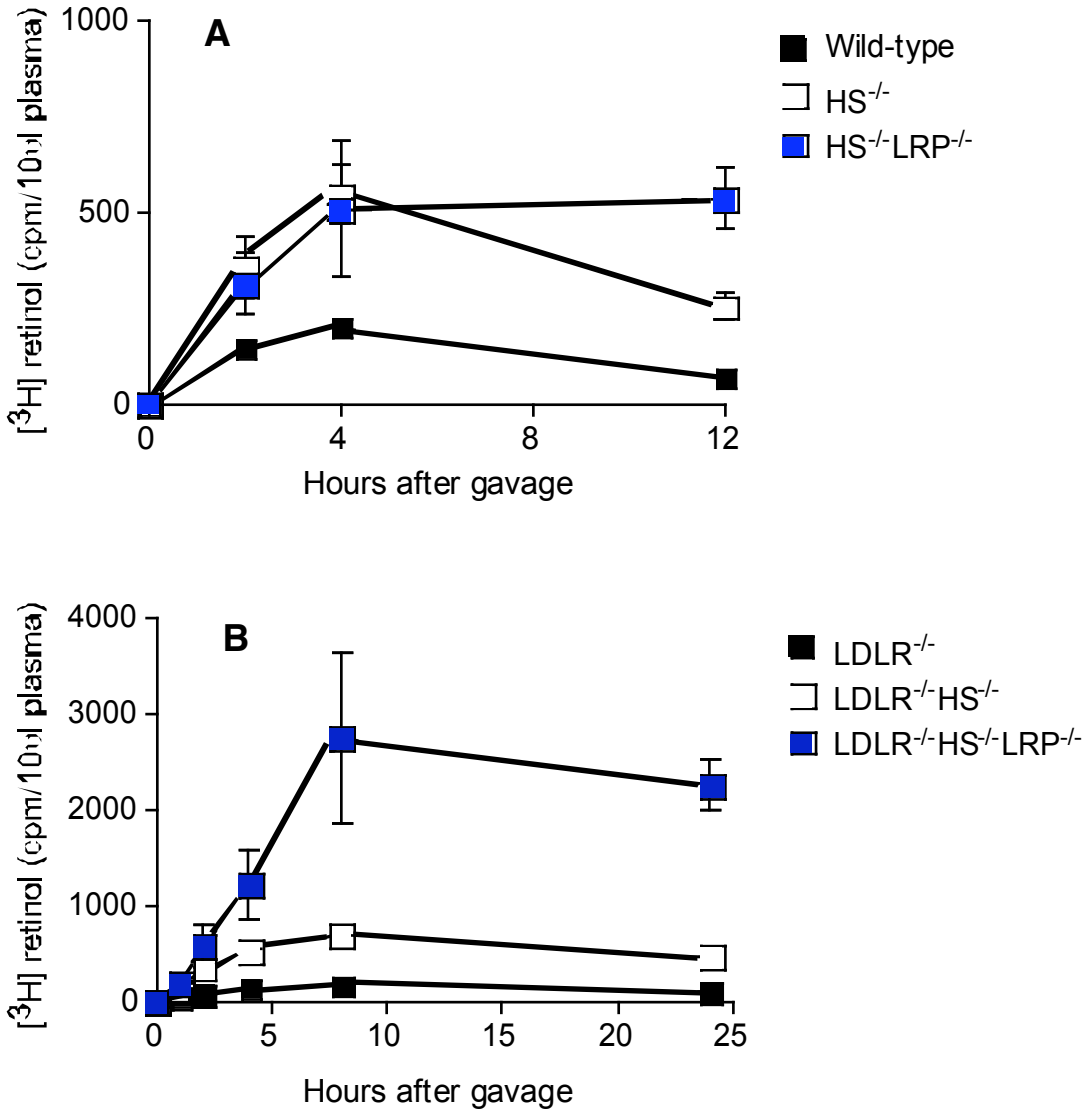


Figure 4-3. *Ldlr*$^{-/-}$*Ndst1*$^{f/f}$*Lrp1*$^{f/f}$*AlbCre*$^{+}$ mice exhibit delayed plasma clearance of dietary triglycerides. Retinyl ester excursions were measured at the times indicated in (A) Wild-type (black squares, n = 3), *HS*$^{-/-}$ (open squares, n = 3), and *HS*$^{-/-}$*Lrp*$^{-/-}$ (bluesquares, n = 3), and (B) *Ldlr*$^{-/-}$ (black squares, n = 3), *Ldlr*$^{-/-}$*HS*$^{-/-}$ (n = 3), and *Ldlr*$^{-/-}$*HS*$^{-/-}$*Lrp*$^{-/-}$ (blue squares, n = 3). Overnight-fasted animals of the indicated genotypes were given 200µl of corn oil containing 5.4µCi [^{3}H] retinol by gavage. Blood samples were taken at the indicated times, and radioactivity remaining in 10 µl of serum was determined scintillation counting in triplicate.

The accumulation of particles in *Ldlr*$^{-/-}$*Ndst1*$^{f/f}$*Lrp1*$^{f/f}$*AlbCre*$^{+}$ mice could reflect increased secretion of lipoproteins as opposed to decreased clearance of reuptake of

particles after secretion (24). As determined after injection of animals with Triton WR-1339 to inhibit lipolysis and lipoprotein clearance, triglyceride secretion rates did not differ significantly between *Ldlr*$^{-/-}$*Ndst1*$^{f/f}$*Lrp1*$^{f/f}$*AlbCre*$^{+}$ mice and any other genotype (data not shown). This finding indicates that the accumulation of triglycerides is most likely a result of a decrease in clearance or uptake.

4.3.3 LDLR and HS mediate binding, uptake, and degradation of VLDL.

To determine if the various lipoprotein receptors could directly mediate binding of lipoproteins, hepatocytes were isolated from wild-type mice and incubated with ^{125}I-VLDL at 4^{o}C. Wild-type hepatocytes bound VLDL in a saturable manner, and the signal was reduced by the addition of heparin (data not shown). Fitting the data to a conventional single-site binding equation yielded a B_{max} value of 5.9 $\pm$ 0.3 μg VLDL protein/mg cell protein (~1.4 x 10^{6} sites per cell) and a K_D 40 $\pm$ 5 (R^2 = 0.9), assuming that the average size particle had a diameter of 40 nm, a mass of 2 x 10^{7} Da, and that protein represents 1.8% of the mass. To determine if binding was dependent on HS, Ldlr, or Lrp1, hepatocytes were isolated from various mutant mice. As shown in Fig 4-4, the absence of HS significantly reduced binding compared to wild-type hepatocytes. The absence of Ldlr, however, had reduced binding at low concentrations of VLDL, but behaved similarly to wild-type hepatocytes at high concentrations of VLDL. The *HS*$^{-/-}$*Lrp1*$^{-/-}$ hepatocytes showed no greater reduction in binding than the *Sdc1*$^{-/-}$ hepatocytes, implying that in the presence of the Ldlr, Lrp1 does not have an effect on binding. *Ldlr*$^{-/-}$*HS*$^{-/-}$ and *Ldlr*$^{-/-}$*HS*$^{-/-}$*Lrp1*$^{-/-}$ hepatocytes, however, showed virtually no binding, suggesting that Ldlr and HS are the two predominant receptors in

VLDL clearance, and in their absence there is little or no binding of VLDL particles.

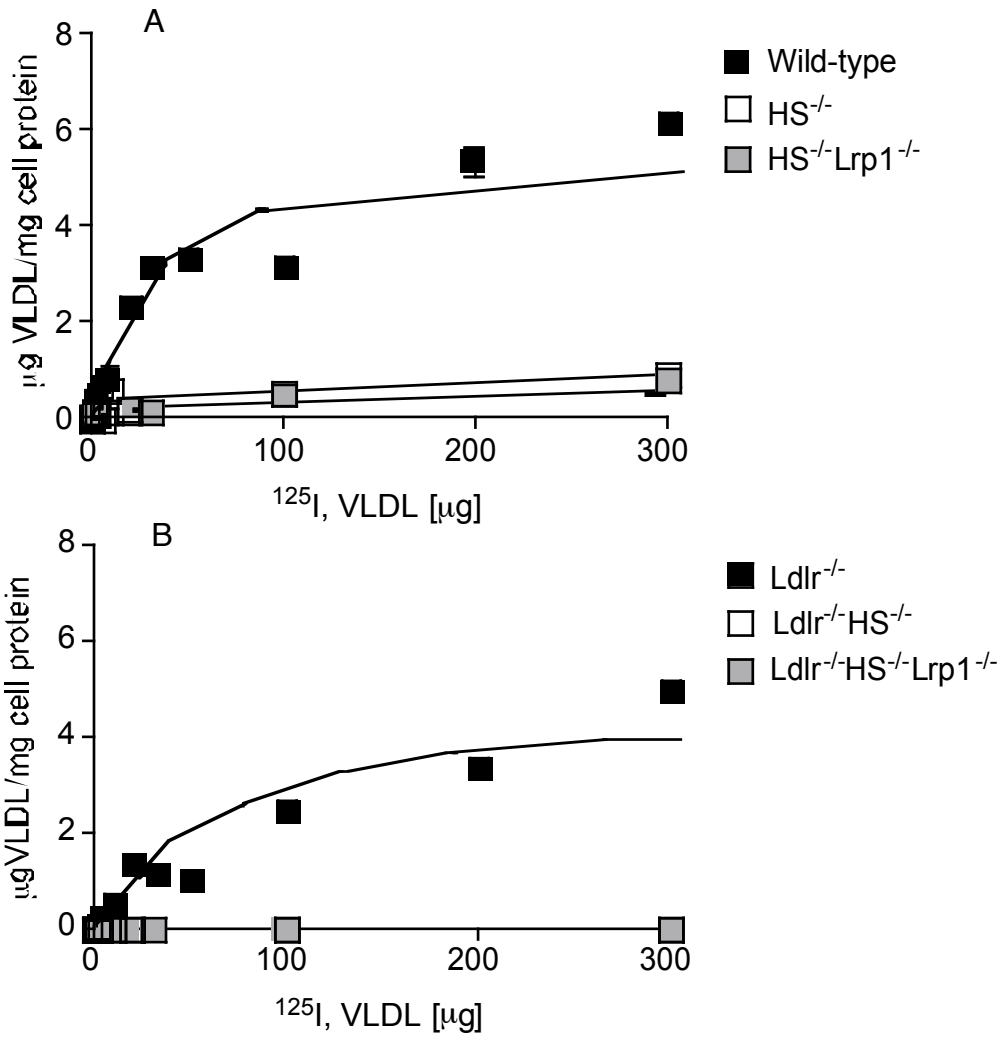


Figure 4-4. HS, LDLR mediates binding of VLDL. (A) Wild-type, *HS*$^{-/-}$, *HS*$^{-/-}$*Lrp*$^{-/-}$, and (B) *Ldlr*$^{-/-}$, *Ldlr*$^{-/-}$*HS*$^{-/-}$, and *Ldlr*$^{-/-}$*HS*$^{-/-}$*Lrp*$^{-/-}$ hepatocytes were incubated with the indicated concentrations of ^{125}I-VLDL in the presence of 10U heparin for 1 hour at 4^{o}C. The amount of binding observed in the presence of heparin was subtracted from the total to obtain specific binding (data not shown). Deletion of HS and LDLR reduced maximal binding.

We also examined uptake and degradation of VLDL by incubating wild-type, *Sdc1*$^{-/-}$, and *Ldlr*$^{-/-}$ with 20μg/ml of ^{125}I-VLDL at 37^{o}C. After one hour, wild-type cells bound and internalized 4.9 $\pm$ 0.4 μg VLDL/mg cell protein (Fig 4-5A), which was ~40% higher than the amount bound at 4^{o}C (2.6 μg/mg cell protein at 20 μg/ml

VLDL, Fig. 4-4). Uptake via syndecan-1 led to degradation of 2.4 μg/mg cell protein in one hour, as measured by the appearance of acid-soluble, non-chloroform extractable ^{125}I-counts in the growth medium. *Sdc1*$^{-/-}$ hepatocytes showed a dramatic increase in both uptake (2.0 ± 0.0 μg VLDL/mg cell protein; $P < 0.005$) and degradation (0.4 ± 0.1 μg VLDL/mg cell protein; $P < 0.02$) under these conditions. *Ldlr*$^{-/-}$ hepatocytes, however, behaved similarly to wild-type hepatocytes, with uptake of 4.2 ± 0.6 μg VLDL/mg cell protein and degradation.

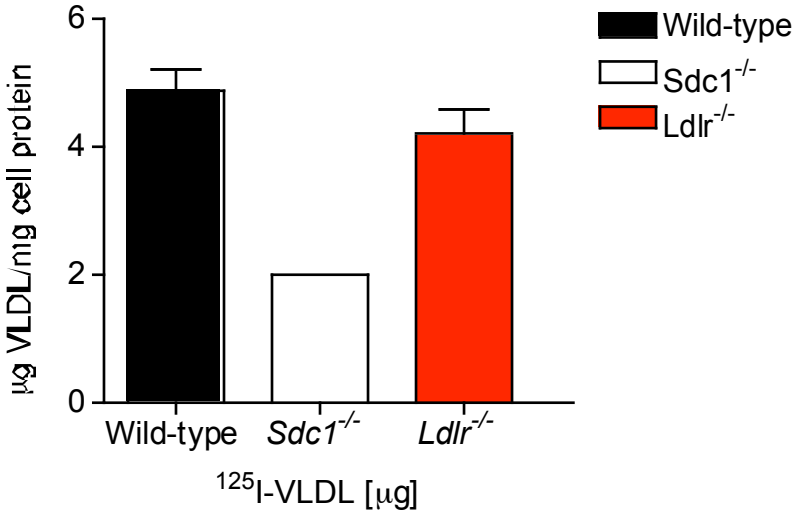


Figure 4-5. Binding, uptake and degradation of VLDL at 37°C. Uptake and degradation of VLDL was measured in wild-type (filled bars) , *Sdc1*$^{-/-}$ (open bars), and *Ldlr*$^{-/-}$ (red bars) hepatocytes after 1 hr incubation with 20 μg/ml of ^{125}I-VLDL. The bars represent the sum of binding and internalization under these conditions, or the amount of degradation as determined by acid soluble,non-chloroform extractable counts in the medium. Binding plus uptake was reduced 2.7 fold in *Sdc1*$^{-/-}$ cells, compared to 0.2 fold in *Ldlr*$^{-/-}$ cells . Degradation was reduced by nearly 6-fold.

4.3.4 The three receptors, LDLR, HS, and LRP1 do not compensate for each other.

We have clearly shown that both Ldlr and HS can mediate the clearance of VLDL particles. Since the absence of two receptors (Ldlr and HS) suggests a synergistic accumulation of triglycerides and cholesterol compared to the absence of either single receptor, we wanted to determine if in the absence of two receptors, the third was up-regulated. By qPCR analysis, we examined several genotypes of mice to determine if this was the case. LDLR and LRP1 were not up-regulated by in any either the *Ndst1*$^{f/f}$*AlbCre*$^{+}$, *Ndst1*$^{f/f}$*Lrp1*$^{f/f}$*AlbCre*$^{+}$, *Ldlr*$^{-/-}$,or *Ldlr*$^{-/-}$*Ndst1*$^{f/f}$*AlbCre*$^{+}$ mice. Interestingly, in the *Ldlr*$^{-/-}$ and *ApoE*$^{-/-}$, NDST1 was slightly up-regulated. This is expected as apoE binds to a region of heparan sulfate which is highly *N*-sulfated. The increase in NDST1 may be to increase the potential for binding of apoE-enriched particles to HS and mediate clearance (Fig. 4-6). Interestingly, in *Lrp*$^{f/f}$*AdCre* animals, qPCR analysis did not show a change in mRNA expression of LDLR; however examination of protein levels revealed an increase in LDLR expression (9). Thus, protein levels of all receptors in various mutant mice should be examined before conclusions can be made from this data.

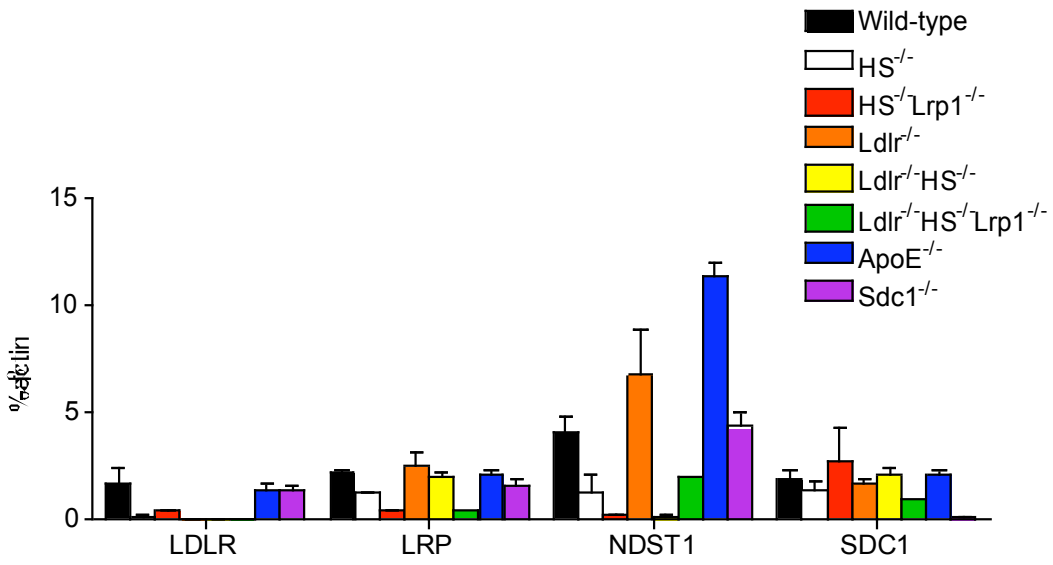


Figure 4-6. RT-PCR analysis of hepatocyte lipoprotein receptors. (A) Transcript levels of the various receptors were measured in isolated hepatocytes. The numbers represent the level of expression compared to the housekeeping gene β-actin, using C_T values from triplicate assays according to Stratagene manual. Comparable results were obtained in three independent assays.

4.4 Discussion

The major finding presented in this report is that LDLR and HSPGs are essential in the clearance of cholesterol- and triglyceride-rich lipoproteins, and only in their absence is LRP1 involved in the clearance of these particles. This conclusion is based on the fact that fasted *Ldlr*$^{-/-}$*Ndst1*$^{f/f}$*AlbCre*$^{+}$ mice have triglyceride and cholesterol levels seven-fold and four-fold over wild-type mice, and fasted *Ldlr*$^{-/-}$ *Ndst1*$^{f/f}$*Lrp1*$^{f/f}$*AlbCre*$^{+}$ mice have triglyceride and cholesterol levels fourteen- and twelve-fold greater than wild-type mice. The majority of this triglyceride and cholesterol is found in the VLDL particles (Fig 1 and 2), and the *Ldlr*$^{-/-}$ *Ndst1*$^{f/f}$*Lrp1*$^{f/f}$*AlbCre*$^{+}$ mice exhibit a greater delay in clearance of dietary fat compared to the *Ldlr*$^{-/-}$*Ndst1*$^{f/f}$*AlbCre*$^{+}$ mice (Fig. 3). Importantly, there is no apparent

compensation of the receptors; in the absence of any two, the third is not upregulated, suggesting that they each work independently of each other and perhaps mediate different types of lipoprotein particles (Fig 4-6). Taken together these data suggest that LDLR and HS are the primary receptors involved in lipoprotein remnant clearance and that in there absence there is little or no clearance of large VLDL particles.

Our genetic studies provide the first clear evidence that each of the three receptors works independently of the other two. Previous work had suggested that HSPG and LRP worked together (21), however the $HS^{-/-}Lrp1^{-/-}$ mice show no triglyceride accumulation over that of the $HS^{-/-}$ mice, genetically confirming that HS can act independently of LRP1. Additionally, because the $Ldlr^{-/-}Ndst1^{f/f}Lrp1^{f/f}AlbCre^{+}$ has a greater accumulation than the $Ldlr^{-/-}Ndst1^{f/f}AlbCre^{+}$, demonstrating that in the absence of LDLR and HS, LRP1 does play a role in lipoprotein remnant clearance. These studies also confirm that LDLR and HSPGs are the primary receptors involved in lipoprotein remnant clearance. While it has been previously demonstrated that HSPGs can independently take up VLDL remnants (11, 22), our data confirms that there are more HSPG receptors than LDL-receptors in hepatocytes, and these receptors are high affinity, low capacity receptors which are more likely to take up VLDL remnants than either LDLR or LRP1, and in the absence of either HS or Sdc1 (22), a 60% reduction in uptake is observed, compared to only a 10% reduction observed in the absence of LDLR, but the presence of HS at the same concentration (Fig. 8).

ApoE has been identified as a potential ligand for the LDLR, LRP1, and HSPGs (7, 12, 16, 18). Previous work in our laboratory has provided genetic evidence suggesting that apoE is not the ligand through which VLDL binds HS (K.I.S. and J.D.E., unpublished observations). If apoE was the primary ligand for all three receptors, then the phenotype observed in the absence of all three receptors would be similar to that of the *ApoE*$^{-/-}$ mouse. Interestingly, while the cholesterol levels that accumulate in the *ApoE*$^{-/-}$ mouse and the *Ldlr*$^{-/-}$*Ndst1*$^{f/f}$*Lrp1*$^{f/f}$*AlbCre*$^{+}$ animals are similar, and both mice accumulate cholesterol-rich VLDL, the *Ldlr*$^{-/-}$ *Ndst1*$^{f/f}$*Lrp1*$^{f/f}$*AlbCre*$^{+}$ mice have triglyceride levels ten-fold over the *ApoE*$^{-/-}$ mice, and the triglyceride accumulates in the VLDL fraction. This would suggest that of the three receptors that are missing (LDLR, LRP1, and HS), apoE is not the primary ligand for all three receptors. Other groups have demonstrated that the *Ldlr*$^{-/-}$*ApoE*$^{-/-}$ mouse does not have an accumulation of cholesterol, or a delay in post-prandial clearance, greater than that of the *ApoE*$^{-/-}$ mouse, suggesting that the clearance of VLDL particles through the LDLR is dependent on apoE (7). The data also implemented that there was another receptor, besides the LDLR, responsible for ~18% of apoE-dependent clearance, and that this receptor could be either LRP1 or HS. Because the *Ldlr*$^{-/-}$*Lrp1*$^{-/-}$ mice have the same triglyceride and cholesterol accumulation as the *Ldlr*$^{-/-}$ mice (9), it would imply that both apoE is the ligand for both LDLR and LRP1, and HS actually binds and internalizes VLDL particles through a different ligand.

The potential VLDL ligands required for HS binding are Lpl, HL, and apoB; because the VLDL particles that accumulate are large and triglyceride rich, Lpl is the

most likely candidate (1). We would hypothesize that hepatocyte HS binds Lpl on VLDL in order to hydrolyze the large, triglyceride-rich VLDL particles, and in the absence of hepatocyte HS these particles are unable to be hydrolyzed and remain as large, buoyant particles in the circulation.

Lpl is a key enzyme in the metabolism of triglyceride-rich lipoproteins (TRLs) (30). It catalyzes the hydrolysis of triglycerides in the core of TRLs, releasing fatty acids for uptake in skeletal, cardia, and adipose tissues. Lpl binds to heparan sulfate (31, 32) and was thought until recently to be bound predominantly to HSPGs present in capillary beds based in part on its rapid release by intravenous injection of heparain (33). Recent work by Young *et al* has cast doubt on this hypothesis; mice deficient in the Lpl-binding protein GPIHBP-1 have reduced Lpl activity and exhibit massive hypertriglyceridema and hyperchylomicronemia (34, 35). Thus, injected heparin may bind to Lpl and prevent its interaction with GPIHBP-1, rather than blocking Lpl interaction with endothelial cell HS. Lpl is also present in the liver and space of Disse where it can be slowly endocytosed. Injection of heparin can cause the release of hepatic Lpl back into the circulation, suggesting that it may by bound to HSPGs in this location (37, 38). Lpl can also associate with TRLs and act as a bridging molecule, which might facilitate lipoprotein uptake by way of HSPGs (1). It is possible that Lpl is acting in this manner, and in the absence of all three receptors there is no way to hydrolyze the triglyceride-rich particles because there is no HS with which to bind. In the absence of HS alone, there was no change observed in Lpl activity (11), but it may be the case that there is more Lpl associated with the particles that are accumulating in the circulation because they have no way to be cleared (36, 47). Further genetic and

biochemical studies are needed to confirm that Lpl is, in fact, the ligand required for the binding of TRLs to heparan sulfate and heparan sulfate proteoglycans.

In conclusion, we have established that HS and LDLR are the two primary receptors involved in lipoprotein clearance. It appears that the ligand required for binding and uptake through each of the various receptors is different; LDLR and LRP1 required apoE, while HS requires Lpl. More work is required to confirm this and establish potential relationships with a human population who may have mutations in these various receptors, or in potential ligands for the receptors.

4.5 Experimental Procedures

4.5.1 Mice and animal husbandry

Ndst1$^{f/f}$*AlbCre*$^{+}$ mice were described by MacArthur et al (11). *Ldlr* and *ApoE* knockout mice and *Lrp1*$^{f/f}$ mice were obtained from The Jackson Laboratories.. All mice were backcrossed >10 generations on a C57BL/6 background. All animals were housed and bred in vivaria approved by the Association for Assessment and Accreditation of Laboratory Animal Care located in the School of Medicine, University of California, San Diego, following standards and procedures approved by the local Institutional Animal Care and Use Committee. Mice were weaned at 3 weeks, maintained on a 12 hr light-dark cycle, and fed *ad libitum* with water and standard rodent chow (Harlan-TekLad). Genotyping was performed as described in the cited publications.

4.5.2 Lipoprotein Analysis.

Plasma samples were prepared from blood drawn by retro-orbital bleeding from mice fasted for 6 hr in the morning. Total cholesterol and triglyceride levels were determined enzymatically using an automated reader (Cobas Mira; Roche Diagnostics) and kits (Cholesterol High-Performance Reagent, Roche Diagnostics and Triglyceride-SL, Diagnostic Chemicals Ltd).

Lipoproteins were prepared from blood drawn by cardiac puncture using sequential preparative ultracentrifugation according to established methods (23). TRLs (δ = 1.006 g/ml) were prepared from pooled plasma samples (*n* = 10 mice, vol = 5 ml) by centrifugation for 12 hours at 45,000 x rpm in a Beckman 50.3Ti rotor. VLDL remnants and IDL were then collected as the δ = 1.006 - 1.019 g/ml fraction and subsequently LDL and HDL were collected as the δ = 1.019-1.063, and δ = 1.063-1.21g/ml fractions, respectively. The isolated lipoproteins were dialyzed against PBS and analyzed for lipid content using kits. Plasma lipoproteins were also separated by gel filtration FPLC. Pooled plasma samples were loaded on a Superose 12 FPLC column (Amersham Biosciences) in 0.15 M sodium chloride containing 1 mM EDTA and 0.02% sodium azide, pH 7.4, and 0.25-ml fractions were collected (0.1 ml/min).

4.5.3 Vitamin A excursion studies.

Clearance of chylomicrons derived from dietary triglyceride was measured by Vitamin A excursion essentially as described (7). Briefly, 27 μCi of [11,12-^{3}H]-retinol (Perkin-Elmer, 44.4Ci/mmol) in ethanol was mixed with 1 ml of corn oil (Sigma) and administered by oral gavage (200 μl/mouse). Retro-orbital sinus blood was sampled at the times indicated and radioactivity was measured in triplicate (10 μl of serum) by

scintillation counting. Triglycerides were measured enzymatically using a plate reader and kits.

4.5.4 Analysis of apolipoprotein composition.

Equal volumes of the $\delta < 1.006$ g/ml and $\delta = 1.063$-1.21g/ml float fraction were concentrated on the Microcon-30s (Millipore), and proteins were resolved by SDS-PAGE on 4%-15% Ready Gels (Bio-Rad). Proteins were visualized by Coomassie blue and silver stain, or by western blot. Western blots were performed by transfer of the gel of 0.45 μm nitrocellulose (NuPAGE) using a wet transfer apparatus in NuPAGE transfer buffer. Membranes were blocked in Superblock (Pierce) for 1 hour, then incubated overnight at 4^{o}C with α-mouse apoB48/100, apoE, apoAI, apoAIV, apoCII (Santa Cruz Biotechnology), LDLR (a kind gift from Dr. Jay Horton, University of Texas-Southwestern), LRP1, syndecan-1 (a kind gift from Dr. Alan Rapraeger, University of Wisconsin) or 3G10 rabbit polyclonal antibodies. Membranes were washed and incubated with HRP-conjugated goat-α-rabbit secondary antibody, washed and developed with ECL West Pico SuperSignal Reagents (Pierce).

4.5.5 Triglyceride secretion rate.

After a 4-6 hour fast, triglyceride secretion rate (TGSR) was determined by the method previously described by Hirano et al. (24). Briefly, 500mg per kg body weight of Triton WR-1339 (sigma) was injected via tail vein, and triglyceride concentrations were measured in plasma samples taken pre-injection, and 0.5, 1, 1.5, 2, and 24 hours

post-injection. TGSR was calculated from the increment in triglyceride concentration per min multiplied by the plasma volume of the mouse (estimated by 0.035% of body weight in g) and expressed in mg/min.

4.5.6 Immunofluorescence microscopy.

Livers were perfused at 7 ml/min with 30 ml of PBS/EDTA followed by 30 ml of 4% paraformaldehyde. Livers were snap-frozen, and 20-μm sections were cut on a cryostat. Sections were plated on glass coverslips precoated with laminin (2 μg/cm^2). They were then fixed with 2% paraformaldehyde in PBS for 10 min at room temperature, incubated for 10 min with 100 mM glycine, pH 7.4, to quench aldehyde groups, permeabilized in 0.1 % Triton X-100 for 10 min, blocked for 20 min with a solution of 1% bovine serum albumin (BSA) and 0.05% Tween in PBS, and then incubated for 2 hr at room temperature with primary antibodies (Apoprotein E, 1:500, Santa Cruz Biotechnology) in blocking solution. Excess antibody was removed by incubation for 15 min with 0.1% Tween in PBS. Samples were then incubated for 1 hr with Alexa fluor-594-conjugated goat anti-rabbit secondary antibody (1:250, Invitrogen) and then washed 6 times at 5-min intervals with 0.1% Tween in PBS and incubated for 20 min with the nuclear stain DAPI (1:5000) diluted in PBS. Images were captured with a DeltaVision Restoration microscope system (AppliedPrecision) using a Photometrics Sony CoolSAP HQ charge-coupled device (CCD) camera system attached to an inverted, wide-field fluorescence microscope (Nikon TE200). Optical sections were acquired using a 63x Nikon (NA 1.3) oil immersion objective in 0.2-μm steps in the *z*-axis. Fluorescence was detected using a standard DAPI and

Texas Red filter set. Images were saved, processed, and analyzed on SGI workstations (O2, Octane) using the DeltaVision software package softWoRx (version 2.50). Quantification of fluorescence was accomplished using only the linear range of the digital camera.

4.5.7 Quantitative RT-PCR of Membrane HSPGs.

RNA was isolated from purified hepatocytes from various genotypes, as well as C57BL/6 mice as described previously (25). Samples were reverse transcribed (Superscript III, Invitrogen) and amplified using intron spanning primers. Quantitation was done by the $2^{-\Delta\Delta Ct}$ method using β-actin as control RNAs (26). C_T values from triplicate assays were used to calculate fold-expression as compared to β-actin according to the Stratagene manual. Results were verified in three independent assays.

4.5.8 Lipoprotein binding and uptake by hepatocytes.

Human VLDL (δ < 1.006 g/ml, ~1.1 mg protein) was iodinated using 3 mCi and $Na^{125}I$ (1.4×10^2 cpm/ng, NEN/Perkin Elmer) using Iodogen (27). Under these conditions, 13% of the label was lipid soluble. Isolated hepatocytes were treated with the indicated concentration of ^{125}I-VLDL in DMEM media with 2.5 mg/ml lipoprotein-free serum (Biomedical Technologies, Inc., Boston, MA). Cells were incubated at 4^{o}C or 37^{o}C for 1 hr, rinsed three times with PBS and then solubilized with 0.1M NaOH. Protein concentration was determined by Bradford (BioRad) and radioactivity was measured by gamma counting. Degradation of ^{125}I-VLDL was measured by precipitation of 0.25 mL of conditioned media with an equal volume of

50% trichloroacetic acid (28). After 30 min at 4^{o}C, the samples were centrifuged for 30 min. The supernatant was placed in a fresh glass tube, and 5 μL of 40% potassium iodide was added as a carrier. Hydrogen peroxide (30%) was added, and lipid soluble material was extracted by the addition of 2 ml of chloroform. An aliquot of the upper aqueous phase containing iodotyrosine was counted as measure of degradation.

4.5.9 Statistics.

Statistical analyses were performed using PRISM (GraphPad Software). All data is expressed as mean values $\pm$ SD unless otherwise indicated. Significance was determined using an unpaired Student's (two-tailed) t-test or ANOVA. Significance was taken as $P < 0.05$.

4.6 Acknowledgements

The bulk of this work will be submitted in for publication to the *Journal of Biological Chemistry* with coauthors Erin M. Foley, Ingrid R. Niesman, Joseph L. Witztum, and Jeffrey D. Esko. The dissertation author was the primary author of the work contained in this chapter. Together with her coauthors, she thanks Joseph Juliano, Fely Alamazen and Jennifer Pattison at UCSD, David Ditto of the Hematology/Coagulation/Chemistry Core. Work was conducted within the department of Cellular and Molecular Medicine, the Department of Medicine, and the Glycobiology Research and Training Center, University of California, San Diego, La Jolla, California.

4.7 References

1. **Williams, K.J., Fless, G.M., Petrie, K.A., Snyder, M.L., Brocia, R.W., and Swenson, T.L. 1992. Mechanisms by which lipoprotein lipase alters cellular metabolism of lipoprotein(a), low density lipoprotein, and nascent lipoproteins. Roles for low density lipoprotein receptors and heparan sulfate proteoglycans. *J. Biol. Chem.* 267: 13284-13292.**

2. **Mahley, R.W., and Ji, Z.A. 1999. Remnant lipoprotein metabolism: key pathways involving cell-surface heparan sulfate proteoglycans and apolipoprotein E. *J. Lipid Res.* 40: 1-16.**

3. **Vilaro, S. et al. 1988. Lipoprotein lipase in liver. Release by heparin and immunocytochemical localization. *Biochim. Biophys. Acta.* 959: 106-117.**

4. **Sanan, D.A., Fan, J., Bensadoun, A., and Taylor, J.M. 1997. Hepatic lipase is abundant on both hepatocyte and endothelial cell surfaces in the liver. *J. Lipid Res.* 38: 1002-1013.**

5. **Rubinsztein, D.C., et al. 1990. Chylomicron remnant clearance from the plasma is normal in familial hypercholesterolemic homozygotes with defined receptor defects. *J. Clin. Invest.* 86: 1306-1312.**

6. **Kita, T., et al. 1982. Hepatic uptake of chylomicron remnants in WHHL rabbits: a mechanism genetically distinct from the low density lipoprotein receptor. *Proc. Natl. Acad. Sci. U.S.A.* 79: 3623-3627.**

7. **Ishibashi, S., et al. 1996. Role of the low density lipoprotein (LDL) receptor pathway in the metabolism of chylomicron remnants. A quantitative study in knockout mice lacking the LDL receptor, apoliprotein E, or both. *J. Biol. Chem.* 271: 22422-22427.**

8. **Cooper, A.D. 1997. Hepatic uptake of chylomicron remnants. *J. Lipid Res.* 38: 2173-2192.**

9. **Rohlmann, A., Gotthardt, M., Hammer, R.E., and Herz, J. 1998. Inducible inactivation of hepatic LRP gene by cre-mediated recombination confirms role of LRP in clearance of chylomicron remnants. *J. Clin. Invest.* 101: 689-695.**

10. **Fujino, T., et al. 2003. Low-density lipoprotein receptor-related protein 5 (LRP5) is essential for normal cholesterol metabolism and glucose-induced insulin secretion. *Proc. Natl. Acad. Sci. U.S.A.* 100: 229-234.**

11. MacArthur, J.M., Bishop, J.R., Stanford, K.I, Wang, L., Bensadoun, A., Witztum, J.L., and Esko, J.D. 2007. Liver heparan sulfate proteoglycans mediate clearance of triglyceride-rich lipoproteins independently of LDL receptor family members. *J. Clin. Invest.* 117: 153-164.

12. Ji, Z.S., et al. 1993. Role of heparan sulfate proteoglycans in the binding and uptake of apolipoprotein E-enriched remnant lipoproteins by cultured cells. *J Biol. Chem.* 268: 10160-10167.

13. Ji, Z.S., Fazio, S., and Mahley, R.W. 1994. Variable heparan sulfate proteoglycan binding of apolipoprotein E variants may modulate the expression of type III hyperlipoproteinemia. *J. Biol. Chem.* 269: 13421-13428.

14. Ji, Z.S., et al. 1994. Enhanced binding and uptake of remnant lipoproteins by hepatic lipase-secreting hepatoma cells in culture. *J. Biol. Chem*. 269: 13429-13436.

15. Ji, Z.S., and Mahley, R.W. 1994. Lactoferrin binding to heparan sulfate proteoglycans and the LDL receptor-related protein. Further evidence supporting the importance of direct binding of remnant lipoproteins to HSPG. *Arterioscler. Thromb.* 14: 2025-2031.

16. Al-Haideri, M., et al. 1997. Heparan sulfate proteoglycan-mediated uptake of apolipoprotein E-triglyceride-rich lipoprotein particles: a major pathway at physiological particle concentrations *Biochemistry* 36: 12766-12772.

17. Fuki, I.V., et al. 1997. The syndecan family of proteoglycans. Novel receptors mediating internalization of atherogenic lipoproteins in vitro. *J. Clin. Invest.* 100: 1611-1622.

18. Ji, Z.S., Dichek, H.L., Miranda, R.D., and Mahley, R.W. 1997. Heparan sulfate proteoglycans participate in hepatic lipase- and apolipoprotein E-mediated binding and uptake of plasma lipoproteins, including high density lipoproteins. *J. Biol. Chem.* 272: 31285-31292.

19. Zeng, B.J., Mortimer, B.C., Martins, I.J., Seydel, U., and Redgrave, T.G. 1998. Chylomicron remnant uptake is regulated by the expression and function of heparan sulfate proteoglycan in hepatocytes. *J. Lipid. Res.* 39: 845-860.

20. Fuki, I.V., Iozzo, R.V., and Williams, K.J. 2000. Perlecan heparan sulfate proteolgycan. Novel receptor that mediates a distinct pathway for ligand catabolism. *J. Biol. Chem.* 275: 25742-25750.

21. Wilsie, L.C., and Orlando, R.A. 2003. The low density lipoprotein receptor-related protein complexes with cell surface heparan sulfate proteoglycans to regulate proteoglycan-mediated lipoprotein catabolism.

22. Stanford, K.I., Bishop, J.R., Niesman, I.R., Witztum, J.L., and Esko, J.D. 2009. Syndecan-1 is the primary heparan sulfate proteoglycan mediating hepatic clearance of triglyceride-rich lipoproteins *in vivo*.

23. Kelley, J.L., and Kruski, A.W. 1986. Density gradient ultracentrifugation of serum lipoproteins in a swinging bucket rotor. *Methods Enzymol*. 128: 170-181.

24. Hirano, T., et al. 2001. Apoprotein C-III deficiency markedly stimulates triglyceride secretion in vivo: comparison with apoprotein E. *Am. J. Physiol. Endocrinol. Metab.* 281: E665-E669.

25. Bishop, J.R., and Esko, J.D. 2005. The elusive role of heparan sulfate in Toxoplasma gondii infection. *Mol. Biochem. Parasitol.* 139: 267-269.

26. Livak, K.J., and Schmittgen, T.D. 2001. Analysis of relative gene expression data using real-time quantitative PCR and the 2(-Delta Delta C(T)) Method. *Methods* 25: 402-408.

27. Salacinski, P.R., McLean, C., Sykes, J.E., Clement-Jones, V.V., and Lowry, P.J. 1981. Iodination of proteins, glycoproteins, and peptides using solid-phase oxidizing agent, 1,3,4,6-tetrachlora-3 alpha, 6 alpha-diphenyl glycoluril (Iodogen). *Anal. Biochem.* 117: 136-146.

28. Williams, K.J. 2001. Interactions of lipoproteins with proteoglycans. *Methods Mol. Biol.* 171: 457-477.

29. Paszty, C., Maeda, N., Verstuyft, J., and Rubin, E.M. 1994. Apolipoprotein AI transgene corrects apolipoprotein E deficiency-induced atherosclerosis in mice. *J. Clin. Invest.* 94: 899-903.

30. Goldberg, I.J., and Merkel, M. 2001. Lipoprotein lipase: physiology, biochemistry, and molecular biology. *Front Biosci.* 6: D388-405.

31. Parthasarathy, N., Goldberg, I.J., Sivaram, P., et al. 1994. Oligosaccharide sequences of endothelial cell surface heparan sulfate

proteoglycan with affinity for lipoprotein lipase. *J. Biol. Chem*. 269: 22391-22396.

32. Spillmann, D., Lookene, A., and Olivercrona, G. 2006. Isolation and characterization of low sulfated heparan sulfate sequences with affinity for lipoprotein lipase. *J. Biol. Chem.* 281: 23405-23413.

33. Anfinsen, C.B., Boyle, E., and Brown, R.K. 1952. The role of heparin in lipoprotein metabolism. *Science* 115: 583-586.

34. Beigneux, A.P., Davies, B.S., Gin, P., et al. 2007. Glycosylphosphatidylinositol-anchored high-density lipoprotein-binding protein 1 (GPIHBP1) plays a critical role in the lipolytic processing of chylomicrons. *Cell Metab*. 5: 279-291.

35. Young, S.G., Davies, B.S., Fong, L.G., et al. GPIHBP1: an endothelial cell molecule important for the lipolytic processing of chylomicrons. *Curr. Opin. Lipidol.* 18: 389-396.

36. Bishop, J.R., Stanford, K.I., and Esko, J.D. 2008. Heparan sulfate proteoglycans and triglyceride-rich lipoprotein metabolism. *Curr. Opin. Lipidol.* 19: 307-313.

37. Wallinder, L., Peterson, J., Olivercrona, T., and Bengtsson-Olivercrona, G. 1984. Hepatic and extrahepatic uptake of intravenously injected lipoprotein lipase. *Biochim. Biophys. Acta* 795: 513-524.

38. Olivercrona, T., and Bengtsson-Olivercrona, G. 1993. Lipoprotein lipase and hepatic lipase. *Curr. Opin. Lipidol.* 4: 187-196.

39. Sorci-Thomas, M., Prack, M.M., Dashti, N., Johnson, F., Rudel, L.L., and Williams, D.L. 1988. *J. Biol. Chem.* 263: 5183-5189.

40. Williamson, R., Lee, D., Hagaman, J., and Maeda, N. 1992. *Proc. Natl. Acad. Sci. U.S.A.* 89: 7134-7138.

41. Walsh, A., Ito, Y., and Breslow, J.L. 1989. *J. Biol. Chem.* 264: 6488-6494.

42. Plump, A.S., Scott, C.J., and Breslow, J.L. 1994. *Proc. Natl. Acad. Sci. U.S.A.* 91: 9607-9611.

43. Fielding, C.J., and Fielding, P.E. 1995. *J. Lipid Res.* 36: 211-228.

44. Tall, A.R. 1990. *J. Clin. Invest.* 86: 379-384.

45. Zhang, S.H., Reddick, R.L., Burkey, B., and Maeda, N. 1994. *J. Clin. Invest.* 94: 937-945.

46. Spangenberg, J., and Curtiss, L.K. 1997. Influence of macrophage-derived apoprotein E on plasma lipoprotein distribution of apolipoprotein A-I in apoprotein E-deficient mice. *Biochim. Biophys. Acta* 1349: 109-121.

47. Hu, L., ven der Hoogt, C.C., Espirito Santo, S.M.S., Out, R., Kypreos, K.E., van Vlijmen, B.J.M., Van Berkel, T.J.C., Romijn, J.A., Havekes, L.M., Willems van Dijk, K., and Rensen P.C.N. 2008. The hepatic uptake of VLDL in lrp^{-}ldlr$^{-/-}$vldlr$^{-/-}$ mice is regulated by LPL activity and involves proteoglycans and SR-B1.

CHAPTER 5

CONCLUSIONS AND FUTURE DIRECTIONS

5.1 Summary

The work described in this thesis demonstrates the essential role of heparan sulfate proteoglycans in lipoprotein remnant metabolism. Several conclusions can be drawn from this data. First, the clearance of TRLs depends not on the overall sulfation, but rather on the *N*-sulfate and 2-*O*-sulfate groups.. This implies that a specific ligand on VLDL requires a particular sequence of sulfated sugars in heparan sulfate in order to be taken up into hepatocytes. Secondly, we have established that syndecan 1 is the only HSPG involved in lipoprotein remnant clearance. Finally, this work shows that heparan sulfate and the LDLR are the two predominant receptors involved in TRL clearance. In the absence of these two receptors, LRP plays a role in TRL clearance.

5.2 *N*- and 2-*O*-sulfation are required for the binding and uptake of triglyceride-rich lipoproteins

We have established that the absence of either *N*- or 2-*O*-sulfate groups results in defective clearance of TRL particles. While this data helps to establish the role of heparan sulfate as a receptor involved in VLDL clearance, it still raises a series of

questions as to the importance of the exact pattern of sulfation required for VLDL binding. One of the interesting effects of altering 2-O-sulfation of heparan sulfate in hepatocytes is the nearly stoichiometric increase in N-sulfation and 6-O-sulfation, which maintains the overall charge of the chain. In spite of this "compensation", triglycerides accumulate in the mutants lacking *N*-sulfated and 2-*O*-sulfates and VLDL uptake is reduced in isolated hepatocytes in a parallel manner, suggesting that the ligand on the lipoprotein particles exhibits specificity for the arrangement of sulfated residues.

Similar "compensation" occurs in Chinese hamster ovary cells containing a mutation in Hs2st (62) and model organisms lacking the Hs2st orthologs (1, 63-66). The mechanism responsible for these coordinated changes in sulfation remain unknown. GlcNAc N-deacetylation and N-sulfation precedes all of the other modification reactions and creates the preferred substrate for HsC5epi, which epimerizes glucuronic acids located to the reducing side of the N-sulfoglucosamine units to L-iduronic (IdoA) (67). The resulting IdoA is then preferentially sulfated at C-2 by Hs2st, although the enzyme can also work less efficiently on glucuronic acids (67). Although we have not measured GlcNAc N-deacetylase/N-sulfotransferase activity in mutant hepatocytes, *N*-sulfotransferase activity in Hs2st-deficient CHO cells was unchanged (62), suggesting that the presence of 2-*O*-sulfated residues somehow decreases the rate or extent of the *N*-deacetylase/*N*-sulfotransferase reaction. This explanation suggests that the length of the N-sulfated blocks might be greater in the absence of Hs2st, which is borne out by analysis of the sulfated segments (NS-domains) in mouse gene trap mutant allele in Hs2st (1).

Using chemically modified heparin, we showed that 6-*O*-sulfate groups are not required for binding of TRLs, as their absence did not impair the ability of wild-type heparin to bind VLDL. We have not, however, examined this effect *in vivo*. By crossing the *Hs6st*$^{f/f}$ mouse to a mouse carrying the *AlbCre* promoter, we will be able to address this question. Also, disaccharide analysis of these chains will allow us to determine if, in the absence of 6-*O*-sulfation, *N*- or 2-*O*-sulfation is affected.

Along these lines, we have not yet addressed the importance of hepatocyte 3-*O*-sulfation. It would be possible to treat wild-type hepatocytes with siRNA for the various *Hs3sts* (1-7) and determine if silencing this gene would alter binding and uptake of VLDL *in vitro.* Analysis of triglycerides in plasma samples of *Hs3st1* or *Hs3st2* mutant mice (68, 72) would allow us to determine if either of these isoforms contribute to binding and uptake of TRLs.

The precise oligosaccharide sequence has yet to be determined; we would predict that it would be a relative short sequence rich in *N*- and 2-*O*-sulfate groups.but more work is necessary to determine the exact sequence. We could create a column of the potential ligand (Lpl, HL, apoB) and run partially digested liver HS through the column. We could then purfy the oligosaccharide that binds the ligand and determine the exact sequence that binds the column using nitrous acid to determine the amount of GlcA vs. IdoA content and various heparin lyases to determine disaccharide composition (69, 70).

5.2.1 Determine the ligand required for VLDL binding to heparan sulfate

While determining the sequence in heparan sulfate required for VLDL binding would be interesting, in order to truly understand the mechanism of binding and

uptake, it is necessary to identify the protein ligand on TRLs required for binding and uptake. Several mechanisms have been suggested to explain how heparan sulfate interactions with apolipoproteins and/or enzymes affect lipoprotein processing in the liver. Mahley et al have suggested that remnant lipoprotein particles entering the space of Disse bind to HSPGs via apoE, resulting in their sequestration prior to further processing and receptor-mediated endocytosis (2). Lipoprotein lipase and hepatic lipase also can act in this way, since both enzymes can bind to heparan sulfate and to the lipoprotein particles, thus acting a bridging molecule (2, 3). Apparently, one or more of these ligands contains a binding site that requires N-sulfation and 2-*O*-sulfation. Many of these ligands bind most avidly to segments enriched in the tri-sulfated disaccharide, GlcNS6S-IdoA2S, but less sulfated structures may suffice (7-18). Thus, the available structural data does not allow us to determine which if any of these proteins serve as the relevant ligand for heparan sulfate dependent clearance.

ApoE (2,3), apoB48, apoB100 (7-9), hepatic lipase (HL) (10, 11), and lipoprotein lipase (Lpl) (12-18) contain domains that bind to HS. ApoE emerged as a primary candidate for VLDL binding to HS because there is a known binding site for apoE on HS (4, 5). However, work in our laboratory, has shown that a *Ndst1*$^{f/f}$*AlbCre*$^{+}$*ApoE*$^{-/-}$ mice accumulate plasma triglycerides to a greater extent than compared to *ApoE*$^{-/-}$, *Ndst1*$^{f/f}$*AlbCre*$^{+}$, or *Sdc1*$^{-/-}$ mice, suggesting that HS clears TRLs in an apoE independent manner (K.I.S. and J.D.E., unpublished results). Other groups have demonstrated that the *Ldlr*$^{-/-}$*ApoE*$^{-/-}$ mouse accumulate cholesterol and exhibit delayed clearance in post-prandial clearance like the *ApoE*$^{-/-}$ mouse, suggesting that the clearance of VLDL particles through the LDLR is dependent on apoE (21).

The data also implied that there was another receptor, besides the LDLR, responsible for ~18% of apoE-dependent clearance, and that this receptor is most likely LRP1 (7). Because the *Ldlr*$^{-/-}$*Lrp*$^{-/-}$ mice have the same triglyceride accumulation as the *ApoE*$^{-/-}$ mice (22), it would imply that apoE is the ligand for both LDLR and LRP1. Thus, HS binds and internalizes VLDL particles through a different ligand.

Other possible candidates include apoB48, apoB100, HL, and Lpl as potential ligands for TRL binding to HS. It would be possible to generate a mouse model of *Ndst1*$^{f/f}$*AlbCre*$^{+}$ crossed to a mouse expressing apoB100-only, or a mouse expressing apoB48-only (6) and observe effects of triglyceride accumulation in mice. If apoB100 is the ligand required for VLDL binding to HS, the *Ndst1*$^{f/f}$*AlbCre*$^{+}$*ApoB100-only* mouse would not accumulate triglyceride-rich particles over either single mutant; the same is true for the *Ndst1*$^{f/f}$*AlbCre*$^{+}$*ApoB48-only* mouse if apoB48 is the primary ligand. One could take VLDL from the various over-expresser mice and inject it into wild-type and HS-deficient mice. Since the VLDL is from mice that were created using a human transgene, the injected VLDL can be traced using MB47, a human mAb to apoB (71). This way, we can determine if apoB100 or apoB48 is the ligand required for binding of VLDL to HS.

Hepatic lipase (HL) has been shown to serve as a ligand for lipoprotein particle binding and uptake via proteoglycans and receptor pathways, independent of its enzymatic function (10, 11). HL has also been shown to aid in lowering plasma remnant and HDL concentrations; patients who are HL-deficient have a mild hypertriglyceridemia and increased atherosclerosis, emphasizing the role of HL in remnant metabolism (19). HL, however, also plays a role in HDL cholesterol

metabolism, and mice deficient in HL have no effect on triglcyeride levels, suggesting that it may not be the ligand involved in the clearance of TRLs through HSPGs, at least in mice (20). Lipoprotein lipase (Lpl), however, remains a primary candidate to bind HS and regulate TRL metabolism. Lpl is a key enzyme in the metabolism of TRLs (23). It catalyzes the hydrolysisof triglycerides in the core of TRLs, releasing fatty acids for uptake in skeletal, cardiac, and adipose tissue. Lpl binds to heparan sulfate (13-15) and was thought until recently to be bound predominantly to HSPGs present in capillary beds based in part on its rapid release by intravenous injection of heparin (24). Recent work by Young et al. cast doubt on this hypothesis; mice deficient in the Lpl-binding protein Gpihbp-1 have reduced Lpl activity and exhibit massive hypertriglyceridemia and hyperchylomicronemia (25, 26). Thus, injected heparin may bind to Lpl and prevent its interaction with Gpihbp-1, rather than blocking Lpl interaction with endothelial cell HS.

Lpl is also present in the liver and space of Disse where it can be endocytosed. Injection of heparin can cause the release of hepatic Lpl back into the circulation, suggesting that it may be bound to HSPGs in this location (27, 28). Lpl can also associate with TRLs and act as a bridging molecule, which might facilitate lipoprotein uptake by way of HSPGs (29). If correct, this model predicts that Lpl associated with the particles that are accumulating in circulation in the $Ldlr^{-/-}HS^{-/-}Lrp1^{-/-}$ mice may be enriched with Lpl (31, 32).

The Lpl-deficient mouse dies 18h post-birth, but the $Lpl^{+/-}$ mouse survives and has and elevated triglyceride levels without a corresponding increase in cholesterol, similar to the HS-deficient mouse (33). Various mutants of Lpl exist, as such it would

be interesting to knock-in an enzymatically active form of Lpl that lacks the ability to bind HS. If this form of Lpl exhibited normal enzymatic activity in the periphery and retained the ability to bind Gpihbp1, and only lacked the ability to bind HS, we would expect to see an accumulation of VLDL triglycerides.

5.3 Why do large particles accumulate in the *Ldlr$^{-/-}$HS$^{-/-}$Lrp1$^{-/-}$* mice?

The absence of the three receptors (LDLR, LRP1, and HS) resulted in the accumulation of large, triglyceride- and cholesterol-rich VLDL particles, as discussed in Chapter 4. The particles that accumulate in the *Ldlr$^{-/-}$HS$^{-/-}$Lrp1$^{-/-}$* mice are different than those that accumulate in the *ApoE$^{-/-}$* mice, as discussed in Chapter 4. Both mutants accumulate cholesterol-rich VLDL particles, however *Ldlr$^{-/-}$HS$^{-/-}$Lrp1$^{-/-}$* also accumulate triglyceride-rich VLDL, while there is virtually no accumulation of triglyceride in the *ApoE$^{-/-}$* mice. Little has been done, however, to characterize these particles and establish why they are unable to be cleared and metabolized in this mouse. Preliminary data suggests that these particles migrate as preβ (VLDL) particles. Very little HDL remaining, similar to the phenotype of the *ApoE$^{-/-}$* mouse. Additionally, apoAI, which is usually associated with HDL, is shifted to the preβ VLDL fraction in both strains. Production of apoAI is a determinant of plasma HDL concentrations *in vivo* (34). The loss of apoE (in *ApoE$^{-/-}$* mice) decreases plasma HDL cholesterol, and induces several changes in apoprotein composition of VLDL and IDL. The *ApoE$^{-/-}$* mice possess a substantial increase of apoAI and apoAIV in their VLDL and IDL fractions (41); because the apoAI mRNA levels remain unchanged it has been suggested that in the absence of apoE, apoAI remains on remnant particles and thereby

limits HDL production (41, 42). It has also been suggested that apoAI accumulate on VLDL serve as an essential structural component of these abnormal lipoproteins (42); it is possible that that is the reason apoAI remains on the VLDL particles in the *Ldlr*$^{-/-}$ *HS*$^{-/-}$*Lrp1*$^{-/-}$ mice. It is also possible that the apoAI remains associated with VLDL to provide a potential mechanism of clearance: as the three primary receptors involved in VLDL clearance have been removed from these mice, perhaps the HDL receptor SR-B1, which recognizes apoAI (32), clears apoAI-enriched VLDL particles. SR-B1 levels need to be examined in these mutant mice to determine if this receptor is up-regulated in the absence of the other three.

5.4 Syndecan 1 is the primary hepatocyte HSPG involved in lipoprotein remnant metabolism

The work presented in chapter 3 establishes that syndecan1 is the primary hepatocyte HSPG involved in the clearance of lipoprotein remnant particles, and that in the absence of Sdc1 TRLs accumulate in the plasma. The compound mutant deficient in Sdc1 and hepatocyte Ndst1 (*Sdc1*$^{-/-}$*Ndst1*$^{f/f}$*AlbCre*$^{+}$) does not show an additive phenotype over either single mutant, implying that it is the HS chains of Sdc1 that are involved. Syndecan 1, however, has five possible GAG attachment sites; three for HS and two for chondroitin sulfate (CS) (43). It is unclear if more than one chain is involved in the binding and uptake of TRL particles. Hepatocyte HS chains are approximately 14-25kDa (44, 45), or 50-100 monosaccharides, which is extended would measure ~40-80nm. Interestingly, this is approximately the same size as TRL remnants. Since the docking sites on the ligand and the HS chan are all subdomains,

we propose the idea of a proteoglycan "hug"; the idea that multiple chains are interacting with the VLDL particle, wrapping around it to facilitate binding and internalization into the hepatocyte. Future studies to address the model involve creating different mutant forms of Sdc1, e.g. deletions of one or more chains. Adenoviral infection of liver by injection of recombinant AdSdc virus into mutant *Sdc1*$^{-/-}$ mice will allow us to determine the function of the individual chains.

We can also create mutations in various domains of the Sdc1 proteoglycan. By creating mutations in the protease cleavage site in the ectodomain, in the transmembrane domain, or in the cytoplasmic C-terminal domain, we can gain insight into the mechanism by which Sdc1 facilitates uptake.

Little is known about the mechanism through which Sdc1 takes the TRL particle into the hepatocyte. We know that, for example, the Ldlr takes up particles through a fast ($t_{1/2}$ = 5-10min), clathrin-mediated pathway (46). Proteoglycan uptake in cells other than hepatocytes is slower ($t_{1/2}$ = 20-60min) and occurs through a clathrin-independent mechanism (47-50). In order to determine the mechanism through which syndecan 1 takes TRLs into the cell, we will use ^{125}I-VLDL in the presence of various inhibition of endocytosis. We will use Methyl-β-Cyclodextrin and Statins to inhibit lipid-raft mediated uptake, Monodansylcadaverine to inhibit uptake by coated pits, and Amiloride to inhibit uptake by macropinocytosis (52). We can then measure uptake and determine which pathway affects lipoprotein uptake. Additionally, we can use immunofluorescence microscopy to track syndecan-1 and TRLs after they have been taken up into the cell.

5.4.1 Regulation of Sdc1 uptake by dietary triglyceride

It has been well established that levels of exogenous and endogenous cholesterol can regulate Ldlr expression on the cell surface (51). It is unknown, however, if Sdc1 can be regulated in the same manner. Edwards et al. examined the regulation of Sdc1 in prostate epithelial cells by ω-3 polyunsaturated acids. By feeding animals a diet enriched in ω-3 polyunsaturated fatty acids and then examining prostate tissue of mice, they were able to determine that mice on this diet had an increase in Sdc1 mRNA (57). The question arises that in this system, is liver syndecan 1 expression altered, and does this have any affect on triglyceride levels? One way to address this question is to treat isolated hepatocytes with free fatty acids, such as ω-3 and ω-6 (as described above). By incubating cultured cells with varying amounts of fatty acids, and then using qPCR or western blot techniques to establish expression or quantity of Sdc1, we would be able to determine if Sdc1 can be regulated by dietary factors.

Previous work has shown that ω-3 polyunsaturated fatty acids (PUFA) enriched LDL, inhibited proliferation, and induced apoptosis in human breast cancer cells. The ω-3 LDL delivered both eicosapentaenoic acid (EPA) and docosahexaenoic acid (DHA) to the cells (53-55). When delivered to the cell via albumin complexes, DHA was able to stimulate apoptosis in a pathway involving the activation of PPARγ (54). Interestingly, Sdc1 has an upstream PPARγ binding site, suggesting that ω-3 activation led to increased Sdc1 expression which resulted in apoptosis. These functions raise the interesting possibility that the lipid-lowering effect of ω-3 fatty acids may be mediated through induction of Sdc1 (55, 56).

5.5 Conclusions

Hypertriglyceridemia is prevalent in the United States, affecting as many as 10-20% of the population (58-60). Acquired hypertriglyceridemia has a complex etiology and may arise from conditions such as uncontrolled diabetes mellitus, metabolic syndrome, chronic alcohol consumption, hypothyroidism, steroids (estrogen), and certain drug treatments. This effect may be compounded by non-esterified free fatty acids in the circulation, which also appear to alter HSPG expression (61). We posit that complications of these disorders may alter liver HS structure. The fact that relatively mild changes in HS structure can lead to triglyceride accumulation would support this notion (30). Furthermore, changes in LDLR expression compounded with alterations in hepatic HS could explain the accentuated accumulation of plasma triglycerides in some individuals. Based on these studies, we suggest that screening of patients with hypertriglyceridemia for changes in HS structure and polymorphisms in candidate genes involved in HSPG expression may reveal novel associations between glycan biosynthesis and lipoprotein metabolism.

We have identified several candidate genes that could be involved in human hypertriglyceridemia, including *Ndst1*, *Hs2st*, or *Sdc1*. It is possible that small nucleotide polymorphisms (SNPs) would allow us to examine variations at a single site in a patients DNA sequence, allowing us to correlate a candidate gene with a certain type of human hypertriglyceridemia. By selecting a patient population with a mild hypertriglyceridemia, or with hypercholesteremia accompanied by hypertriglyceridemia, we would have a potential patient base that may have a mutation in a heparan sulfate proteoglycan, or a heparan sulfate biosynthetic enzyme

5.6 References

1. **Merry, C.L., Bullock, S.L., Swan, D.C., Backen, A.C., Lyon, M., Beddington, R.S., Wilson, V.A., and Gallagher, J.T. 2001. The molecular phenotype of heparan sulfate in the Hs2st$^{-/-}$ mutant mouse. *J. Biol. Chem.* 276: 35429-35434.**

2. **Mahley, J., and Ji, Z.S. (1999). *J. Lipid Res.* 40, 1-16.**

3. **Williams, K.J., and Fuki, I.V. (1997). *Curr. Opin. Lipidol.* 8, 253-262.**

4. **Libeu, C.P., Lunk-Katz, S., Phillips, M.C., et al. 2001. New insights into the heparan sulfate proteoglycan-binding activity of apolipoprotein E. *E. J. Biol. Chem.* 276: 39138-39144.**

5. **Dong, J., Peters-Libeu, C.A., Weisgraber, K.H., et al. 2001. Interaction of the N-terminal domain of apolipoprotein E4 with heparin. *Biochemistry* 40: 2826-2834.**

6. **Veniant, M.M., Pierotti, V., Newland, D., Cham, C.M., Sanan, D.A., Walzem, R.L., and Young, S.G. 1997. Susceptibility to atherosclerosis in mice expressing exclusively apolipoprotein B48 or apolipoprotein B100. *J. Clin. Invest.* 100: 180-188.**

7. **Goldberg, I.J., Wagner, W.D., Pang, L., Curtiss, L.K., DeLozier, J.A., Shelness, G.S., Young, C.S., and Pillarisetti, S. 1998. The NH2-terminal region of apolipoprotein B is sufficient for lipoprotein assocation with glycosaminoglycans. *J. Biol. Chem.* 273: 35355-35361.**

8. **Boren J., Olin, K., Lee, I., Chait, A., Wight, T.N., and Innerarity, T.L. 1998. Identification of the principal proteoglycan-binding site in LDL. A single-point mutation in apoB100 severely affects proteoglycan interaction without affecting LDL receptor binding. *J. Clin. Invest.* 101: 2658-2664.**

9. **Flood, C., Gustafsson, M., Richardson, P.E., Harvey, S.C., Segrest, J.P., and Boren, J. 2002. Identification of the proteoglyacn binding site in apolipoprotein B48. *J. Biol. Chem.* 277: 32228-32233.**

10. **Dichek, H.L., Brecht, W., Fan, J., Ji, Z.S., McCormick, S.P., Akeefe, H., Conzo, L., Sanan, D.A., Weisgraver, K.., Young, S.G., et al. 1998. Overexpression of hepatic lipase in transgenic mice**

decreases apolipoprotein B-containing and high density lipoproteins. Evidence that hepatic lipase acts as a ligand for lipoprotein uptake. *J. Biol. Chem.* 273: 1896-1903.

11. Dichek, H.L., Johnson, S.M., Akeefe, H., Lo, G.T., Sage, E., Yap, C.E., and Mahley, R.W. 2001. Hepatic lipase overexpression lowers remnant and LDL levels by a noncatalytic mechanism in LDL receptor-deficient mice. *J. Lipid Res.* 42: 201-210.

12. Ledin, J., Staatz, W., Li, J.P., Gotte, M., Selleck, S., Kjellen, L., and Spillmann, D. 2004. Heparan sulfate structure in mice with genetically modified heparan sulfate production. *J. Biol. Chem.* 279: 42732-42741.

13. Shimada, K., Gill, P.J., Silbert, J.E., Douglas, W.H., and Fanburg, B.L. 1981.Involvement of cell surface heparan sulfate in the binding of lipoprotein lipase to cultured bovine endothelial cells. *J. Clin. Invest.* 68: 995-1002.

14. Parthasarathy, N., Goldberg, I.J., Sivaram, P., Mulloy, B., Flory, D.M., and Wagner, W.D. 1994. Oligosaccharide sequences of endothelial cell surface heparan sulfate proteoglycan with affinity for lipoprotein lipase. *J. Biol. Chem.* 269: 22391-22396.

15. Spillmann, D., Lookene, A., and Olivercrona, G. 2006. Isolation and characterization of low sulfated heparan sulfate sequences with affinity for lipoprotein lipase. *J. Biol. Chem.* 281: 23405-23413.

16. Kinnunen, T., Raulo, E., Nolo, R., Maccarana, M., Lindahl, U., and Rauvala, H. 1996. Neurite outgrowth in brain neurons induced by heparin-binding growth-associated molecule (HB-GAM) depends on the specific interaction of HB-GAM with heparan sulfate at the cell surface. *J. Biol. Chem.* 27: 2243-2248.

17. Beisiegel, U., Weber, W., and Bengtsson-Olivercrona, G. 1991. Lipoprotein lipase enhances the binding of chylomicrons to low density lipoprotein receptor-related protein. *Proc. Natl. Acad. Sci. U.S.A.* 88: 8342-8346.

18. Safaiyan, F., Lindahl, U., and Salmivirta, M. 2000. Stuctural diversity of N-sulfated heparan sulfate domains: distinct modes of glucuronyl C5 epimerization, iduronic acid, 2-O-sulfation, and glucosaamine 6-O-sulfation. *Biochemistry* 39: 10823-10830.

19. Brunzell, J.D., and Deeb, S.S. 2001. Familial lipoprotein lipase deficiency, apoC-11 deficiency, and hepatic lipase deficiency, In The Metabolic and Molecular Bases of Inherited Disease, C.R. Scriver, W.S. Sly, B. Childs, A.L. Beaudet, D. Valle, KW. Kinzler, and B. Vogelstein, eds. (New York: McGraw-Hill), pp. 2789-2816.

20. Homanics, G.E., de Silva, H.V., Osada, J., Zhang, S.H., Wong, H., Borensztajn, J., and Maeda, N. 1995. Mild dyslipidemia in mice following targeted inactivation of the hepatic lipase gene. *J. Biol. Chem.* 270: 2974-2980.

21. Ishibashi, S., et al. 1996. Role of the low density (LDL) receptor pathway in the metabolism of chylomicron remnants. A quantitative study in knockout mice lacking the LDL receptor, apolipoprotein E, or both. *J. Biol. Chem*. 271: 22422-22427.

22. Rohlmann, A., Gotthardt, M., Hammer, R.E., and Herz, J. 1998. Inducible activation of hepatic LRP gene by cre-mediated recombination confirms role of LRP in clearance of chylomicron remnants. *J. Clin. Invest.* 101: 689-695.

23. Goldberg, I.J., and Merkel, M. 2001. Lipoprotein lipase: physiology, biochemistry, and molecular biology. *Front. Biosci.* 6: D388-405.

24. Anfinsen, C.B., Boyle, E., and Brown, R.K. 1952. The role of heparin in lipoprotein metabolism. *Science*. 115: 583-586.

25. Beigneux, A. P., Davies, D.S., Gin, P., et al. 2007. Glycosylphosphatidylinositol-anchored high-density lipoprotein-binding protein 1 (GPIHBP1) plays a critical role in the lipolytic processing of chylomicrons. *Cell Metab*. 5: 279-291.

26. Young, S.G., Davies, B.S., Fong, L.G., et al. 2007. GPIHBP1: an endothelial cell molecule important for the lipolytic processing of chylomicrons. *Curr. Opin. Lipidol.* 18: 389-396.

27. Wallinder, L., Peterson J., Olivercrona, T., and Bengtsson-Olivercrona, G. 1984. Hepatic and extrahepatic uptake of intravenously injected lipoprotein lipase. *Biochim. Biophys. Acta* 795: 513-524.

28. Olivercrona, T., and Bengtsson-Olivercrona, G. 1993. Lipoprotein lipase and hepatic lipase. *Curr. Opin. Lipidol.* 4: 187-196.

29. Williams, K.J., Fless, G.M., Petrie, K.A., Snyder, M.L., Brocia, R.W., and Swenson, T.L. 1992. Mechanisms by which lipoprotein lipase alters cellular metabolism of lipoprotein(a), low density lipoprotein, and nascent lipoproteins. Roles for low density lipoprotein receptors and heparan sulfate proteoglycans. *J. Biol. Chem.* 267: 13284-13292.

30. MacArthur, J.M., Bishop, J.R., Stanford, K.I., Wang, L., Bensadoun, A., Witztum, J.L., and Esko, J.D. (2007). Liver heparan sulfate proteoglycans mediate clearance of triglyceride-rich lipoproteins independently of LDL receptor family members. *J Clin Invest.* 117, 153-164.

31. Bishop, J.R., Stanford, K.I., and Esko, J.D. 2008. Heparan sulfate proteoglycans and triglyceride-rich lipoprotein metabolism. *Curr. Opin. Lipidol.* 19: 307-313.

32. Hu, L., ven der Hoogt, C.C, Espirito Santo, S.M.S., Out, R., Kypreos, K.E., van Vlijmen, B.J.M., Van Berkel, T.J.C., Romijn, J.A., Havekes, L.M., Willems van Dijk, K., and Rensen, P.C.N. 2008. The hepatic uptake of VLDL in lrp^{-}ldlr$^{-/-}$vldlr$^{-/-}$ mice is regulated by LPL activity and involves proteoglycans and SR-B1.

33. Weinstock, P.H., Bisgaier, C.L., Aalto-Setala, K., Radner, H., Ramakrishnan, R., Levak-Frank, S., Essenburg, A.D., Zechner, R., and Breslow, J.L. 1995. Severe hypertriglyceridemia, reduced high density lipoprotein, and neonatal death in lipoprotein lipase knockout mice. *J. Clin. Invest.* 96: 2555-2568.

34. Sorci-Thomas, M., Prack, M.M., Dashti, N., Johnson, F., Rudel, L.L., and Williams, D.L. 1988. Apolipoprotein A-I production and mRNA abundance explain plasma apoA-I and high density lipoprotein differences between two nonhuman primate species with high and low susceptibilities to diet-induced hypercholesterolemia. *J. Biol. Chem.* 263: 5183-5189.

35. Paszty, C., Maeda, N., Verstuyft, J., and Rubin, E.M. 1994. Apolipoprotein AI transgene corrects apolipoprotein E deficiency-induced atherosclerosis in mice. *J. Clin. Invest.* 94: 899-903.

36. Williamson, R., Lee, D., Hagaman, J., and Maeda, N. 1992. Marked reduction of high density lipoprotein cholesterol in mice genetically modified to lack apolipoprotein A-I. *Proc. Natl. Acad. Sci. U.S.A.* 89: 7134-7138.

36. **Walsh, A., Ito, Y., and Breslow, J.L. 1989. High levels of human apolipoprotein AI in transgenic mice result in increased plasma levels of small high density lipoprotein (HDL) articles comparable to human HDL3. *J. Biol. Chem.* 264: 6488-6494.**

37. **Plump, A.S., Scott, C.J., and Breslow, J.L. 1994. Human apolipoprotein AI gene expression increases high density lipoprotein and suppresses atherosclerosis in the apolipoprotein E-deficient mouse. *Proc. Natl. Acad. Sci. U.S.A.* 91: 9607-9611.**

38. **Fielding, C.J., and Fielding, P.E. 1995. Molecular physiology of reverse cholesterol transport. *J. Lipid Res.* 36: 211-228.**

39. **Tall, A.R. 1990. Plasma high density lipoproteins. Metabolism and relationship to atherogenesis. *J. Clin. Invest.* 86: 379-384.**

40. **Zhang, S.H., Reddick, R.L., Burkey, B., and Maeda, N. 1994. Diet-induced atherosclerosis in mice heterozygous and homozygous for apolipoprotein E gene disruption. *J. Clin. Invest.* 94: 937-945.**

41. **Spangenberg, J., and Curtiss, L.K. 1997. Influence of macrophage-derived apoprotein E on plasma lipoprotein distribution of apolipoprotein A-I in apoprotein E-deficient mice. *Biochim. Biophys Acta* 1349: 109-121.**

42. **Bernfield, M., Gotte, M., Park, P.W., Reizes, O., Fitzgerald, M.L., Lincecum, J., and Zako, M. 1999. Functions of cell surface heparan sulfate proteoglycans. *Annu Rev Biochem* 68:729-777.**

43. **Oldberg, A., Kjellen, L., and Hook, M. 1979. Cell-surface heparan sulfate. Isolation and characterization of a proteoglycan from rat liver membranes. *J. Biol. Chem.* 254: 8505-8510.**

44. **Lyon, M., Deakin, J.A., and Gallagher, J.T. 1994. Liver heparan sulfate structure. A novel molecular design. *J. Biol. Chem.* 269: 11208-11215.**

45. **Brown, M.S., Anderson, R.G., and Goldstein, J.L. 1983. Recycling receptors: the roundtrip itinerary of migrant membrane proteins. *Cell* 32:663-667.**

46. **Fuki, I.V., Meyer, M.E., and Williams, K.J. 2000. Transmembrane and cytoplasmic domains of syndecan mediate a multi-step endocytic pathway involving detergent insolublemembrane rafts.**

Biochem J **351:607-612.**

48. Wilsie, L.C., Gonzales, A.M., and Orlando, R.A. 2006. Syndecan-1 mediates internalization of apoE-VLDL through a low density lipoprotein receptor-related protein (LRP)-independent, non-clathrin-mediated pathway. ***Lipids Health Dis*** **5:23.**

49. Thankamony, S.P., and Knudson, W. 2006. Acylation of CD44 and its association with lipid rafts are required for receptor and hyaluronan endocytosis. ***J Biol Chem*** **281:34601-34609.**

50. Tkachenko, E., Lutgens, E., Stan, R.V., and Simons, M. 2004. Fibroblast growth factor 2 endocytosis in endothelial cells proceed via syndecan-4-dependent activation of Rac1 and a Cdc42-dependent macropinocytic pathway. ***J Cell Sci*** **117:3189-3199.**

51. Issandou, M., Guillard, R., Boullay, A.B., Linhard, V., and Lopez-Perez, E. 2004. Up-regulation of low-density lipoprotein receptor in human hepatocytes is induced by sequestration of free cholesterol in the endosomal/lysosomal compartment. ***Biochem. Pharmacol.*** **67: 2281-2289.**

52. Ivanov, A.I. 2008. Pharmacological inhibition of endocytic pathways: is it specific enough to be useful? ***Methods Mol. Biol.*** **440: 15-33.**

53. Edwards, I.J., Berquin, I.M., Sun, H., O'Flaherty, J.T., Daniel, L.W., Thomas, M.J., Rudel, L.L., Wykle, R.L., and Chen, Y.Q. 2004. Differential effects of delivery of omega-3 fatty acids to human cancer cells by low-density lipoproteins versus albumin. ***Clin. Cancer Res.*** **10: 8275-8283.**

54. Sun, H., Berquin, I.M., and Edwards, I.J. 2005. Omega-3 polyunsaturated fatty acids regulate syndecan-1 expression in human breast cancer cells. ***Cancer Res.*** **65: 4442-4447.**

55. Sun, H., Berquin, I.M., Owens, R.T., O'Flaherty, J.T., and Edwards, I.J. 2008. Peroxisome proliferators-activated receptor gamma-mediated up-regulation of syndecan-1 by n-3 fatty acids promotes apoptosis of human breast cancer cells. ***Cancer Res.*** **68: 2912-2919.**

56. Edwards, I.J., and O'Flaherty, J.T. 2008. Omega-3 fatty acids and

PPARgamma in Cancer. *PPAR Res.* 2008: 358052.

57. Edwards, I.J., Sun, H., Hu, Y., Berquin, I.M., O'Flaherty, J.T., Cline, J.M., Rudel, L.L., and Chen, Y.Q. 2008. *In vivo* and *in vitro* regulation of syndecan-1 in prostate cells by *n*-3 polyunsaturated fatty acids. *J. Biol. Chem.* 283: 18441-18449.

58. Nordestegaard BG, Benn M, Schnohr P, and Tybjaerg-Hansen A. 2007. Nonfasting triglycerides and risk of myocardial infarction, ischemic heard disease, and death in men and women. *JAMA* 298: 299-308.

59. Bansal S, Buring JE, Rifai N, *et al*. 2007. Fasting compared with nonfasting triglycerides and risk of cardiovascular events in women. *JAMA* 24: 213-15.

60. Yuan G, Al-Shlai KZ, and Hegele RA. 2007. Hypertriglyceridemia: its etiology, effects, and treatment. *CMAJ* 176: 1113-20.

61. Rodriguez-Lee M, Bondjers G, and Camejo G. 2007. Fatty acid-induced atherogenic changes in extracellular matrix proteoglycans. *Curr Opin Lipidol* 18: 546-53.

62. Bai X., and Esko J.D. 1996. An animal cell mutant defective in heparan sulfate hexuronic acid 2-O-sulfation. *J. Biol. Chem.* 271: 17711-117717.

63. Hudson, M.L., Kinnunen, T., Cinar, H.N., and Chisholm, A.D. 2006. C. elegands Kallmann syndrome protein KAL-1 interacts with syndecan and glypican to regulate neuronal cell migrations. *Dev. Biol.* 294: 352-365.

64. Bulow, H.E., Berry, K.L., Topper, L.H., Peles, E., and Hobert, O. 2002. Heparan sulfate proteoglycan-dependent induction of axon branching and axon misrouting by the Kallmann syndrome gene kal-1. *Proc. Natl. Acad. Sci., U.S.A.* 99: 6346-6351.

65. Bulow, H.E., and Hobert, O. 2004. Differential sulfations and epimerization define heparan sulfate specificity in nervous system development. *Neuron* 41: 723-736.

66. **Kamimura, K., Koyama, T., Habuchi, H., Ueda, R., Masu, M., Kimata, K., and Nakato, H. 2006. Specific and flexible role of heparan sulfate modifications in Drosophila FGF signaling. *J. Cell. Biol.* 174: 773-778.**

67. **Esko, J.D., and Selleck, S.B. (2002). *Annu. Rev. Biochem.* 71, 435 – 471.**

68. **HajMohammadi, S., Eniyoji,K., Princivalle, M., Christi, P., Lech, M., Beeler, D., Rayburn, H., Schwartz, J.J., Barzegar, S., de Agostini, A.I., Post, M.J., Rosenberg, R.D., and Shworak, N.W. 2003. Normal levels of anticoagulant heparan sulfate are not essential for normal hemostasis. *J. Clin. Invest.* 111: 989-999.**

69. **Lawrence, R., Lu, H., Rosenburg, R.D., Esko, J.D., and Zhang, L. (2008). Disaccharide structure code for the easy representation of constituent oligosaccharides from glycosaminoglycans. *Nat Methods* 5, 291-2.**

70. **Shively, J.E., and Conrad, HE. 1976. Formation of anhydrosugars in the chemical depolymerization of heparin. *Biochemistry* 15, 3932-3942.**

71. **Young S.G., Smith, R.S., Hogel, D.M., Curtiss, L.K., and Witztum, J.L. 1986. Two new monoclonal antibody-based enzyme-linked assays of apolipoprotein B. *Clin. Chem.* 32, 1484-1490.**

72. **Hasegawa, H., and Wang, F. 2008. Visualizing mechanosensory endings of TrkC-expressing neurons in HS3ST-2-hPLAP mice. *J. Comp. Neurol.* 511: 543-56.**

APPENDIX A

DELETION OF BASEMENT MEMBRANE HEPARAN SULFATE PROTEOGLYCAN TYPE XVIII COLLAGEN CAUSES HYPERTRIGLYCERIDEMIA

Abstract

Lipoprotein lipase (Lpl) acts on triglyceride-rich lipoproteins in the peripheral circulation, liberating free fatty acids for energy metabolism or storage. The enzyme binds to heparan sulfate and heparin, but is bound to the endothelial cell surface primarily by a specific receptor, Gpihbp1. Here we report the surprising finding that a null allele of the basement membrane heparan sulfate proteoglycan, Type XVIII collagen (Col18), decreases presentation of Lpl on endothelia and reduces plasma levels of enzyme, resulting in mild fasting hypertriglyceridemia and transient diet-induced hyperchylomicronemia. Injection of heparin released normal amounts of Lpl from subendothelial stores into the circulation and lowered plasma triglycerides, indicating that normal amounts of enzyme were made and that the accumulated lipoproteins were susceptible to lipolysis and clearance. The expression of Lpl and Gpihbp1 and the rate of triglyceride synthesis and hepatic clearance of triglyceride-rich lipoproteins were otherwise normal in the mutant. The defect was specifically due to altered presentation of Lpl in extrahepatic tissue based on the observation that humans with Knobloch Syndrome caused by a null mutation in the vascular form of

Col18 also exhibited fasting hypertriglyceridemia, a previously unrecognized phenotype in these patients.

Introduction

Heparan sulfate proteoglycans present in basement membranes aid in the formation of tissue barriers and facilitate cell adhesion and migration during development (1). The major basement membrane heparan sulfate proteoglycans include Type XVIII Collagen (Col18) and perlecan, which are found ubiquitously in the vascular basement membrane zones of tissues, and agrin, a critical component of the neuromuscular junction basement membrane (2-4). Loss of function mutations in perlecan and agrin are lethal in mice due to defective cartilage/bone development or formation of neuromuscular junctions, respectively (5-7). In contrast, Col18-deficient mice (*Col18a1*$^{-/-}$) are viable but exhibit major ocular defects including abnormal retinal vessel development and poor anchoring of vitreal collagen fibrils to the inner lining membrane of the retina (8-10). Col18-deficiency also leads to increased vascular permeability of large and small blood vessels and thickened basement membranes in organs such as the heart, kidney, and skin (9, 11).

Lipoprotein lipase (Lpl) is the major enzyme responsible for the hydrolysis of triglycerides from triglyceride-rich lipoproteins in the circulation, liberating free fatty acids and monoacylglycerol for storage or energy production. The enzyme is made by the parenchymal cells of adipose tissue, heart, and skeletal muscle and migrates from its site of synthesis to its site of action on the luminal side of endothelial cells where it encounters circulating lipoproteins (12). Lpl binds to heparin and for many years

heparan sulfate proteoglycans were considered the receptors for presenting Lpl on the luminal side of the endothelium. However, the discovery of Gpihbp1 has cast doubt on the importance of this interaction. Genetic ablation of Gpihbp1 reduces presentation of Lpl and causes striking hypertriglyceridemia, whereas altering endothelial heparan sulfate has no effect on circulating Lpl or plasma triglycerides (13, 14). Nevertheless, Lpl binds to heparan sulfate and heparin injection releases the enzyme into the circulation most likely by displacing it from the Gpihbp1 and from subendothelial pools (14). As Lpl transits through tissue from its site of synthesis to the endothelium, it presumably encounters heparan sulfate proteoglycans in vascular basement membranes that surround parenchymal cells and blood vessels. The interaction of Lpl with proteoglycans may facilitate its transit or stabilize the enzyme. A heparin-binding mutant form of Lpl with preserved activity was found to be less stable and failed to localize lipid uptake to muscles (15). Genetic studies have not yet confirmed if interactions between Lpl and proteoglycans have physiological significance.

In this work we show that deletion of Col18 in mice decreases plasma Lpl and presentation of Lpl in the vasculature, resulting in hypertriglyceridemia due to delayed lipolysis in the peripheral circulation. The level of expression of the Lpl and Gpihbp1 were unaffected and hepatic clearance of remnant lipoproteins remained unchanged. We also show that elevated plasma triglycerides occurs in humans with Knobloch Syndrome, who bear a mutation that only affects the NC11-303 form of Col18 present in extrahepatic, vascular basement membranes (Knobloch Syndrome, OMIM 267750) (16). We interpret these findings to suggest that Col18 facilitates the transit of Lpl from its site of synthesis in the parenchyma of tissues to the vascular compartment and

that the reduction of Lpl in Col18-deficiency leads to delayed hydrolysis of triglycerides in the plasma.

Results

Reduced plasma Lpl and enzyme presentation on endothelial cells in *Col18a1*$^{-/-}$ mice. Lpl transits from its site of synthesis in the parenchymal cells of adipose, cardiac, and skeletal muscle across basement membranes and endothelial cells to reach its site of action on the luminal side of capillary beds. The enzyme presumably encounters extracellular matrix proteoglycans as it diffuses, suggesting that altering their composition might affect Lpl transit. Since Type XVIII collagen (Col18) constitutes a major heparan sulfate proteoglycan present in basement membranes, we first examined the effect of its deletion on plasma Lpl levels. By ELISA, Lpl was markedly reduced in *Col18a1*$^{-/-}$ mice compared to wild type controls (25 ± 6 ng/ml in controls, n=7 *vs*. 6 ± 4 ng/ml in mutants, n = 7; P = 0.006, Fig. 1A). The decrease in plasma Lpl was not caused by reduced expression of the enzyme, since intravenous heparin injection, which releases Lpl from its receptor Gpihbp1 and from subendothelial stores (14), liberated comparable amounts of enzyme in *Col18a1*$^{-/-}$ and wild type mice (314 ng/ml ± 42 vs. 336 ng/ml ± 15 respectively, n = 4, P = 0.7) (Fig. 1B). Furthermore, quantitative RT-PCR of Lpl transcripts in adipose, heart, and muscle showed normal levels of Lpl mRNA under fasting or fed conditions compared to wild type mice (supplemental Fig. S1A).

Gpihbp1$^{-/-}$ mice also exhibit reduced plasma levels of Lpl presumably due to shedding of newly transported enzyme and rapid clearance in the liver (17-19). To test if Col18-deficiency affected the expression or localization of Gpihbp1, we measured its level in adipose, heart, and muscle tissue by qPCR. No significant differences in transcript levels were detected in mutant and wild type animals (Supplemental Fig.

S1B). We also isolated primary cardiac endothelial cells and reacted them with a monoclonal antibody to Gpihbp1 (20). Both wild type and mutant cells showed similar reactivity, indicating normal levels of protein expression (Supplemental Fig. S1C). Direct binding studies with biotinylated Lpl to heart microvascular endothelial cells derived from *Col18a1*$^{-/-}$ and wild type mice also did not show any significant differences (data not shown).

Mice lacking Gpihbp1 have little enzyme that can be released by intravenous injection of Intralipid, which forms chylomicron like particles in the blood and displaces only Lpl bound to luminal receptors on the endothelium (14, 17). When we examined the time course of Lpl release after a bolus injection of Intralipid, we found little release of Lpl into the plasma in *Col18a1*$^{-/-}$ mice compared to the wild type (Fig. 1C). Comparing the area under the curves after correction for the normal plasma pool of Lpl (Fig. 1A) showed a dramatic difference in displaceable enzyme in the mutant (75 ng/ml in wild type vs. 8.2 ng/ml in mutants, $n = 8$ in two separate experiments). Since Lpl is rapidly cleared by receptors in the liver (18, 19), this technique may somewhat underestimate the amount of Lpl bound to the endothelium. Nevertheless, the levels are significantly lower in *Col18a1*$^{-/-}$ mice compared to the wild type. Thus, *Col18a1*$^{-/-}$ mice have reduced amounts of plasma and receptor-bound Lpl, yet make normal amounts of enzyme and receptors.

Reduced plasma Lpl presentation results in hypertriglyceridemia. The reduction in plasma and endothelium-bound Lpl suggested that *Col18a1*$^{-/-}$ mice might exhibit hypertriglyceridemia. Fasting plasma triglyceride levels in 8-week old

Col18a1$^{-/-}$ mice fed normal chow were elevated ~2-fold compared to wild type littermate controls (Fig. 2A) (65 ± 13 mg/dl in control mice *vs*. 119 ± 25 mg/dl in mutants, n = 10, $P < 0.0001$), and the values did not change significantly when the animals were fasted for 8 hr instead of 4 hr, with age (2 - 12 months) or sex. A slight, consistent decrease in plasma cholesterol also occurred, but the difference did not achieve statistical significance (Fig. 2B) (132 ± 17 mg/dl in wild type *vs*. 115 ± 24 in mutants, n = 10, $P = 0.101$). In contrast, *Col18a1*$^{+/-}$ heterozygotes did not display any changes in plasma lipids (data not shown). Interestingly, the elevation in plasma triglycerides was specific to Col18-deficiency, since *Hspg2*$^{\Delta 3/\Delta 3}$ mice, which produce perlecan lacking heparan sulfate chains (21), showed no change in fasting triglyceride (44 ± 15 mg/dL, n = 11 vs. 48 ± 4 mg/dL, n = 12) or cholesterol levels (69 ± 8 vs. 71 ± 3). Similar findings were recently reported by Tran-Lundmark et al in *Hspg2*$^{\Delta 3/\Delta 3}$ mice lacking apoE (22).

Pooled plasma samples from fasted animals were analyzed by LipoSEARCH profiling, which uses curve fitting algorithms to analyze the relative amounts of lipoprotein subclasses separated by gel filtration FPLC. These profiles indicated triglyceride accumulation in large diameter particles similar in size to chylomicrons and all VLDL subclasses in the mutant (Fig. 2C). Separation of lipoproteins by ultracentrifugation showed that the plasma triglycerides accumulated as lipoproteins of $\delta < 1.006$ g/ml (Supplementary Fig. S2A) and they contained apolipoproteins B-48 (apoB-48) and E (apoE) (Supplementary Fig. S2B), consistent with their identification as VLDL or remnant particles derived from chylomicrons. However, the preparations

from the mutant were enriched in particles of average diameter > 50 nm (Fig. 2D), suggesting delayed lipolysis.

Col18a1$^{-/-}$ mice also accumulated plasma triglycerides in response to dietary fat challenge. After oral gavage of corn oil the plasma of *Col18a1*$^{-/-}$ mice was milky in appearance compared to controls (data not shown), and triglyceride-rich lipoproteins of $\delta<1.006$ were elevated 2-fold compared to wild type mice (Fig. 3A). Electron micrographs of these lipoproteins showed that large particles of diameter > 100 nm accumulated in the mutant (Fig. 3B and Fig. S2C). Mice were also orally gavaged with corn oil containing [^{3}H]retinol, which is converted into fatty acylated retinyl esters and packaged into chylomicrons. Like plasma triglycerides, plasma levels of [^{3}H]retinyl esters were elevated >2-fold within 2 hours in *Col18a1*$^{-/-}$ mice compared to wild type animals (Fig. 3C). The ^{3}H-counts remained elevated in the mutant for four hours and thereafter disappeared at a rate similar to that observed in wild type mice. Clearance of plasma triglycerides mimicked the retinol clearance curves over the course of the assay (data not shown). The rapid onset of accumulation in *Col18a1*$^{-/-}$ mice resembles that observed previously in Lpl heterozygotes (23), but differs from that reported for a mutant lacking hepatic proteoglycan clearance receptors (24). Since the later phase of turnover reflects hepatic clearance of particles after Lpl-mediated hydrolysis in the peripheral circulation, hepatic turnover of remnants appeared to be unaffected in the *Col18a1*$^{-/-}$ mice (25). To confirm this conclusion, animals were injected with human VLDL and plasma samples were analyzed by ELISA with a monoclonal antibody that reacts only with human apoB100. As shown in Fig. 3D, hepatic clearance of injected human VLDL was the same in mutant and wild type animals.

We also examined other factors that can affect plasma triglyceride levels. The rate of synthesis of triglycerides was identical in *Col18a1*$^{-/-}$ and wild type mice as measured by plasma triglyceride levels after injection of Triton WR-1339, which blocks triglyceride hydrolysis and uptake (0.032 ± 0.001 mg triglyceride/min in wild type *vs*. 0.032 ± 0.004 mg triglyceride/min in mutant mice; n = 3, *P* = 1.0) (26). No differences were observed after oral gavage of corn oil as well (0.055 ± 0.005 mg triglyceride/min in controls, n = 3 *vs*. 0.051± 0.002 mg triglyceride/min in the mutants, n = 3; *P* = 0.2131), indicating normal intestinal secretion of dietary lipids. The level of angiopoietin-like 4 (27), caveolin-1 (28), and apoC-II (29) were unaffected (data not shown).

Injection of heparin has long been known to rapidly clear plasma triglycerides via the release of Lpl into the plasma and subsequent rapid lipolysis and hepatic clearance. Heparin injection caused the rapid disappearance of plasma triglycerides in fasting *Col18a1*$^{-/-}$ and wildtype mice (Supplemental Fig. S3A). Identical results were obtained after heparin injection of animals previously challenged by oral gavage of corn oil (Supplemental Fig. S3B). Thus, triglyceride-rich lipoproteins accumulating in the mutant were fully capable of undergoing lipolysis when exposed to Lpl released by heparin. Taken together, these findings suggest that the hypertriglyceridemia manifested by *Col18a1*$^{-/-}$ mice was most likely due to decreased Lpl levels and reduced rates of lipolysis in the vasculature.

Hypertriglyceridemia occurs in Knobloch Patients lacking the vascular form of COL18. In humans, loss of function mutations in COL18 cause Knobloch

syndrome (OMIM 267750). This extremely rare disorder is characterized primarily by ocular defects, including myopia, vitreoretinal and macular degeneration, retinal detachments, and occipital encephalocele defects thought to arise from altered basement membrane structures (30-36). Several of the ocular defects are similar to defects observed in *Col18a1*$^{-/-}$ mice (8). A large consanguineous family of Knobloch patients was identified in a remote farming community in Bahia State, Brazil (35). Linkage analysis studies showed that this family carries a null mutation predicted to disrupt specifically the NC11-303 isoform (short) of *COL18A1* common to vascular basement membranes, which is distinct from long form splice variant expressed abundantly in the liver and heart (37). Although small in number, the members of this rare family constituted an ideal study group to test if a more specific deficiency in vascular COL18 might give rise to elevated plasma triglycerides as well. Furthermore, normal, heterozygous, and homozygous individuals had similar diets, shared living quarters, and were of similar age. Plasma cholesterol, glucose, and triglyceride levels in plasma samples taken from seven Knobloch patients were compared to six heterozygous carriers of the mutation and seven normal controls (see *Methods* for study inclusion criteria Supplemental Table 1). Fasted plasma triglycerides were elevated to >200 mg/dl in 6 of 7 affected patients compared to <150 mg/dl in unaffected family members ($P = 0.02$), but no significant difference was noted in heterozygotes compared to normal ($P = 0.27$) (Fig. 4A). Ultracentrifugal analysis showed that the triglycerides accumulated in lipoproteins of $\delta < 1.006$ g/ml (Fig. 4B). Plasma cholesterol was elevated slightly, but the number of individuals available for analysis was too small for the difference to achieve statistical significance. One of the

patients (F1020-36) was borderline diabetic (blood glucose = 130 mg/dl) in the field measurement, but tested normal by later colorimetric assay. Thus, the hypertriglyceridemia seen was not due to diabetes or other diseases diagnosed by their attending physician. A single plasma sample from a Knobloch patient from the same family but living in Sao Paulo, Brazil, was compared to four household members with similar results (plasma triglycerides 529 mg/dl in the affected patient *vs*. 232 ± 48 mg/dl in controls, n = 4). The extreme remote location of most family members and local dietary restraints precluded postprandial studies.

Discussion

In this report, we demonstrate that Col18-deficiency results in elevated plasma triglycerides. To our knowledge, this is the first demonstration of a requirement for a specific extracellular matrix heparan sulfate proteoglycans in triglyceride metabolism *in vivo*. This function was unique to Col18 and not associated with another basement membrane heparan sulfate proteoglycan, perlecan. Previous studies showed that altering the expression of a specific sulfotransferase involved in the formation of heparan sulfate chains in hepatocytes affected hepatic clearance of triglyceride-rich lipoproteins. In contrast, the defect in *Col18a1*$^{-/-}$ mice appears to be due to reduced lipolysis of triglyceride-rich lipoproteins in the peripheral circulation due to decreased presentation of Lpl in the plasma compartment. Data supporting this conclusion derives from the large size of triglyceride-rich lipoproteins that accumulate in the mutant under fasting and post-prandial conditions, differences in the initial turnover of [^{3}H]retinol-labeled post-prandial lipoproteins, and the lack of any effect on hepatic

turnover of remnant lipoproteins derived from dietary triglyceride and injected human VLDL. Additional evidence was provided by studies of human Knobloch patients bearing a mutation that only affects the vascular form of Col18.

These findings raise the question, "How can a proteoglycan located in basement membranes affect presentation of Lpl in the plasma and at the lumenal surface of the endothelium?" Lpl is secreted by adipocytes and cardiac and skeletal myocytes and migrates from its site of secretion through surrounding basement membranes and across the endothelium (12). During its transport, the enzyme presumably encounters the resident heparan sulfate proteoglycans in the matrix. Since Lpl contains one or more heparin binding sites (38-41), it presumably can interact with the heparan sulfate chains on Col18 or other matrix proteoglycans (10). Binding to Col18 could facilitate diffusion or protect Lpl, perhaps in the same way heparan sulfate proteoglycans have been suggested to affect the rate of diffusion or turnover of heparan sulfate-binding morphogens during early development (*e.g.,* Wnts, Hedgehog, FGFs, BMPs) (42-45). The inefficient presentation Lpl could also reflect the expansion of basement membranes that occurs in various tissues (1.4 to 2-fold) due to Col18 deficiency (11). Since a quadratic relationship exists between time and distance when considering freely diffusing molecules (46), small changes in distance could greatly slow the rate of diffusion of Lpl. In either model, the delay in transport could decrease the rate at which the enzyme appears in the blood compartment. Since Lpl is displaced from Gpihbp1 by circulating triglyceride-rich lipoproteins and rapidly cleared in the liver, a decrease in its rate of diffusion through the tissue could result in diminished steady-state amount of enzyme bound to Gpihbp1 and in the plasma.

Although simple in concept, proving this model has proven to be difficult due to the absence of suitable in vitro models for measuring transport through tissues and the lack of high affinity antibodies to mouse Lpl for assessing the enzyme distribution in tissues using immunohistochemistry and immuno-electron microscopy.

Interestingly, the phenotype of *Col18a1*$^{-/-}$ mice closely resembles that seen in Lpl heterozygotes in that both strains have reduced plasma levels of Lpl, mild hypertriglyceridemia in both the fasted and post-prandial states, and acute accumulation of plasma lipids after oral gavage (23). *Col18a1*$^{-/-}$ mice also have many similarities to Gpihbp1-deficient animals, but differ in one important way. Both mutants express decreased plasma Lpl and Lpl associated with the endothelium, and injection of heparin causes the appearance of wild type levels of Lpl in both strains of mice. However, the release of Lpl in *Gpihbp1*$^{-/-}$ mice enzyme does not lower plasma triglycerides (14), whereas its release in *Col18a1*$^{-/-}$ mice, which have a normal complement of Gpihbp1 receptors, led to rapid lipolysis and clearance. These findings suggest that engagement of Lpl with Gpihbp1 receptors might be necessary for lipolysis to proceed .

Recent large cohort clinical trials have shown that mild elevated triglycerides are a major risk factor for coronary heart disease (47, 48). The work presented here suggesting that disruption of COL18 in humans might lead to an increase in plasma triglycerides also suggest that decreased COL18 expression or mutations affecting the heparan sulfate chains might account for some cases of hypertriglyceridemia. For example, patients with diabetes mellitus exhibit slowed metabolism of dietary triglycerides in post-prandial studies (49, 50). The direct cause of post-prandial

hyperlipidemia in these patients remains unknown, but it is interesting to note that thickening of basement membranes has been documented in the intima of the aorta as well as muscle, glomerular and retinal capillaries in diabetes (51, 52). The continuous turnover of COL18 in tissues and its cleavage to endostatin in the circulation (3) suggest a simple plasma test to determine whether some forms of hypertriglyceridemia might arise from altered COL18 expression in hyperlipidemic patients.

Methods

Mice and animal husbandry. Mice deficient in Col18 (*Col18a1*$^{-/-}$), and perlecan (*Hspg2*$^{\Delta 3/\Delta 3}$) were described previously (8-10, 53-55). All mice were backcrossed >10 generations on a C57/Bl6 background. All animals were housed and bred in vivaria approved by the Association for Assessment and Accreditation of Laboratory Animal Care located in the School of Medicine, University of California, San Diego, following standards and procedures approved by the local Institutional Animal Care and Use Committee. Mice were weaned at 3 weeks, maintained on a 12 hr light-dark cycle, and fed *ad libitum* with water and standard rodent chow (Harlan-TekLad) unless indicated otherwise. Genotyping was performed as described in the original publications.

Human Subjects. Knobloch patients were recruited from a large family diagnosed and characterized previously at the Human Genome Center in São Paulo, SP, Brazil (35). Most members of this large family live in a remote farming community in Bahia State, Brazil and family members typically had similar diets and shared living quarters. After obtaining signed informed consent, a study investigator obtained a medical history and patients were fasted for 4 hr after which a plasma sample was taken. Glucose measurements were taken immediately with a glucometer. Study participants with >200 mg/dl blood glucose, previously diagnosed diabetes, heavy alcohol consumption (5 alcoholic drinks per day), and tobacco use were excluded from the study (4 total). Plasma triglyceride, cholesterol, and glucose levels from 7 homozygous patients, 6 heterozygotes, and 6 age-matched normal subjects from the family were measured using kits (Wako). A second affected family member

living in São Paulo, Brazil along with 4 wild type controls living in the same household was tested.

Triglyceride secretion rates in mice. Triglyceride secretion rates were determined by the method of Hirano et al. (26). Briefly Triton WR-1339 (500 mg/kg body weight, Sigma) was injected *via* the tail vein into mice fasted for 4 hr, and triglyceride concentrations were measured in plasma samples taken 30, 60, and 90 min post-injection. The secretion rate (mg/min) was calculated from the increment in triglyceride concentration per min multiplied by the plasma volume of the mouse (estimated as 0.035% of body weight in grams). To determine the intestinal triglyceride secretion rate, Triton WR-1339 was injected into mice that had been given a bolus of corn oil by gavage (0.2 ml/mouse).

Human VLDL clearance in mice. Clearance of human VLDL was performed by measuring the level of human apoB-100 present in plasma at timed intervals following i.v. injection of VLDL purified from fasted, healthy human donors. Human apoB-100 was measured by ELISA using MB47, which binds human but not murine apoB-100, exactly as described in (24).

Lipoprotein analysis. Plasma was prepared from retroorbital bleeds after fasting the animals for 4 hr in the morning and plasma triglyceride and cholesterol levels were determined enzymatically (Wako). Pooled mouse plasma lipoproteins were also separated by gel filtration FPLC (LipoSEARCH, Skylight Biotech Inc.). Lipoproteins were prepared from human plasma or blood drawn by cardiac puncture from mice using sequential preparative ultracentrifugation according to established methods (56). Pooled plasma samples were centrifuged for 20 hr at 45,000 x rpm in a

Beckman 50.3Ti rotor at δ = 1.006 g/ml to collect triglyceride-rich lipoproteins. Isolated lipoproteins were dialyzed against PBS and analyzed for lipid content.

Electron microscopy. Lipoproteins of δ < 1.006 g/ml were purified by ultracentrifugation from pooled plasma obtained from fasted animals after oral gavage of 0.2 ml corn oil (n = 3 or each genotype). To determine particle size, samples were coded, negatively stained with 2% potassium phosphotungstate (pH 7.6), and imaged by transmission electron microscopy (Jenny Wong, Gladstone Institute). The diameters of particles in 8 fields were measured, and the data from two separate experiments were pooled.

Retinol excursion studies in mice. Retinol excursion studies were done essentially as described (25). Briefly, 27 μCi of [11,12-^{3}H]retinol (Perkin-Elmer, 44.4 Ci/mmol) in ethanol was mixed with 1 ml of corn oil (Sigma) and administered by oral gavage (200 μl/mouse). Blood was sampled at the times indicated by retro-orbital sinus bleed and radioactivity was measured in triplicate (10 μl of serum) by scintillation counting.

Heparin and Intralipid injection. Intravenous injection of heparin (0.5 U/g body weight) or 20% Intralipid (7.5 ml/kg body weight) was used to clear plasma triglycerides or release Lpl into the plasma. Blood samples were taken by retro-orbital bleeding prior to injection and various times after injection. Lpl mass in plasma samples was measured by ELISA with a specific antibody as described previously (57).

Statistics. Statistical analyses were performed using PRISM (GraphPad Software). All data are expressed as mean values ± S.D unless otherwise indicated. Significance was determined using an unpaired Student's (two-tailed) t test. Significance was taken as $P < 0.05$.

Acknowledgments

This work has been submitted to the *Proceedings of the National Academy of Sciences*, and the dissertation author is a co-author of this manuscript. Together with her co-authors, Joseph R. Bishop, Maria Rita Passos-Bueno, Jon C. Gonzales, Erika Yeh, Andre Bensadoun, Joseph L. Witztum, Karen S. Moulton, and Jeffrey D. Esko, she thank Dr. Raija Soininen for plasma samples from the *Hspg2* knockout mice and the members of the Esko and Passos-Bueno lab for support and technical assistance on this manuscript. A special thanks to the people of Euclides de Cunha, Bahia State, Brazil. We acknowledge Jinny Wong at the Gladstone Institute for EM studies. This work was supported by National Institutes of Health Grants GM33063 and HL57345 (J.D.E.), HL087228 (A.B.), (HL67255 (K.S.M), CEPID/FAPESP and CNPq (M.R.S.B-P.), a Department of Medicine Pilot Grant (K.S.M) at the University of Colorado, Denver, and by the Leducq Foundation (J.L.W.). J.R.B. is funded by a Scientist Development Grant 0735038N from the American Heart Association.

References

1. **Iozzo RV (2005) Basement membrane proteoglycans: from cellar to ceiling. *Nat Rev Mol Cell Biol* 6(8):646-656.**

2. **Bezakova G & Ruegg MA (2003) New insights into the roles of agrin. *Nat Rev Mol Cell Biol* 4(4):295-308.**

3. **Marneros AG & Olsen BR (2005) Physiological role of collagen XVIII and endostatin. *FASEB J* 19(7):716-728.**

4. **Knox SM & Whitelock JM (2006) Perlecan: how does one molecule do so many things? *Cell Mol Life Sci* 63(21):2435-2445.**

5. **Arikawa-Hirasawa E, Watanabe H, Takami H, Hassell JR, & Yamada Y (1999) Perlecan is essential for cartilage and cephalic development. *Nat Genet* 23(3):354-358.**

6. **Gautam M, *et al.* (1996) Defective neuromuscular synaptogenesis in agrin-deficient mutant mice. *Cell* 85:525-535.**

7. **Serpinskaya AS, Feng G, Sanes JR, & Craig AM (1999) Synapse formation by hippocampal neurons from agrin-deficient mice. *Dev Biol* 205(1):65-78.**

8. **Fukai N, *et al.* (2002) Lack of collagen XVIII/endostatin results in eye abnormalities. *Embo J* 21(7):1535-1544.**

9. **Moulton KS, *et al.* (2004) Loss of collagen XVIII enhances neovascularization and vascular permeability in atherosclerosis. *Circulation* 110(10):1330-1336.**

10. **Marneros AG, *et al.* (2004) Collagen XVIII/endostatin is essential for vision and retinal pigment epithelial function. *EMBO J* 23(1):89-99.**

11. **Utriainen A, *et al.* (2004) Structurally altered basement membranes and hydrocephalus in a type XVIII collagen deficient mouse line. *Hum Mol Genet* 13(18):2089-2099.**

12. **Goldberg IJ & Merkel M (2001) Lipoprotein lipase: physiology, biochemistry, and molecular biology. *Front Biosci* 6:D388-405.**

13. Beigneux AP, *et al.* (2007) Glycosylphosphatidylinositol-anchored high-density lipoprotein-binding protein 1 plays a critical role in the lipolytic processing of chylomicrons. *Cell Metab* 5(4):279-291.

14. Weinstein MM, *et al.* (2008) Abnormal Patterns of Lipoprotein Lipase Release into the Plasma in GPIHBP1-deficient Mice. (Translated from eng) *J Biol Chem* 283(50):34511-34518 (in eng).

15. Lutz EP, *et al.* (2001) Heparin-binding defective lipoprotein lipase is unstable and causes abnormalities in lipid delivery to tissues. *J Clin Invest* 107(9):1183-1192.

16. Suzuki OT, *et al.* (2002) Molecular analysis of collagen XVIII reveals novel mutations, presence of a third isoform, and possible genetic heterogeneity in Knobloch syndrome. *Am J Hum Genet* 71(6):1320-1329.

17. Qi D, *et al.* (2006) Acute intralipid infusion reduces cardiac luminal lipoprotein lipase but recruits additional enzyme from cardiomyocytes. (Translated from eng) *Cardiovasc Res* 72(1):124-133 (in eng).

18. Wallinder L, Bengtsson G, & Olivecrona T (1979) Rapid removal to the liver of intravenously injected lipoprotein lipase. (Translated from eng) *Biochim Biophys Acta* 575(1):166-173 (in eng).

19. Vilaro S, Llobera M, Bengtsson-Olivecrona G, & Olivecrona T (1988) Lipoprotein lipase uptake by the liver: localization, turnover, and metabolic role. *Am J Physiol* 254(5 Pt 1):G711-722.

20. Gin P, *et al.* (2008) The Acidic Domain of GPIHBP1 Is Important for the Binding of Lipoprotein Lipase and Chylomicrons. (Translated from eng) *J Biol Chem* 283(43):29554-29562 (in eng).

21. Rossi M, *et al.* (2003) Heparan sulfate chains of perlecan are indispensable in the lens capsule but not in the kidney. *EMBO J* 22(2):236-245.

22. Tran-Lundmark K, *et al.* (2008) Heparan sulfate in perlecan promotes mouse atherosclerosis: roles in lipid permeability, lipid retention, and smooth muscle cell proliferation. *Circ Res* 103(1):43-52.

23. Weinstock PH, *et al.* (1995) Severe hypertriglyceridemia, reduced high density lipoprotein, and neonatal death in lipoprotein lipase knockout mice. Mild hypertriglyceridemia with impaired very low density lipoprotein clearance in heterozygotes. *J Clin Invest* 96(6):2555-2568.

24. MacArthur JM, *et al.* (2007) Liver heparan sulfate proteoglycans mediate clearance of triglyceride-rich lipoproteins independently of LDL receptor family members. *J Clin Invest* 117:153-164.

25. Ishibashi S, *et al.* (1996) Role of the low density lipoprotein (LDL) receptor pathway in the metabolism of chylomicron remnants. A quantitative study in knockout mice lacking the LDL receptor, apolipoprotein E, or both. *J Biol Chem* 271(37):22422-22427.

26. Hirano T, *et al.* (2001) Apoprotein C-III deficiency markedly stimulates triglyceride secretion in vivo: comparison with apoprotein E. *Am J Physiol Endocrinol Metab* 281(4):E665-669.

27. Koster A, *et al.* (2005) Transgenic angiopoietin-like (angptl)4 overexpression and targeted disruption of angptl4 and angptl3: regulation of triglyceride metabolism. *Endocrinology* 146(11):4943-4950.

28. Frank PG, Pavlides S, Cheung MW, Daumer K, & Lisanti MP (2008) Role of caveolin-1 in the regulation of lipoprotein metabolism. (Translated from eng) *Am J Physiol Cell Physiol* 295(1):C242-248 (in eng).

29. Brunzell JD & Deeb SS (2001) Familial lipoprotein lipase deficiency, apoC-II deficiency, and hepatic lipase deficiency. *The Metabolic and Molecular Bases of Inherited Disease*, eds Scriver CR, Sly WS, Childs B, Beaudet AL, Valle D, Kinzler KW, & Vogelstein B (McGraw-Hill, New York), 8th Ed Vol 2, pp 2789-2816.

30. Keren B, *et al.* (2007) CNS malformations in Knobloch syndrome with splice mutation in COL18A1 gene. (Translated from eng) *Am J Med Genet A* 143A(13):1514-1518 (in eng).

31. Menzel O, *et al.* (2004) Knobloch syndrome: novel mutations in COL18A1, evidence for genetic heterogeneity, and a functionally impaired polymorphism in endostatin. (Translated from eng) *Hum Mutat* 23(1):77-84 (in eng).

32. Saarela J, Rehn M, Oikarinen A, Autio-Harmainen H, & Pihlajaniemi T (1998) The short and long forms of type XVIII collagen show clear tissue specificities in their expression and location in basement membrane zones in humans. (Translated from eng) *Am J Pathol* 153(2):611-626 (in eng).

33. Saarela J, Ylikarppa R, Rehn M, Purmonen S, & Pihlajaniemi T (1998) Complete primary structure of two variant forms of human type XVIII collagen and tissue-specific differences in the expression of the corresponding transcripts. (Translated from eng) *Matrix Biol* 16(6):319-328 (in eng).

34. Wilson C, Aftimos S, Pereira A, & McKay R (1998) Report of two sibs with Knobloch syndrome (encephalocoele and viteroretinal degeneration) and other anomalies. (Translated from eng) *Am J Med Genet* 78(3):286-290 (in eng).

35. Passos-Bueno MR*, et al.* (1994) Knobloch syndrome in a large Brazilian consanguineous family: confirmation of autosomal recessive inheritance. (Translated from eng) *Am J Med Genet* 52(2):170-173 (in eng).

36. Seaver LH, Joffe L, Spark RP, Smith BL, & Hoyme HE (1993) Congenital scalp defects and vitreoretinal degeneration: redefining the Knobloch syndrome. (Translated from eng) *Am J Med Genet* 46(2):203-208 (in eng).

37. Sertie AL*, et al.* (1996) A gene which causes severe ocular alterations and occipital encephalocele (Knobloch syndrome) is mapped to 21q22.3. (Translated from eng) *Hum Mol Genet* 5(6):843-847 (in eng).

38. Sendak RA, Berryman DE, Gellman G, Melford K, & Bensadoun A (2000) Binding of hepatic lipase to heparin: identification of specific heparin-binding residues in two distinct positive charge clusters. *J.Lipid Res.* 41(2):260-268.

39. Berryman DE & Bensadoun A (1993) Site-directed mutagenesis of a putative heparin binding domain of avian lipoprotein lipase. *J.Biol.Chem.* 268:3272-3276.

40. Hata A*, et al.* (1993) Binding of lipoprotein lipase to heparin. Identification of five critical residues in two distinct segments of the amino-terminal domain. (Translated from eng) *J Biol Chem* 268(12):8447-8457 (in eng).

41. Ma Y*, et al.* (1994) Mutagenesis in four candidate heparin binding regions (residues 279-282, 291-304, 390-393, and 439-448) and identification of residues affecting heparin binding of human lipoprotein lipase. *J.Lipid Res.* 35:2049-2059.

42. Baeg GH, Selva EM, Goodman RM, Dasgupta R, & Perrimon N (2004) The Wingless morphogen gradient is established by the cooperative action of Frizzled and Heparan Sulfate Proteoglycan receptors. *Dev Biol* 276(1):89-100.

43. Bornemann DJ, Park S, Phin S, & Warrior R (2008) A translational block to HSPG synthesis permits BMP signaling in the early Drosophila embryo. *Development* 135(6):1039-1047.

44. Nybakken K & Perrimon N (2002) Heparan sulfate proteoglycan modulation of developmental signaling in Drosophila. *Biochim Biophys Acta Gen Subj* 1573(3):280-291.

45. Lander AD, Nie Q, & Wan FY (2002) Do morphogen gradients arise by diffusion? *Dev Cell* 2(6):785-796.

46. Lander AD (2007) Morpheus unbound: reimagining the morphogen gradient. (Translated from eng) *Cell* 128(2):245-256 (in eng).

47. Nordestgaard BG, Benn M, Schnohr P, & Tybjaerg-Hansen A (2007) Nonfasting triglycerides and risk of myocardial infarction, ischemic heart disease, and death in men and women. *Jama* 298(3):299-308.

48. Bansal S*, et al.* (2007) Fasting compared with nonfasting triglycerides and risk of cardiovascular events in women. *Jama* 298(3):309-316.

49. Orchard TJ, Chang YF, Ferrell RE, Petro N, & Ellis DE (2002) Nephropathy in type 1 diabetes: a manifestation of insulin resistance and multiple genetic susceptibilities? Further evidence from the Pittsburgh Epidemiology of Diabetes Complication Study. (Translated from eng) *Kidney Int* 62(3):963-970 (in eng).

50. Wingard DL, Barrett-Connor E, Criqui MH, & Suarez L (1983) Clustering of heart disease risk factors in diabetic compared to nondiabetic adults. (Translated from eng) *Am J Epidemiol* 117(1):19-26 (in eng).

51. Beisswenger PG & Spiro RG (1970) Human glomerular basement membrane: chemical alteration in diabetes mellitus. (Translated from eng) *Science* 168(931):596-598 (in eng).

52. Frank RN, Keirn RJ, Kennedy A, & Frank KW (1983) Galactose-induced retinal capillary basement membrane thickening: prevention by Sorbinil. (Translated from eng) *Invest Ophthalmol Vis Sci* 24(11):1519-1524 (in eng).

53. Park PW, Pier GB, Hinkes MT, & Bernfield M (2001) Exploitation of syndecan-1 shedding by Pseudomonas aeruginosa enhances virulence. *Nature* 411(6833):98-102.

54. Reizes O, *et al.* (2001) Transgenic expression of syndecan-1 uncovers a physiological control of feeding behavior by syndecan-3. *Cell* 106(1):105-116.

55. Echtermeyer F, *et al.* (2001) Delayed wound repair and impaired angiogenesis in mice lacking syndecan-4. *J Clin Invest* 107(2):9-14.

56. Kelley JL & Kruski AW (1986) Density gradient ultracentrifugation of serum lipoproteins in a swinging bucket rotor. *Methods Enzymol* 128:170-181.

57. Page S, Judson A, Melford K, & Bensadoun A (2006) Interaction of lipoprotein lipase and receptor-associated protein. *J Biol Chem* 281(20):13931-13938.

Figure Legends

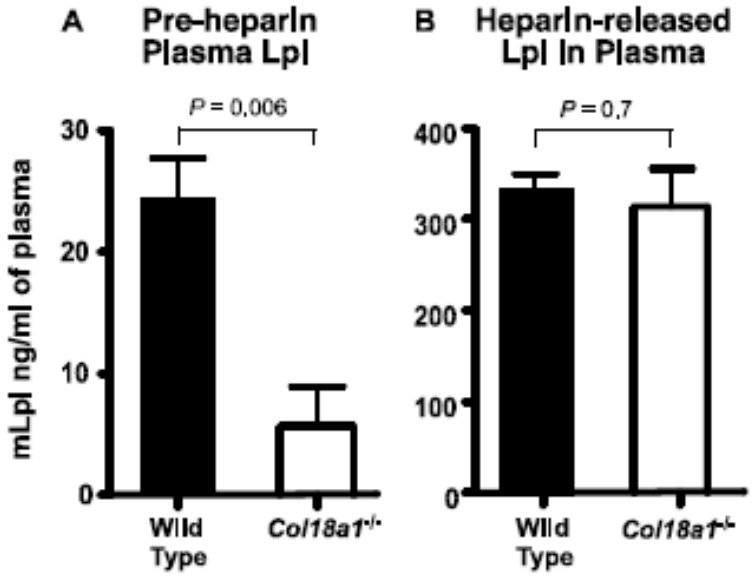
Figure 1. Lipoprotein Lipase in *Col18a1*$^{-/-}$ mice. (A) Plasma level of Lpl was lower in *Col18a1*$^{-/-}$ mice. Plasma levels of Lpl were measured by sandwich ELISA in wild type (black bars) and *Col18a1*$^{-/-}$ mice (white bars) (n=7 for each strain; $P < 0.006$). **(B)** Heparin displacement of Lpl. Wild type and *Col18a1*$^{-/-}$ mice were injected i.v. with heparin (0.5 U/g body weight) and the levels of Lpl in the plasma were measured 15 min later (n=7 for each strain, $P = 0.7$). Results are representative of two separate experiments. **(C)** Intralipid displacement of Lpl. Mice were injected i.v. with a bolus of Intralipid to mimic hyperchylomicronemia and plasma Lpl was measured at the times indicated (n=4 for each strain; $P < 0.004$). Results are representative of two separate experiments.

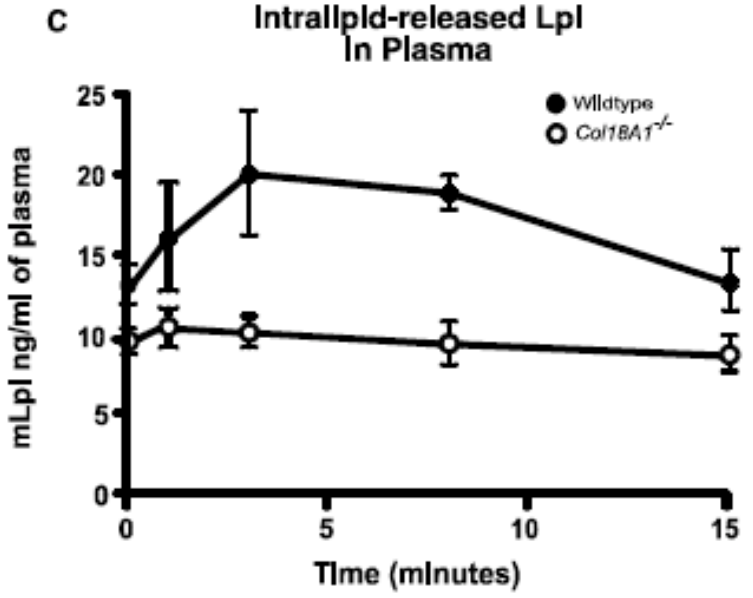
Figure 2. Hypertriglyceridemia in fasted *Col18a1*$^{-/-}$ mice. (A) Total plasma triglycerides were measured in wild type and *Col18a1*$^{-/-}$ after fasting the animals for 4 hrs in the morning. Blood was taken from the retro-orbital sinus for analysis (n = 10, $P < 0.0001$). **(B)** Plasma cholesterol was analyzed in the same samples. **(C)** Triglyceride distribution across plasma lipoprotein subclasses. Plasma was pooled from 4 mice of each genotype and triglyceride in lipoprotein size classes was determined by LipoSEARCH FPLC. Control mice, filled bars; *Col18a1*$^{-/-}$ mice, open bars. Chylomicron (CM) > 80 nm particle diameter; VLDL, 30-80 nm; LDL, 16-30 nm; and HDL, 8-16nm. The experiment was performed twice and the error bars represent the average recovery of triglycerides across the two experiments. **(D)** Equal volumes of lipoproteins of $\delta < 1.006$ g/ml (pooled from n = 3 mice of each genotype) were analyzed by negative staining transmission electron microscopy (inset, 20,000X magnification). The diameters of particles present in eight fields were analyzed in a blinded fashion. The experiment was repeated twice with comparable results.

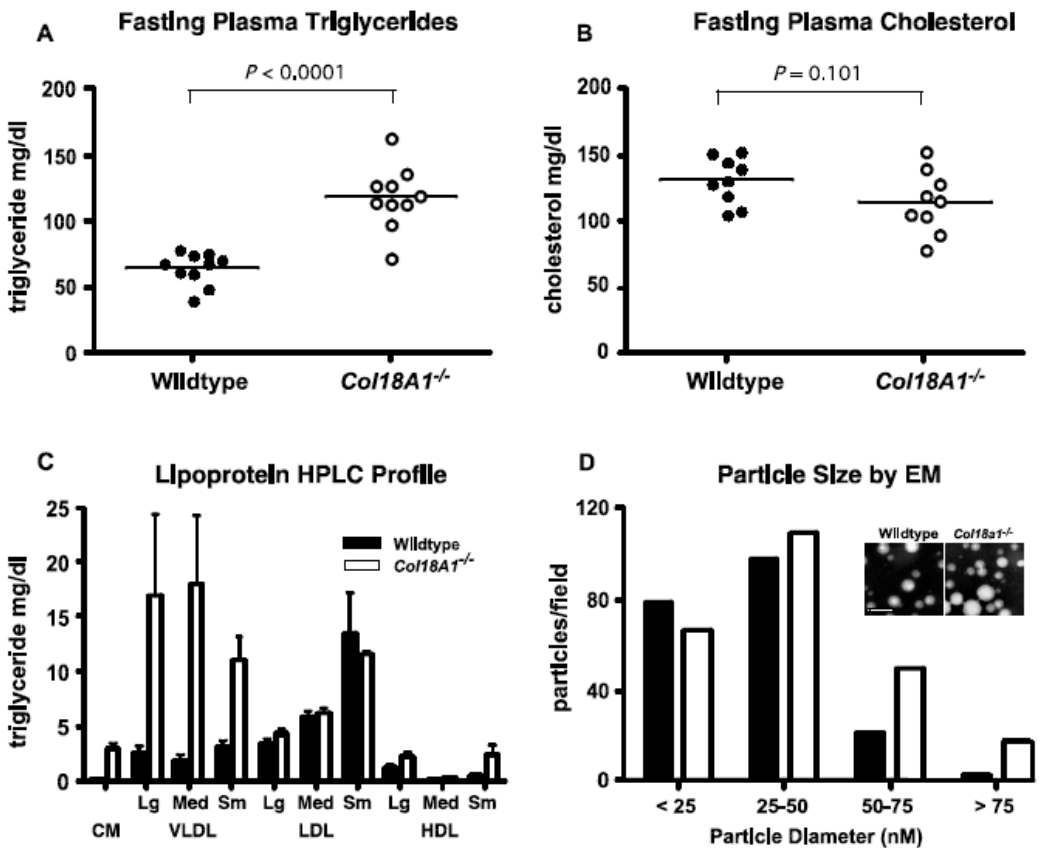
Figure 3. Characterization of hyperchylomicronemia in *Col18a1*$^{-/-}$ mice. (A) Mice (n=6) were fasted 4 hrs in the morning and given a bolus of corn oil by oral gavage. After 2 hrs, blood was collected by cardiac puncture and lipoproteins of $\delta < 1.006$ g/ml were prepared by ultracentrifugation. The triglyceride concentration was determined from equal volumes of sample and related back to the volume of plasma that had been centrifuged. **(B)** Particle size of triglyceride-rich lipoproteins after oral gavage of corn oil. Equal volumes of lipoproteins of $\delta < 1.006$ g/ml were negative-stained and imaged by electron microscopy (20,000X magnification). The diameters of all particles in 8 fields were measured in a blinded fashion and the percentage of lipoproteins greater than 100 nm in diameter was determined. **(C)** Chylomicron clearance by retinyl ester excursion. Fasted wildtype (closed circles, n=4) and *Col18a1*$^{-/-}$ mice (open circles, n=4) were given 200 µl of corn oil containing [^{3}H]retinol by oral gavage. Blood samples were taken at the indicated times and radioactivity remaining in 10 µL of serum was determined by scintillation counting in triplicate. The values are expressed as mean ± SD and are representative of three separate experiments. **(D) VLDL clearance in *Col18a1*$^{-/-}$ mice.** Turnover of VLDL was

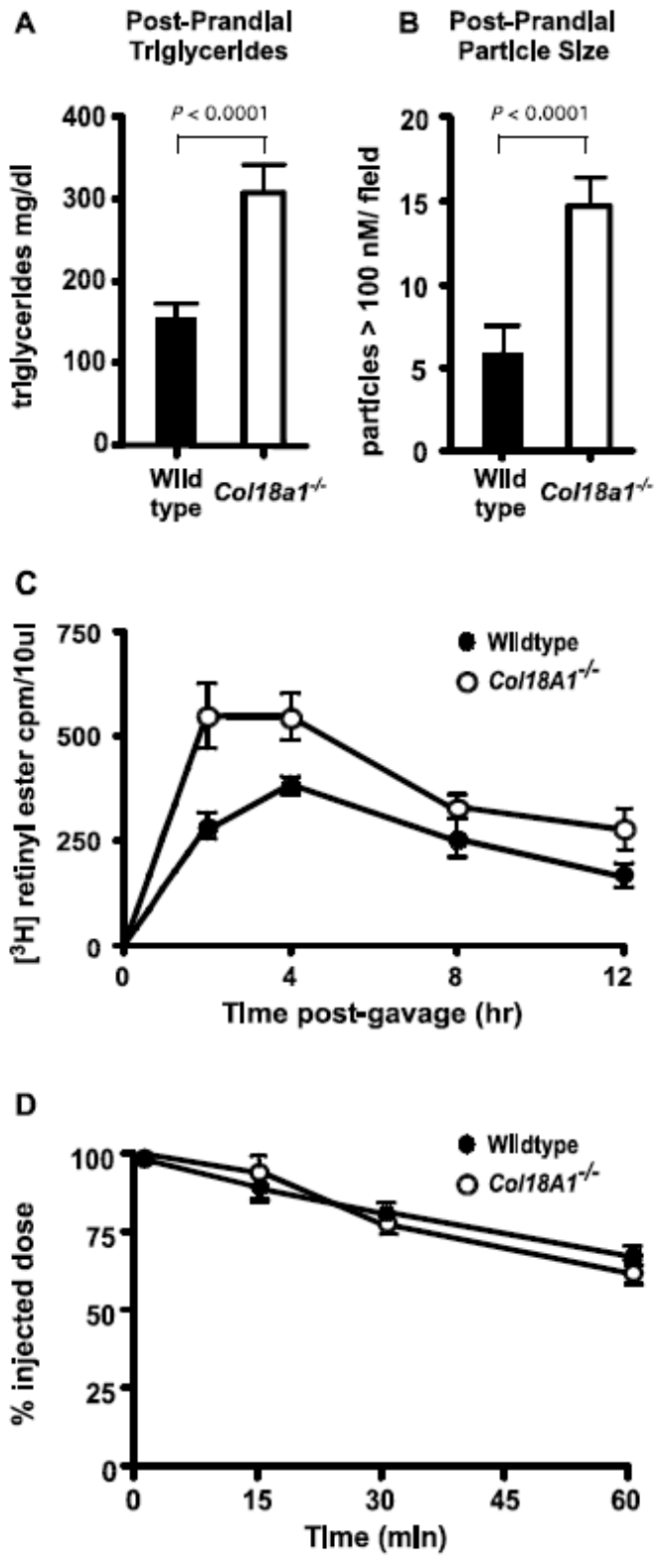
measured in *Col18a1*$^{-/-}$ mice (open circles, n = 4) compared to controls (closed circles, n = 4). Human VLDL was injected intravenously and blood was drawn from the retro-orbital sinus at the indicated times. ApoB-100 remaining in the circulation was detected by ELISA with a human-specific monoclonal antibody. Results are expressed as a percentage of the injected dose. The values are representative of two separate experiments.

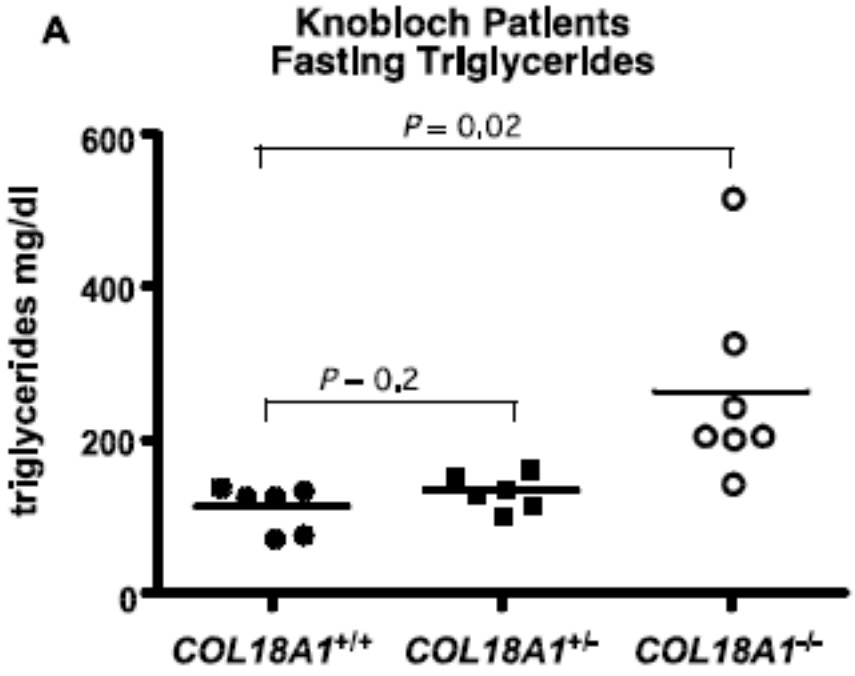
Figure 4. Hypertriglyceridemia in Knobloch patients. (A) Plasma triglycerides were measured in blood samples collected from patients with Knobloch syndrome (*COL18A1*$^{-/-}$) (open circles, *n*=7), heterozygous carriers (*COL18A1*$^{+/-}$, closed squares, n=6) and normal control subjects (*COL18A1*$^{+/+}$, closed circles, n=6). (B) Plasma from 6 individuals was pooled and centrifuged to separate the lipoprotein classes. Triglycerides accumulate in particles of $\delta < 1.006$ g/ml. No error bars are shown since the samples were pooled and only one set of Knobloch patients was studied.

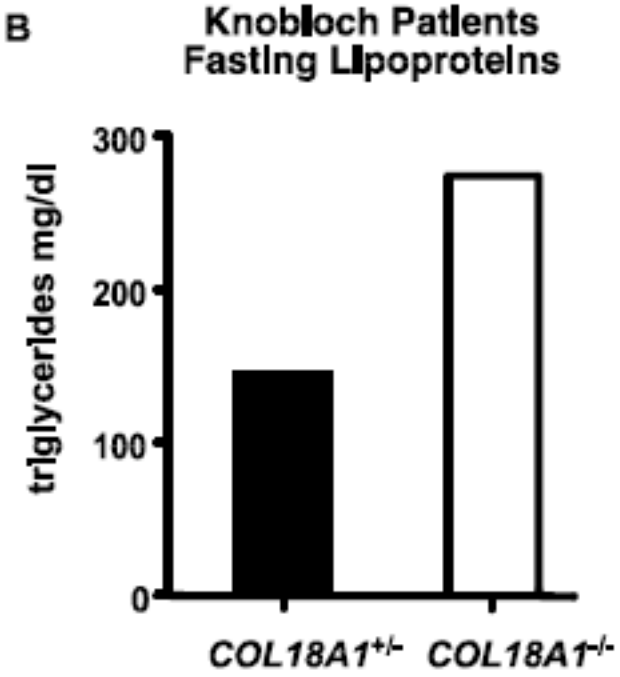

A
Pre-heparin
Plasma Lpl
P = 0.006
mLpl ng/ml of plasma
30
20
10
0
Wild
Type
Col18a1-/-
B
Heparin-released
Lpl in Plasma
P = 0.7
400
300
200
100
0
Wild
Type
Col18a1-/-


C
Intralipid-released Lpl
In Plasma
Wildtype
Col18A1-/-
mLpl ng/ml of plasma
25
20
15
10
5
0
0
5
10
15
Time (minutes)


A
Fasting Plasma Triglycerides
P < 0.0001
triglyceride mg/dl
200
150
100
50
0
Wildtype
Col18A1-/-
B
Fasting Plasma Cholesterol
P = 0.101
cholesterol mg/dl
200
150
100
50
0
Wildtype
Col18A1-/-
C
Lipoprotein HPLC Profile
triglyceride mg/dl
25
20
15
10
5
0
Wildtype
Col18A1-/-
Lg Med Sm Lg Med Sm Lg Med Sm
CM
VLDL
LDL
HDL
D
Particle Size by EM
particles/field
120
80
40
0
Wildtype
Col18a1-/-
< 25
25-50
50-75
> 75
Particle Diameter (nM)


A
Post-Prandial Triglycerides
P < 0.0001
triglycerides mg/dl
400
300
200
100
0
Wild type
Col18a1-/-
B
Post-Prandial Particle Size
P < 0.0001
particles > 100 nM/ field
20
15
10
5
0
Wild type
Col18a1-/-
C
[3H] retinyl ester cpm/10ul
750
500
250
0
Wildtype
Col18A1-/-
0
4
8
12
Time post-gavage (hr)
D
% injected dose
100
75
50
25
0
Wildtype
Col18A1-/-
0
15
30
45
60
Time (min)


A
Knobloch Patients
Fasting Triglycerides
P = 0,02
P – 0,2
triglycerides mg/dl
600
400
200
0
COL18A1+/+
COL18A1+/-
COL18A1-/-


B
Knobloch Patients
Fasting Lipoproteins
triglycerides mg/dl
300
200
100
0
COL18A1+/-
COL18A1-/-

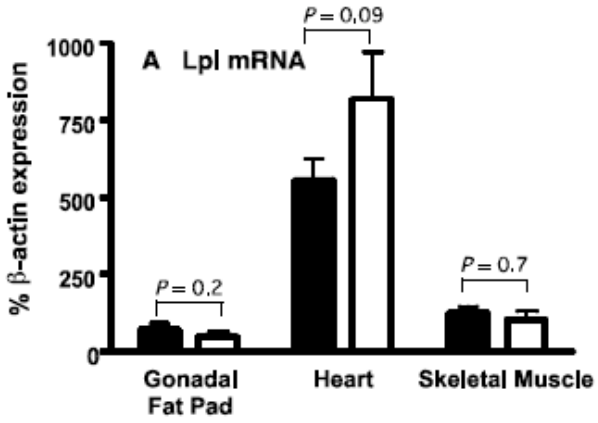
Supplemental Figure Legends

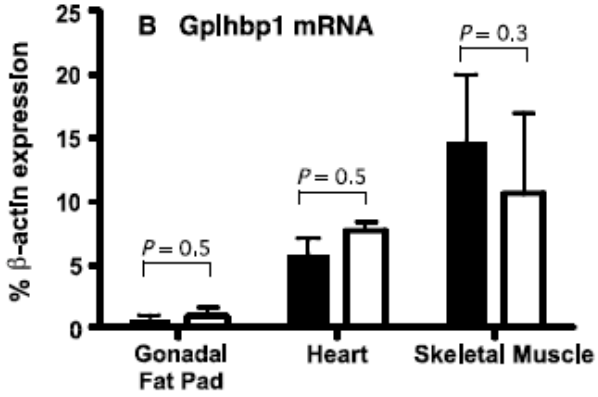
Figure S1. Quantitative RT-PCR analysis of Lpl and Gpihbp1 transcripts. Lpl (A) and Gpihbp1 (B) mRNA expression was determined in samples isolated from gonadal fat pad, heart, and soleus muscle from fasted wild type and *Col18a1*$^{-/-}$ mice (n=4, for each strain). RNA was isolated (10 mg/tissue, Trizol reagent), reverse transcribed (Superscript III, Invitrogen) and amplified using gene specific intron spanning primers to Lpl or GPIHBP. Primer sequences, LPL 5'-AGGTGGACATCGGAGAACTG and 3' –TTTGTCCAGTGTCAGCCAGA and GPIHBP1 5'AACATGATCCCTGGAAGCAG and 3'-ACAGTGTGGACTGGCAACAG. Quantitation was done by the $2^{-\Delta\Delta Ct}$ method using β-actin as a control RNA in a Stratagene MxP3500 {Livak, 2001 #21}. Final numbers represent fold-expression compared to β-actin (100%). Ct values from triplicate assays were used to calculate fold expression according to Stratagene manual. Results were verified in two independent assays. (C) Heart endothelial cell GPIHBP1 detection by FACs analysis. Primary heart endothelial cells were isolated from control (solid line) and *Col18a1*$^{-/-}$ mice (dashed line) by magnetic bead separation with CD31 antibodies following collagenase digestion. GPIHBP1 was detected with a specific polyclonal antibody and Alexa-488 labeled anti-rabbit secondary antibodies followed by FACs analysis. Unshifted cells represent control IgG incubated with secondary antibodies. No difference was seen between mutant and control. Data are representative of 3 separate experiments.

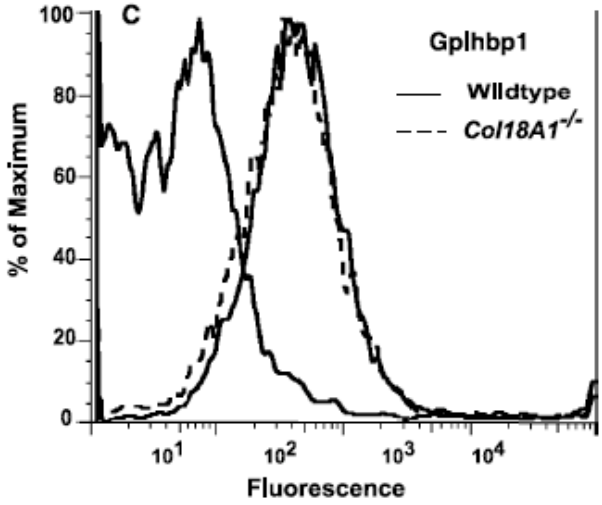
Figure S2. Characterization of fasting lipoproteins accumulating in *Col18a1*$^{-/-}$ mice. (A) Lipoproteins were isolated from pooled plasma by density ultracentrifugation at δ< 1.006 g/ml and triglycerides were measured in equal aliquots of samples prepared from mutant and wild type mice. **(B)** Equal volumes of δ< 1.006 g/ml lipoproteins were concentrated by membrane filtration (Microcon-30s, Millipore) and apolipoproteins were resolved by SDS-PAGE on 4-20% ReadyGels (BioRad). Proteins were visualized by Western blotting with rabbit anti-mouse apoB-48/B-100 (1:2000) and apoE (1:5000) polyclonal antibodies. Membranes were washed and incubated with HRP-conjugated donkey anti-rabbit secondary antibody (1:5000), washed and developed with ECL West Pico Super Signal Reagents (Pierce). Data are representative of 3 separate experiments. In **(C)** and **(D)**, samples were obtained *Col18a1*$^{-/-}$ and wild type mice 2 hr after challenge with a bolus of corn oil by oral gavage. In **(C)** equal volumes of lipoproteins of δ < 1.006 g/ml (pooled from n = 3 mice of each genotype) were analyzed by negative staining transmission electron microscopy (20,000X magnification). **(D)** Samples were processed as in panel (B).

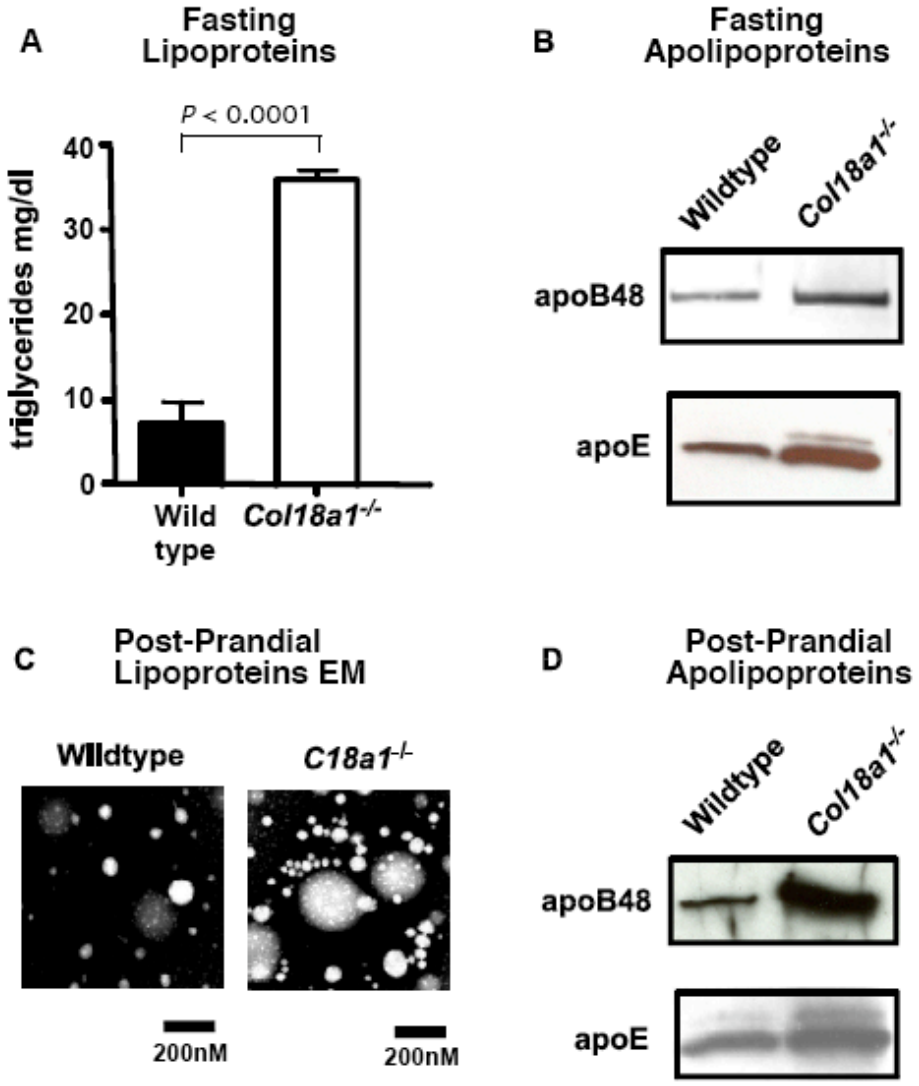
Figure S3. Heparin-induced clearance of plasma triglycerides. Plasma triglycerides were measured pre- and post-heparin injection in fasted mice **(A)** or 2 hrs post-fat challenge **(B)** in the wild type and *Col18a1*$^{-/-}$ mice. Heparin was injected

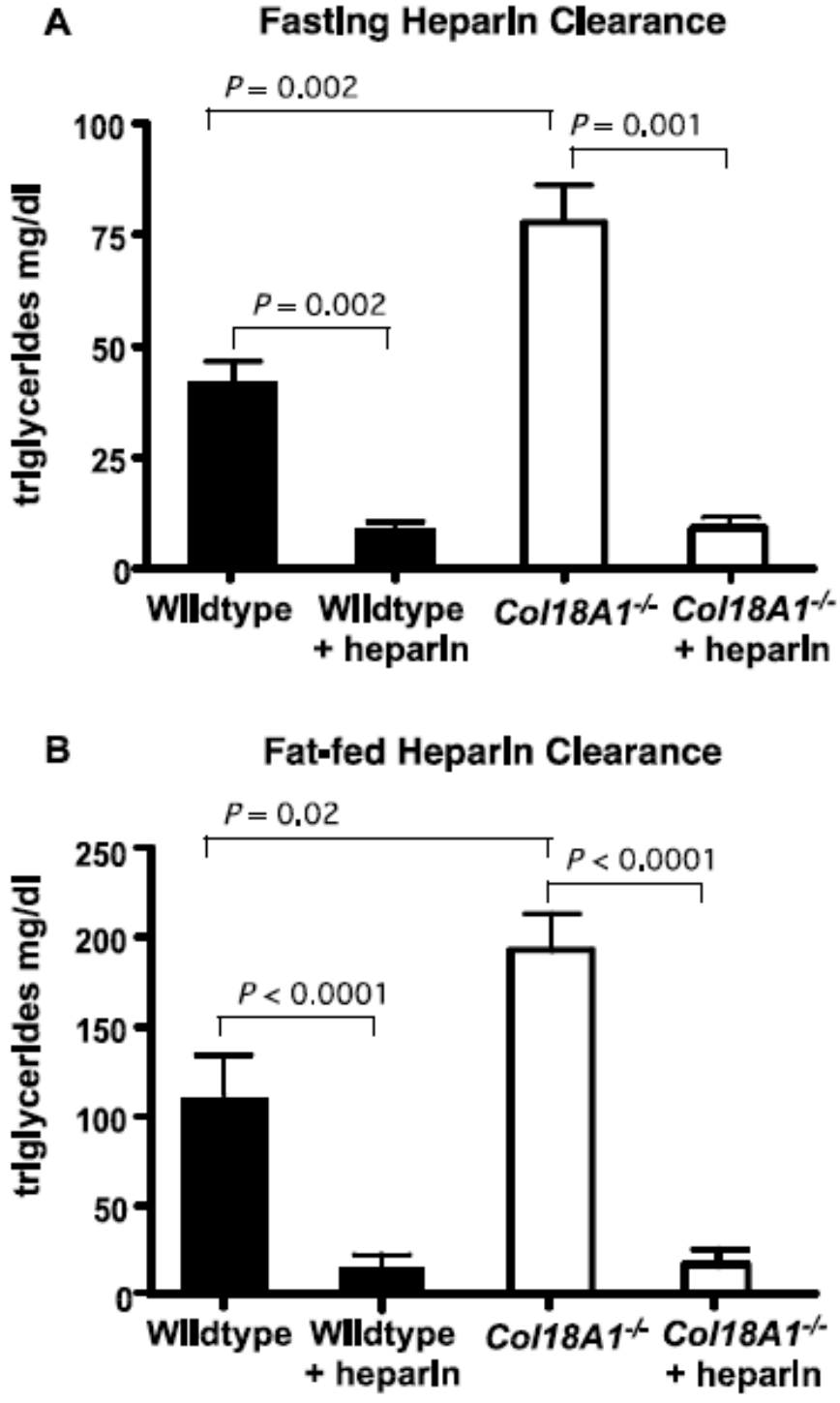
intravenously (0.5 U/g body weight) and blood was sampled from the retro-orbital sinus 10 min post injection. Results were verified in two independent assays.


A Lpl mRNA
% β-actin expression
1000
750
500
250
0
P = 0,09
P = 0,2
P = 0.7
Gonadal Fat Pad
Heart
Skeletal Muscle


B Gplhbp1 mRNA
% β-actin expression
25
20
15
10
5
0
P = 0.3
P = 0.5
P = 0,5
Gonadal Fat Pad
Heart
Skeletal Muscle


C
Gplhbp1
Wildtype
Col18A1-/-
% of Maximum
100
80
60
40
20
0
10¹
10²
10³
10⁴
Fluorescence


A
Fasting Lipoproteins
P < 0.0001
triglycerides mg/dl
40
30
20
10
0
Wild type
Col18a1-/-
B
Fasting Apolipoproteins
Wildtype
Col18a1-/-
apoB48
apoE
C
Post-Prandial Lipoproteins EM
Wildtype
C18a1-/-
200nM
200nM
D
Post-Prandial Apolipoproteins
Wildtype
Col18a1-/-
apoB48
apoE


A
Fasting Heparin Clearance
P = 0.002
P = 0.001
P = 0.002
triglycerides mg/dl
100
75
50
25
0
Wildtype
Wildtype + heparin
Col18A1-/-
Col18A1-/- + heparin
B
Fat-fed Heparin Clearance
P = 0.02
P < 0.0001
P < 0.0001
triglycerides mg/dl
250
200
150
100
50
0
Wildtype
Wildtype + heparin
Col18A1-/-
Col18A1-/- + heparin

Supplemental Table 1. Knobloch patient data. Fasted blood samples were taken from Knobloch patients and analyzed for glucose, triglycerides and cholesterol.

Patient I.D	Col18 genotype	fasting glucose mg/dl	fasting triglycerides mg/dl	fasting cholesterol mg/dl
F1020-03	+/+	91	144.1	107.5
F1020-17	+/+	83	139.3	81.4
F1020-39	+/+	91	118.9	86.6
F1020-45	+/+	89	130.6	79.9
F1020-46	+/+	72	104.8	85.8
F1020-50	+/+	86	133.8	84.0
F1251-04	+/+	85	118.8	118.
mean		85 ± 6	117 ± 12	92 ± 15
F1020-05	+/-	82	169.6	74.6
F1020-40	+/-	89	144.4	90.7
F1020-47	+/-	75	143.8	92.9
F1020-46	+/-	72	104.8	85.8
F1020-48	+/-	85	133.5	86.9
F1020-54	+/-	103	81.9	71.6
mean		84 ± 11, $P = 0.85$	135 ± 9, $P = 0.27$	84 ± 9, $P = 0.43$
F1020-06	-/-	92	540.1	107.9
F1020-09	-/-	87	205.4	107.5
F1020-35	-/-	95	248.4	93.3
F1020-34	-/-	89	122.9	122.4
F1020-36	-/-	130*	330.6	101.1
F1020-37	-/-	82	210.9	75.0
F1020-38	-/-	93	209.4	82.5
mean		95 ± 15, $P = 0.14$	267 ± 51, $P = 0.02$	99 ± 16, $P = 0.26$

Wt – wildtype, +/-, heterozygous carriers of Col18 mutation, -/-, Knobloch Syndrome, homozygous Col18 mutation. * borderline diabetic. All P values compared to wildtype.